Synthesis of Drug/Dye Incorporated Copolymer-Protein Hybrids and Novel Curcumin Derivatives for Imaging and Therapeutic Applications.

By

Sukanta Dolai

A dissertation submitted to the graduate Faculty in Chemistry in partial fulfillment of the requirement for the degree of Doctor of Philosophy, The City University of New York.

2010

This manuscript has been read and accepted for the Graduate Faculty in Chemistry in satisfaction of the dissertation requirement for the degree of Doctor of Philosophy.

Prof. Krishnaswami Raja

_____	_____
Date	Chair of Examining Committee

Prof. Mahesh K. Lakshman

_____	_____
Date	Executive Officer

Prof. Probal Banerjee

_____

Prof. Michal Kruk

_____

Prof. Carol Steiner

_____

Supervisory Committee

THE CITY UNIVERSITY OF NEW YORK

Abstract

Synthesis of Drug/Dye Incorporated Copolymer-Protein Hybrids and Novel Curcumin Derivatives for Imaging and Therapeutic Applications.

By

Sukanta Dolai

Advisor: **Prof. Krishnaswami Raja**

This thesis describes novel synthetic methodologies towards: (a) novel polymer-protein hybrids with a significantly increased number of functional units attached per protein and (b) the synthesis of curcumin derivatives with increased solubility and amplified bioactivity.

Azide terminated poly(*tert*-butyl acrylate) was synthesized via atom transfer radical polymerization [ATRP]. Subsequent deprotection was performed to yield poly(acrylic acid) (PAA) possessing a reactive chain-end. A one pot sequential amidation of the PAA with the amine derivatives of a near infrared fluorescent dye (ADS832WS) and glucose produced NIRF dye incorporated water soluble copolymers. End-group modifications were performed to produce alkyne/biotin terminated copolymers which were further employed to generate dye incorporated polymer-protein hybrids via the biotin-avidin interaction with avidin or "click" bioconjugation with azide modified bovine serum albumen or apoferritin. We have overcome two fundamental limitations in the synthesis of bioconjugates: (a) the basic restriction in the diversity of copolymers

which can be synthesized for producing bioconjugates, (b) the limitation in the number of dyes/drug molecules that can be attached per protein molecule. The copolymers possessed enhanced optical properties compared to the dye due to increased solubility in water. Potential utility of these copolymers and conjugates in multiwell plate based assays, cell surface imaging and *in vivo* animal imaging were explored.

In order to overcome the difficulties associated with the low water/plasma solubility of the potent anti-oxidant, anti-inflammatory, anti-carcinogenic, anti-Alzheimer's active curcumin we have successfully synthesized several mono-functional derivatives via one-two step covalent modification methods. Freely water soluble derivatives or adducts of curcumin e.g. curcumin sugar conjugate, dendrimer-curcumin conjugate were synthesized. Antibody-curcumin adduct was produced to develop an intelligent drug delivery system. The curcumin mono-carboxylic acid was able to stain and dissolute amyloid-beta plaques at a much lower concentrations compared to curcumin. A curcumin sugar conjugate which was able to modulate Aβ aggregation in nM concentrations was synthesized compared to curcumin which is effective in μM concentrations, the sugar conjugate is ~1000 times more potent. The curcumin sugar conjugate was found to be neuro-protective as well. The curcumin dimer which have the same numbers of free phenolic-OH as curcumin, was able to selectively destroy human neurotumor cells. The dendrimer-curcumin conjugate displays curcumin in a polyvalent architecture, it was freely soluble in water and was effective against BT459 mammalian cancer cells at much lower concentrations than curcumin. Towards the synthesis of targeted drug delivery module for curcumin, the synthesis of Antibody-curcumin adduct showed a great promise in destroying GL261 glioblastoma cells as well as B16F10

melanoma cells in nM concentrations compared to curcumin which is effective in μM concentrations. The *in vivo* studies in both glioblastoma and melanoma models for brain tumors indicated that mice treated with antibody-curcumin conjugate resulted in significant decrease in tumor size and a significant increase in survival life span.

I dedicate this dissertation to my Grand Parents, Mr. & Mrs. Haripada Maity, who sowed the seed of success in my early childhood and throughout my educational carrier provided me love, encouragement and enormous support to create a complete and successful persona.

ACKNOWLEDGEMENTS

I wish to express my sincere gratitude to my supervisor Professor Krishnaswami S. Raja, Department of Chemistry at College of Staten Island, The City University of New York, New York, for his valuable guidance, stimulating inspiration and all the supports throughout my research career.

My grateful thanks are due to my research committee members; Professor Probal Banerjee, Department of Chemistry, College of Staten Island (CUNY), Professor Michal Kruk, Department of Chemistry, College of Staten Island (CUNY), and Professor Carol Steiner, Department of Chemical Engineering, City College (CUNY) for being in my committee and for providing me valuable suggestions throughout my research career.

My special thanks are due to Dr. Wei Shi, for his endless help and inspiration throughout my research career. I gratefully acknowledge my other colleagues Mr. Chong Sun, Mr. Amit Mogha, Mr. Christopher Corbo, Mr. Manik Mandal, Mr. Arijit Sengupta, Ms. Janhavi Shah, Ms. Phyllis Langone, Ms. Sreyashi Sammadar, Ms. Shawon Debnath for their help and encouragement and also for providing me a friendly atmosphere in the department.

I also acknowledge the help and support of my previous and current undergrads, Mr. Saadyah Averick, Mr. Jose Saltos, Mr. Eric Rios-Doria, Mr. Zeeshan, Mr. Adam Chin, Mr. Christopher Santana, Ms. Dinali Obeysekera, Ms. Olga Vishneva, Ms. Hina Naveed.

I sincerely acknowledge Dr. Boris Arshava (Department of Chemistry, College of Staten Island) and Mr. Tai Park (Department of Chemistry, College of Staten Island) for their help with various analytical techniques.

Mr. Chong Sun, Mr. Christopher Corbo, Mr. Amit Mogha, Ms. Phyllis Langone

and Ms. Shawon Debnath are acknowledged for their help in biological experiments towards my thesis.

The source of inspiration and inclination towards my career has been my beloved parents Mr. Lakshmikanta Dolai and Mrs. Krishna Maity (Dolai) who were my strength throughout my career. I wish to thank them for their valuable guidance, support and encouragement. My thanks are also due to my beloved sisters and brother for their love and support.

I especially thank my beautiful wife Mrs. Rupita Dolai, the love of my life, whose unconditional love, support and encouragements throughout my career was my life-line to reach my goal. My son Debameet, the little wonder, helped me to be more focused towards my destiny.

I wish to express my sincere thanks to Dr. Alok Sarkar, Dr. Rajesh Sardar, Dr. Bharathi Balagam, Dr. Rema Balambika whose advise and support was a valuable gift throughout my career.

Sukanta Dolai

Staten Island, NY

Table of Contents

List Of Tables

List of Illustrations (Schemes)

List of Illustrations (Figures)

CHAPTER I

Background Information and Rationale for the Research.

PART I

Synthesis and applications of the drug/dye incorporated copolymer-protein hybrids.

1. BACKGROUND INFORMATION

Since the first report of synthesis of protein/peptide-synthetic polymer hybrids in the early 1950's, it has drawn a lot of interest as it provides unique opportunities to combine the best of two worlds: the chemical and the biological (*1, 2*). One of the very first reports was on the synthesis of mescaline-glycyl-L-leucine-poly(vinylpyrrolidone) conjugate, which was designed to act as a depot to allow enzyme-mediated drug release. Davis et al and Abuchowski et al. in the 1970's have covalently attached poly(ethylene glycol) (PEG) to bovine serum albumin (BSA) and bovine liver catalase, PEG attachment served as an excellent strategy to reduce or eliminate the immunogenicity of these proteins and increase their blood circulation times (*3, 4*). In the mid-1980s Maeda et al. studied the pharmacokinetics of the antitumor protein neocarzinostatin (NCS) and styrene-maleic anhydride copolymer conjugates (*5-7*). These conjugates were preferentially accumulated in tumor tissue due to a passive targeting mechanism, the enhanced permeability and retention (EPR) effect. In the early years using appropriate synthetic polymer macroinitiators a variety of hybrid di- and tri-block copolymers were prepared by ring-opening polymerization of R-amino acid N-carboxyanhydrides (NCA's) (*8-12*).

Several synthetic strategies are available to synthesize these hybrid materials.

Usually three main techniques/methods are employed towards the synthesis of peptide/protein part of the hybrid materials namely (*13*), (a) ring-opening polymerization (ROP) of *R*-amino acid *N*-carboxyanhydride, (b) solid phase peptide synthesis (SPPS), and (c) bio-synthesis of proteins. The most commonly applied method for the large-scale preparation of synthetic polypeptides and polypeptide-block copolymer hybrids is ring-opening polymerization of *R*-amino acid *N*-carboxyanhydride which uses simple starting materials, allows the preparation of high molecular weight polypeptides, and does not affect the stereochemistry of the amino acid building blocks (*13-17*). The synthesized polypeptides can be conjugated to the synthetic polymers via either convergent (e.g. 'click' coupling of R-alkyne/R-azido polypeptides with alkyne/azide functionalized synthetic polymers) (*18-20*) or divergent methods (e.g. one-pot synthesis using dual initiators for NCA ring-opening polymerization and NMP/ATRP) (*21-23*). The biggest drawback of this method is that it can yield neither perfectly monodisperse nor sequence specific polypeptides. To tackle this problem, over the past few years, a number of techniques have been developed. One approach is to achieve a "living" NCA ring-opening polymerization using transition-metal-based initiators such as Ni(COD), Co $(PMe_3)_4$, or (dppe)Pt(MBS-H) (*24-26*).

Solid phase peptide synthesis has recently became a routine technique to produce polypeptides containing up to 50 amino acid residues with perfect control over chain length and monomer sequence (*27, 28*). The convergent synthesis of a broad range of peptide-synthetic polymer hybrids can be achieved via selective modification of a suitable reactive chain-ended polymer or via functionalization of appropriate reactive side chains (*29*). The main drawback of the traditional peptide coupling conditions which are

frequently used for the synthesis of peptide-synthetic polymer conjugates is that these reactions are usually not bioorthogonal and cannot be used to synthesize conjugates in homogeneous (aqueous) solution from unprotected peptides. Several bioorthogonal techniques (*29*) used or invented include various Pd^0-catalyzed coupling reactions, Staudinger ligation, cycloaddition reactions (e.g. Diels-Alder, 1,3-dipolar cycloaddition), reductive alkylation, oxime and hydrazone formation, thiol addition reactions, and oxidative coupling and the Huisgen 1,3-dipolar cycloaddition reaction (more commonly known as 'click' reaction) have been employed in several instances for the synthesis of peptide-synthetic polymer conjugates (*30-34*). On the other hand the divergent synthesis can be carried out both on the solid phase as well as in homogeneous solution. The divergent solid phase synthesis of peptide-polymer conjugates is frequently carried out using commercially available Tentagel resins in which poly(ethylene glycol) chains are attached to the solid support via a labile linker (*35-38*). The synthetic polymer segment can also be grown from appropriate initiator modified resin-bound peptides using controlled radical polymerization techniques (e.g. atom transfer radical polymerization; ATRP, reversible addition-fragmentation chain transfer polymerization; RAFT) instead of grafting the peptide segment step-by-step from a soluble or insoluble synthetic polymer support (*39-41*). Another divergent approach for the synthesis of these hybrid materials is based on the polymerization of peptide-based monomers (*29*). A variety of peptide-based monomers have recently been polymerized via conventional free radical polymerization (*42, 43*), ring-opening metathesis polymerization (ROMP) (*44-46*), or controlled radical polymerization (ATRP/RAFT) (*47, 48*).

Biosynthetic methods helped to overcome some of the limitations towards the

protein/peptide-synthetic polymer hybrids imposed by the NCA ring-opening polymerization (no precise control over chain length and monomer sequence) and Solid phase peptide synthesis methods (maximum chain length restricted to ~50 amino acids). This technique can be used to produce high molecular weight proteins with precisely controlled chain lengths and peptide sequences by introducing an appropriately engineered recombinant plasmid into a bacterial host (*49*). Davis et al. prepared the first protein-synthetic polymer conjugates following a convergent strategy involving a reaction between a PEG-dichlorotriazine derivative with either bovine liver catalase or bovine serum albumin (*3, 4*). Over the past few decades PEGylation has evolved as a well-established technology to modify therapeutic proteins and improve their stability and solubility, reduce renal clearance, enhance circulation half-life, reduce immunogenicity and antigenicity, and prevent proteolytic degradation. Nowadays, a variety of PEGylated protein based drugs are available on the market, including drugs such as Pegintron, Pegasys, Neulasta, and Mircera which are used to treat diseases like Hepatitis C, cancer, and others (*13, 50*). In the early years the PEGylation agents in addition to PEG-dichlorotriazine included PEG-succinimidyl carbonate, PEG-trichlorophenyl carbonate, PEG-tresylate, PEG-benzotriazole carbonate, PEG-p-nitrophenyl carbonate, PEG-carbonylimidazole, and PEG-succinimidyl succinate, have successfully generated the desired conjugates but also suffered from several drawbacks due to PEG impurities, the restriction to low molecular weight PEG derivatives, the formation of unstable linkages, and lack of selectivity in modification (*51*). Some of the above mentioned problems were successfully overcame by next-generation PEGylation agents including PEG-aldehyde derivatives, PEG-iodoacetamide, PEG-maleimide, PEG-

NHS, PEG-vinylsulfone, and PEG-o-pyridyl disulfide (*51*). A wide range of bioorthogonal coupling reactions is available for the synthesis of such precision protein-synthetic polymer conjugates including the widely used 'click' reaction (*29, 34*).

Peptide-synthetic polymer conjugates have attracted interest for a number of reasons. First of all, the peptide segment both in solution and in the solid state, can provide these materials with unique self-assembly properties and induce the formation of hierarchically organized nanoscale structures with a much higher level of complexity as compared to e.g. ordinary block copolymers. The peptide secondary structure is sensitive to environmental parameters such as temperature, pH, or ion strength and the conjugation of synthetic polymers allows to reversibly manipulate the nanoscale structure formation of these hybrid materials. Covalently combining proteins and synthetic polymers is of interest for numerous reasons. The conjugation of an appropriate synthetic polymer can modulate the biological activity of a protein. Again, looking from the other side, the attachment of a protein may endow a synthetic polymer with unique functional and structural properties. **Table 1** lists several selected examples of the wide range of attractive properties and diverse applications of peptide/protein-synthetic polymer conjugates reported in recent years.

Table 1.1. Overview of Selected Functions and Applications of Peptide/Protein-Synthetic Polymer Conjugates. (Adapted from Macromolecules 2009, 42, 7990–8000)

drug and gene delivery	• peptide-synthetic hybrid block copolymers as carriers for drug and gene delivery (*52, 53*) • functionalization of synthetic polymers with peptide sequences to allow targeted delivery (*54, 55*) and guide intracellular trafficking (*56, 57*)
mechanical properties	• silk-inspired peptide-synthetic hybrid multiblock copolymers (*58, 59*) • modulation of the mechanical properties of synthetic polymers by blending self-assembled peptide-synthetic polymer hybrid nanofibers (*60*)
hydrogels	• hydrogel formation driven by peptide self-assembly; coiled coil formation, (*61-65*) entanglement of β-sheet peptide based peptide-synthetic polymer nanotubes (*66*) • bioactive hydrogels: incorporation of cell-adhesion peptide sequences and protease substrates (*67, 68*) • hybrid hydrogels formed by self-assembly of recombinant coiled coil protein-synthetic polymer conjugates (*61, 69*) • bioactive hydrogels based on recombinant proteins containing cell adhesion sequences and protease substrates (*70, 71*) • "dynamic" hydrogels based on proteins that undergo large conformational changes upon binding of a substrate (*71-75*)
directing mineralization	• PEG-b-PAsp and PEG-b-PGlu as additives for the mineralization of $CaCO_3$ and $BaSO_4$ (*76-78*) • peptide-synthetic polymer nanotapes as a template for the formation of silica composite nanofibers (*79*)
enzymes	• separation, recovery, recycling and modulation of activity via attachment of thermosensitive polymers (*80-83*)
viral capsids and protein cages	• polymer-modified viral capsids as vectors for gene delivery (*84-88*)
therapeutic proteins	• modification of therapeutic proteins to improve stability and solubility, reduce renal clearance, enhance circulation half-life, reduce immunogenicity and antigenicity, and prevent proteolytic degradation (*50, 89, 90*) • reversible PEGylation and polymer masking-unmasking protein therapy (PUMPT) to avoid loss of activity upon polymer conjugation and obviate the need for site-specific modification (*91-93*)

2. RATIONALE FOR OUR RESEARCH

Our current research is focused on the synthesis of well-defined functional biopolymer-synthetic polymer hybrids, which are targeted at addressing relevant biotechnological and biomedical problems. A major goal of our research was to develope a bioconjugation technology towards new generations of targeted imaging agents, detection reagents and targeted drugs with amplified efficiency. The protein components (biopolymer) employed would be avidin (*89, 94*), Bovine Serum Albumin (BSA), secondary antibodies (Anti-Rabbit IgG) and bio-nanoparticles (*90*). The protein components could be attached to living copolymers with unique reactive chain ends; the multifunctional polymers would be composed of several copies of water soluble poly(ethylene glycol)/poly(acrylic acid)/poly(aminoethyl methacrylate) units and imaging/therapeutic agent/targeting ligands attached covalently in a brush polymer architecture. The main therapeutic/imaging agents we proposed to employ was a Near Infrared Fluorescence Dye (ADS832WS) and Glucose as the biocompatible/water-solubilizing group.

It should be noted that Near-infrared (NIR)-absorbing dyes have opened new avenues in optical imaging with direct applications in pharmacology, cellular biology, and diagnostics as living subjects can be monitored with safe, non-invasive optical imaging/contrasting techniques (*95*). Since last two decades, semiconductor nanocrystals (*96-99*), fluorescent proteins (*100, 101*), and NIR fluorescent molecules have been used as powerful optical sensors or probes (*102-104*). In comparison to other dyes, NIR fluorescent dyes are better candidate for *in vitro* and *in vivo* imaging because hemoglobin in red blood cells and water are the major absorbers of visible and infrared light but have very low absorption in the NIR region (650-900 nm). Significant reduction of background absorption, enhanced fluorescence, the availability of

low-cost sources of irradiation, and the versatility of different reporter probes are among the numerous advantages of optical imaging in the NIR region (700-1100 nm). Cyanine dyes (*105-107*) are superior compared to other long-wavelength fluorophores [e.g. BODIPY (*108*), rhodamine (*109, 110*), and oxazine (*111*)] as they display large molar extinction coefficients and moderate-to-high fluorescence quantum yields (*112-114*).

Our approach towards these conjugates involves three steps: (i) the synthesis of well-defined living polymers containing reactive chain-end and functional side-chain pendant groups in which the chain end and side chain possesses orthogonal reactivity, (ii) the attachment of a number of water soluble, biocompatible moieties and imaging/therapeutic agents to the functional polymer side chains, and (iii) attachment of the polymers (via the reactive polymer chain end) with proteins to produce the final bioconjugates.

Scheme 1.1. Schematic representation of synthesis of drug/dye incorporated copolymer-protein/peptide conjugates.

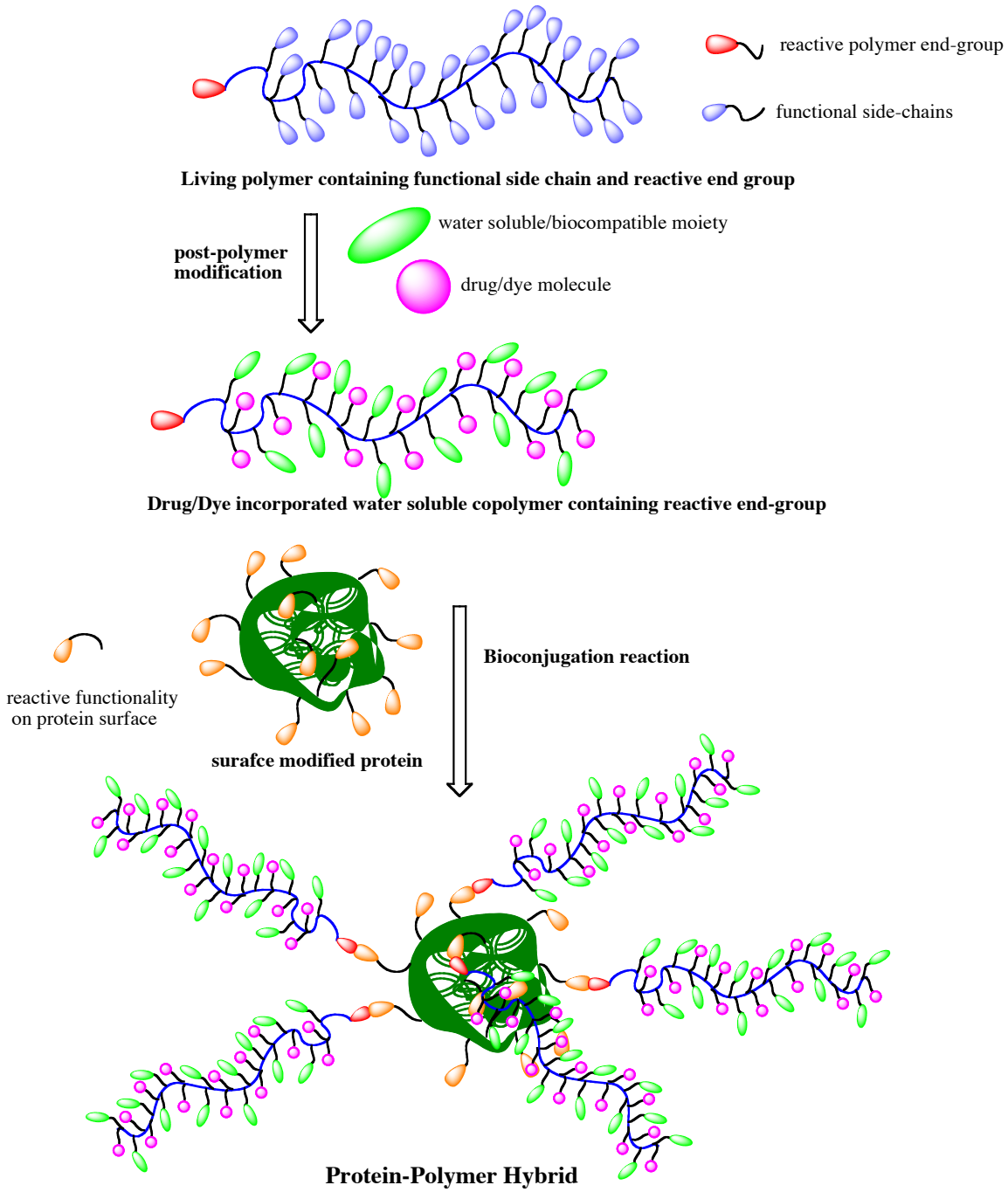

PART II

Synthesis and applications of novel functional curcumin derivatives.

3. BACKGROUND INFORMATION

Curcumin, the primary active ingredient in the spice turmeric, is essentially a hydrophobic polyphenol derived from the rhizome of the herb *Curcuma longa* and has been shown to have a wide spectrum of biological and pharmacological activities (*115*). Chemically, curcumin is an unsaturated diketone containing two phenolic-OH, which exhibits keto-enol tautomerism showing a predominant keto form in acidic and neutral solutions and stable enol form in alkaline medium. Commercially available curcumin contains approximately 77% curcumin, 17% demethoxycurcumin, and 6% bisdemethoxy-curcumin (*115*). Traditionally, turmeric has been used as a spice in South Asian cooking, as a cosmetic and in the ancient Ayurvedic system of medicine (*116*) particularly as an anti-inflammatory agent, and also curcumin has been identified as the active component of turmeric (*117*). Curcumin has been shown to exhibit antioxidant, anti-inflammatory (*118-121*), antimicrobial, and anti-carcinogenic (*122-126*) activities. Additionally, the hepato- and nephro-protective (*127-129*), thrombosis suppressing (*130*), myocardial infarction protective (*131-133*), hypoglycemic (*134-137*), and antirheumatic (*138*) effects of curcumin are also well established. Various animal models (*139, 140*) or human studies (*141-144*) proved that curcumin is extremely safe even at very high doses. The pharmacological safety and efficacy of curcumin makes it a potential compound for treatment and prevention of a wide variety of human diseases. In spite of its efficacy and

safety, curcumin has not yet been approved as a therapeutic agent, and the lack of relative bioavailability of curcumin has been highlighted as a major problem for this. The reasons for reduced bioavailability of any agent within the body are low intrinsic activity, poor absorption, high rate of metabolism, inactivity of metabolic products and/or rapid elimination and clearance from the body (*115*). One of the major observations related to curcumin studies involves the observation of extremely low serum levels. Earlier and recent studies by several groups e.g. Wahlstrom et al. (*145*), Ravindranath et al. (*146, 147*), Pan et al. (*148*), Perkins et al. (*149*), Sharma et al. (*150*), Yang et al. (*151*), Marczylo et al. (*152*) clearly suggest the role of route of administration on achievable serum levels of curcumin and further indicate that the serum levels of curcumin in rats and in human are not directly comparable.

Systemic elimination or clearance of curcumin from the body is also an important factor, which determines its relative biological activity. Several groups have studied the elimination half-life of curcumin both in humans and in mouse models. Curcumin was administered orally, intraveneously (i.v.) or intraperitonially (i.p.) and in some cases radiolabeled curcumin was used to determine the pathway. Regardless of the type of drugs and mode of administration, the major route of elimination of the curcumin was found to be through feces; no detectable amount of curcumin was found in urine regardless of the dose, although some of the derivatives like curcumin glucuronide and sulfates were observed in the recovered metabolites (*145, 153, 154*). The absorption and elimination half-lives of orally administered curcumin (2 g/kg) in mouse models were reported to be 0.31 h, but in humans, the same dose of curcumin did not allow the

calculation of these half-life values because the serum curcumin levels were below the detection limit at most of the time points in most of the experimental subjects (*144*).

Various studies have also evaluated the metabolism of curcumin in mouse and in humans. Once absorbed, curcumin is subjected to conjugations like sulfonation and glucuronidation at various tissue sites. Liver was indicated as the major organ responsible for metabolism of curcumin (*145, 155, 156*). Several groups have reported that the major biliary metabolites of curcumin are curcumin–glucuronoside, dihydrocurcumin (DHC)–glucuronoside, tetrahydrocurcumin (THC)–glucuronoside, and THC and hexahydrocurcumin (HHC) and minor biliary metabolite was dihydroferulic acid together with traces of ferulic acid (*153*). Thus, it seemed that curcumin undergoes extensive reduction, most likely through alcohol dehydrogenase, followed by conjugation. While most studies indicate that curcumin glucuronides and THC are less active than curcumin itself (*157, 158*), there are other studies which suggest that they may actually be more active than curcumin (*159-164*).

The absorption, biodistribution, metabolism, and elimination studies of curcumin have, unfortunately, shown only poor absorption, rapid metabolism, and elimination of curcumin as major reasons for poor bioavailability of this interesting polyphenolic compound (*115*). Some of the possible ways to overcome these problems are via the use of (i) adjuvants, which can block metabolic pathways of curcumin, and are one of the major means that are being used to improve its bioavailability (*165-169*), (ii) nanoparticles, liposomes, micelles, phospholipid complexes and other promising novel formulations, which appear to provide longer circulation, better permeability, and resistance to metabolic processes (*170-179*). On the other hand, bioconjugates can

increase the cellular uptake and hence better bioavailability of curcumin. For example, Biocurcumax, a formulation where curcuminoids combined with turmeric oil (turmerons) in a specific proportion enhanced the bioavailability and showed better absorption into blood and had longer retention time compared to curcumin (*115*). This product showed 700% more activity and 7–8 times more bioavailability over curcumin as confirmed by human clinical trials (*115*). Currently a multicenter, phase II, randomized, double-blinded, placebo controlled clinical study is ongoing to assess the efficacy and safety of Biocurcumax (BCM-95) in oral premalignant lesions/cervical cancer (http://www.bcm95.com). In another study, curcumin bioconjugates containing glycine, alanine, and/or piperic acid were found to show improved antimicrobial properties over curcumin, suggesting increased cellular uptake or reduced metabolism of these bioconjugates resulting in increased concentration inside the infected cells (*180*).

Another strategy to improve the biological activity of curcumin was to chelate it with metals. The presence of two phenolic groups and one active methylene group in a curcumin molecule makes it an excellent ligand for any chelation. Several metal chelates of curcumin are reported to possess biological activity over that of free curcumin. John et al. studied the antitumor activities of curcumin, piperonylcurcumin, 2-hydroxynaphthylcurcumin, cinnamylcurcumin, and their copper complexes. Copper complexes of curcumin and its derivatives were found to be better antitumor agents than the parent compounds (*181*). Studies by Sui et al. showed that the modest activity of curcumin as an *in vitro* inhibitor of HIV-1and HIV-2 proteases is enhanced more than 10-fold when curcumin is complexed with boron. The curcumin-boron complexes were observed to lower the IC50 values significantly (*182*). Further, the curcumin-copper

complex was equally effective as curcumin against cadmium induced oxidative damage in mice (*183*). Similarly, it was demonstrated that curcumin-manganese complex exhibited a more potent neuroprotective activity than curcumin both *in* v*itro* and *in vivo* suggesting that this complex may be useful as a neuroprotective agent in the treatment of acute brain pathologies associated with NO-induced neurotoxicity and oxidative stress-induced neuronal damage such as epilepsy, stroke, and traumatic brain injury (*184-187*). A vanadyl-curcumin complex ($VO(cur)_2$) was reported to show a 2-fold increase in antirheumatic activity and a 4-fold increase in inhibiting smooth muscle cell proliferation as compared to free curcumin *in* v*itro*. Further, this complex was more effective as an anticancer agent, compared to uncomplexed curcumin (*188*). Both *in* v*itro* and *in* v*ivo* evaluations of a series of indium and gallium complexes of curcumin derivatives and curcumin have shown that the structural modification and/or complex formation of curcumin with metal ions may yield gallium and indium curcuminoids with potential therapeutic applications (*189*). Although many curcumin analogues are found to show improved biological activity over curcumin, specific evaluations of structural analogues and/or derivatives of curcumin to show improved tissue and plasma distribution are lacking. However, the promising biological effects over curcumin showed by structural modifications throws light into the possibility of modulating bioavailability of curcumin and much needs to be done to prove that the improved biological activity of structurally modified curcumin is due to its increased bioavailability.

4. RATIONALE FOR OUR RESEARCH

The chemical structure of curcumin bearing an α,β-diketone unit and two phenolic-OH groups plays a pivotal role in its biological activity. For example, isomerization has been proved to have an influence on antioxidant activity of curcumin (*189*). Thus, researchers hope to achieve improved biological activity of curcumin by structural modifications. Numerous studies dealing with the enhanced biological activity of curcumin derivatives and/or analogues can be found in a recent literature-review by Mosley et al. (*190*), for example, systematically describes several studies dealing with the biological activity relationships of curcumin and its derivatives. The terminal elimination half-life and plasma clearance values for *i.v.* administration of curcumin analog designated as EF-24 were reported to be 73.6 min and 0.482 L/min/ kg, respectively. Peak plasma concentrations of nearly 1000 nM were detected 3 min after the dose was given intraperitonially and the absorption and elimination half-life values were 177 and 219 min, respectively and the bioavailability of oral and i.p. EF-24 was 60% and 35%, respectively (*190*). A series of curcumin analogues including symmetrical 1,5-diarylpentadienone compounds whose aromatic rings possess two alkoxy substitutes were synthesized and screened for anticancer activity. New analogues that exhibit growth-suppressive activity 30 times that of curcumin and other commonly used anticancer drugs were identified in this study. Moreover, these analogues showed no *in vivo* toxicities (*191*). Although there has been considerable effort to synthesize curcumin derivatives, formulations, chelated conjugates etc. in order to make curcumin more water/plasma soluble, bioavailable and effective, the direct functionalization of curcumin moiety is very rare (*192*). The development of a synthetic methodology to produce curcumin

conjugates with water soluble polymers and targeting proteins can potentially enhance the therapeutic efficacy of curcumin. Higher molecular weight plant polyphenols have been shown to possess amplified physiological properties such as antioxidant or anticancer properties compared to their low molecular weight analogs (*193*). The chemical synthesis of therapeutically relevant, well-defined high molecular weight polyphenols is very rare.

Hence, we plan to develop convenient routes to water soluble curcumin conjugates and polyvalent curcumin polymers via the synthesis of novel mono-functional curcumin derivatives in which one of the phenolic groups of curcumin has been chemically modified with reactive groups (azide, alkyne, carboxylic acid, amine, alcohol, NHS etc.) (**Scheme 2**). The synthesis of mono-functional curcumin derivatives affords two advantages: (a) The presence of at least one free phenolic group is necessary for the biological activity of many antioxidants like curcumin (*194*) (b) Bioconjugation and polymer modifications using mono-functional derivatives produce soluble conjugates in high yields whereas bi-functional derivatives would result in insoluble cross-linked products (*195*). There has been a recent report describing the multi-step synthesis of a mono-functional alkyl fluoride derivative of curcumin starting from a vanillin derivative (*165*), in contrast to the previous report, the approach we plan involves direct one/two step covalent modification of curcumin to produce reactive mono-functional derivatives. To the best of my knowledge this is the first study describing a general methodology for preparing reactive mono-functional curcumin derivatives; the unique carboxylic acid/azide/alkyne groups serve as covalent functional handles for modifying both synthetic polymers and proteins.

Scheme 1.2. Schematic representation of functionalization of curcumin.

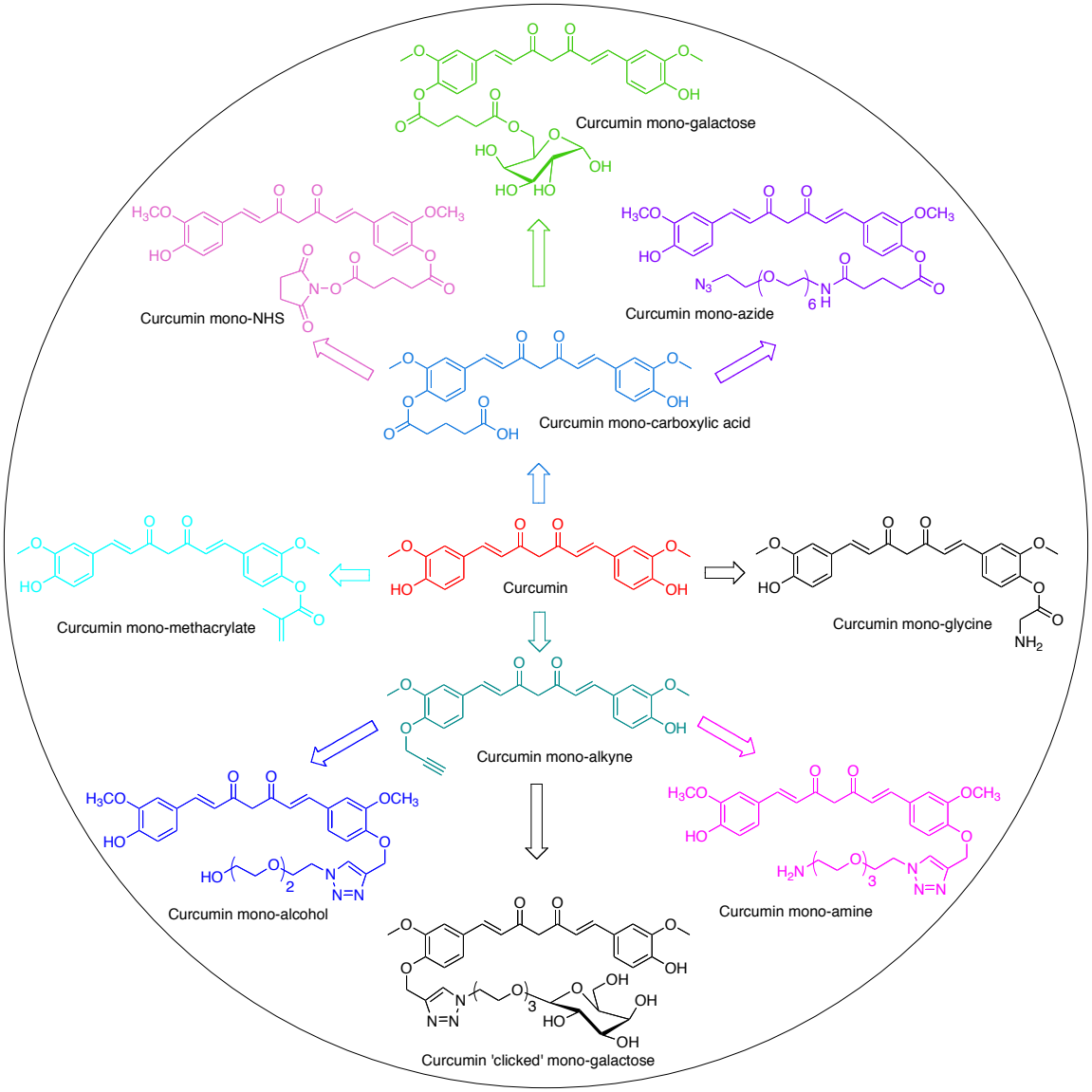

5. REFERENCES

(1) Jatzkewitz, H. (1954) The incorporation of a physiologically active substance in a colloid blood plasma substitute. I. Incorporation of a mescaline-peptide into poly(vinylpyrrolidinone) (PVP). *Physiologische Chemie 297*, 149-156.

(2) Jatzkewitz, H. (1955) A peptamine (glycyl-L-leucylmescaline) bound to a colloidal blood plasma substitute (polyvinylpyrrolidone) as a new type of depot for a biologically active primary amine (mescaline). *Zeitschrift fuer Naturforschung 10*, 27-31.

(3) Abuchowski, A., Van Es, T., Palczuk, N. C., and Davis, F. F. (1977) Alteration of immunological properties of bovine serum albumin by covalent attachment of polyethylene glycol. *Journal of Biological Chemistry 252*, 3578-3581.

(4) Abuchowski, A., McCoy, J. R., Palczuk, N. C., van Es, T., and Davis, F. F. (1977) Effect of covalent attachment of polyethylene glycol on immunogenicity and circulating life of bovine liver catalase. *J Biol Chem 252*, 3582-6.

(5) Maeda, H., Takeshita, J., and Kanamaru, R. (1979) A lipophilic derivative of neocarzinostatin. A polymer conjugation of an antitumor protein antibiotic. *Int J Pept Protein Res 14*, 81-7.

(6) Maeda, H., Ueda, M., Morinaga, T., and Matsumoto, T. (1985) Conjugation of poly(styrene-co-maleic acid) derivatives to the antitumor protein neocarzinostatin: pronounced improvements in pharmacological properties. *J Med Chem 28*, 455-61.

(7) Matsumura, Y., and Maeda, H. (1986) A new concept for macromolecular therapeutics in cancer chemotherapy: mechanism of tumoritropic accumulation of proteins and the antitumor agent smancs. *Cancer Res 46*, 6387-92.

(8) Spach, G. R., Leonard; Loucheux, Marie H.; Parrod, Jacques. (1969) Synthesis of block copolymers in which one block is a polypeptide. *Journal of Polymer Science, Polymer Symposia 16*, 4705-4712.

(9) Reibel, L., Spach, G., and Dufour, C. (1973) Physicochemical study of trisequence copolymers, poly(gamma-benzyl-L-glutamate)-poly(ethylene oxide)-poly(gamma-benzyl-L-glutamate). Role of polydispersity in the determination of conformation of the molecules in dilute solution. *Biopolymers 12*, 2391-2408.

(10) Perly, B., Douy, A., and Gallot, B. (1974) Synthesis of the polybutadiene-poly(benzyl-L-glutamate) sequential copolymers and structural study of their mesophases. *Comptes Rendus des Seances de l'Academie des Sciences, Serie C: Sciences Chimiques 279*, 1109-1111.

(11) Perly, B., Douy, A., and Gallot, B. (1976) Block copolymers polybutadiene/poly(benzyl-L-glutamate) and polybutadiene/poly(N5-hydroxypropylglutamine). Preparation and structural study by x-ray and electron microscopy. *Makromolekulare Chemie 177*, 2569-2589.

(12) Yamashita, Y., Iwaya, Y., and Ito, K. (1975) Block copolymerization. 9. Polymerization of the NCA [N-carboxy anhydride] of methyl D-glutamate by telechelic polystyrene having glycyl groups as active chain ends. *Makromolekulare Chemie 176*, 1207-1216.

(13) Klok, H.-A. (2009) Peptide/Protein-Synthetic Polymer Conjugates: Quo Vadis. *Macromolecules 42*, 7990-8000.

(14) Deming, T. J. (1997) Polypeptide materials. New synthetic methods and applications. *Advanced Materials 9*, 299-311.

(15) Deming, T. J. (2000) Living polymerization of α-amino acid-N-carboxyanhydrides. *Journal of Polymer Science, Part A: Polymer Chemistry 38*, 3011-3018.

(16) Deming, T. J. (2006) Polypeptide and polypeptide hybrid copolymer synthesis via NCA polymerization. *Advances in Polymer Science 202*, 1-18.

(17) Kricheldorf, H. R. (2006) Polypeptides and 100 years of chemistry of α-amino acid N-carboxyanhydrides. *Angewandte Chemie, International Edition 45*, 5752-5784.

(18) Agut, W., Taton, D., and Lecommandoux, S. (2007) A Versatile Synthetic Approach to Polypeptide Based Rod-Coil Block Copolymers by Click Chemistry. *Macromolecules 40*, 5653-5661.

(19) Schatz, C., Louguet, S., Le Meins, J.-F., and Lecommandoux, S. (2009) Polysaccharide-block-polypeptide copolymer vesicles: towards synthetic viral capsids. *Angewandte Chemie, International Edition 48*, 2572-2575.

(20) Wang, K., Liang, L., Lin, S., and He, X. (2008) Synthesis of well-defined ABC triblock copolymers with polypeptide segments by ATRP and click reactions. *European Polymer Journal 44*, 3370-3376.

(21) Steig, S., Cornelius, F., Witte, P., Staal, B. B. P., Koning, C. E., Heise, A., and Menzel, H. (2005) Synthesis of polypeptide based rod-coil block copolymers. *Chemical Communications 43*, 5420-5422.

(22) Steig, S., Cornelius, F., Heise, A., Knoop, R. J. I., Habraken, G. J. M., Koning, C. E., and Menzel, H. (2007) Synthesis of rod-coil block copolymers using two controlled polymerization techniques. *Macromolecular Symposia 248*, 199-206.

(23) Knoop, R. J. I., Habraken, G. J. M., Gogibus, N., Steig, S., Menzel, H., Koning, C. E., and Heise, A. (2008) Synthesis of poly(benzyl glutamate-b-styrene) rod-coil block copolymers by dual initiation in one pot. *Journal of Polymer Science, Part A: Polymer Chemistry 46*, 3068-3077.

(24) Deming, T. J. (1997) Facile synthesis of block copolypeptides of defined architecture. *Nature 390*, 368-389.

(25) Deming, T. J. (1999) Cobalt and Iron Initiators for the Controlled Polymerization of α-Amino Acid-N-Carboxyanhydrides. *Macromolecules 32*, 4500-4502.

(26) Peng, Y.-L., Lai, S.-L., and Lin, C.-C. (2008) Preparation of Polypeptide via Living Polymerization of Z-Lys-NCA Initiated by Platinum Complexes. *Macromolecules 41*, 3455-3459.

(27) Fields, G. B., and Noble, R. L. (1990) Solid-phase peptide synthesis utilizing 9-fluorenylmethoxycarbonyl amino acids. *International Journal of Peptide & Protein Research 35*, 161-214.

(28) Chan, W. C., and White, P. D. (2000) *Fmoc Solid Phase Peptide Synthesis - A Practical Approach.*, Oxford University Press, New York.

(29) Gauthier, M. A., and Klok, H.-A. (2008) Peptide/protein-polymer conjugates: synthetic strategies and design concepts. *Chemical Communications 23*, 2591-2611.

(30) Parrish, B., Breitenkamp, R. B., and Emrick, T. (2005) PEG- and peptide-grafted aliphatic polyesters by click chemistry. *J Am Chem Soc 127*, 7404-10.

(31) Dirks, A. J., Van Berkel, S. S., Hatzakis, N. S., Opsteen, J. A., Van Delft, F. L., Cornelissen, J. J. L. M., Rowan, A. E., Van Hest, J. C. M., Rutjes, F. P. J. T., and Nolte, R. J. M. (2005) Preparation of biohybrid amphiphiles via the copper catalyzed Huisgen [3+2] dipolar cycloaddition reaction. *Chemical Communications 33*, 4172-4174.

(32) Lutz, J.-F., Boerner, H. G., and Weichenhan, K. (2006) Combining ATRP and "Click" Chemistry: a Promising Platform toward Functional Biocompatible Polymers and Polymer Bioconjugates. *Macromolecules 39*, 6376-6383.

(33) Lutz, J.-F., Boerner, H. G., and Weichenhan, K. (2007) Click Bioconjugation of a Well-Defined Synthetic Polymer and a Protein Transduction Domain. *Australian Journal of Chemistry 60*, 410-413.

(34) Shi, W., Dolai, S., Averick, S., Fernando, S. S., Saltos, J. A., L'Amoreaux, W., Banerjee, P., and Raja, K. (2009) A General Methodology Toward Drug/Dye Incorporated Living Copolymer-Protein Hybrids: (NIRF Dye-Glucose) Copolymer-Avidin/BSA Conjugates as Prototypes. *Bioconjug Chem*.

(35) Rosler, A., Klok, H. A., Hamley, I. W., Castelletto, V., and Mykhaylyk, O. O. (2003) Nanoscale structure of poly(ethylene glycol) hybrid block copolymers

containing amphiphilic beta-strand peptide sequences. *Biomacromolecules 4*, 859-63.

(36) Hentschel, J., Krause, E., and Borner, H. G. (2006) Switch-peptides to trigger the peptide guided assembly of poly(ethylene oxide)-peptide conjugates into tape structures. *J Am Chem Soc 128*, 7722-3.

(37) Burkoth, T. S., Benzinger, T. L. S., Jones, D. N. M., Hallenga, K., Meredith, S. C., and Lynn, D. G. (1998) C-Terminal PEG blocks the irreversible step in β-amyloid(10-35) fibrillogenesis. *Journal of the American Chemical Society 120*, 7655-7656.

(38) Burkoth, T. S., Benzinger, T. L. S., Urban, V., Lynn, D. G., Meredith, S. C., and Thiyagarajan, P. (1999) Self-Assembly of Aβ(10-35)-PEG Block Copolymer Fibrils. *Journal of the American Chemical Society 121*, 7429-7430.

(39) Becker, M. L., Liu, J., and Wooley, K. L. (2003) Peptide-polymer bioconjugates: hybrid block copolymers generated via living radical polymerizations from resin-supported peptides. *Chemical Communications 2*, 180-181.

(40) Mei, Y., Beers, K. L., Byrd, H. C., VanderHart, D. L., and Washburn, N. R. (2004) Solid-phase ATRP synthesis of peptide-polymer hybrids. *J Am Chem Soc 126*, 3472-6.

(41) Becker, M. L., Liu, J., and Wooley, K. L. (2005) Functionalized micellar assemblies prepared via block copolymers synthesized by living free radical polymerization upon peptide-loaded resins. *Biomacromolecules 6*, 220-8.

(42) Ding, H., Kopeckova, P., and Kopecek, J. (2007) Self-association properties of HPMA copolymers containing an amphipathic heptapeptide. *J Drug Target 15*, 465-74.

(43) Kasuya, Y., Lu, Z. R., Kopeckova, P., Minko, T., Tabibi, S. E., and Kopecek, J. (2001) Synthesis and characterization of HPMA copolymer-aminopropylgeldanamycin conjugates. *J Control Release 74*, 203-11.

(44) Maynard, H. D., Okada, S. Y., and Grubbs, R. H. (2000) Synthesis of Norbornenyl Polymers with Bioactive Oligopeptides by Ring-Opening Metathesis Polymerization. *Macromolecules 33*, 6239-6248.

(45) Breitenkamp, R. B., Ou, Z., Breitenkamp, K., Muthukumar, M., and Emrick, T. (2007) Synthesis and Characterization of Polyolefin-graft-oligopeptide Polyelectrolytes. *Macromolecules 40*, 7617-7624.

(46) Biagini, S. C. G., and Parry, A. L. (2007) Investigation into the ROMP copolymerization of peptide- and PEG-functionalized norbornene derivatives. *Journal of Polymer Science, Part A: Polymer Chemistry 45*, 3178-3190.

(47) Fernandez-Trillo, F., Dureault, A., Bayley, J. P. M., van Hest, J. C. M., Thies, J. C., Michon, T., Weberskirch, R., and Cameron, N. R. (2007) Elastin-Based Side-Chain Polymers: Improved Synthesis via RAFT and Stimulus Responsive Behavior. *Macromolecules 40*, 6094-6099.

(48) Ayres, L., Vos, M. R. J., Adams, P. J. H. M., Shklyarevskiy, I. O., and Van Hest, J. C. M. (2003) Elastin-Based Side-Chain Polymers Synthesized by ATRP. *Macromolecules 36*, 5967-5973.

(49) van Hest, J. C. M., and Tirrell, D. A. (2001) Protein-based materials, toward a new level of structural control. *Chemical Communications 19*, 1897-1904.

(50) Bailon, P., and Won, C.-Y. (2009) PEG-modified biopharmaceuticals. *Expert Opinion on Drug Delivery 6*, 1-16.

(51) Roberts, M. J., Bentley, M. D., and Harris, J. M. (2002) Chemistry for peptide and protein PEGylation. *Adv Drug Deliv Rev 54*, 459-76.

(52) Osada, K., and Kataoka, K. (2002) Drug and gene delivery based on supramolecular assembly of PEG-polypeptide hybrid block copolymers. *Advances in Polymer Science 202*, 113-153.

(53) Yokoyama, M., Kwon, G. S., Okano, T., Sakurai, Y., Seto, T., and Kataoka, K. (1992) Preparation of micelle-forming polymer-drug conjugates. *Bioconjugate Chemistry 3*, 295-301.

(54) Mitra, A., Nan, A., Papadimitriou, J. C., Ghandehari, H., and Line, B. R. (2006) Polymer-peptide conjugates for angiogenesis targeted tumor radiotherapy. *Nucl Med Biol 33*, 43-52.

(55) Rothenfluh, D. A., Bermudez, H., O'Neil, C. P., and Hubbell, J. A. (2008) Biofunctional polymer nanoparticles for intra-articular targeting and retention in cartilage. *Nat Mater 7*, 248-54.

(56) Lee, H., Jeong, J. H., and Park, T. G. (2001) A new gene delivery formulation of polyethylenimine/DNA complexes coated with PEG conjugated fusogenic peptide. *J Control Release 76*, 183-92.

(57) Kwon, E. J., Bergen, J. M., and Pun, S. H. (2008) Application of an HIV gp41-derived peptide for enhanced intracellular trafficking of synthetic gene and siRNA delivery vehicles. *Bioconjug Chem 19*, 920-7.

(58) Rathore, O., and Sogah, D. Y. (2001) Nanostructure Formation through β-Sheet Self-Assembly in Silk-Based Materials. *Macromolecules 34*, 1477-1486.

(59) Rathore, O., and Sogah, D. Y. (2001) Self-assembly of beta-sheets into nanostructures by poly(alanine) segments incorporated in multiblock copolymers inspired by spider silk. *J Am Chem Soc 123*, 5231-9.

(60) Hentschel, J., and Borner, H. G. (2009) Blendable peptide-polymer nanofibers to modulate mechanical properties of polymers. *Macromol Biosci 9*, 187-94.

(61) Wang, C., Stewart, R. J., and Kopecek, J. (1999) Hybrid hydrogels assembled from synthetic polymers and coiled-coil protein domains. *Nature 397*, 417-20.

(62) Yang, J., Xu, C., Kopeckova, P., and Kopecek, J. (2006) Hybrid hydrogels self-assembled from HPMA copolymers containing peptide grafts. *Macromol Biosci 6*, 201-9.

(63) Yang, J., Xu, C., Wang, C., and Kopecek, J. (2006) Refolding Hydrogels Self-Assembled from N-(2-Hydroxypropyl)methacrylamide Graft . *Biomacromolecules 7*, 1187-1195.

(64) Wu, K., Yang, J., Konak, C., Kopeckova, P., and Kopecek, J. (2008) Novel synthesis of HPMA copolymers containing peptide grafts and their self-assembly into hybrid hydrogels. *Macromolecular Chemistry and Physics 209*, 467-475.

(65) Jing, P., Rudra, J. S., Herr, A. B., and Collier, J. H. (2008) Self-assembling peptide-polymer hydrogels designed from the coiled coil region of fibrin. *Biomacromolecules 9*, 2438-46.

(66) Tzokova, N., Fernyhough, C. M., Topham, P. D., Sandon, N., Adams, D. J., Butler, M. F., Armes, S. P., and Ryan, A. J. (2009) Soft hydrogels from nanotubes of poly(ethylene oxide)-tetraphenylalanine conjugates prepared by click chemistry. *Langmuir 25*, 2479-85.

(67) Lutolf, M. P., Raeber, G. P., Zisch, A. H., Tirelli, N., and Hubbell, J. A. (2003) Cell-responsive synthetic hydrogels. *Advanced Materials 15*, 888-892.

(68) Lutolf, M. P., Weber, F. E., Schmoekel, H. G., Schense, J. C., Kohler, T., Muller, R., and Hubbell, J. A. (2003) Repair of bone defects using synthetic mimetics of collagenous extracellular matrices. *Nat Biotechnol 21*, 513-8.

(69) Wang, C., Kopecek, J., and Stewart, R. J. (2001) Hybrid hydrogels cross-linked by genetically engineered coiled-coil block proteins. *Biomacromolecules 2*, 912-20.

(70) Rizzi, S. C., and Hubbell, J. A. (2005) Recombinant protein-co-PEG networks as cell-adhesive and proteolytically degradable hydrogel matrixes. Part I: Development and physicochemical characteristics. *Biomacromolecules 6*, 1226-38.

(71) Rizzi, S. C., Ehrbar, M., Halstenberg, S., Raeber, G. P., Schmoekel, H. G., Hagenmuller, H., Muller, R., Weber, F. E., and Hubbell, J. A. (2006) Recombinant protein-co-PEG networks as cell-adhesive and proteolytically

degradable hydrogel matrixes. Part II: biofunctional characteristics. *Biomacromolecules 7*, 3019-29.

(72) Murphy, W. L., Dillmore, W. S., Modica, J., and Mrksich, M. (2007) Dynamic hydrogels: translating a protein conformational change into macroscopic motion. *Angew Chem Int Ed Engl 46*, 3066-9.

(73) Sui, Z., King, W. J., and Murphy, W. L. (2007) Dynamic materials based on a protein conformational change. *Advanced Materials 19*, 3377-3380.

(74) Sui, Z., King, W. J., and Murphy, W. L. (2008) Protein-based hydrogels with tunable dynamic responses. *Advanced Functional Materials 18*, 1824-1831.

(75) Yuan, W., Yang, J., Kopeckova, P., and Kopecek, J. (2008) Smart hydrogels containing adenylate kinase: translating substrate recognition into macroscopic motion. *J Am Chem Soc 130*, 15760-1.

(76) Kasparova, P., Antonietti, M., and Coelfen, H. (2004) Double hydrophilic block copolymers with switchable secondary structure as additives for crystallization control. *Colloids and Surfaces, A: Physicochemical and Engineering Aspects 250*, 153-162.

(77) Guo, X.-H., Yu, S.-H., and Cai, G.-B. (2006) Crystallization in a mixture of solvents by using a crystal modifier: morphology control in the synthesis of highly monodisperse CaCO3 microspheres. *Angewandte Chemie, International Edition 45*, 3977-3981.

(78) Guo, X.-H., Xu, A.-W., and Yu, S.-H. (2008) Crystallization of Calcium Carbonate Mineral with Hierarchical Structures in DMF Solution under Control of Poly(ethylene glycol)-b-poly(L-glutamic acid): Effects of Crystallization

Temperature and Polymer Concentration. *Crystal Growth & Design 8*, 1233-1242.

(79) Kessel, S., and Boerner, H. G. (2008) High rate silicification of peptide-polymer assemblies toward composite nanotapes. *Macromolecular Rapid Communications 29*, 419-424.

(80) Chen, G., and Hoffman, A. S. (1993) Preparation and properties of thermoreversible, phase-separating enzyme-oligo(N-isopropylacrylamide) conjugates. *Bioconjug Chem 4*, 509-14.

(81) Stayton, P. S., Shimoboji, T., Long, C., Chilkoti, A., Chen, G., Harris, J. M., and Hoffman, A. S. (1995) Control of protein-ligand recognition using a stimuli-responsive polymer. *Nature 378*, 472-4.

(82) Pennadam, S. S., Lavigne, M. D., Dutta, C. F., Firman, K., Mernagh, D., Gorecki, D. C., and Alexander, C. (2004) Control of a multisubunit DNA motor by a thermoresponsive polymer switch. *J Am Chem Soc 126*, 13208-9.

(83) De, P., Li, M., Gondi, S. R., and Sumerlin, B. S. (2008) Temperature-regulated activity of responsive polymer-protein conjugates prepared by grafting-from via RAFT polymerization. *J Am Chem Soc 130*, 11288-9.

(84) Raja, K. S., Wang, Q., Gonzalez, M. J., Manchester, M., Johnson, J. E., and Finn, M. G. (2003) Hybrid virus-polymer materials. 1. Synthesis and properties of PEG-decorated cowpea mosaic virus. *Biomacromolecules 4*, 472-6.

(85) Cheng, X., Ming, X., and Croyle, M. A. (2003) PEGylated adenoviruses for gene delivery to the intestinal epithelium by the oral route. *Pharm Res 20*, 1444-51.

(86) Ogawara, K., Rots, M. G., Kok, R. J., Moorlag, H. E., Van Loenen, A. M., Meijer, D. K., Haisma, H. J., and Molema, G. (2004) A novel strategy to modify adenovirus tropism and enhance transgene delivery to activated vascular endothelial cells in vitro and in vivo. *Hum Gene Ther 15*, 433-43.

(87) Fisher, K. D., Stallwood, Y., Green, N. K., Ulbrich, K., Mautner, V., and Seymour, L. W. (2001) Polymer-coated adenovirus permits efficient retargeting and evades neutralising antibodies. *Gene Ther 8*, 341-8.

(88) Green, N. K., Herbert, C. W., Hale, S. J., Hale, A. B., Mautner, V., Harkins, R., Hermiston, T., Ulbrich, K., Fisher, K. D., and Seymour, L. W. (2004) Extended plasma circulation time and decreased toxicity of polymer-coated adenovirus. *Gene Ther 11*, 1256-63.

(89) Kochendoerfer, G. G. (2005) Site-specific polymer modification of therapeutic proteins. *Curr Opin Chem Biol 9*, 555-60.

(90) Gaberc-Porekar, V., Zore, I., Podobnik, B., and Menart, V. (2008) Obstacles and pitfalls in the PEGylation of therapeutic proteins. *Curr Opin Drug Discov Devel 11*, 242-50.

(91) Filpula, D., and Zhao, H. (2008) Releasable PEGylation of proteins with customized linkers. *Adv Drug Deliv Rev 60*, 29-49.

(92) Shechter, Y., Mironchik, M., Rubinraut, S., Tsubery, H., Sasson, K., Marcus, Y., and Fridkin, M. (2008) Reversible pegylation of insulin facilitates its prolonged action in vivo. *Eur J Pharm Biopharm 70*, 19-28.

(93) Duncan, R., Gilbert, H. R., Carbajo, R. J., and Vicent, M. J. (2008) Polymer masked-unmasked protein therapy. 1. Bioresponsive dextrin-trypsin and -

melanocyte stimulating hormone conjugates designed for alpha-amylase activation. *Biomacromolecules 9*, 1146-54.

(94) M. G. Savage (1992) *Avidin-Biotin Chemistry: A Handbook*, *Pierce Chemical company*, *Rockford, Illinois*.

(95) Daehne, S., Resch-Genger, U., and Wolfbeis, O. S. (1998) *Near-Infrared Dyes for High Technology Applications*, Vol. 52, Kluwer Academic, Dordrecht.

(96) Michalet, X., Pinaud, F. F., Bentolila, L. A., Tsay, J. M., Doose, S., Li, J. J., Sundaresan, G., Wu, A. M., Gambhir, S. S., and Weiss, S. (2005) Quantum dots for live cells, in vivo imaging, and diagnostics. *Science 307*, 538-44.

(97) Dubertret, B., Skourides, P., Norris, D. J., Noireaux, V., Brivanlou, A. H., and Libchaber, A. (2002) In vivo imaging of quantum dots encapsulated in phospholipid micelles. *Science 298*, 1759-62.

(98) So, M. K., Xu, C., Loening, A. M., Gambhir, S. S., and Rao, J. (2006) Self-illuminating quantum dot conjugates for in vivo imaging. *Nat Biotechnol 24*, 339-43.

(99) Ballou, B., Lagerholm, B. C., Ernst, L. A., Bruchez, M. P., and Waggoner, A. S. (2004) Noninvasive imaging of quantum dots in mice. *Bioconjug Chem 15*, 79-86.

(100) Bhaumik, S., and Gambhir, S. S. (2002) Optical imaging of Renilla luciferase reporter gene expression in living mice. *Proc Natl Acad Sci U S A 99*, 377-82.

(101) Contag, C. H., and Bachmann, M. H. (2002) Advances in in vivo bioluminescence imaging of gene expression. *Annu Rev Biomed Eng 4*, 235-60.

(102) Cheng, Z., Levi, J., Xiong, Z., Gheysens, O., Keren, S., Chen, X., and Gambhir, S. S. (2006) Near-infrared fluorescent deoxyglucose analogue for tumor optical imaging in cell culture and living mice. *Bioconjug Chem 17*, 662-9.

(103) Weissleder, R., Tung, C. H., Mahmood, U., and Bogdanov, A., Jr. (1999) In vivo imaging of tumors with protease-activated near-infrared fluorescent probes. *Nat Biotechnol 17*, 375-8.

(104) Becker, A., Hessenius, C., Licha, K., Ebert, B., Sukowski, U., Semmler, W., Wiedenmann, B., and Grotzinger, C. (2001) Receptor-targeted optical imaging of tumors with near-infrared fluorescent ligands. *Nat Biotechnol 19*, 327-31.

(105) Hilderbrand, S. A., Kelly, K. A., Weissleder, R., and Tung, C. H. (2005) Monofunctional near-infrared fluorochromes for imaging applications. *Bioconjug Chem 16*, 1275-81.

(106) Lin, Y., Weissleder, R., and Tung, C. H. (2002) Novel near-infrared cyanine fluorochromes: synthesis, properties, and bioconjugation. *Bioconjug Chem 13*, 605-10.

(107) Mader, O., Reiner, K., Egelhaaf, H. J., Fischer, R., and Brock, R. (2004) Structure property analysis of pentamethine indocyanine dyes: identification of a new dye for life science applications. *Bioconjug Chem 15*, 70-8.

(108) Zhao, W., and Carreira, E. M. (2006) Conformationally restricted aza-BODIPY: highly fluorescent, stable near-infrared absorbing dyes. *Chemistry- A European Journal 12*, 7254-63.

(109) Liu, J., Diwu, Z., Leung, W.-Y., Lu, Y., Patch, B., and Haugland, R. P. (2003) Rational design and synthesis of a novel class of highly fluorescent rhodamine

dyes that have strong absorption at long wavelengths. *Tetrahedron Letters 44*, 4355-4359.

(110) Bandichhor, R., Petrescu, A. D., Vespa, A., Kier, A. B., Schroeder, F., and Burgess, K. (2006) Synthesis of a new water-soluble rhodamine derivative and application to protein labeling and intracellular imaging. *Bioconjug Chem 17*, 1219-25.

(111) Jose, J., and Burgess, K. (2006) Benzophenoxazine-based fluorescent dyes for labeling biomolecules. *Tetrahedron Letters 62*, 11021-11037.

(112) Patonay, G., Salon, J., Sowell, J., and Strekowski, L. (2004) Noncovalent labeling of biomolecules with red and near- infrared dyes. *Molecules 9*, 40-9.

(113) Tung, C. H. (2004) Fluorescent peptide probes for in vivo diagnostic imaging. *Biopolymers 76*, 391-403.

(114) Zaheer, A., Lenkinski, R. E., Mahmood, A., Jones, A. G., Cantley, L. C., and Frangioni, J. V. (2001) In vivo near-infrared fluorescence imaging of osteoblastic activity. *Nat Biotechnol 19*, 1148-54.

(115) Anand, P., Kunnumakkara, A. B., Newman, R. A., and Aggarwal, B. B. (2007) Bioavailability of curcumin: problems and promises. *Mol Pharm 4*, 807-18.

(116) Chattopadhyay, I., Biswas, K., Bandyopadhyay, U., and Banerjee, R. K. (2004) Turmeric and curcumin: Biological actions and medicinal applications. *Current Science 87*, 44-53.

(117) Aggarwal, B. B., Kumar, A., and Bharti, A. C. (2003) Anticancer potential of curcumin: preclinical and clinical studies. *Anticancer Res 23*, 363-98.

(118) Sharma, O. P. (1976) Antioxidant activity of curcumin and related compounds. *Biochem Pharmacol 25*, 1811-2.

(119) Ruby, A. J., Kuttan, G., Babu, K. D., Rajasekharan, K. N., and Kuttan, R. (1995) Anti-tumour and antioxidant activity of natural curcuminoids. *Cancer Lett 94*, 79-83.

(120) Sugiyama, Y., Kawakishi, S., and Osawa, T. (1996) Involvement of the beta-diketone moiety in the antioxidative mechanism of tetrahydrocurcumin. *Biochem Pharmacol 52*, 519-25.

(121) Srimal, R. C., and Dhawan, B. N. (1973) Pharmacology of diferuloyl methane (curcumin), a non-steroidal anti-inflammatory agent. *J Pharm Pharmacol 25*, 447-52.

(122) Jordan, W. C., and Drew, C. R. (1996) Curcumin--a natural herb with anti-HIV activity. *J Natl Med Assoc 88*, 333.

(123) Mahady, G. B., Pendland, S. L., Yun, G., and Lu, Z. Z. (2002) Turmeric (Curcuma longa) and curcumin inhibit the growth of Helicobacter pylori, a group 1 carcinogen. *Anticancer Res 22*, 4179-81.

(124) Kim, M. K., Choi, G. J., and Lee, H. S. (2003) Fungicidal property of Curcuma longa L. rhizome-derived curcumin against phytopathogenic fungi in a greenhouse. *J Agric Food Chem 51*, 1578-81.

(125) Reddy, R. C., Vatsala, P. G., Keshamouni, V. G., Padmanaban, G., and Rangarajan, P. N. (2005) Curcumin for malaria therapy. *Biochem Biophys Res Commun 326*, 472-4.

(126) Kuttan, R., Bhanumathy, P., Nirmala, K., and George, M. C. (1985) Potential anticancer activity of turmeric (Curcuma longa). *Cancer Lett 29*, 197-202.

(127) Kiso, Y., Suzuki, Y., Watanabe, N., Oshima, Y., and Hikino, H. (1983) Antihepatotoxic principles of Curcuma longa rhizomes. *Planta Med 49*, 185-7.

(128) Venkatesan, N. (1998) Curcumin attenuation of acute adriamycin myocardial toxicity in rats. *Br J Pharmacol 124*, 425-7.

(129) Venkatesan, N., Punithavathi, D., and Arumugam, V. (2000) Curcumin prevents adriamycin nephrotoxicity in rats. *Br J Pharmacol 129*, 231-4.

(130) Srivastava, R., Dikshit, M., Srimal, R. C., and Dhawan, B. N. (1985) Anti-thrombotic effect of curcumin. *Thromb Res 40*, 413-7.

(131) Dikshit, M., Rastogi, L., Shukla, R., and Srimal, R. C. (1995) Prevention ofischaemia-induced biochemical changes by curcumin & quinidine in the cat heart. *Indian J. Med. Res. 101*, 31-35.

(132) Nirmala, C., and Puvanakrishnan, R. (1996) Protective role of curcumin against isoproterenol induced myocardial infarction in rats. *Mol Cell Biochem 159*, 85-93.

(133) Nirmala, C., and Puvanakrishnan, R. (1996) Effect of curcumin on certain lysosomal hydrolases in isoproterenol-induced myocardial infarction in rats. *Biochem Pharmacol 51*, 47-51.

(134) Srinivasan, M. (1972) Effect of curcumin on blood sugar as seen in a diabetic subject. *Indian J. Med. Sci. 26*, 269-270.

(135) Babu, P. S., and Srinivasan, K. (1995) Influence of dietary curcumin and cholesterol on the progression of experimentally induced diabetes in albino rat. *Mol Cell Biochem 152*, 13-21.

(136) Babu, P. S., and Srinivasan, K. (1997) Hypolipidemic action of curcumin, the active principle of turmeric (Curcuma longa) in streptozotocin induced diabetic rats. *Mol Cell Biochem 166*, 169-75.

(137) Arun, N., and Nalini, N. (2002) Efficacy of turmeric on blood sugar and polyol pathway in diabetic albino rats. *Plant Foods Hum Nutr 57*, 41-52.

(138) Deodhar, S. D., Sethi, R., and Srimal, R. C. (1980) Preliminary study on antirheumatic activity of curcumin (diferuloyl methane). *Indian J Med Res 71*, 632-4.

(139) Shankar, T. N., Shantha, N. V., Ramesh, H. P., Murthy, I. A., and Murthy, V. S. (1980) Toxicity studies on turmeric (Curcuma longa): acute toxicity studies in rats, guineapigs & monkeys. *Indian J Exp Biol 18*, 73-5.

(140) Qureshi, S., Shah, A. H., and Ageel, A. M. (1992) Toxicity studies on Alpinia galanga and Curcuma longa. *Planta Med 58*, 124-7.

(141) Lao, C. D., Demierre, M. F., and Sondak, V. K. (2006) Targeting events in melanoma carcinogenesis for the prevention of melanoma. *Expert Rev Anticancer Ther 6*, 1559-68.

(142) Lao, C. D., Ruffin, M. T. t., Normolle, D., Heath, D. D., Murray, S. I., Bailey, J. M., Boggs, M. E., Crowell, J., Rock, C. L., and Brenner, D. E. (2006) Dose escalation of a curcuminoid formulation. *BMC Complement Altern Med 6*, 10.

(143) Cheng, A. L., Hsu, C. H., Lin, J. K., Hsu, M. M., Ho, Y. F., Shen, T. S., Ko, J. Y., Lin, J. T., Lin, B. R., Ming-Shiang, W., Yu, H. S., Jee, S. H., Chen, G. S., Chen, T. M., Chen, C. A., Lai, M. K., Pu, Y. S., Pan, M. H., Wang, Y. J., Tsai, C. C., and Hsieh, C. Y. (2001) Phase I clinical trial of curcumin, a chemopreventive

agent, in patients with high-risk or pre-malignant lesions. *Anticancer Res 21*, 2895-900.

(144) Shoba, G., Joy, D., Joseph, T., Majeed, M., Rajendran, R., and Srinivas, P. S. (1998) Influence of piperine on the pharmacokinetics of curcumin in animals and human volunteers. *Planta Med 64*, 353-6.

(145) Wahlstrom, B., and Blennow, G. (1978) A study on the fate of curcumin in the rat. *Acta Pharmacol Toxicol (Copenh) 43*, 86-92.

(146) Ravindranath, V., and Chandrasekhara, N. (1980) Absorption and tissue distribution of curcumin in rats. *Toxicology 16*, 259-65.

(147) Ravindranath, V., and Chandrasekhara, N. (1981) Metabolism of curcumin--studies with [3H]curcumin. *Toxicology 22*, 337-44.

(148) Pan, M. H., Huang, T. M., and Lin, J. K. (1999) Biotransformation of curcumin through reduction and glucuronidation in mice. *Drug Metab Dispos 27*, 486-94.

(149) Perkins, S., Verschoyle, R. D., Hill, K., Parveen, I., Threadgill, M. D., Sharma, R. A., Williams, M. L., Steward, W. P., and Gescher, A. J. (2002) Chemopreventive efficacy and pharmacokinetics of curcumin in the min/+ mouse, a model of familial adenomatous polyposis. *Cancer Epidemiol Biomarkers Prev 11*, 535-40.

(150) Sharma, R. A., Euden, S. A., Platton, S. L., Cooke, D. N., Shafayat, A., Hewitt, H. R., Marczylo, T. H., Morgan, B., Hemingway, D., Plummer, S. M., Pirmohamed, M., Gescher, A. J., and Steward, W. P. (2004) Phase I clinical trial of oral curcumin: biomarkers of systemic activity and compliance. *Clin Cancer Res 10*, 6847-54.

(151) Yang, K. Y., Lin, L. C., Tseng, T. Y., Wang, S. C., and Tsai, T. H. (2007) Oral bioavailability of curcumin in rat and the herbal analysis from Curcuma longa by LC-MS/MS. *J Chromatogr B Analyt Technol Biomed Life Sci 853*, 183-9.

(152) Marczylo, T. H., Verschoyle, R. D., Cooke, D. N., Morazzoni, P., Steward, W. P., and Gescher, A. J. (2007) Comparison of systemic availability of curcumin with that of curcumin formulated with phosphatidylcholine. *Cancer Chemother Pharmacol 60*, 171-7.

(153) Holder, G. M., Plummer, J. L., and Ryan, A. J. (1978) The metabolism and excretion of curcumin (1,7-bis-(4-hydroxy-3-methoxyphenyl)-1,6-heptadiene-3,5-dione) in the rat. *Xenobiotica 8*, 761-8.

(154) Sharma, R. A., McLelland, H. R., Hill, K. A., Ireson, C. R., Euden, S. A., Manson, M. M., Pirmohamed, M., Marnett, L. J., Gescher, A. J., and Steward, W. P. (2001) Pharmacodynamic and pharmacokinetic study of oral Curcuma extract in patients with colorectal cancer. *Clin Cancer Res 7*, 1894-900.

(155) Garcea, G., Jones, D. J., Singh, R., Dennison, A. R., Farmer, P. B., Sharma, R. A., Steward, W. P., Gescher, A. J., and Berry, D. P. (2004) Detection of curcumin and its metabolites in hepatic tissue and portal blood of patients following oral administration. *Br J Cancer 90*, 1011-5.

(156) Hoehle, S. I., Pfeiffer, E., Solyom, A. M., and Metzler, M. (2006) Metabolism of curcuminoids in tissue slices and subcellular fractions from rat liver. *J Agric Food Chem 54*, 756-64.

(157) Ireson, C., Orr, S., Jones, D. J., Verschoyle, R., Lim, C. K., Luo, J. L., Howells, L., Plummer, S., Jukes, R., Williams, M., Steward, W. P., and Gescher, A. (2001)

Characterization of metabolites of the chemopreventive agent curcumin in human and rat hepatocytes and in the rat in vivo, and evaluation of their ability to inhibit phorbol ester-induced prostaglandin E2 production. *Cancer Res 61*, 1058-64.

(158) Sandur, S. K., Pandey, M. K., Sung, B., Ahn, K. S., Murakami, A., Sethi, G., Limtrakul, P., Badmaev, V., and Aggarwal, B. B. (2007) Curcumin, demethoxycurcumin, bisdemethoxycurcumin, tetrahydrocurcumin and turmerones differentially regulate anti-inflammatory and anti-proliferative responses through a ROS-independent mechanism. *Carcinogenesis 28*, 1765-73.

(159) Pfeiffer, E., Hoehle, S. I., Walch, S. G., Riess, A., Solyom, A. M., and Metzler, M. (2007) Curcuminoids form reactive glucuronides in vitro. *J Agric Food Chem 55*, 538-44.

(160) Kim, J. M., Araki, S., Kim, D. J., Park, C. B., Takasuka, N., Baba-Toriyama, H., Ota, T., Nir, Z., Khachik, F., Shimidzu, N., Tanaka, Y., Osawa, T., Uraji, T., Murakoshi, M., Nishino, H., and Tsuda, H. (1998) Chemopreventive effects of carotenoids and curcumins on mouse colon carcinogenesis after 1,2-dimethylhydrazine initiation. *Carcinogenesis 19*, 81-5.

(161) Okada, K., Wangpoengtrakul, C., Tanaka, T., Toyokuni, S., Uchida, K., and Osawa, T. (2001) Curcumin and especially tetrahydrocurcumin ameliorate oxidative stress-induced renal injury in mice. *J Nutr 131*, 2090-5.

(162) Naito, M., Wu, X., Nomura, H., Kodama, M., Kato, Y., and Osawa, T. (2002) The protective effects of tetrahydrocurcumin on oxidative stress in cholesterol-fed rabbits. *J Atheroscler Thromb 9*, 243-50.

(163) Pari, L., and Amali, D. R. (2005) Protective role of tetrahydrocurcumin (THC) an active principle of turmeric on chloroquine induced hepatotoxicity in rats. *J Pharm Pharm Sci 8*, 115-23.

(164) Murugan, P., and Pari, L. (2006) Effect of tetrahydrocurcumin on plasma antioxidants in streptozotocin-nicotinamide experimental diabetes. *J Basic Clin Physiol Pharmacol 17*, 231-44.

(165) Ryu, E. K., Choe, Y. S., Lee, K. H., Choi, Y., and Kim, B. T. (2006) Curcumin and dehydrozingerone derivatives: synthesis, radiolabeling, and evaluation for beta-amyloid plaque imaging. *J Med Chem 49*, 6111-9.

(166) Cruz-Correa, M., Shoskes, D. A., Sanchez, P., Zhao, R., Hylind, L. M., Wexner, S. D., and Giardiello, F. M. (2006) Combination treatment with curcumin and quercetin of adenomas in familial adenomatous polyposis. *Clin Gastroenterol Hepatol 4*, 1035-8.

(167) Verma, S. P., Salamone, E., and Goldin, B. (1997) Curcumin and genistein, plant natural products, show synergistic inhibitory effects on the growth of human breast cancer MCF-7 cells induced by estrogenic pesticides. *Biochem Biophys Res Commun 233*, 692-6.

(168) Fang, J. Y., Hung, C. F., Chiu, H. C., Wang, J. J., and Chan, T. F. (2003) Efficacy and irritancy of enhancers on the in-vitro and in-vivo percutaneous absorption of curcumin. *J Pharm Pharmacol 55*, 1175.

(169) Balasubramanian, S., and Eckert, R. L. (2004) Green tea polyphenol and curcumin inversely regulate human involucrin promoter activity via opposing

effects on CCAAT/enhancer-binding protein function. *J Biol Chem 279*, 24007-14.

(170) Bisht, S., Feldmann, G., Soni, S., Ravi, R., Karikar, C., and Maitra, A. (2007) Polymeric nanoparticle-encapsulated curcumin ("nanocurcumin"): a novel strategy for human cancer therapy. *J Nanobiotechnology 5*, 3.

(171) Tiyaboonchai, W., Tungpradit, W., and Plianbangchang, P. (2007) Formulation and characterization of curcuminoids loaded solid lipid nanoparticles. *Int J Pharm 337*, 299-306.

(172) Li, L., Ahmed, B., Mehta, K., and Kurzrock, R. (2007) Liposomal curcumin with and without oxaliplatin: effects on cell growth, apoptosis, and angiogenesis in colorectal cancer. *Mol Cancer Ther 6*, 1276-82.

(173) Kunwar, A., Barik, A., Pandey, R., and Priyadarsini, K. I. (2006) Transport of liposomal and albumin loaded curcumin to living cells: an absorption and fluorescence spectroscopic study. *Biochim Biophys Acta 1760*, 1513-20.

(174) Suresh, D., and Srinivasan, K. (2007) Studies on the in vitro absorption of spice principles--curcumin, capsaicin and piperine in rat intestines. *Food Chem Toxicol 45*, 1437-42.

(175) Ma, Z., Shayeganpour, A., Brocks, D. R., Lavasanifar, A., and Samuel, J. (2007) High-performance liquid chromatography analysis of curcumin in rat plasma: application to pharmacokinetics of polymeric micellar formulation of curcumin. *Biomed Chromatogr 21*, 546-52.

(176) Gatti, G., and Perucca, E. (1994) Plasma concentrations of free and conjugated silybin after oral intake of a silybin-phosphatidylcholine complex (silipide) in healthy volunteers. *Int J Clin Pharmacol Ther 32*, 614-7.

(177) Kimura, T., Takeda, K., Kageyu, A., Toda, M., Kurosaki, Y., and Nakayama, T. (1989) Intestinal absorption of dolichol from emulsions and liposomes in rats. *Chem Pharm Bull (Tokyo) 37*, 463-6.

(178) Liu, A., Lou, H., Zhao, L., and Fan, P. (2006) Validated LC/MS/MS assay for curcumin and tetrahydrocurcumin in rat plasma and application to pharmacokinetic study of phospholipid complex of curcumin. *J Pharm Biomed Anal 40*, 720-7.

(179) Letchford, K., Liggins, R., and Burt, H. (2008) Solubilization of hydrophobic drugs by methoxy poly(ethylene glycol)-block-polycaprolactone diblock copolymer micelles: theoretical and experimental data and correlations. *J Pharm Sci 97*, 1179-90.

(180) Mishra, S., Narain, U., Mishra, R., and Misra, K. (2005) Design, development and synthesis of mixed bioconjugates of piperic acid-glycine, curcumin-glycine/alanine and curcumin-glycine-piperic acid and their antibacterial and antifungal properties. *Bioorg Med Chem 13*, 1477-86.

(181) John, V. D., Kuttan, G., and Krishnankutty, K. (2002) Anti-tumour studies of metal chelates of synthetic curcuminoids. *J Exp Clin Cancer Res 21*, 219-24.

(182) Sui, Z., Salto, R., Li, J., Craik, C., and Ortiz de Montellano, P. R. (1993) Inhibition of the HIV-1 and HIV-2 proteases by curcumin and curcumin boron complexes. *Bioorg Med Chem 1*, 415-22.

(183) Eybl, V., Kotyzova, D., and Bludovska, M. (2004) The effect of curcumin on cadmium-induced oxidative damage and trace elements level in the liver of rats and mice. *Toxicol Lett 151*, 79-85.

(184) Vajragupta, O., Boonchoong, P., Watanabe, H., Tohda, M., Kummasud, N., and Sumanont, Y. (2003) Manganese complexes of curcumin and its derivatives: evaluation for the radical scavenging ability and neuroprotective activity. *Free Radic Biol Med 35*, 1632-44.

(185) Vajragupta, O., Boonchoong, P., and Berliner, L. J. (2004) Manganese complexes of curcumin analogues: evaluation of hydroxyl radical scavenging ability, superoxide dismutase activity and stability towards hydrolysis. *Free Radic Res 38*, 303-14.

(186) Eybl, V., Kotyzova, D., Leseticky, L., Bludovska, M., and Koutensky, J. (2006) The influence of curcumin and manganese complex of curcumin on cadmium-induced oxidative damage and trace elements status in tissues of mice. *J Appl Toxicol 26*, 207-12.

(187) Thompson, K. H., Bohmerle, K., Polishchuk, E., Martins, C., Toleikis, P., Tse, J., Yuen, V., McNeill, J. H., and Orvig, C. (2004) Complementary inhibition of synoviocyte, smooth muscle cell or mouse lymphoma cell proliferation by a vanadyl curcumin complex compared to curcumin alone. *J Inorg Biochem 98*, 2063-70.

(188) Mohammadi, K., Thompson, K. H., Patrick, B. O., Storr, T., Martins, C., Polishchuk, E., Yuen, V. G., McNeill, J. H., and Orvig, C. (2005) Synthesis and

characterization of dual function vanadyl, gallium and indium curcumin complexes for medicinal applications. *J Inorg Biochem 99*, 2217-25.

(189) Shen, L., and Ji, H. F. (2007) Theoretical study on physicochemical properties of curcumin. *Spectrochim Acta A Mol Biomol Spectrosc 67*, 619-23.

(190) Mosley, C. A., Liotta, D. C., and Snyder, J. P. (2007) Highly active anticancer curcumin analogues. *Adv Exp Med Biol 595*, 77-103.

(191) Ohori, H., Yamakoshi, H., Tomizawa, M., Shibuya, M., Kakudo, Y., Takahashi, A., Takahashi, S., Kato, S., Suzuki, T., Ishioka, C., Iwabuchi, Y., and Shibata, H. (2006) Synthesis and biological analysis of new curcumin analogues bearing an enhanced potential for the medicinal treatment of cancer. *Mol Cancer Ther 5*, 2563-71.

(192) Shi, W., Dolai, S., Rizk, S., Hussain, A., Tariq, H., Averick, S., L'Amoreaux, W., El ldrissi, A., Banerjee, P., and Raja, K. (2007) Synthesis of monofunctional curcumin derivatives, clicked curcumin dimer, and a PAMAM dendrimer curcumin conjugate for therapeutic applications. *Org Lett 9*, 5461-4.

(193) Ihara, N., Schmitz, S., Kurisawa, M., Chung, J. E., Uyama, H., and Kobayashi, S. (2004) Amplification of inhibitory activity of catechin against disease-related enzymes by conjugation on poly(epsilon-lysine). *Biomacromolecules 5*, 1633-6.

(194) Aggarwal, B. B., and Shishodia, S. (2006) Molecular targets of dietary agents for prevention and therapy of cancer. *Biochem Pharmacol 71*, 1397-421.

(195) Hermanson, G. T. (1996) *Bioconjugate Techniques*, Academic Press, San Diego, California.

CHAPTER II

Synthesis of Drug/Dye Incorporated Copolymers via Atom Transfer Radical Polymerization.

1. INTRODUCTION

Antibody molecules are important members in nearly every field of the life sciences as it encompasses a broad variety of applications like immunoassay, targeting, drug delivery and detection techniques. Ehrlich recognized the potential of antibodies as therapeutic agents in the early 20th century (*1*). Humanized monoclonal antibodies (mAbs) have been developed for the treatment of several diseases and for preclinical imaging applications (*2*). The mounting success of the antibody molecule as a therapeutic agent is based on the facts that (a) the antigen binding sites of the antibody permits with exquisite specificity and affinity and (b) a molecular mass of at least 150 kDa permits a circulatory half-life of up to 21 days. Upon binding to cell surface antigens, many mAbs are taken up by receptor-mediated endocytosis. Mylotarg,® the only FDA approved toxin conjugate is a recombinant humanized monoclonal antibody covalently linked with the anti-tumor drug calicheamicin and is used to treat acute myeloid leukemia (*3*). The current approach to convert humanized mAbs into drugs is to attempt to conjugate them to radionucleotides or cytotoxic drugs (*4*). Most initial antibody conjugate efforts involved radionucleotides; however, the procedure is costly and requires that drugs be generated immediately prior to use. Toxin conjugates are a challenging chemical problem; for e.g., many anticancer drugs like taxol are not water soluble. In addition, standard routes of chemical modification of antibodies involve modification at random sites on the mAb surface which can lead to deactivation of the active sites (*4*). This problem has been addressed to some extent by developing few site specific conjugation methods by reducing the inter-chain disulfides present in the antibodies or by introducing novel cysteine residues genetically (*4*). Using current technologies, the number of copies

of cytotoxic drugs/radionucleotides that can be chemically conjugated to an antibody is very limited. Extensive modification of antibodies with several copies of a cytotoxic molecule would cause chemical modification and deactivation of the antigen binding sites and the introduction of a unique reactive site like cysteine residues genetically allows for the attachment of only few cytotoxic molecules per antibody molecule. Dye-labeled antibodies are used as detection reagents for a range of biological imaging applications. This technology is also limited by the number of dyes one can covalently conjugate to a single antibody or protein. Future applications and breakthroughs of this field depend critically on developing general strategies for attaching several copies of drug molecules and imaging agents per protein molecule (antibody, avidin/streptavidin, BSA, etc.) without compromising the binding specificity and affinity. Such an approach would reduce the amount of antibody/proteins required for targeting, therapy or imaging; thereby reducing both the price and the toxicity of antibody/protein based drugs and imaging agents.

Modification or attachment of synthetic polymers with proteins is beneficial for both *in vivo* and *in vitro* applications. Polymer modification of proteins can induce increased biocompatibility, lower immune response, increase in *in vivo* stability, and delayed clearance by the reticuloendothelial system *(5)*. Polymer attachment can provide cryoprotection for low-temperature sensitive proteins. Surface modification by polymers can also effectively mask the intrinsic characteristics of the surface, preventing nonspecific protein adsorption. Polymers with multivalent reactive sites can be coupled to numerous small molecules creating pharmacologically active agents that possess long half-lives in biological systems. Hence, polymer-protein hybrids, a newly emerging class

of bioconjugates, have found several applications in biotechnology, biopharmaceutical chemistry and other life science areas *(4-7)*. There are however some fundamental limitations in the current methodologies available for the synthesis of these hybrids: (a) using current technologies, the number of copies of cytotoxic drugs/dyes that can be chemically conjugated to a protein (antibody, avidin/streptavidin, etc.) is limited (b) there is a basic limitation in the diversity of copolymers which can be synthesized for bioconjugation. The former limitation arises from the fact that extensive modification of proteins with several copies of a drug/dye would cause deactivation of the active sites and because of the limited numbers of functional groups available per protein molecule for bioconjugation. The latter limitation (in the diversity of copolymers synthesized for bioconjugation) arises from: (a) widely different reactivity between monomers; and (b) the lack of reactivity of many biologically relevant acrylates (e.g. an acrylate derivative of the anticancer drug candidate curcumin can be synthesized but will not polymerize since the molecule is a radical quencher) (*8*). Biological properties (e.g. bioactivity and self-assembly) of polymer-protein hybrids demand the synthesis of well defined polymers for bioconjugation *(9-11)*. In the early embodiments, the polymer component of the conjugates was synthesized via uncontrolled free radical polymerization techniques (*12*).

The synthesis of well defined polymer-protein hybrids in which the polymers are synthesized via controlled radical polymerization methods (such as atom transfer radical polymerization [ATRP] or reversible addition-fragmentation chain transfer polymerization [RAFT] is a rich newly emerging field of research (*13-21*). The synthesis of polymer-protein hybrid materials has, however, been restricted to a few acrylate/methacrylate monomers such as poly(ethylene glycol) acrylate/methacrylate and

poly(*N*-isopropyl) acrylamide; the recently reported streptavidin conjugates with biotinylated polymers *(13, 15, 16)* and thiol-terminated glycopolymers (*22*) serve as examples

Our current research mainly focused on the synthesis of well-defined functional biopolymer-synthetic polymer hybrids, which are targeted at addressing relevant biotechnological and biomedical problems. A major goal of our research is to develop a bioconjugation technology towards new generations of targeted imaging agents, detection reagents and targeted drugs with amplified efficiency. Herein, we present a general methodology for significantly increasing the number of dye/drug molecules which can be attached per protein molecule. The diversity of copolymers which can be synthesized for bioconjugation with proteins has also been considerably expanded. The synthesis of poly(acrylic acid) based Near Infrared Fluorescence (NIRF) dye and glucose incorporated novel copolymers which were further employed for bioconjugation to avidin, bovine serum albumen (BSA) and apoferritin demonstrates this breakthrough. It should be noted that Near-infrared (NIR)-absorbing dyes have opened new avenues in optical imaging with direct applications in pharmacology, cellular biology, and diagnostics as living subjects can be monitored with safe, noninvasive optical imaging/contrasting techniques (*23-26*). *In vitro* and *in vivo* imaging with cyanine based NIRF dyes are advantageous due to significant reduction of background absorption, enhanced fluorescence, the availability of low-cost sources of irradiation, the versatility of different reporter probes, large molar extinction coefficients and moderate-to-high fluorescence quantum yields (*27-29*).

2. MATERIALS AND METHODS

2.1. General Information.

Reagent-grade acetone, HPLC grade tetrahydrofuran, methylene chloride, N,N-dimethylformamide, methanol, toluene, ethylacetate were used without further purification. Solvents used for reactions were purified using *Puresolv*^{TM} system. 2-(2-(2-chloroethoxy)ethoxy)ethanol, 2-bromoisobutyryl bromide, methyl 2-bromopropanoate, *tert*-butyl acrylate, 1,1,4,7,7-pentamethyldiethylenetriamine, trifluoroacetic acid, D(+)-glucosamine, N-Hydroxybenzotriazole (HOBt), Copper (II) Sulfate and sodium ascorbate were obtained from Sigma-Aldrich. D(+)-Biotin was obtained from Acros Organics. 1-Ethyl-3-(3-dimethyllaminopropyl)carbodiimide hydrochloride (EDC.HCl) was obtained from Pierce Biotechnology. NIRF-Dye (ADS832WS) was obtained from American Dye Source, Inc. CupriSorb® was obtained from Seachem Laboratories Inc. Silica gel 60 F 254 plates for thin-layer chromatography (TLC) were purchased from Fisher Scientific. Column chromatographic separations were performed using silica gel (Fisher) with a particle size of 0.040-0.063 mm. Nuclear magnetic resonance (NMR) spectra were recorded on Oxford NMR 600 (600 MHz) spectrometer. Mass spectra (ESI-MS) were recorded using an Agilent LC/MS mass spectrometer. The Mol. Wt. of polymers were determined using Waters HPLC system equipped with either PLgel 5µm Mixed-D or PLaquagel-OH Mixed 8µm columns and Breeze software. Poly(methyl methacrylate) and poly(ethylene glycol) standards were used for organic soluble and water soluble polymers respectively.

2.2. Synthetic Protocols

2.2.1. Synthesis of Bromide-Terminated Methyl propanoate Poly(tert-butyl acrylate)

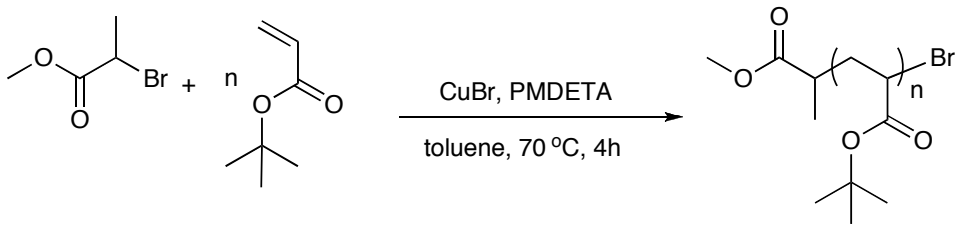

A 250 mL flask was charged with CuBr (0.448g, 3.12 mmol), and a septum was placed over the stem of the stopcock. Under positive pressure of Ar, *tert*-butyl acrylate (10 mL, 68.18 mmol), methyl 2-bromopropanoate (0.12 mL, 1.09 mmol), and pentamethyldiethylenetriamine (PMDETA) (0.63 mL, 3.05 mmol) were added via syringe, followed by addition of 1 ml degassed toluene. Following three freeze-pump-thaw degassing cycles, the reaction was allowed to stir for 4 h at 70 ^{0}C. After quenching of the polymerization by submerging the flask in liquid nitrogen, the mixture was allowed to warm to ambient temperature. The reaction mixture was diluted with THF and Cuprisorb was added, after stirring for ca. 15 minutes, the solution was filtered and solvent was removed under vacuum. The crude product was dissolved in small amount THF to yield a sticky mixture and precipitated two times from 10% methanol in deionized water. Isolated yield was 8.35 g (93%). *M*n=5889 g/mole, M_w/M_n= 1.1. ^{1}H NMR (CD_3OD, 300 MHz) δ(ppm): 3.66 (s, CH_3-CH-COOCH_3), 2.27 (b, -C*H*-CH_2-C*H*-Br), 1.84-1.96 (bm, -CH-CH_2-CH-Br), 1.45 (s, -CH-COOC-(CH_3)$_3$), 1.17 (s, CH_3-CH-$COOCH_3$); IR (cm^{-1}): 3434, 2977, 2933, 2258, 1991, 1728, 1479, 1449, 1392, 1367, 1259, 1155, 1035, 917, 845, 734.

2.2.2. Synthesis of Azido-Terminated Methyl propanoate Poly(tert-butyl acrylate)

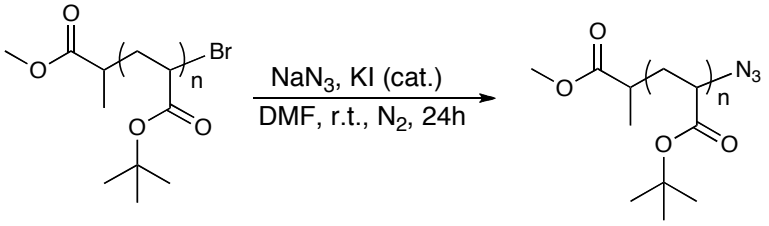

Bromide-terminated methyl propanoate Poly(tert-butyl acrylate) (1.51 g, 0.26 mmol) was dissolved in DMF (12 mL), and NaN_3 (0.1 g, 1.55 mmol) and KI (cat.) were added to the solution, which was stirred at room temperature for 24 h under N_2 atmosphere. The mixture was slowly added into plenty of 15% methanol, deionized water solution. The precipitated product was washed with water to obtain white gluey paste. The crude product was dissolved in CH_2Cl_2, dried with Na_2SO_4, filtered, dried under vacuum, and finally solid polymer was obtained. Mn=5775 g/mole, M_w/M_n= 1.20. ^{1}H NMR (CD_3OD, 300 MHz) δ(ppm): 3.66 (s, CH_3-CH-COOCH_3), 2.25 (b, -CH-CH_2-CH-N_3), 1.72-1.84 (bm, -CH-CH_2-CH-N_3), 1.45 (s, -CH-COOC-(CH_3)$_3$), 1.17 (s, CH_3-CH-$COOCH_3$); IR (cm^{-1}): 3434, 2978, 2933, 2258, 2113, 1991, 1730, 1479, 1392, 1367, 1257, 1155, 1035, 917, 846, 734.

2.2.3. Synthesis of Azido-Terminated Methyl propanoate Poly(acrylic acid)

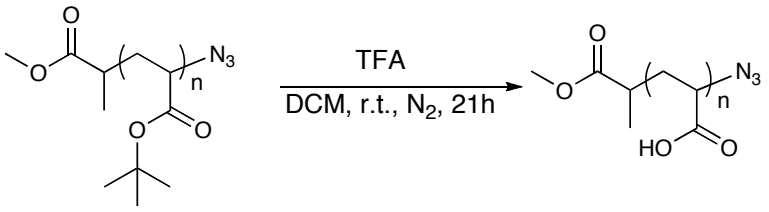

Azide-terminated methyl propanoate Poly(tert-butyl acrylate) (1g) was dissolved in a solution of trifluoroacetic acid (3.5 mL, 46 mmol) in dichloromethane (12 mL). The reaction was allowed to stir at ambient temperature for overnight. The solvent was removed under vacuum, and the resulting solid was dissolved in water. The solution was transferred to a dialyzed bag (MWCO 3.5 kDa), and the solution was dialyzed against a continuous flow of deionized water for 24 h. The final water soluble polymer was isolated by lyophilization: Isolated yield 0.575 g, (87%). ^{1}H NMR (DMSO, 300 MHz) δ(ppm): 12.27 (s, CH-COO*H*), 3.58 (s, CH_3-CH-COOC*H*$_3$), 2.22 (s, -C*H*-CH_2-C*H*-N_3), 1.76 (b, -C*H*-COOC-$(CH_3)_3$, -C*H*-COOH), 1.52 (bm, -CH-COOC-$(CH_3)_3$, -C*H*$_2$-CH-COOH), 1.24 (s, C*H*$_3$-CH_2-CH-COOH), 1.08 (s, C*H*$_3$-CH_2-CH-$COOCH_3$); IR (cm^{-1}): 3022, 2118, 1989, 1681, 1454, 1182, 1142, 1113, 1057, 921, 809.

About 4% tert-butyl acrylate group wasn't removed and confirmed via ^{1}H NMR by comparing the integral of protons (-C*H*-CH_2-C*H*-N_3) from the repeat units at δ = 2.22 ppm to COO*H* (δ = 12.27 ppm) from the carboxylic acid component.

2.2.4. Synthesis of Azido-Terminated Methyl propanoate Poly(acrylic acid)-poly(NIRF dye) [low dye loading]

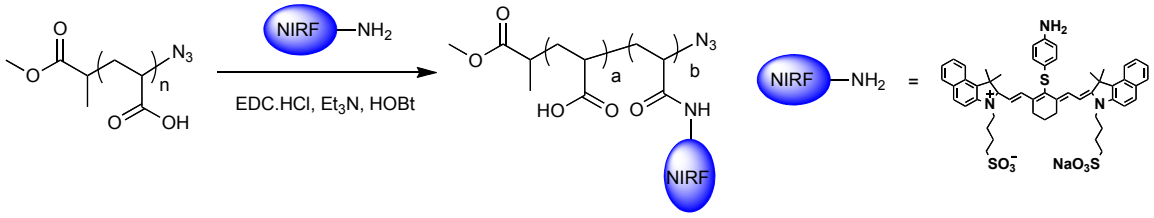

Azido-terminated methyl propanoate Poly(acrylic acid) (72 mg, 0.99 mmol), near infrared absorption dye ADS832WS (20 mg, 0.02 mmol), EDC·HCl (25 mg, 0.13 mmol), and HOBt (16.3 mg, 0.12 mmol) were dissolved in DMF (3.8 mL), Triethylamine(0.03

mL, 0.17 mmol) was added. The mixture was stirred 2.5 day at room temperature. After stopping of the reaction, the solution was transferred to a dialysis bag (MWCO 3.5 KDa), and the solution was dialyzed against a continuous flow of deionized water for 24 h. After dialysis, filtered, and lyophilized, green brown cotton shape crude product was obtained. The final water soluble polymer was isolated after purification by Sephadex™ LH-20 column and lyophilization: Isolated yield was 38 mg. ^{1}H NMR (CD_3OD, 300 MHz) δ(ppm): 8.93 (bd), 8.18 (bd), 7.98 (bm), 7.62 (bs), 7.47 (bm), 7.12 (bm), 6.45 (bm), 4.31 (bs), 3.66 (s), 3.21 (m), 2.86 (s), 2.45 (bs), 1.93 (bs), 1.69 (bm), 1.30 (m), 1.12(m). IR (cm^{-1}): 3440, 2932, 2114, 1967, 1715, 1537, 1503, 1430, 1392, 1353, 1269, 1236, 1169, 1139, 1116, 1063, 1039, 1012, 922, 894.

The NMR results showed the loading number of dye ADS832WS was 8.10 %.

2.2.5. Synthesis of Azido-Terminated Methyl propanoate Poly(acrylic acid)-poly(NIRF dye) [medium dye loading]

Azido-terminated methyl propanoate Poly(acrylic acid) (72 mg, 0.99 mmol), near infrared absorption dye ADS832WS (40 mg, 0.04 mmol), EDC·HCl (25 mg, 0.13 mmol), and HOBt (16.3 mg, 0.12 mmol) were dissolved in DMF (3.8 mL), Triethylamine (0.03 mL, 0.17 mmol) was added. The mixture was stirred 2.5 day at room temperature. After stopping of the reaction, the solution was transferred to a dialysis bag (MWCO 3.5 KDa), and the solution was dialyzed against a continuous flow of deionized water for 24 h. After dialysis, filtered, and lyophilized, green brown cotton shape crude product was obtained. The final water soluble polymer was isolated via Sephadex™ LH-20 column and lyophilization: Isolated yield was 48 mg. ^{1}H NMR (CD_3OD, 300 MHz) δ(ppm): 8.91

(bd), 8.15 (bm), 7.91 (bm), 7.57 (bs), 7.42 (bm), 7.1 (bm), 6.48 (bm), 4.23 (bs), 3.59 (s), 3.49 (s), 3.15 (m), 2.85 (m), 2.42 (s), 1.93 (s), 1.69 (bm), 1.25 (m), 1.06(m). IR (cm^{-1}): 3440, 2929, 2860, 2109, 1723, 1538, 1504, 1456, 1393, 1353, 1266, 1233, 1166, 1140, 1115, 1061, 1039, 1012, 923, 894.

The loading number of dye ADS832WS was found to be 13.14 % from NMR.

2.2.6. Synthesis of Azido-Terminated Methyl propanoate Poly(acrylic acid)-poly(NIRF dye) [high dye loading]

Azido-terminated methyl propanoate Poly(acrylic acid) (72 mg, 0.99 mmol), near infrared absorption dye ADS832WS (60 mg, 0.06 mmol), EDC·HCl (25 mg, 0.13 mmol), and HOBt (16.3 mg, 0.12 mmol) were dissolved in DMF (3.8 mL), Triethylamine (0.03 mL, 0.17 mmol) was added. The mixture was stirred 2.5 day at room temperature. After stopping of the reaction, the solution was transferred to a dialysis bag (MWCO 3.5 KDa), and the solution was dialyzed against a continuous flow of deionized water for 24 h. After dialysis, filtered, and lyophilized, green brown cotton shape crude product was obtained. The purified polymer was isolated by Sephadex^{TM} LH-20 column and lyophilization: Isolated yield was 48 mg. ^{1}H NMR (CD_3OD, 300 MHz) δ(ppm): 8.91 (bs), 8.21 (bm), 7.98 (bm), 7.51 (bm), 7.42 (bm), 7.2 (bm), 6.33 (bm), 4.27 (bs), 3.5 (s), 3.17 (m), 2.86 (m), 2.45 (bs), 1.95 (bm), 1.69 (bm), 1.25 (m). IR (cm^{-1}): 3440, 2929, 2860, 2114, 1723, 1538, 1504, 1456, 1393, 1353, 1266, 1233, 1166, 1140, 1115, 1061, 1039, 1012, 923, 894.

NMR results showed the loading number of dye ADS832WS was 38.85 %.

2.2.7. Synthesis of Azido-Terminated Methyl propanoate Poly (glucosamine)-poly(NIRF dye) [low loading]

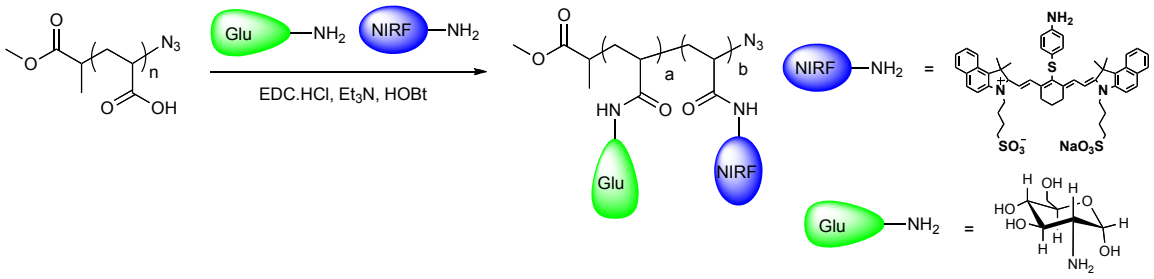

Azido-terminated methyl propanoate Poly(acrylic acid) (72 mg, 0.99 mmol), near infrared absorption dye ADS832WS (20 mg, 0.02 mmol), EDC·HCl (25 mg, 0.13 mmol), and HOBt(16.3 mg, 0.12 mmol) were dissolved in DMF (3.8 mL), Triethylamine(0.03 mL, 0.17 mmol) was added. After stirred 2 days at room temperature, glucosamine (248 mg, 1.15 mmol) in water (1.5 mL), EDC·HCl (218 mg, 1.137 mmol), and HOBt (153 mg, 1.149 mmol) mixture solution in DMF (1.5 mL) were added via syringe. The mixture was stirred another 3 day at room temperature. After stopping of the reaction, the solution was transferred to a dialysis bag (MWCO 3.5 KDa), and the solution was dialyzed against a continuous flow of deionized water for 24 h. After dialysis, filtered, and lyophilized, green brown cotton shape crude product was obtained. The final water soluble copolymer was isolated by Sephadex^{TM} LH-20 column and lyophilization: Isolated yield 195 mg. ^{1}H NMR (DMSO, 300 MHz) δ(ppm): 7.35-8.60 (bm), 6.58 (bm), 5.10 (bs), 4.60 (bm), 3.62 (bs), 3.18 (bs), 1.25-2.30 (bm), 1.04 (bs).

Results showed the loading number of dye ADS832WS and glucose were 11.92% and 81.97% respectively.

2.2.8. Synthesis of Azido-Terminated Methyl propanoate Poly(NIRF dye)-poly(glucose) [medium loading]

Azido-terminated methyl propanoate Poly(acrylic acid) (72 mg, 0.99 mmol), near infrared absorption dye ADS832WS (40 mg, 0.04 mmol), EDC·HCl (25 mg, 0.13 mmol), and HOBt(16.3 mg, 0.12 mmol) were dissolved in DMF (3.8 mL), Triethylamine(0.03 mL, 0.17 mmol) was added. After stirred for 2 days at room temperature, glucosamine (248 mg, 1.15 mmol) in water (1.5 mL), EDC·HCl (218 mg, 1.137 mmol), and HOBt (153 mg, 1.149 mmol) mixture solution in DMF (1.5 mL) were added via syringe. The mixture was stirred another 3 day at room temperature. After stopping of the reaction, the solution was transferred to a dialysis bag (MWCO 3.5 KDa), and the solution was dialyzed against a continuous flow of deionized water for 24 h. After dialysis, filtered, and lyophilized, green brown cotton shape crude product was obtained. The final water soluble copolymer was isolated by Sephadex^{TM} LH-20 column and lyophilization: Isolated yield 195 mg.

Results showed the loading number of dye ADS832WS and glucose were 13.66% and 72.93% respectively.

2.2.9. Synthesis of Azido-Terminated Methyl propanoate Poly(glucose)–poly(NIRF dye) [high loading]

Azido-terminated methyl propanoate Poly(acrylic acid) (72 mg, 0.99 mmol), near infrared absorption dye ADS832WS (60 mg, 0.06 mmol), EDC·HCl (25 mg, 0.13 mmol), and HOBt(16.3 mg, 0.12 mmol) were dissolved in DMF (3.8 mL), Triethylamine(0.03 mL, 0.17 mmol) was added. After stirred 2 day at room temperature, glucosamine (248 mg, 1.15 mmol) in water (1.5 mL), EDC·HCl (218 mg, 1.137 mmol), and HOBt (153 mg, 1.149 mmol) mixture solution in DMF (1.5 mL) were added via syringe. The mixture was stirred another 3 day at room temperature. After stopping of the reaction, the solution was transferred to a dialysis bag (MWCO 3.5 KDa), and the solution was dialyzed against a continuous flow of deionized water for 24 h. After dialysis, filtered, and lyophilized, green brown cotton shape crude product was obtained. The final water soluble copolymer was isolated by Sephadex^{TM} LH-20 column and lyophilization: Isolated yield 180 mg. Results showed the loading number of dye ADS832WS and glucose were 33.65% and 65.46% respectively.

2.2.10. Synthesis of 2-(2-(2-Azidoethoxy)ethoxy)ethanol

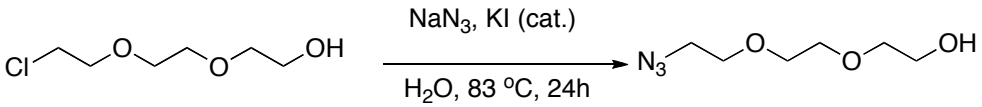

A mixture of 2-(2-(2-chloroethoxy)ethoxy)ethanol (7.04 g, 41.72 mmol), sodium azide (13.65 g, 209.94 mmol) and potassium iodide (1.87 g, 11.25 mmol) in water (72 mL) was stirred at 83 ^{0}C for 24 h. The reaction mixture was extracted with ether, and the organic layer was washed with brine and then dried over anhydrous Na_2SO_4. The solvent

was evaporated and the product was dried under vacuum to give colourless oil. The product was purified via column chromatography, CH_2Cl_2:MeOH, 95:5 was used as the eluent. Yield: 62%. ^{1}H NMR (600 MHz, $CDCl_3$): δ(ppm) 2.85-2.87 (t, 2H), 3.29-3.31 (t, 2H), 3.50-3.51 (m, 2H), 3.57-3.64 (m, 6H). ^{13}C NMR (150 MHz, $CDCl_3$): δ(ppm) 46.58, 57.58, 65.96, 66.31, 66.57, 68.55. ESI-MS m/z = 198.1 (M+Na); IR (KBr, cm^{-1}) 2104.

2.2.11. Synthesis of 2-Bromo-2-methylpropionic acid 2-[2-(2-Azidoethoxy)ethoxy] ethyl ester

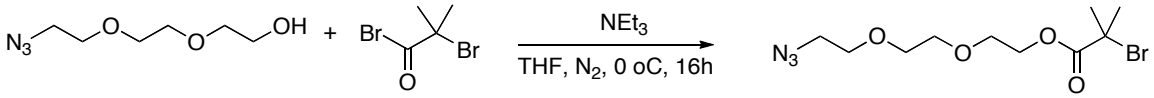

A solution of 2-bromoisobutyryl bromide (4.58 g, 19.9 mmol) and triethylamine (2.18 g, 21.5 mmol) in THF (5 mL) was cooled to 0 °C in a 2-necked round-bottomed flask. A solution of 2-[2-(2-azidoethoxy)ethoxy]ethanol (3 g, 17.1 mmol) in THF (5 mL) was added dropwise with stirring. The reaction mixture was then stirred at room temperature for 16 h, filtered, and the solvent was removed by rotatory evaporator. The crude product was added to a cooled (ice bath) containing 5% aqueous solution of Na_2CO_3 and the resulting mixture was extracted with ethyl acetate (3 x 50 mL). The combined organic layers were washed with brine, dried over anhydrous Na_2SO_4, and solvent was evaporated to provide a dark-yellow oil. Yield: 5 g (90 %). ^{1}H NMR (600 MHz, $CDCl_3$): δ (ppm) 1.88 (s, 6H), 3.56-3.58 (t, 2H), 3.63 (s, 4H), 3.69-3.70 (t, 4H), 4.26-4.28 (t, 2H). ^{13}C NMR (150 MHz, $CDCl_3$): δ (ppm) 30.53, 42.57, 55.54, 64.89, 68.58, 68.60, 70.43, 70.48, 71.15, 171.37.

2.2.12. Synthesis of Azide terminated Poly(tert-butyl acrylate)

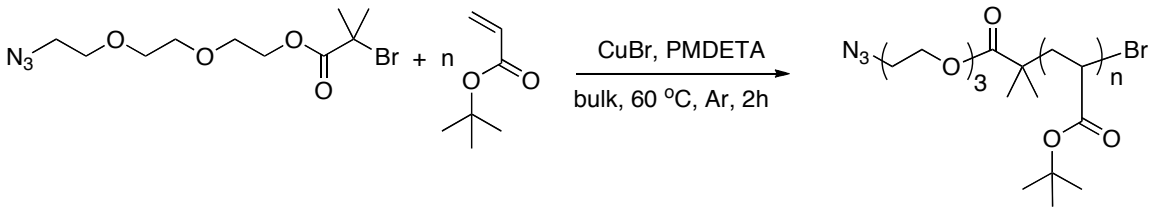

A 100 mL flask fitted with a stopcock was flame-dried under vacuum and allowed to cool at ambient temperature under Ar. The flask was charged with CuBr (115 mg, 0.8 mmol). Under positive pressure of Argon, a solution of 2-Bromo-2-methylpropionic acid 2-[2-(2-Azidoethoxy)ethoxy] ethyl ester (118 mg, 0.36 mmol) dissolved in tert-butyl acrylate (4 mL, 27.55 mmol) was added via syringe, followed by the addition of 1,1,4,7,7-pentamethyldiethylenetriamine (PMDETA) (0.17 mL, 0.8 mmol). Following three freeze-pump-thaw degassing cycles, the reaction was allowed to stir for 2 hour 10 minutes at 60 ^{0}C. Submerging the flask in liquid nitrogen quenched the polymerization, the mixture was allowed to warm to ambient temperature, and diluted with tetrahydrofuran. CupriSorb® was added and stirred ca. 30 minutes for removing copper complex. After filtration, the mixture was poured into a 15% methanol, deionized water solution, white solid product was precipitated. The polymer was further purified via reprecipitation and dried under vacuum, isolated weight was 2.18 g. M_n=8586 g/mol, M_w/M_n=1.21. ^{1}H NMR (600 MHz, $CDCl_3$): δ (ppm) 4.19 (s, 2H), 3.55-3.75 (m, 6H), 3.39 (t, 2H), 2.18-2.30 (bm), 1.85 (s), 1.28-1.62 (bm), 1.15 (s, 6H), 0.89 (m). FTIR (film, cm^{-1}): 3433, 2977, 2289, 2113 (azide), 1727, 1619, 1450, 1367, 1255, 1153, 845, 752.

2.2.13. Synthesis of 5-(2-oxooctahydropyrrolo[3,4-d]imidazol-4-yl)-N-(prop-2-ynyl)pentanamide (Biotin-Alkyne)

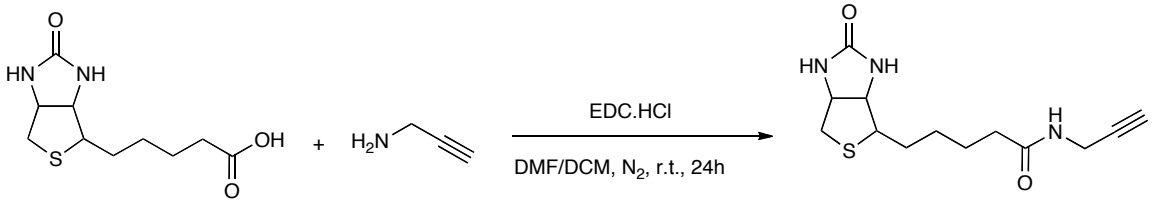

D(+)-biotin (186 mg, 0.76 mmol) was dissolved in 7 mL DMF and a solution of propargylamine (76 mg, 1.37 mmol) in CH_2Cl_2 (7 mL) was added to it followed by EDC.HCl. After being stirred for 24 h at room temperature, the reaction mixture was concentrated in vacuum and diluted by 30 mL of CH_2Cl_2 and the organic layer was washed by water (10 mL×3), dried over Na_2SO_4 and then concentrated in vacuum. The crude product was purified by flash column chromatography ($MeOH/CH_2Cl_2$=5/95-15/85) to obtain the product 160 mg (75%). ^1H NMR (600 MHz, CD_3OD): δ(ppm) 4.48-4.50 (dd, 1H), 4.29-4.31 (dd, 1H), 3.94 (d, 2H), 3.19-3.22 (dt, 1H), 2.91-2.94 (dd, 1H), 2.69-2.41 (d, 2H), 2.58-2.59 (t, 1H), 2.20-2.23 (t, 2H), 1.58-1.74 (m, 4H), 1.42-1.46 (q, 2H); ^{13}C NMR (150 MHz, CD_3OD): δ(ppm) 173.6, 164.1, 78.7, 70.1, 61.3, 59.6, 55.0, 39.1, 34.5, 27.7, 27.4, 24.7.

2.2.14. Synthesis of Biotin Terminated poly(tert-butyl acrylate)

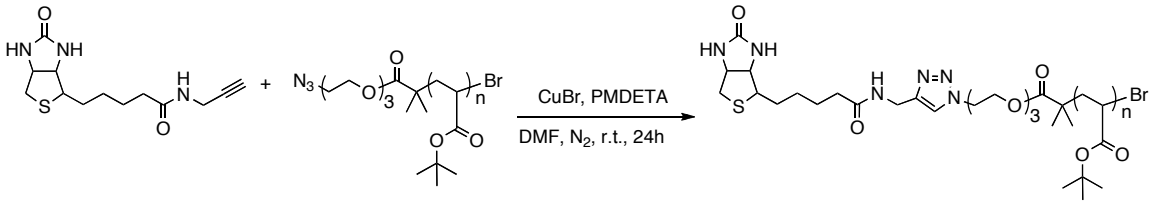

The azide-containing polymer (565 mg, 0.073 mmol of azide groups), biotin-alkyne (25 mg, 0.087 mmol), CuBr (35 mg, 0.024 mmol), and 1,1,4,7,7-

pentamethyldiethylenetriamine (PMDETA) (5.2 μL, 0.025 mmol) were placed in a round-bottom flask. The flask was closed with rubber septum and degassed with N_2. Deoxygenated DMF (3 mL) was added with an argon-purged syringe, and the reaction was stirred for 24 h at room temperature. The mixture was diluted with tetrahydrofuran, CupriSorb® was added and stirred ca. 30 minutes to remove copper complex. Solid residue was filtered off and the mixture was poured into a 15% methanol, deionized water solution where white solid product was precipitated. The product was further purified by re precipitation and dried over vacuum. Yield: 537 mg (92%). M_n=8850 g/mol, M_w/M_n=1.30. ^{1}H NMR (600 MHz, $CDCl_3$), δ(ppm): 7.68 (s), 7.44 (s), 4.48 (s), 4.31 (s), 4.19 (s), 4.00 (s), 3.3803.64 (m), 3.11 (m), 2.73 (d), 2.18-2.30 (bm), 1.79 (s), 1.28-1.62 (bm), 1.10 (s), 0.89 (m). FTIR (film, cm^{-1}): 3433, 2977, 2932, 2720, 2360, 1991, 1728, 1479, 1449, 1392, 1367, 1256, 1150, 1037, 845, 734.

2.2.15. Synthesis of Biotin Terminated poly(acrylic acid)

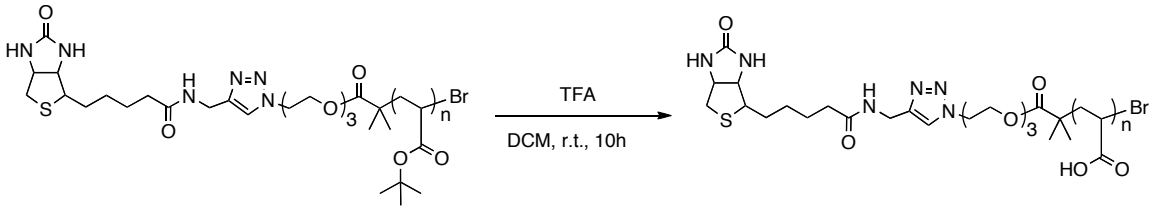

The bitinylated poly(*tert*-butyl acrylate) (489 mg, 0.061 mmol) was dissolved in a solution of trifluoroacetic acid (1.5 mL, 19.5 mmol) in dichloromethane (13 mL). The reaction was allowed to stir at ambient temperature for 10 hrs. The solvent was removed under vacuum, and the resulting solid was dissolved in deionized water. The solution was transferred to a dialysis bag (MWCO 3.5 KDa), and dialyzed against a continuous flow of deionized water for overnight. The final polymer was isolated by lyophilization: Isolated

yield 238 mg, (87%). M_n=43728, M_w=55070, PDI=1.26; ^{1}H NMR (600 MHz, $CDCl_3$): δ(ppm) 12.23 (bs), 7.85 (s), 7.78 (s), 4.47 (t), 4.26-4.30 (m), 4.04 (b), 3.38-3.82, (bm), 3.23-3.25 (t), 3.08 (s), 2.87 (d), 2.80-2.83 (t), 2.68-2.74 (m), 2.19 (bs), 2.07 (t), 1.74 (bm), 1.22-1.60 (bm), 1.07 (bm), 0.88 (m).

2.1.16. Synthesis of Biotin Terminated Poly(D-Glucosamine)-poly(NIRF Dye)

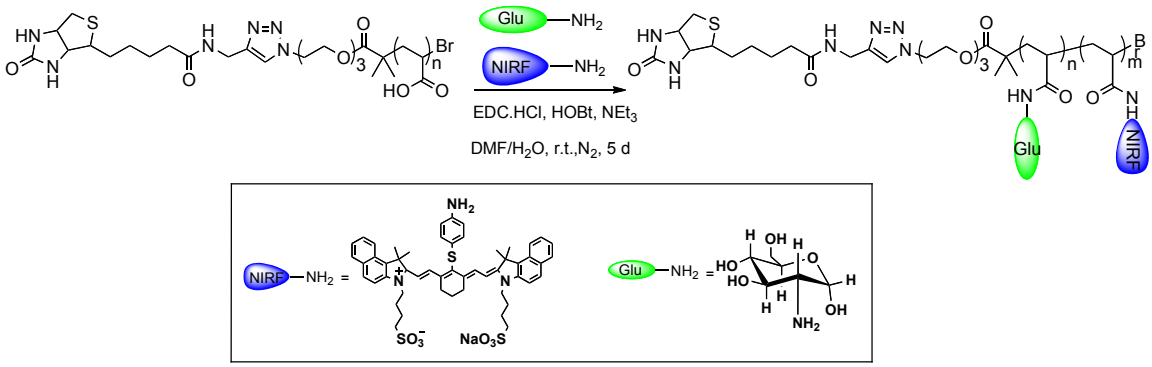

Biotin-terminated poly(acrylic acid) (76 mg, 1.055 mmol), Near infrared absorption dye (ADS832WS) (200 mg, 0.213 mmol), EDC·HCl (213 mg, 1.11 mmol), and HOBt (153 mg, 1.148 mmol) were dissolved in DMF (1.5 mL) in a r.b. followed by the addition of Triethylamine (0.15 mL, 1.08 mmol). After stirring for 2 days at room temperature, D(+)-glucosamine (230 mg, 1.067 mmol) in water (2 mL) and DMF (1 mL) mixture solution was added. EDC·HCl (200 mg, 1.043 mmol) was added, and the mixture was stirred another 3 day at room temperature. After stopping the reaction, the solution was transferred into a dialysis bag (MWCO 3.5 KDa), and the solution was dialyzed against a continuous flow of deionized water for 24 h. The dialyzed reaction mixture was filtered and lyophilized to yield greenish- brown crude product. The crude product was further purified with Sephadex^{TM} LH-20 size-exclusion column with deionized water as eluent and lyophilized. Isolated yield: 249 mg. M_n=23259 g/mol, M_w/M_n=1.48. ^{1}H NMR

(600 MHz, CD_3OD), δ(ppm): 8.98 (d), 7.18-8.34 (bm), 6.68 (m), 6.37 (m), 5.27 (d), 4.63 (s), 4.30 (s), 3.31-3.96 (m), 3.19 (m), 3.12 (m), 2.99-3.02 (m), 2.86-2.91 (m), 2.79 (s), 1.35-2.22 (m), 1.61 (d), 1.19-1.32 (m), 1.08 (m).

2.2.17. Synthesis of Biotin Terminated Poly(acrylic acid)-poly(NIRF Dye)

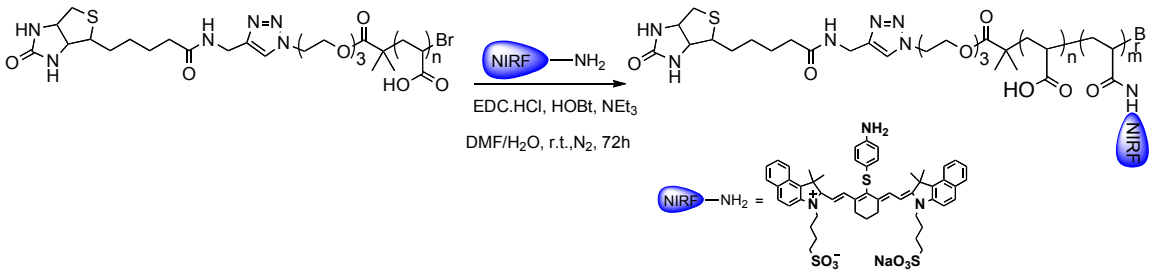

Biotinylated poly(acrylic acid) (76 mg, 1.055 mmol), Near infrared absorption dye (ADS832WS) (498 mg, 0.531 mmol), EDC·HCl (213 mg, 1.11 mmol), and HOBt (153 mg, 1.148 mmol) were dissolved in DMF (1.5 mL) in a r.b. followed by the addition of Triethylamine (0.03 mL, 0.17 mmol). The mixture was stirred 3 days at room temperature. After stopping of the reaction, the solution was transferred into a dialysis bag (MWCO 3.5 KDa), and the solution was dialyzed against a continuous flow of deionized water for 24 h. The dialyzed reaction mixture was filtered and lyophilized to yield greenish-brown cotton shaped crude product. The crude product was further purified with Sephadex^{TM} LH-20 size-exclusion column with deionized water as eluent. Yield: 40 mg. ^{1}H NMR (600 MHz, CD_3OD), δ(ppm): 8.83 (b), 7.13-8.23 (bm), 6.35 (b), 4.04-4.34 (b), 3.09-3.19 (bm), 2.55-3.07 (bm), 1.02-2.48 (bm).

2.2.18. Synthesis of Azide Terminated Poly(Acrylic acid)

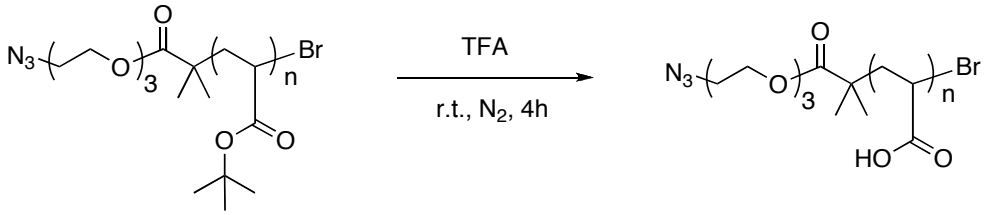

Trifluro acetic acid (2 ml, 27 mmol) of was added drop-wise to a round bottom flask containing azido-poly(*tert*-butyl acrylate) (0.3 g , 0.02 mmol). The reaction was stirred under N_2 for 4 hours. The reaction mixture was dialyzed using 3500 MWCO membrane in distilled water with several exchanges and finally the lyophilization yielded the deprotected polymer as white powder. Yield: 97%, M_n= 42423 M_w= 50570 PDI=1.19; ^{1}H NMR (600 MHz, D_2O), δ (ppm): 1.14-1.18 (m, 8 H), 1.40 (s, 4 H), 1.61 (s, 46 H), 1.73 (s, 112 H), 1.90 (s, 40 H), 2.36 (s, 104 H), 3.67-4.17 (m, 12 H). FT-IR (cm^{-1}): 3022, 2117 (N_3), 1681, 1454.

2.2.19. Synthesis of Azide Terminated Poly(NIRF)-poly(Glucose) copolymer

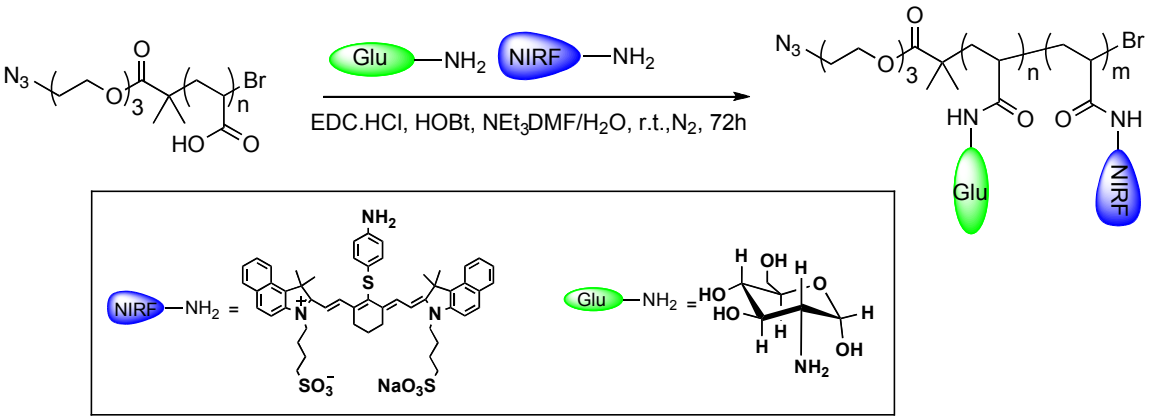

Azide terminated poly(acrylic acid) (72 mg, 0.003 mmol), NIRF dye (ADS832WS) (100 mg, 0.106 mmol), D(+)-Glucosamine (190 mg, 0.9 mmol), EDC.HCl (575 mg, 3.0 mmol) and HOBt (460 mg, 3.0 mmol) were dissolved in 10 ml of DMF in a round bottom flask and was degassed with N_2 and followed by dropwise addition of Et_3N (0.42 ml, 5 mmol). The reaction mixture was stirred at room temperature for 72 hours. The reaction mixture was dialyzed extensively using 10K MWCO membrane and then purified by passing through a Sephadex LH20 column. Finally the product was isolated as black-colored fluffy powder after lyophilization. Yield: 76 %. ^{1}H NMR (600 MHz, D_2O), δ (ppm): 1.03 (bs), 1.52-1.66 (bd), 1.76 (s), 2.01(bs), 2.57(s), 2.80 (s), 2.93 (bs), 3.59 (s), 3.65 (s), 3.75 (s), 5.09-5.22 (bm). FT-IR (cm^{-1}): 3431, 2935, 2111 (N_3), 1714, 1538, 1504, 1443, 1393, 1353, 1266, 1233, 1166, 1140, 1115. GPC (H_2O): Mn= 19469, Mw= 25074, PDI= 1.28.

2.2.20. Synthesis of Alkyne terminated poly(NIRF)-poly(Glucose) copolymer

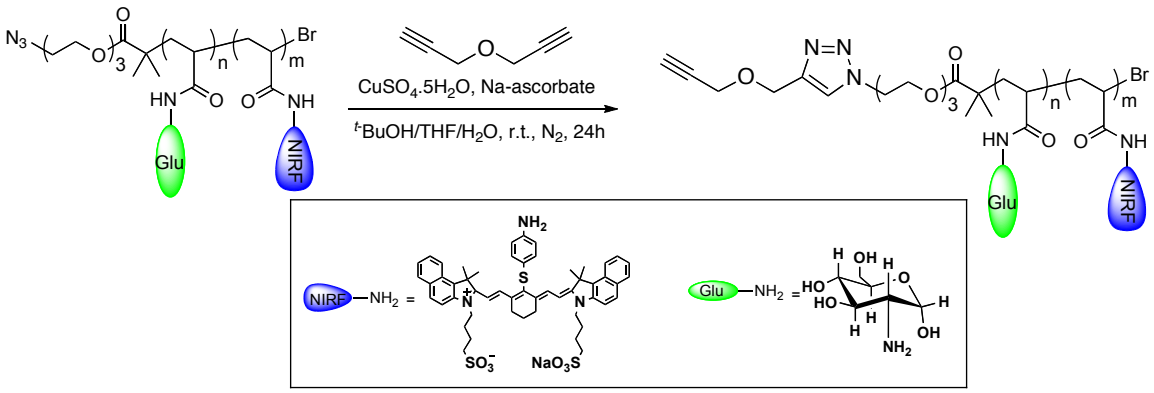

Poly(NIRF dye)-poly(glucose) copolymer (60 mg, 3 µmol) was dissolved in 3 ml of *t*-BuOH/THF/H_2O (1:1:1) and stirred with Propargyl ether (9.14 mg, 10µL, 31.5 eq), $CuSO_4.5H_2O$ (5 mg, 0.02 mmol), Sodium ascorbate (4 mg, 0.02 mmol) in a r.b. flask

under N_2 atmosphere at room temperature for 24 h. The reaction was stopped and the reaction mixture was dialyzed extensively in deionized water using 10 kD MWCO membrane. The dialyzed mixture was further purified via Sephadex-LH 20 size exclusion chromatography and lyophilized. Yield: 42 mg (70%) ^{1}H NMR (600 MHz, D_2O), δ (ppm): 1.03 (bs), 1.52-1.75 (bd), 2.01(bs), 2.58 (s), 2.81 (s), 2.94 (s), 3.36 (s), 3.66-3.73 (bd), 5.06-5.23 (bm), 7.15-8.33 (m). GPC (H_2O): Mn= 19988, Mw= 28168, PDI= 1.40. FT-IR (cm^{-1}): 3299, 2928, (No N_3 peak ~2100), 1648, 1536, 1429, 1389, 1351, 1232, 1155, 1113. The absence of the azide peak (~2100 cm^{-1}) in the FT-IR spectra confirmed that all of the azide-end groups were reacted with dipropargyl ether. The polymer was used for further conjugation as it was.

3. RESULTS AND DISCUSSIONS

3.1. Synthesis of Drug/Dye Incorporated copolymers.

Our approach towards these copolymers involves these steps: (1) the synthesis of well-defined living polymers containing reactive chain-end and functional side-chain pendant groups in which the chain end and side chain possesses orthogonal reactivity, (2) the attachment of a number of water soluble, biocompatible moieties and imaging/therapeutic agents to the functional polymer side chains. Three parallel synthetic designs were employed to establish the feasibility of this concept. According to the first synthetic design (**Scheme 1.1**) azide-terminated poly(acrylic acid) was synthesized. Carboxylic acid side chains were reacted with amine derivatives of a NIRF dye and glucose. The azide terminated drug/dye loaded copolymers could be used to modify protein surfaces. In the second design poly(acrylic acid) with a single reactive biotin chain end was synthesized; straight-forward post-polymerization modification of the polymer yielded the final NIRF dye-glucose copolymers for bioconjugation (**Scheme 1.2**). In the third design, azide and alkyne terminated NIRF dye-glucose copolymers were synthesized which could be used to synthesized drug/dye incorporated protein-polymer hybrids (**Scheme 1.3**).

3.2. Azide-terminated water-soluble NIRF dye copolymers.

The synthesis involved the polymerization of *tert*-butyl acrylate via ATRP (*30*) using an bromo initiator **1** to produce bromo-terminated poly(*tert*-butyl acrylate) **2** (**Scheme 1.1**). Azide group was introduced on the polymer via substitution using NaN_3 in DMF. The insertion of the azide group in the polymer was confirmed by the presence of the azide peak at 2113 cm^{-1} in the IR spectrum of the polymer. Polymer **2** was treated with trifluoro acetic acid (TFA) to produce poly(acrylic acid) (PAA) with a single azide chain end **3**. The rationale for synthesizing PAA with a single chain end is based on the facts that (a) PAA is FDA approved and is generally regarded as safe (GRAS); (b) amine derivatives of a broad spectrum of dyes and a wide range of therapeutic agents are readily available commercially and can be employed using amidation chemistry with PAA to produce copolymers. The amine derivatives, NIRF-NH_2 (ADS832WS) and Glu-NH_2 (D-(+)-glucosamine) were grafted to the PAA polymer **3** using standard amide coupling reagents 1-Ethyl-3-(3-dimethylaminopropyl)carbodiimide hydrochloride (EDC.HCl) and *N*-Hydroxybenzotriazole (HOBt) in DMF to produce a series of acrylic acid-NIRF dye copolymers **4-6** and NIRF dye-glucose copolymers **7-9**. The polymers synthesized were characterized via ^1H NMR, Gel Permeation Chromatograph (GPC) and FT-IR spectroscopy. Based on the NMR results, the dye composition in the copolymer **4** was quantified by comparing the peak area of the protons from NIRF dye at 7.12-8.93 ppm to that of -C*H*$_2$-C*H*- protons from main chain of polymer at 1.69-1.93 ppm, and results revealed that the loading number of NIRF dye was 8.10%. FT-IR peak frequency at 2114 cm^{-1} confirms the presence N_3 group after the side-chain group modifications. Loading amount of dye on copolymer **5** (medium dye loading) was calculated comparing the peak

area of the protons from dye at 7.12-8.93 ppm and -CH_2-CH- protons from polymer backbone at 1.69-1.93 ppm, and results showed the loading number of NIRF dye was 13.14 %. In copolymer 6 the dye loaing was calculated to be 38.8 % comparing peak area of the NMR spectrum of NIRF dye at 7.2-8.91 ppm to that of -CH_2-CH- protons from main chain of polymer at 1.69-1.95 ppm. Azide group was found to be intact in both copolymers **5** and **6** which is evident from the FTIR spectrum. GPC molecular weights

Scheme 2.1. Synthetic design of NIRF dye incorporated living copolymer with reactive azide end-group.

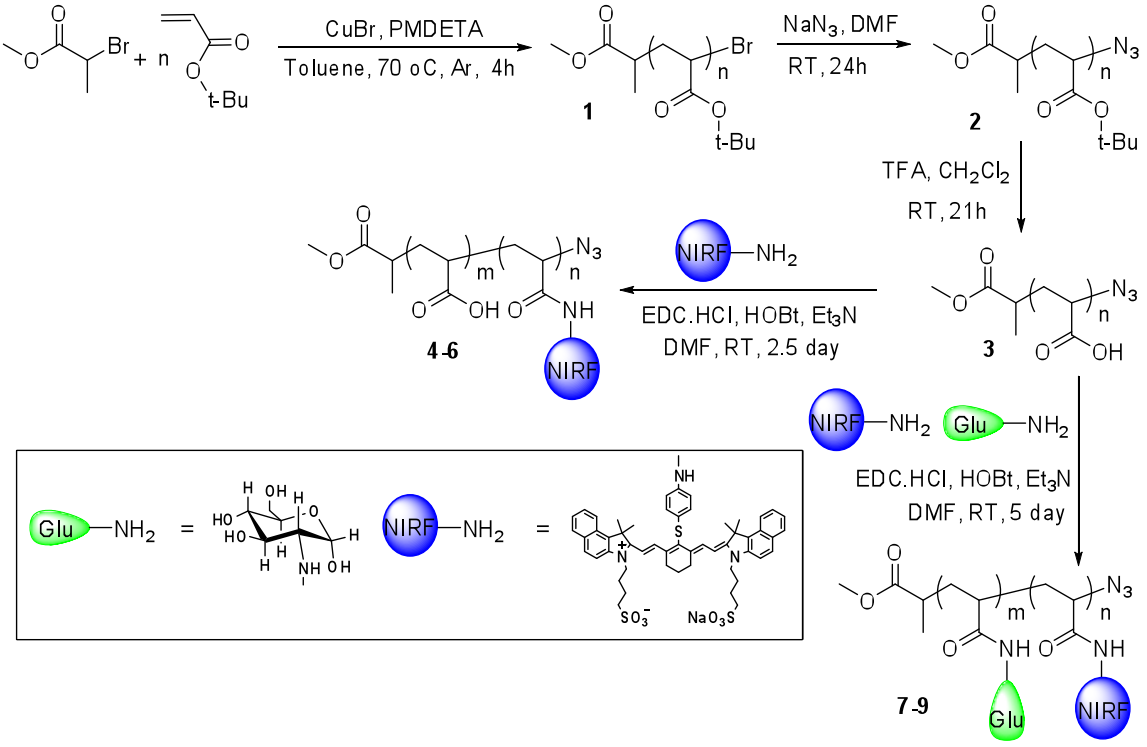

comparison among poly(acrylic acid) polymer and dye incorporated polymers also gave insight about the dye loading on the copolymers. Dye loading values from GPC method and NMR method were comparable to each other. Another series of copolymers containing both NIRF dye and glucose with three different level of dye loading were also synthesized. Incorporation of glucose moiety along with NIRF dye increased polymer

solubility in water. According to GPC molecular weights and NMR peak areas the NIRF dye and glucose loadings on the copolymers were calculated. The dye and glucose on the copolymer **7** were quantified by comparing the peaks area of the protons from dye at 7.35-8.60 ppm, glucosamine at 5.10 and 4.60 ppm, and -CH_2-CH- protons from polymer backbone at 1.25-2.30 ppm and were found to be 11.92% and 81.97% respectively. For copolymer **8** these values were recorded to be 13.66% and 72.93% respectively. Copolymer **9** contained 33.65% NIRF dye and 65.46% glucose, which were determined using NMR peak areas and GPC molecular weights. These water soluble, dye incorporated, reactive chain ended copolymers could be conjugated to alkyne surface modified proteins via azide-alkyne [3+2] cycloaddition reaction to produce protein-polymer hybrids.

Table 2.1: List of polymers and copolymers synthesized

Name	Structure	M_n	M_w	PDI	% of Dye Loading
Poly(*tert*-butyl acrylate) (**1**)	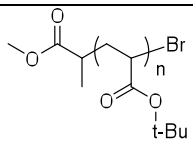	5,889	6,478	1.1	
Azido Poly(*tert*-butyl acrylate) (**2**)	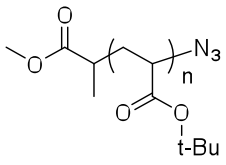	5,775	6,930	1.20	
Azido Poly(acrylic acid) (**3**)	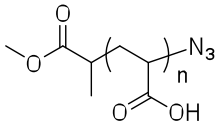	-	-	-	

Azido Poly(acrylic acid)-poly(NIRF dye) copolymer (**4**) (low dye loading)	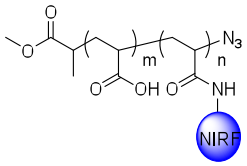	-	-	-	8.1 %
Azido Poly(acrylic acid)-poly(NIRF dye) copolymer (**5**) (medium dye loading)	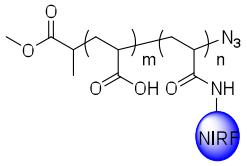	-	-	-	13.14 %
Azido Poly(acrylic acid)-poly(NIRF dye) copolymer (**6**) (high dye loading)	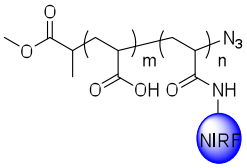	-	-	-	38.85 %
Azido Poly(NIRF dye)-poly(glucose) copolymer (**7**) (low dye loading)	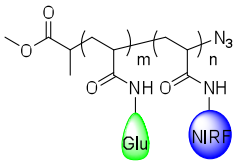	-	-	-	11.92 %
Azido Poly(NIRF dye)-poly(glucose) copolymer (**8**) (medium dye loading)	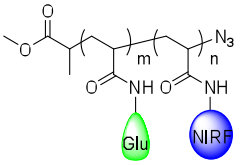	25,662	33,544	1.30	13.66 %
Azido Poly(NIRF dye)-poly(glucose) copolymer (**9**) (high dye loading)	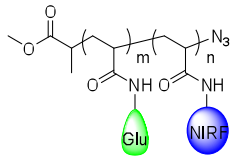	-	-	-	33.65 %

3.3. Biotin terminated water-soluble NIRF dye incorporated coplymers.

The synthesis involved the polymerization of *tert*-butyl acrylate via ATRP (*30*) using an azide incorporated initiator **10** to produce poly(*tert*-butyl acrylate) **11** (**Scheme 1.2**). The intact nature of the azide group in the polymer was confirmed by the presence of the azide peak at 2113 cm^{-1} in the IR spectrum of the polymer. The resulting polymer was reacted with an alkyne derivative of biotin **12** under [3+2] azide-alkyne triazole forming "click" conditions to produce a polymer with a single biotin chain end **13** (**Scheme 1.2**). Peaks arising from the biotin moiety (*17*) at 4.48 ppm and 4.31 ppm were observed in the ^1H NMR of **13**, peaks at 7.68 (s), and 7.44 (s) arising from the triazole protons (*31*) were also observed. Polymer **13** was treated with trifluoro acetic acid (TFA) to produce poly(acrylic acid) (PAA) with a single biotin chain end **14**. The rationale for synthesizing PAA with a single chain end is based on the facts that (a) PAA is FDA approved and is generally regarded as safe (GRAS); (b) amine derivatives of a broad spectrum of dyes and a wide range of therapeutic agents are readily available commercially and can be employed using amidation chemistry with PAA to produce copolymers and (c) azidotriethylene glycol and the ATRP initiator with the azide group employed for the polymerizations are safe (many short chain azides are explosive). The amine derivatives, NIRF-NH_2 (ADS832WS) and Glu-NH_2 (D-(+)-glucosamine) were grafted to the PAA polymer **14** using standard amide coupling reagents 1-Ethyl-3-(3-dimethyllaminopropyl)carbodiimide hydrochloride (EDC.HCl) and *N*-Hydroxybenzotriazole (HOBt) in DMF to produce **15**. The polymers synthesized were characterized via ^1H NMR, Gel Permeation Chromatograph (GPC) and FT-IR spectroscopy.

Comparing the *Mn*=8850 of polymer **13** and *Mn*=23259 of polymer **15,** the percent of dyes per polymer chain were calculated: subtracting the mol.wt. of the chain-end groups from *Mn* of polymer **13**, the number of repeat units in polymer **13** was calculated to be 64, this number was used as the total number of repeat units in the copolymer **15**, employing the following equation the number of dye repeat unit per polymer chain was calculated: $\boldsymbol{ax + b(64 - x) = (Mn - c)}$. Where $\boldsymbol{x}$ = number of dyes per polymer chain, $\boldsymbol{a}$, $\boldsymbol{b}$ & $\boldsymbol{c}$ are mol.wts. of dye repeat unit, sugar repeat unit and chain-ends respectively, and the percentage of dyes per polymer chain was calculated to be ~17%. The quantity of different compositions in the copolymer was further quantified by comparing the peaks area of the protons from dye ADS832WS at 7.35-8.60 ppm, glucosamine at 5.10 and 4.60 ppm, and that of -CH_2-C*H*- protons from main chain of polymer at 1.25-2.30 ppm. Results showed the loading number of dye ADS832WS and glucosamine were 15.92% and 81.97% respectively.

Scheme 2.2. Schematic synthesis of biotinylated poly(NIRF dye)-poly(glucose) copolymers.

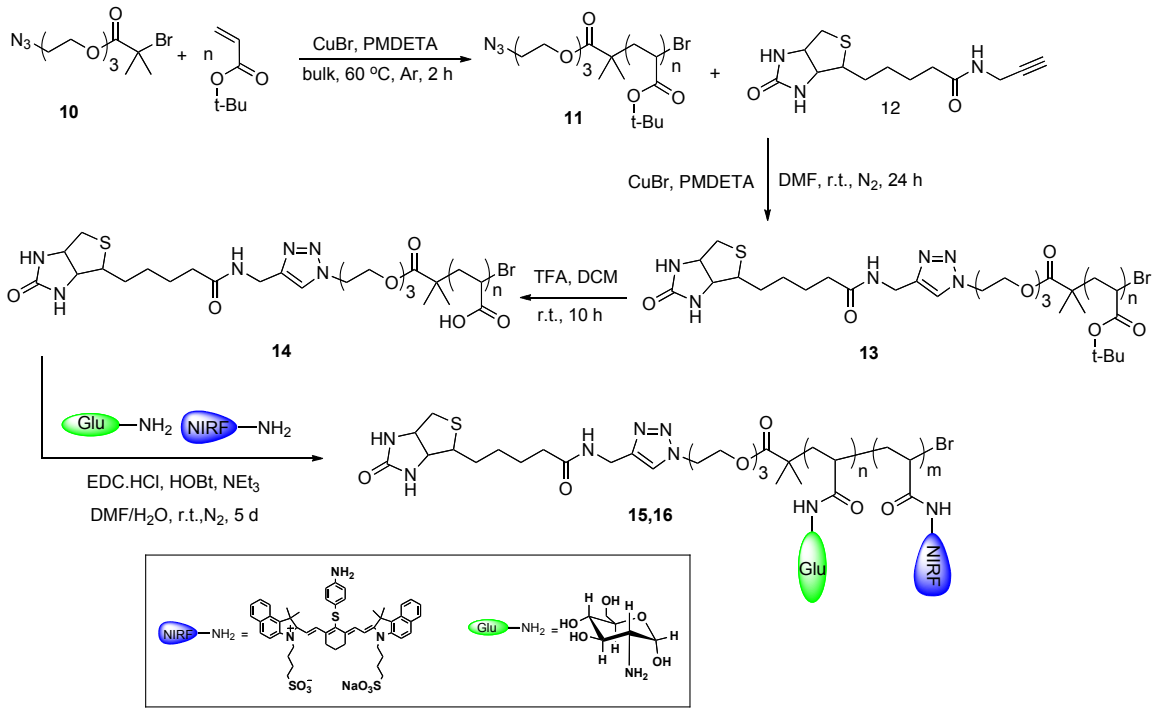

A control polymer **16** (PAA with dye alone) with higher dye loading was also synthesized. Comparing the GPC molecular weights of polymer **13** and copolymer **16** following above-mentioned method the NIRF dye loading on the copolymer 16 was calculated to be 34%. NMR peak area of the protons from dye and that of -C*H*$_2$-C*H*- protons from polymer main chain were compared which indicate the dye loading was ~30 %. However, this copolymer was not readily soluble in water like copolymer **15**. Therefore, copolymer **15** was chosen for further studies due to its better solubility in water. It should be noted that recently, side chain poly(alkyne) polymers were synthesized and various azide molecules were attached to the polymer back-bone via "click" chemistry (*22, 32*). The approach is restricted to a few azides because many small azides are potentially explosive (*22, 32*). Our approach is safe because the initiator is safe and the final polymer has only one azide per polymer chain, a large number of non-toxic glucose molecules. These synthesized dye incorporated polymers could be used to synthesize protein-polymer hybrids via biotin-avidin interaction.

Table 2.2: List of biotin-terminated polymers and copolymers synthesized

Name	Structure	M_n	M_w	PDI	Dye Loading
Poly(*tert*-butyl acrylate) (**11**)	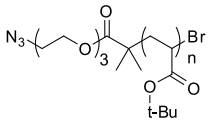	8,586	10,340	1.21	
Biotinylated Poly(*tert*-butyl acrylate) (**13**)	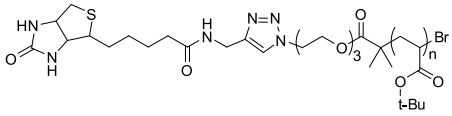	8,850	11,505	1.30	
Biotinylated Poly(acrylic acid) (**14**)	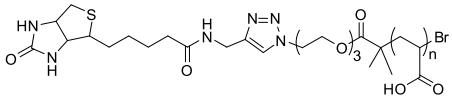	43,728	55,070	1.26	
Biotinylated Poly(NIRF dye)-poly(glucose) copolymer (**15**)	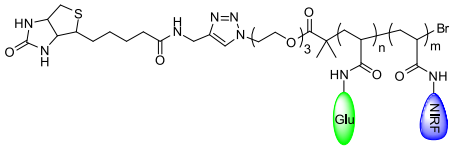	23,259	34,223	1.48	17 %
Biotinylated Poly(acrylic acid)-poly(NIRF dye) copolymer (1**6**)	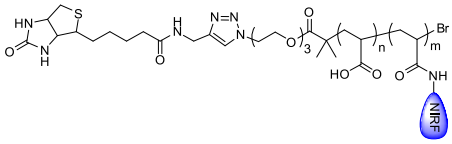	25,662	33,544	1.30	34 %

3.4. Azide and Alkyne terminated NIRF dye copolymers.

In the third synthetic methodology (**Scheme 1.3**) the azide-terminated polymer **11** was treated with TFA to produce PAA with azide chain end **17**. Absence of the proton shifts at 1.85 ppm confirms the complete deprotection of the *tert*-butyl group. The GPC molecular weight of azide-terminated PAA was higher compared to polymer **11**. This is expected as the pKa value of these type of water-soluble poly-carboxylic acids is lower. Due to hydration and as well as the deprotonated carboxy groups which tend to be away from one another, the hydrodynamic radius of this polymer will be much bigger. The FT-IR spectrum reveals intact azide moiety (2117 cm^{-1}) on the polymer. The pendant carboxylic acid side-chains of polymer **17** were grafted with NIRF-NH_2 and Glu-NH_2 via amide-coupling (EDC.HCl and HOBt) in DMF to produce poly(NIRF dye)-poly(glucose) copolymer **18**. Comparing the *Mn*=8586 of polymer **11** and *Mn*=19469 of polymer **18,** the percent of dyes per polymer chain were calculated. Employing the following equation the number of dye repeat unit per polymer chain was calculated: $\boldsymbol{ax + b(64 - x) = (Mn - c)}$. Where $\boldsymbol{x}$ = number of dyes per polymer chain, $\boldsymbol{a}$, $\boldsymbol{b}$ & $\boldsymbol{c}$ are Mol. wts. of dye repeat unit, sugar repeat unit and chain-ends respectively, and the percentage of dyes per polymer chain was calculated to be ~8%. The quantity of different compositions in the copolymer was further quantified by comparing the peak area of the protons from NIRF dye at 7.12-8.93 ppm and -CH_2-CH- protons from polymer backbone at 1.69-1.93 ppm, which the loading number of dye was 8.10%. FT-IR also confirmed the intact nature of the azide chain-end. This azide terminated poly(glucose)-(NIRF dye) copolymer could be conjugated to the alkyne modified proteins to form protein-polymer hybrids via 'click' bioconjugation reaction.

Scheme 2.3. Synthetic design towards azide/alkyne terminated NIRF dye incorporated polymers.

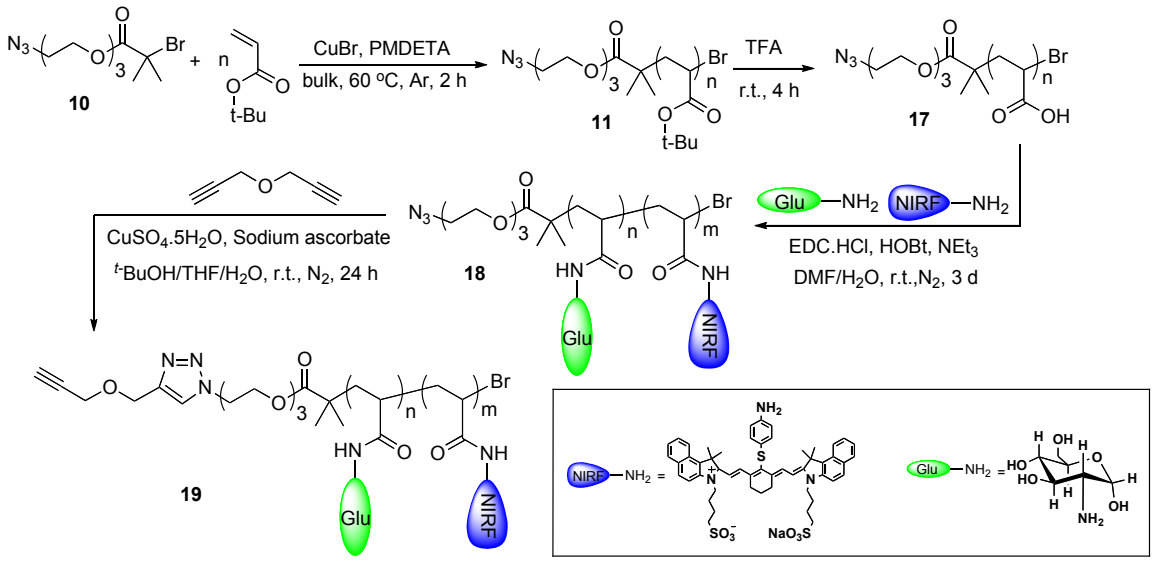

Furthermore, copolymer **18** was reacted with a large excess of di-propargyl ether under "click" conditions in presence of $CuSO_4.5H_2O$ and sodium ascorbate to convert the azide-terminated copolymer to an alkyne-terminated poly(NIRF dye)-poly(glucose) copolymer **19**. The absence of the azide peak (~2100 cm^{-1}) in the FT-IR spectra confirmed the conversion of all the azide-end groups to alkyne. Comparing the M_n =8586 of polymer **11** and M_n =19988 of polymer **19,** the percent of dyes per polymer chain were calculated to be 9%. Comparison of the peak area of the protons from dye at 7.15-8.33 ppm to that of -C*H*$_2$-C*H*- protons from main chain of polymer at 1.52-1.75 ppm resulted loading number of NIRF dye to be 8.7% which is comparable to the GPC result. The aklyne-terminated copolymer could be used to synthesize protein-polymer hybrids reacting at 'click' reaction conditions with azide-modified proteins. The rationale of synthesizing azide/alkyne terminated copolymer with triethylene glycol spacer was the accessibility of the polymer chian-end towards the further reactions. Please note that the

GPC mol. wt. of poly(acrylic acid) was found to be much higher than expected. This is quite normal as the PAAs are ionic in nature and have very low pKa and hence depending on the pH of the system the hydrodynamic radius change as well as the molecular weight.

Table 2.3: List of polymers and copolymers synthesized

Name	Structure	M_n	M_w	PDI	Dye Loading
Azido Poly(acrylic acid) (**17**)	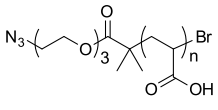	42,423	50,570	1.19	
Azido Poly(NIRF dye)-poly(glucose) copolymer (**18**)	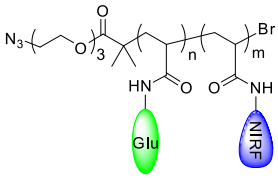	19,469	25,074	1.28	8 %
Alkyne Poly(NIRF dye)-poly(glucose) copolymer (**19**)	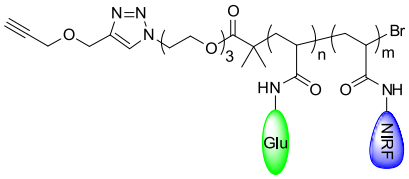	19,988	28,168	1.40	9 %

4. CONCLUSION

In this study we have overcome two fundamental limitations in the synthesis of bioconjugates: (a) the basic restriction in the diversity of copolymers which can be synthesized for producing bioconjugates and (b) the limitation that only a small number of dyes/drug molecules can be attached per protein molecule. Our approach towards these copolymers involves three steps: (1) the synthesis of well-defined living polymers containing reactive chain-end and functional side-chain pendant groups in which the chain end and side chain possesses orthogonal reactivity, (2) the attachment of a number of water soluble, biocompatible moieties and imaging/therapeutic agents to the functional polymer side-chains. To demonstrate our synthetic strategy, three parallel synthetic designs were employed. In the first design, a polymer of well-defined chain length was synthesized with *tert*-butyl acrylate via ATRP comprising of reactive chain-end (azide) and functional side-chain (ester; easily converted to carboxylic acid). Further, via a one pot amidation of poly acrylic acid with NIRF-NH_2 and Glu-NH_2, poly(NIRF dye)-poly(glucose) copolymers with reactive chain ends were synthesized. Several copolymers containing different level of NIRF dye loadings were synthesized and characterized via NMR, FT-IR and GPC techniques. In the second design azide-terminated poly(*tert*-butyl acrylate) was synthesized and further it was clicked with biotin-alkyne to produce biotinylated polymer. After deprotection the pendant carboxylic acid groups were employed via amidation reaction with NIRF-NH_2 and Glucosamine to produce water-soluble copolymers. The biotin chain-end is specific towards the avidin and this fact could be used to produce protein-polymer hybrids. The synthesized polymers and copolymers were successfully characterized via NMR, FT-IR and GPC techniques. In the third methodology azido-ethyleneglycol terminated poly(NIRF dye)-poly(glucose)

copolymer was synthesized. The azide end-group was easily converted to alkyne reacting with dipropargyl ether via 'click' reaction. NMR, FT-IR and GPC techniques were employed to characterize the synthesized copolymers. The azide/alkyne terminated copolymers could be conjugated to alkyne/azide surface modified proteins via 'click' bioconjugation reaction to produce drug/dye incorporated protein-polymer hybrids. The copolymers could be immobilized for potential multiwell plate based assay experiments. The resulting immobilized neoglycopolymers can interact with complementary cell surface receptors/lectins and a convenient platform to study carbohydrate-receptor interactions can be created; by varying the carbohydrates in the polymer and by using dye modified lectins/cell receptors which are Fluorescence Resonance Energy Transfer partners for the NIRF dye on the polymers, a range of lectin /cell receptor interactions can be explored. The synthesized copolymers could be utilized for *in vitro* and *in vivo* imaging. This general synthetic methodology could be utilized to produce a range of bioactive copolymers and protein/antibody conjugates for applications ranging from tissue specific imaging to targeted drug delivery.

5. SPECTRAL CHARACTERIZATION DATA (^{1}H NMR, ^{13}C NMR, FT-IR)

^{1}H NMR of 1

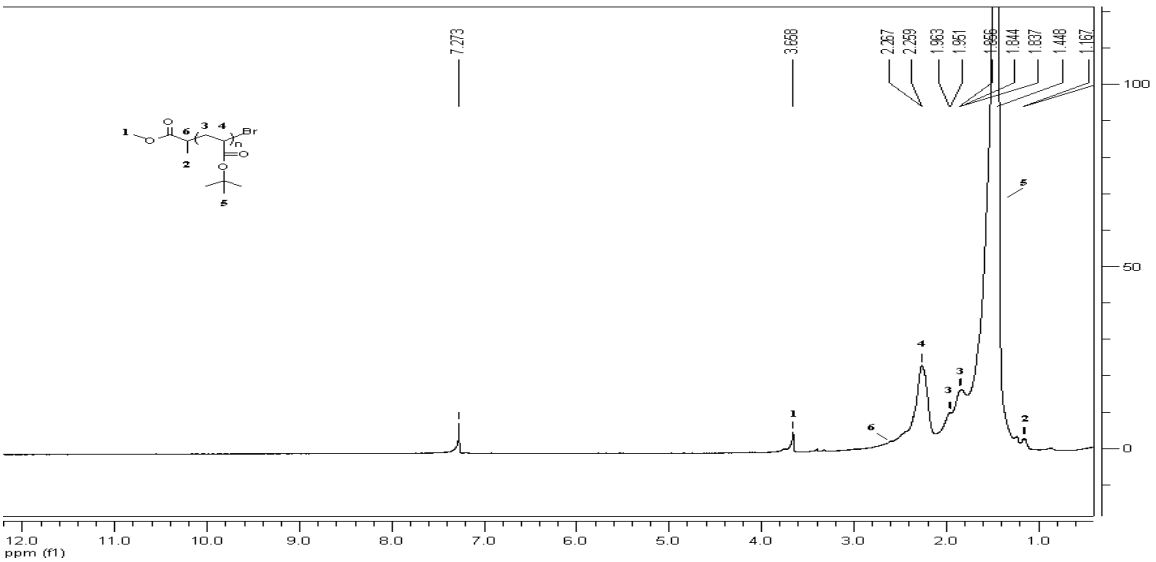

FTIR of 1

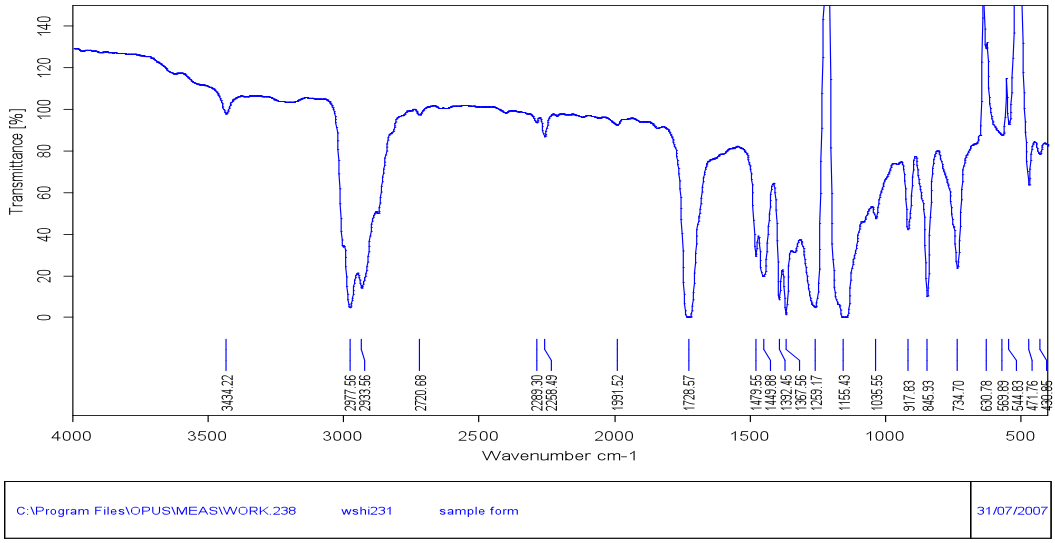

^{1}H NMR 2

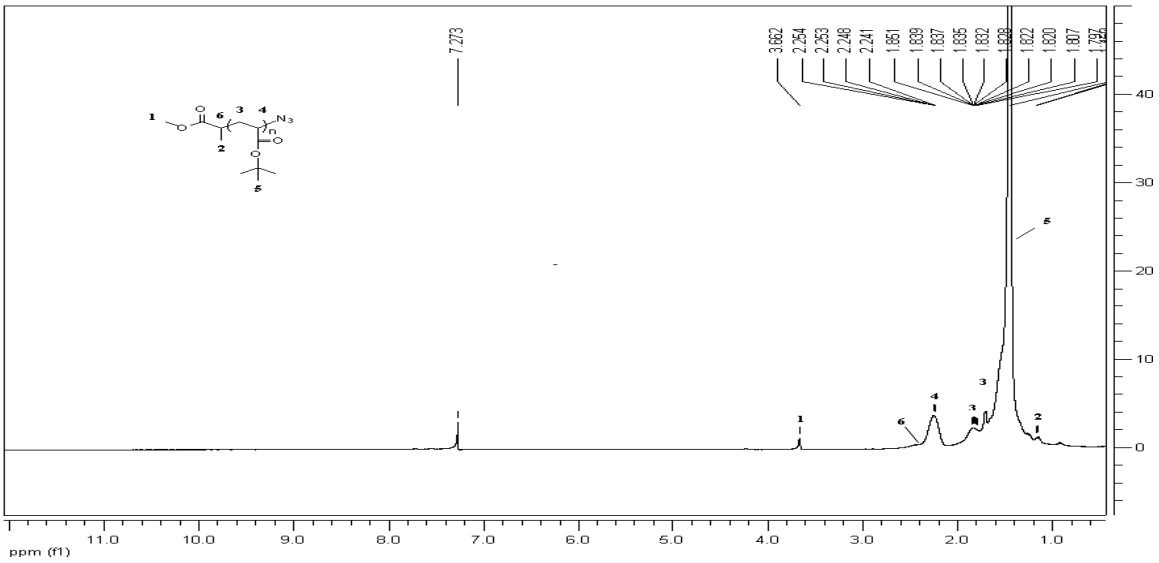

FTIR 2

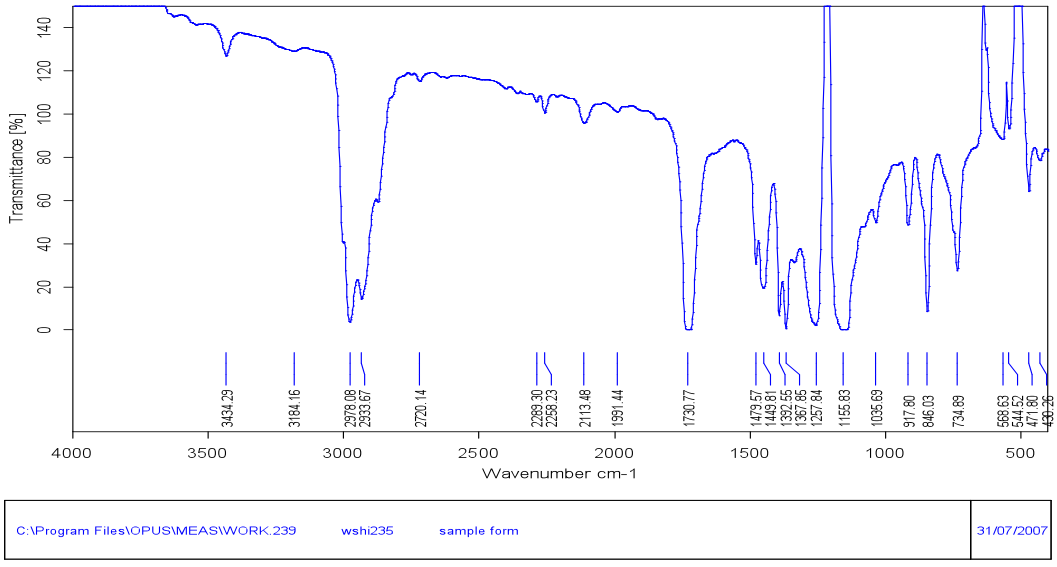

^{1}H NMR 4

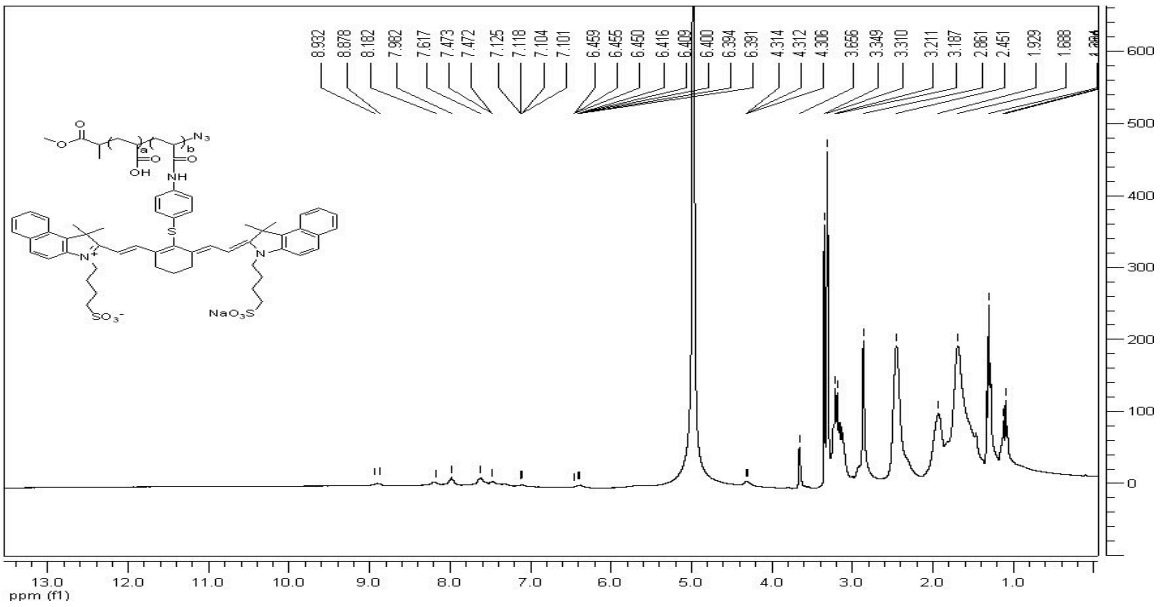

FT-IR of 4

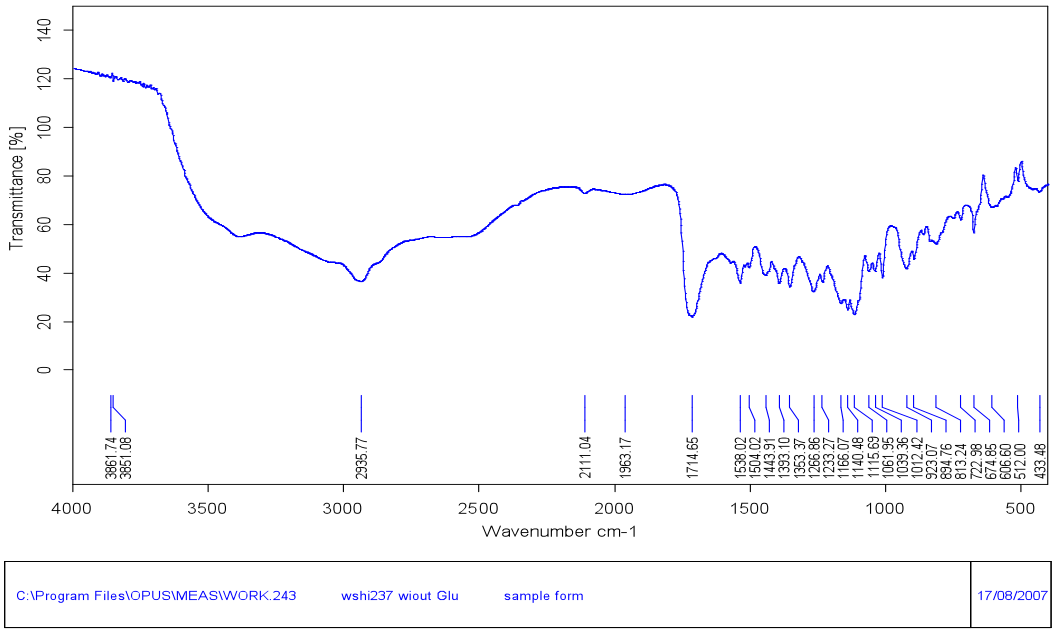

^{1}H NMR of 5

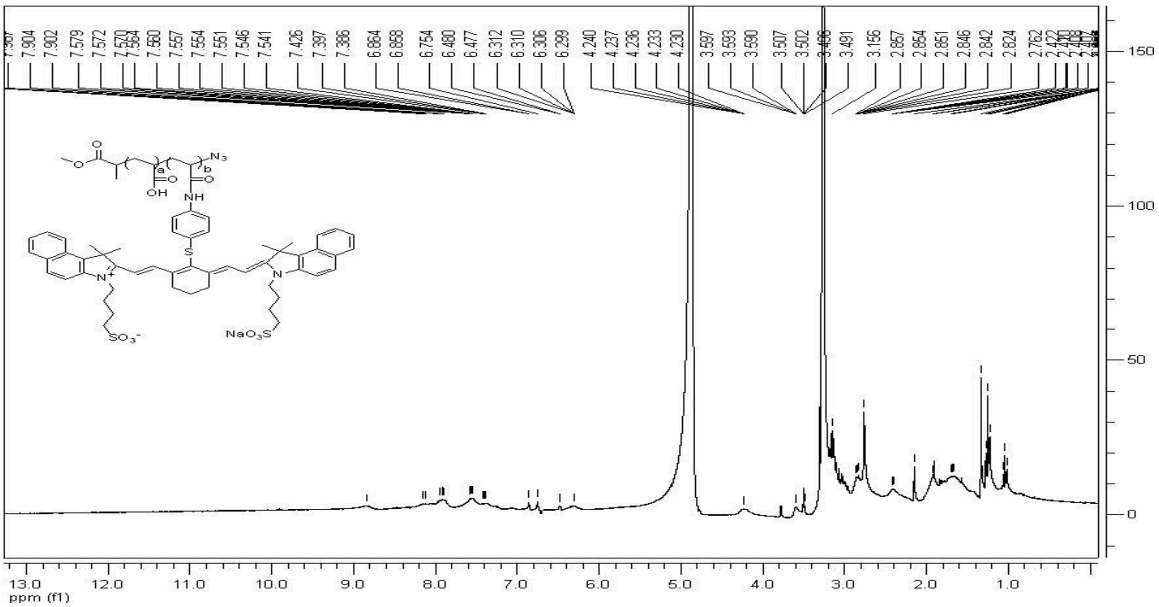

FT-IR of 5

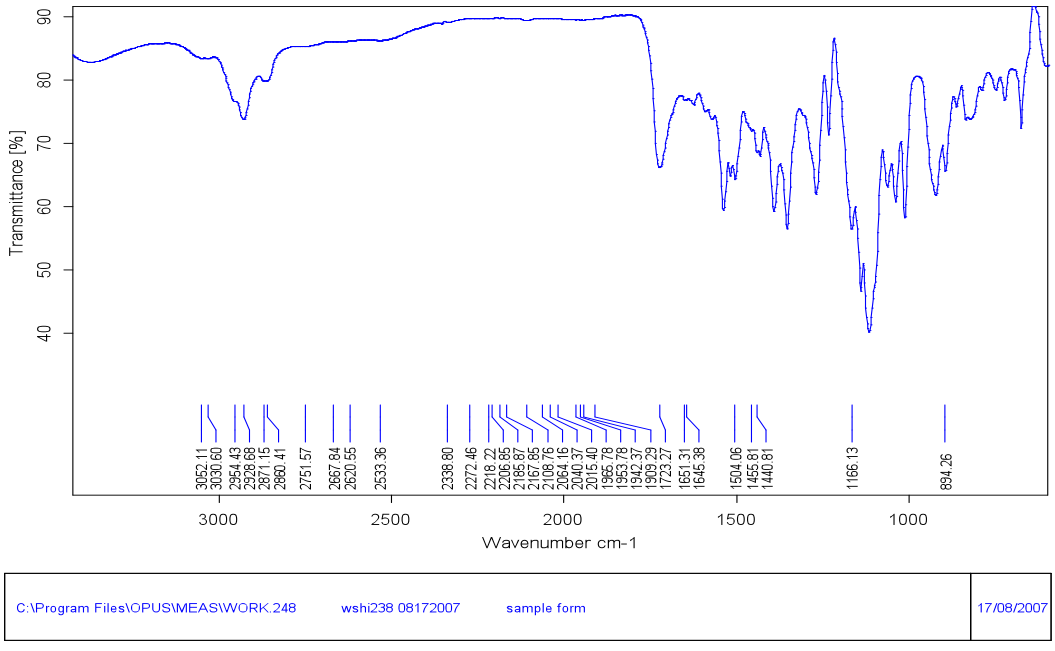

^{1}H NMR of 6

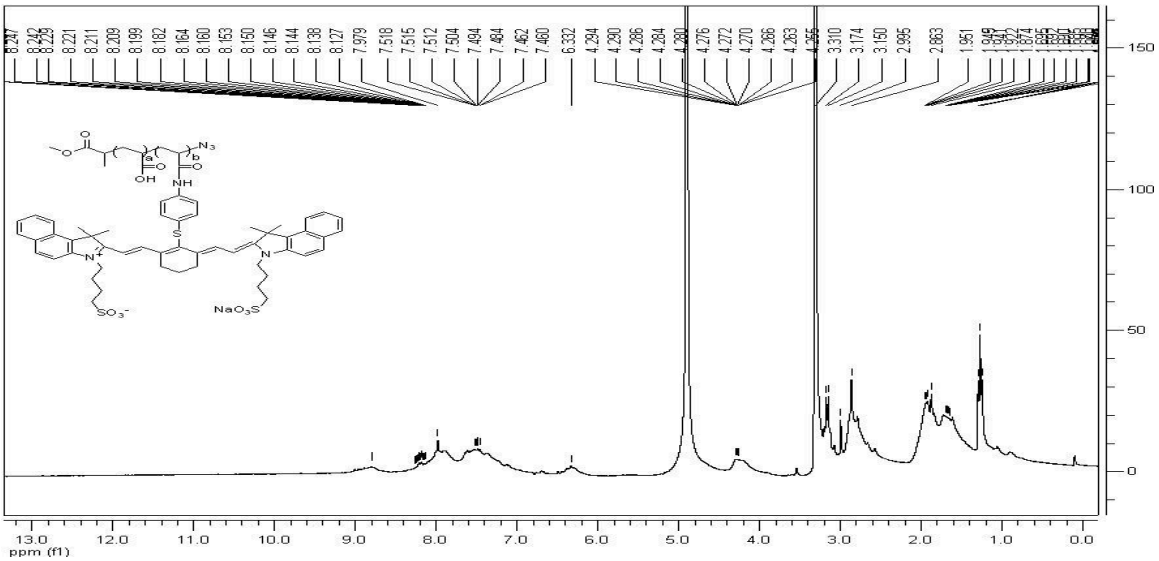

FT-IR of 6

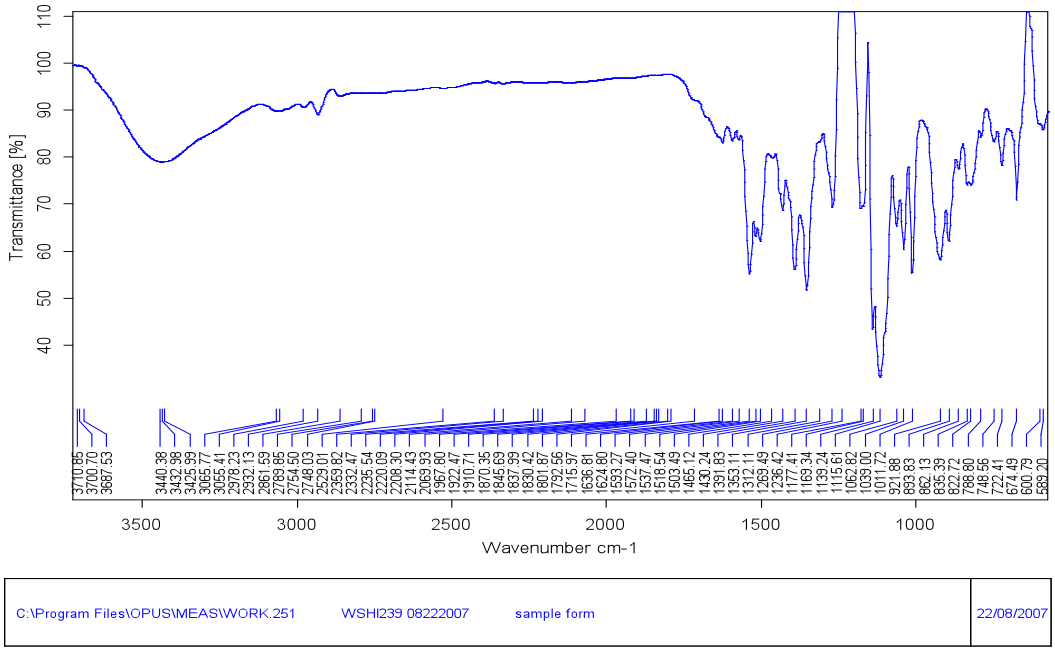

^{1}H NMR of 7

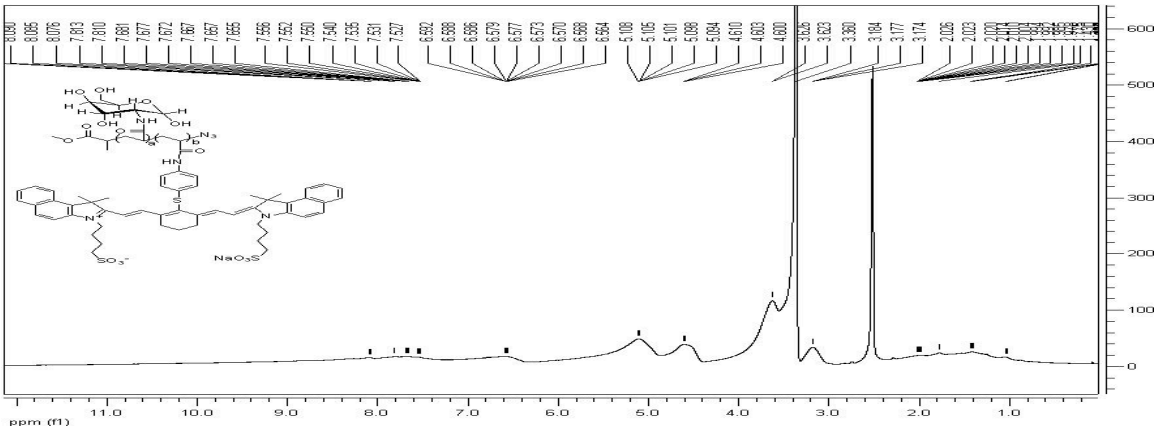

^{1}H NMR of 8

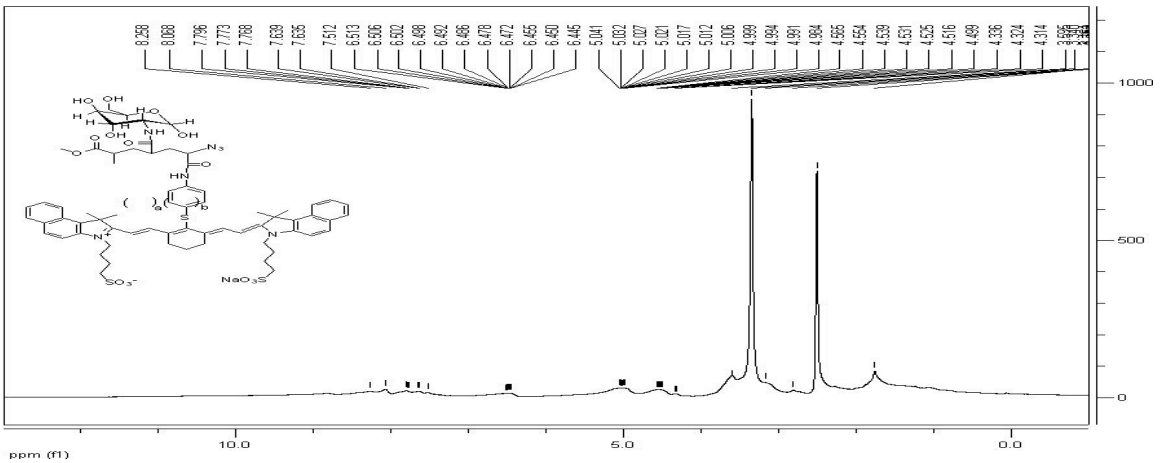

^{1}H NMR of 9

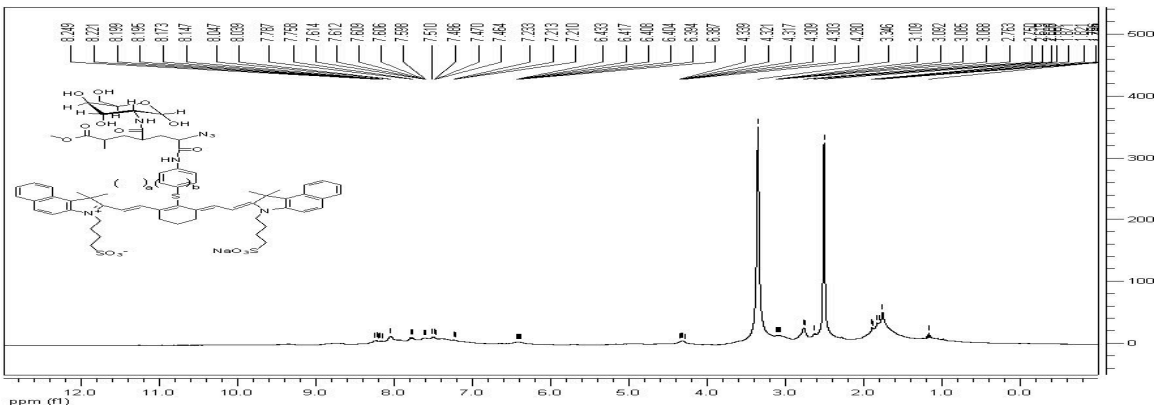

^{1}H NMR

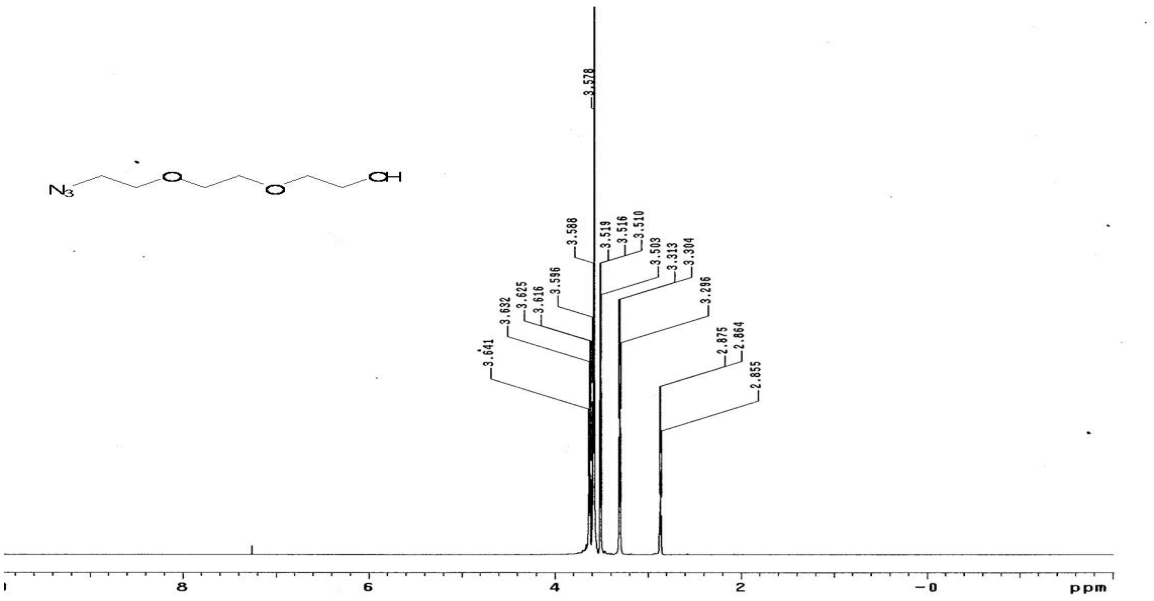

^{13}C NMR

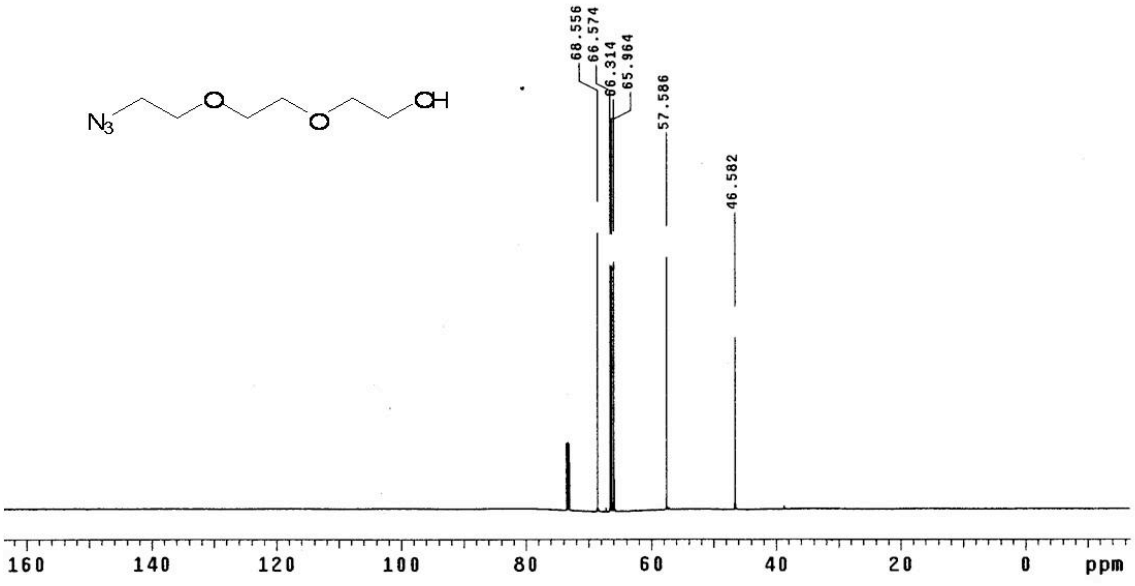

^{1}H NMR of 10

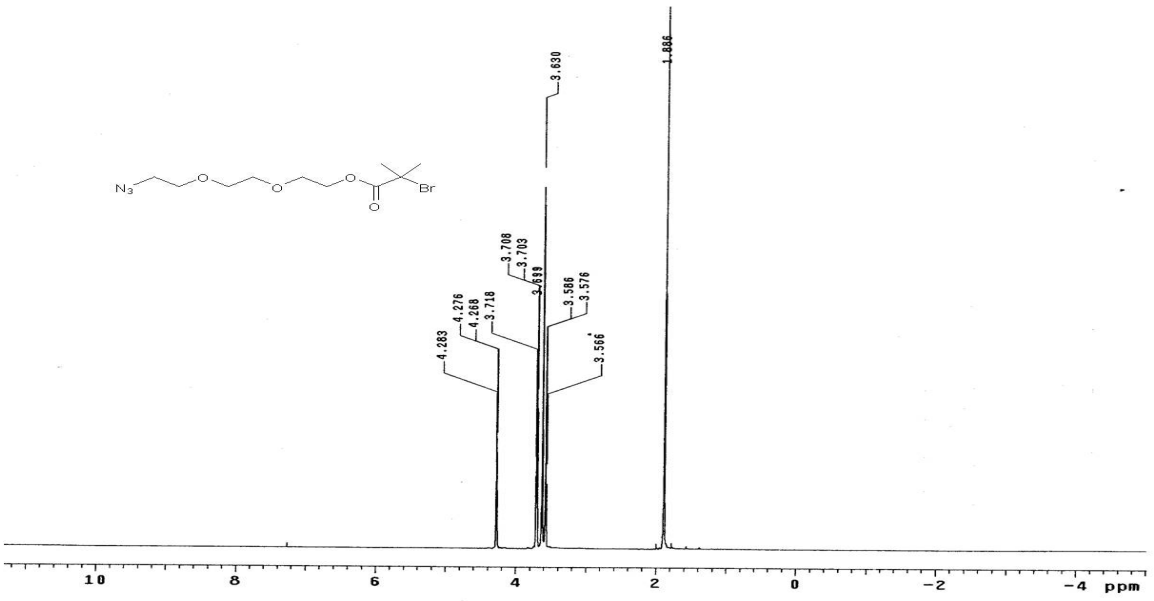

^{13}C NMR of 10

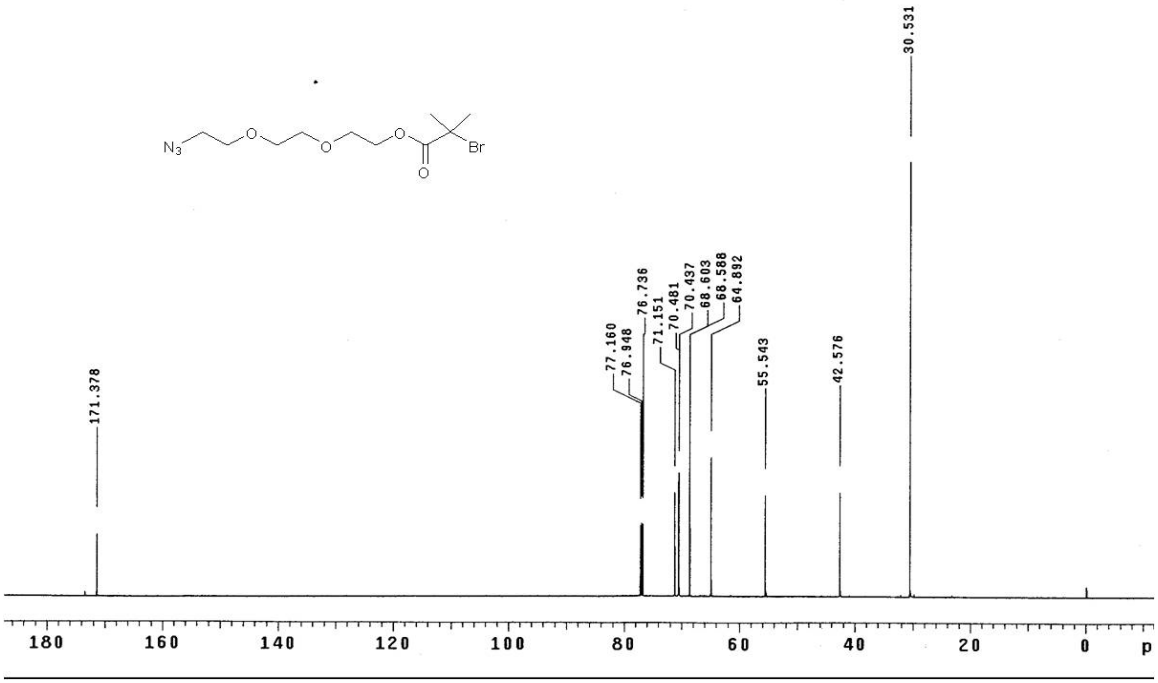

^{1}H NMR of 11

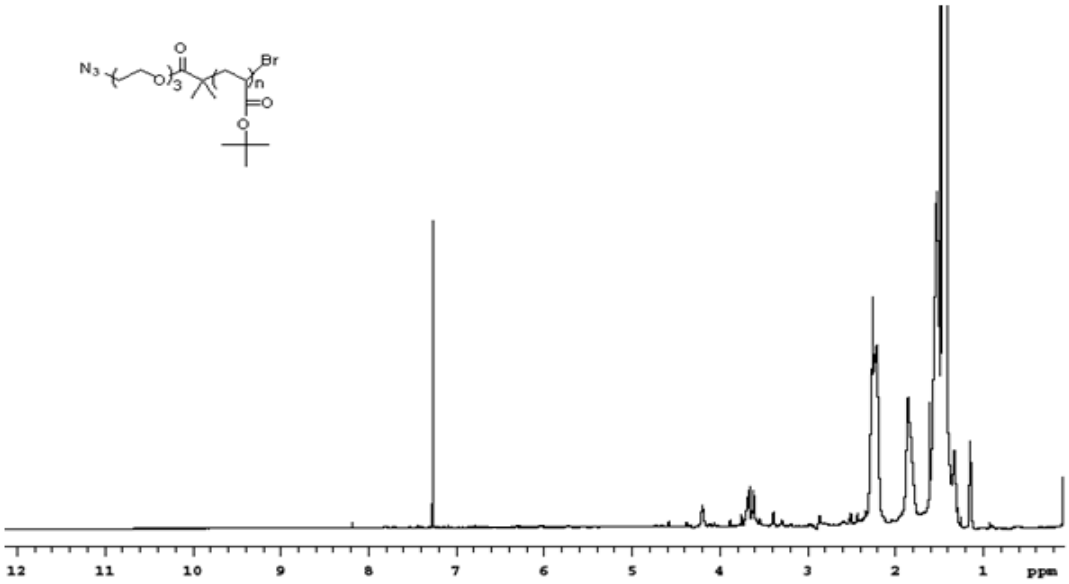

FT-IR of 11

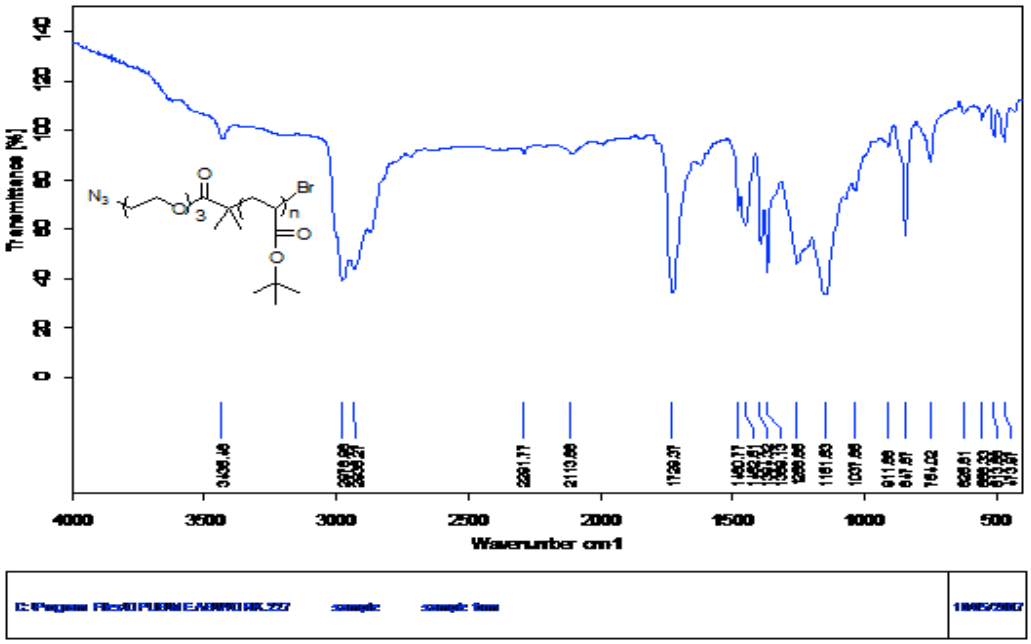

^{1}H NMR of 12

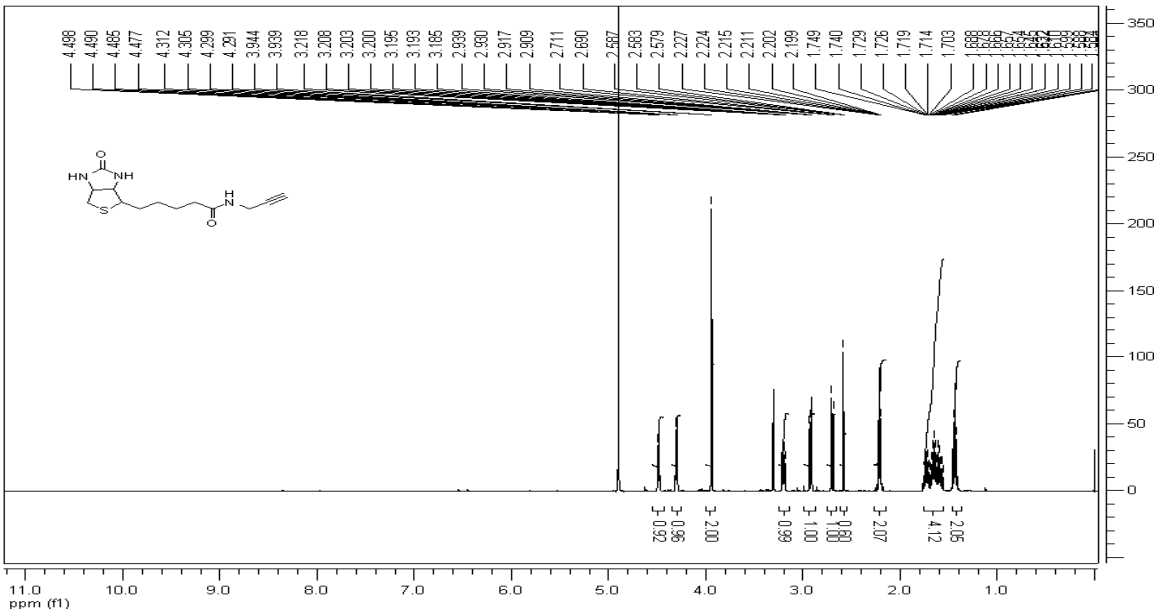

^{13}C NMR of 12

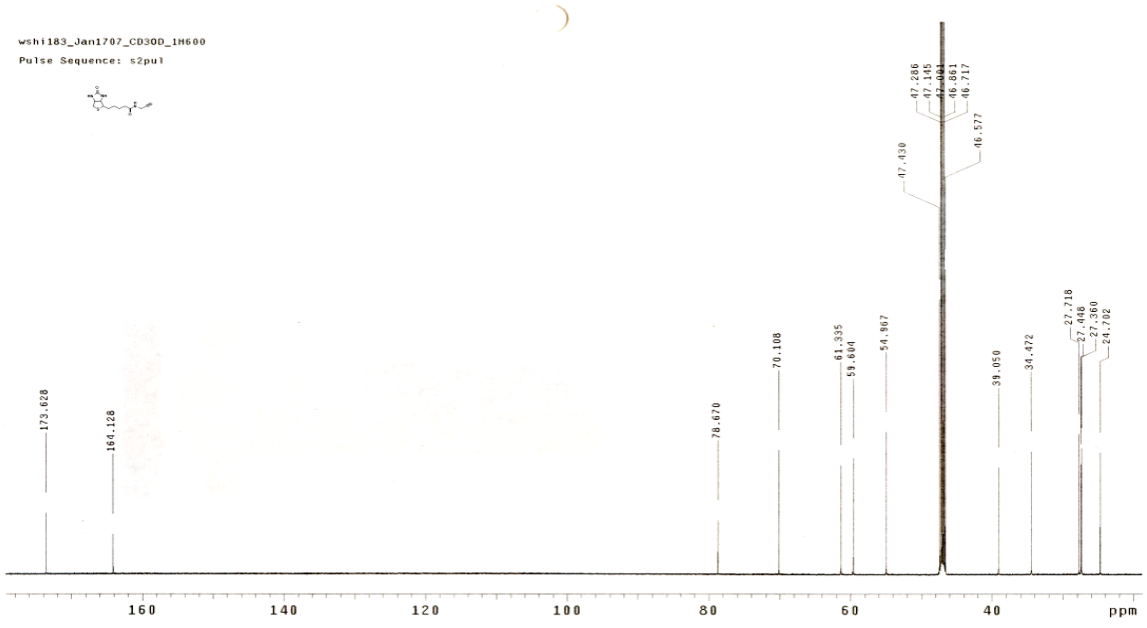

^{1}H NMR of 13

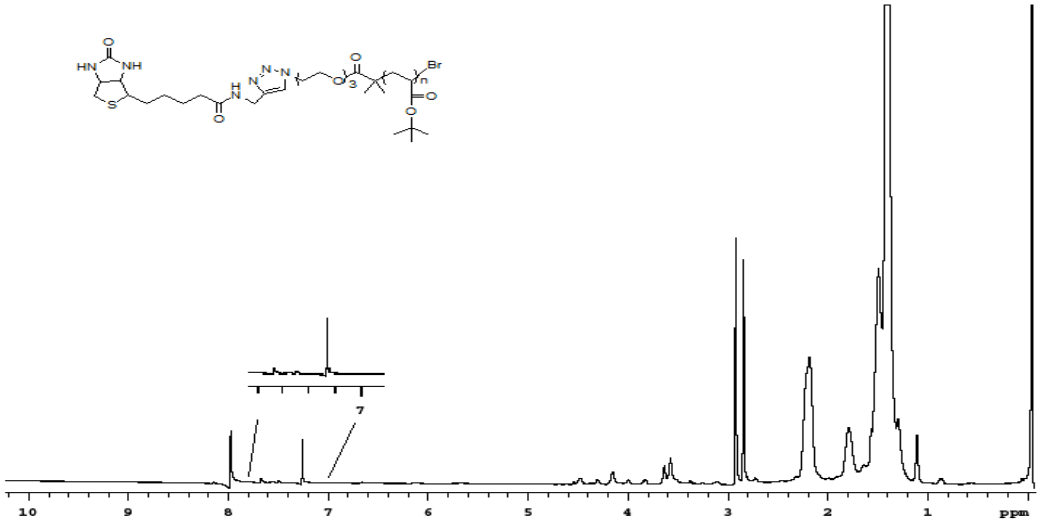

FT-IR of 13

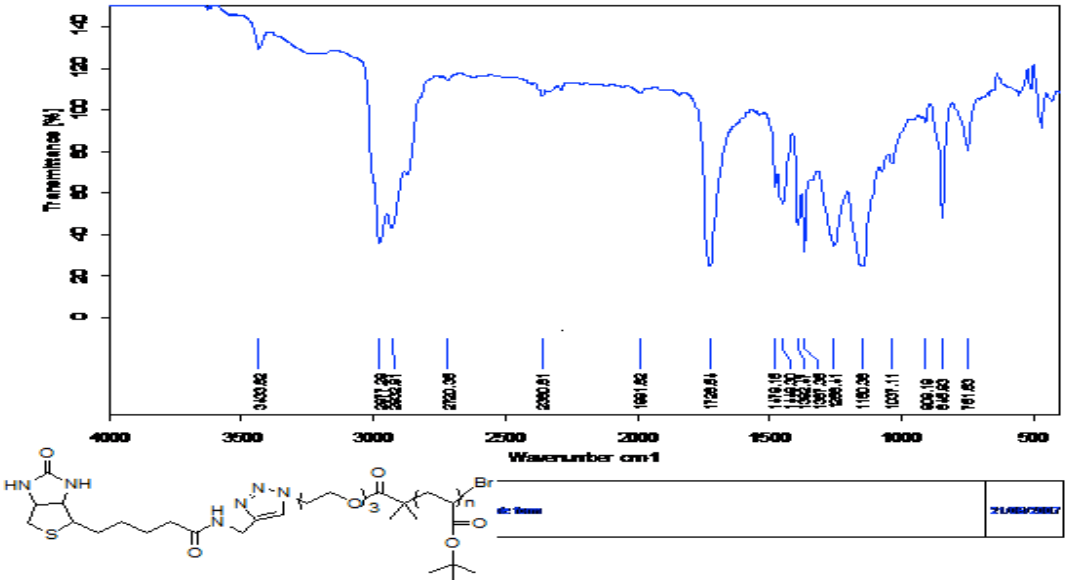

^{1}H NMR of 14

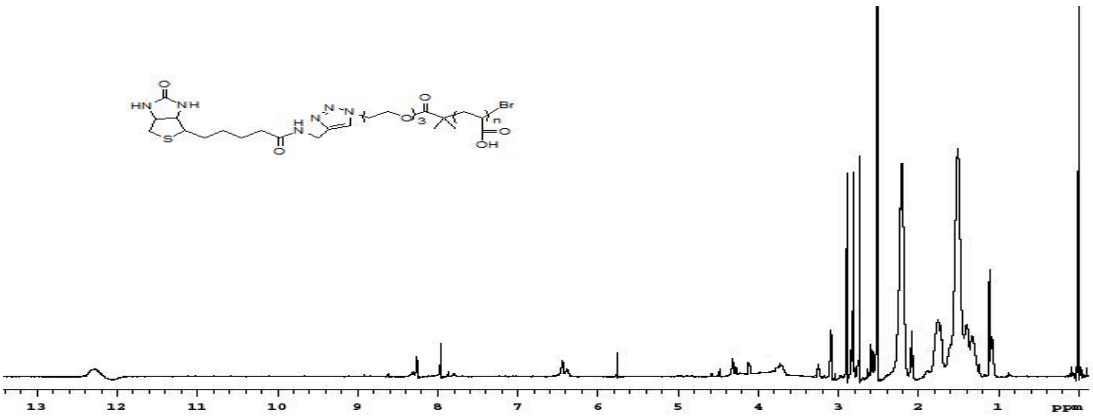

^{1}H NMR of 15

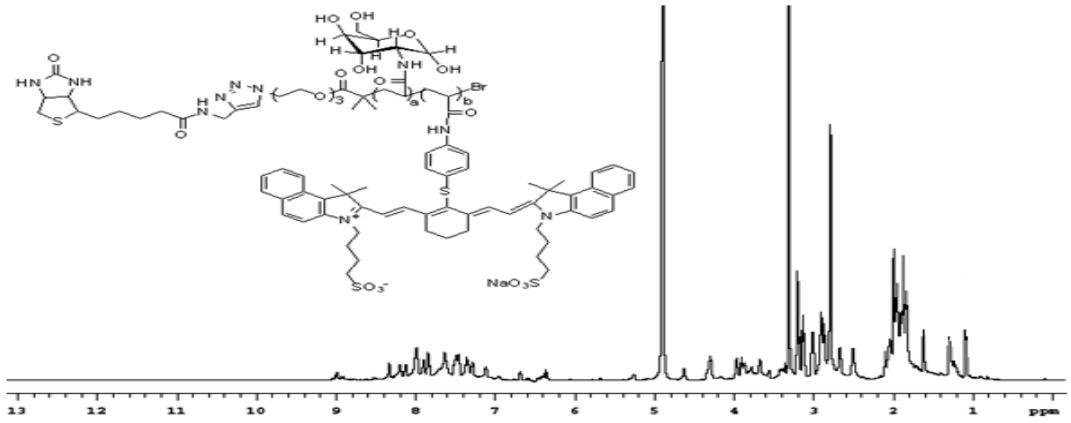

^{1}H NMR of 16

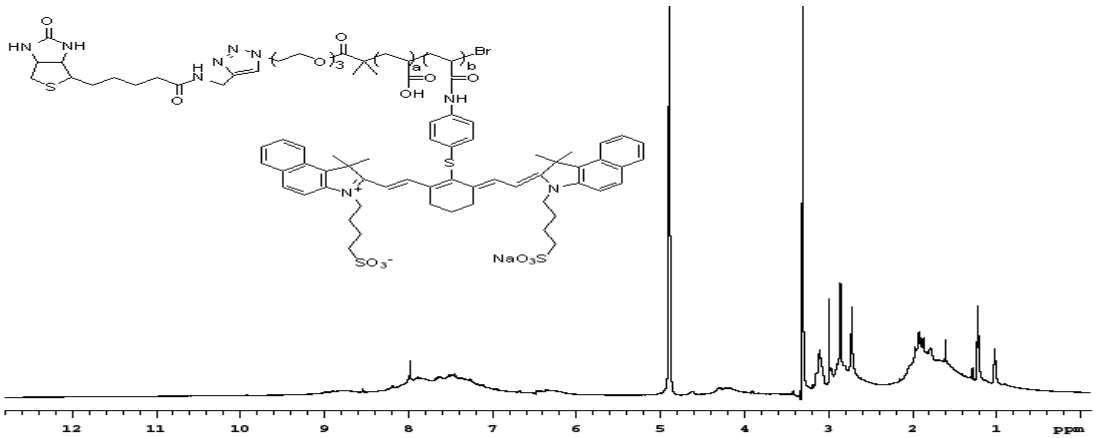

^{1}H NMR of 17

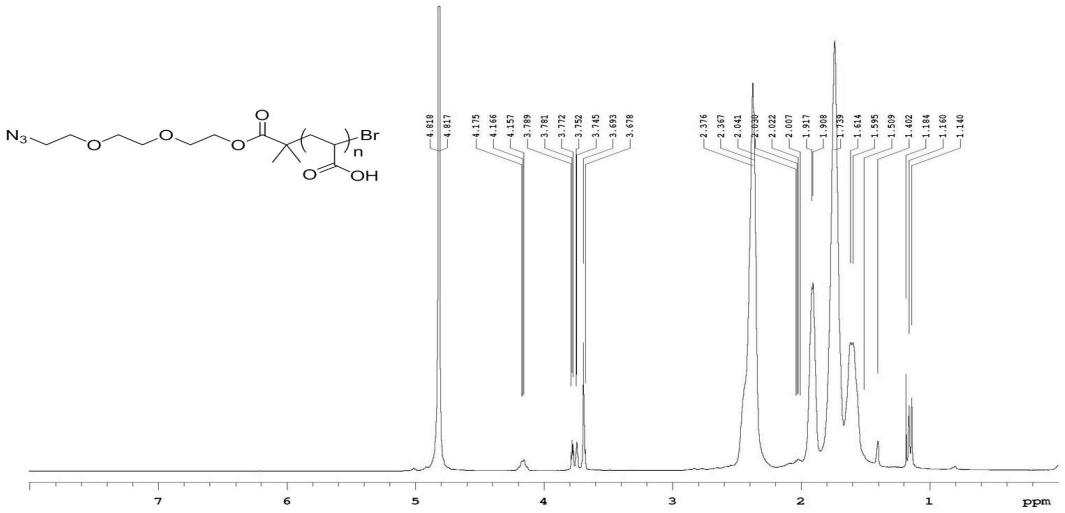

FT-IR of 17

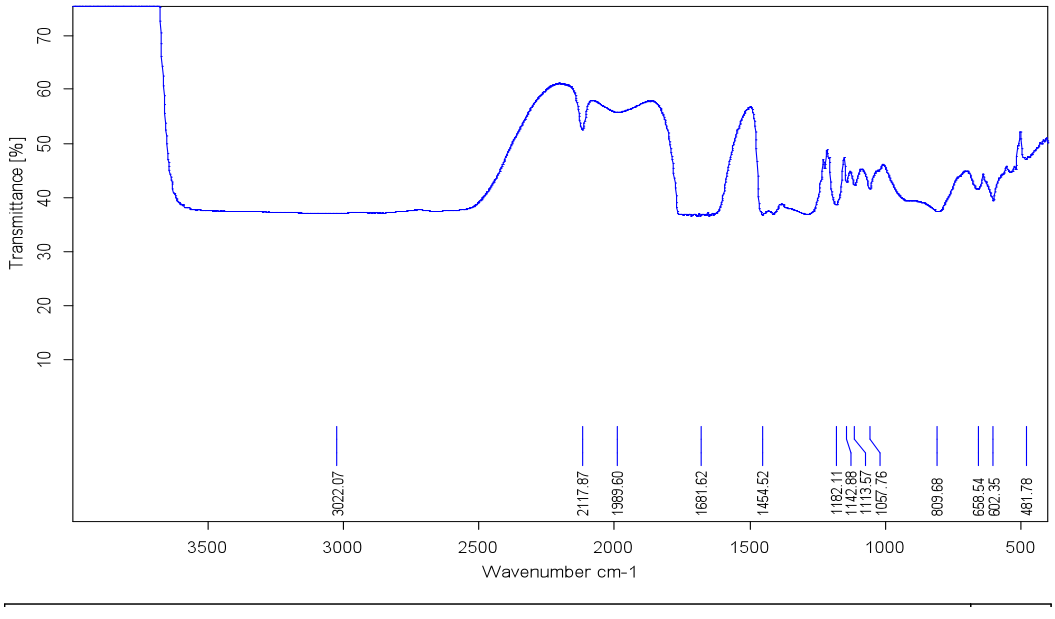

^{1}H NMR of 18

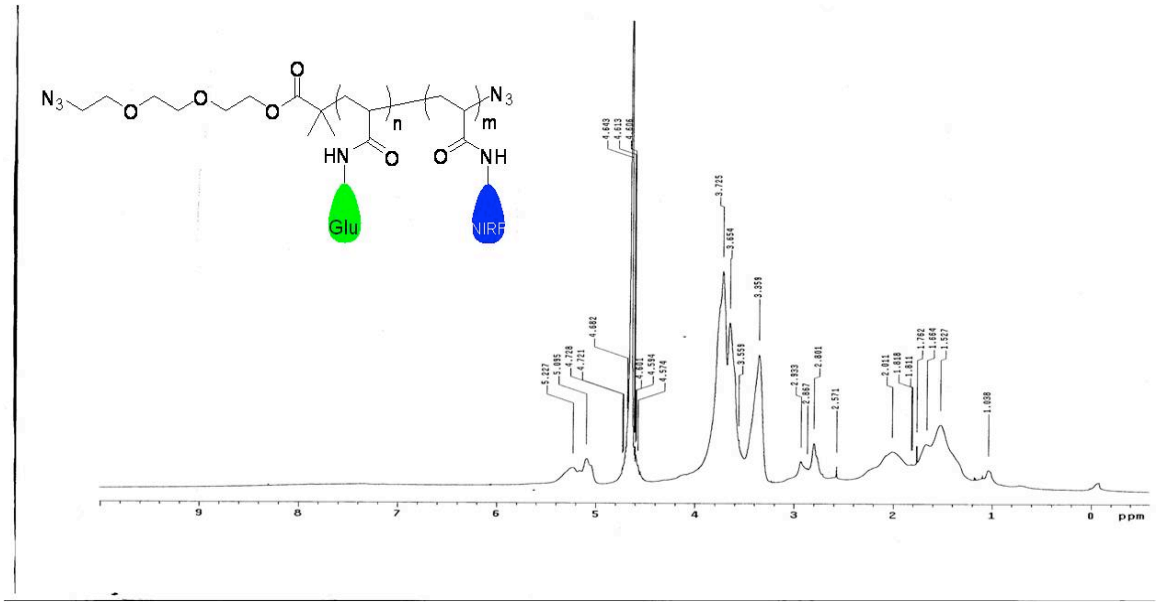

FT-IR of 18

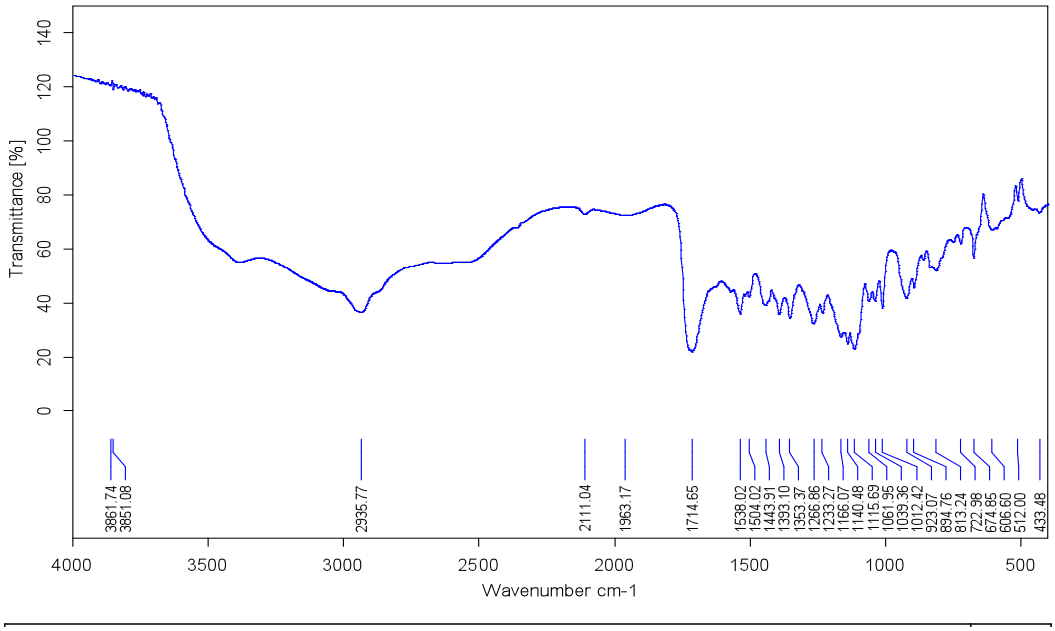

^{1}H NMR of 19

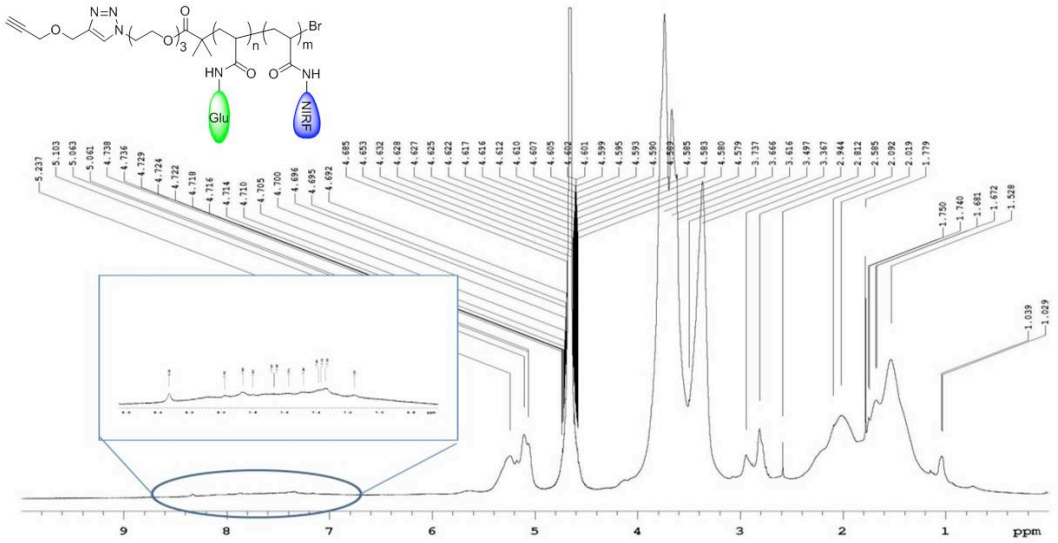

FT-IR of 19

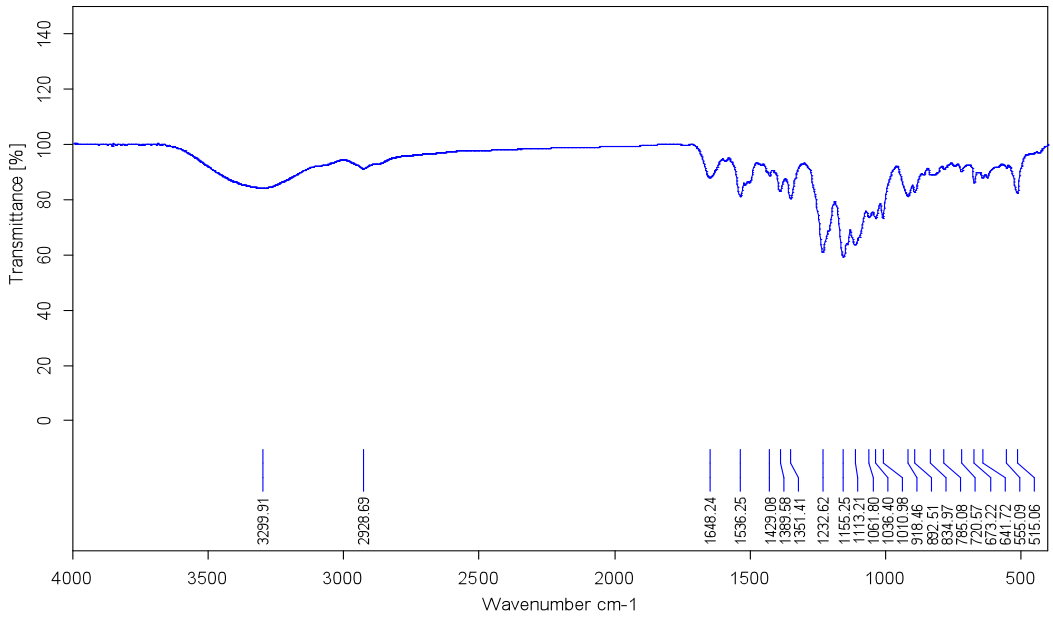

6. REFERENCES

(1) Ehrlich, P. (1960) *The Collected Papers of Paul Ehrlich*, Pergamon, London.

(2) Mullin, R. (2005) *C&En. 83*.

(3) Hata, K. (2006) Efficacy of Mylotarg for acute myeloid leukemia. *Annual Review Ketsueki*, 114-123.

(4) Wu, A. M., and Senter, P. D. (2005) Arming antibodies: prospects and challenges for immunoconjugates. *Nat Biotechnol 23*, 1137-46.

(5) Hermenson, G. T. (2008) *Bioconjugate Techniques, 2nd Ed.*, Academic Press, San Diego, California.

(6) Raja, K., McDonald, R., Tuck, S., Rodriguez, R., Milley, B., and Traquina, P. (2007) One-pot synthesis, purification, and formulation of bionanoparticle-CpG oligodeoxynucleotide hepatitis B surface antigen conjugate vaccine via tangential flow filtration. *Bioconjug Chem 18*, 285-8.

(7) Raja, K. S., Wang, Q., Gonzalez, M. J., Manchester, M., Johnson, J. E., and Finn, M. G. (2003) Hybrid virus-polymer materials. 1. Synthesis and properties of PEG-decorated cowpea mosaic virus. *Biomacromolecules 4*, 472-6.

(8) Shi, W., Dolai, S., Rizk, S., Hussain, A., Tariq, H., Averick, S., L'Amoreaux, W., El ldrissi, A., Banerjee, P., and Raja, K. (2007) Synthesis of monofunctional curcumin derivatives, clicked curcumin dimer, and a PAMAM dendrimer curcumin conjugate for therapeutic applications. *Org Lett 9*, 5461-4.

(9) Hannink, J. M., Cornelissen, J. J., Farrera, J. A., Foubert, P., De Schryver, F. C., Sommerdijk, N. A., and Nolte, R. J. (2001) Protein-Polymer Hybrid Amphiphiles. *Angew Chem Int Ed Engl 40*, 4732-4734.

(10) Velonia, K., Rowan, A. E., and Nolte, R. J. (2002) Lipase polystyrene giant amphiphiles. *J Am Chem Soc 124*, 4224-5.

(11) Kochendoerfer, G. G., Chen, S. Y., Mao, F., Cressman, S., Traviglia, S., Shao, H., Hunter, C. L., Low, D. W., Cagle, E. N., Carnevali, M., Gueriguian, V., Keogh, P. J., Porter, H., Stratton, S. M., Wiedeke, M. C., Wilken, J., Tang, J., Levy, J. J., Miranda, L. P., Crnogorac, M. M., Kalbag, S., Botti, P., Schindler-Horvat, J., Savatski, L., Adamson, J. W., Kung, A., Kent, S. B., and Bradburne, J. A. (2003) Design and chemical synthesis of a homogeneous polymer-modified erythropoiesis protein. *Science 299*, 884-7.

(12) Kovar, M., Strohalm, J., Etrych, T., Ulbrich, K., and Rihova, B. (2002) Star structure of antibody-targeted HPMA copolymer-bound doxorubicin: a novel type of polymeric conjugate for targeted drug delivery with potent antitumor effect. *Bioconjug Chem 13*, 206-15.

(13) Kulkarni, S., Schilli, C., Grin, B., Muller, A. H., Hoffman, A. S., and Stayton, P. S. (2006) Controlling the aggregation of conjugates of streptavidin with smart block copolymers prepared via the RAFT copolymerization technique. *Biomacromolecules 7*, 2736-41.

(14) Sen Gupta, S., Raja, K. S., Kaltgrad, E., Strable, E., and Finn, M. G. (2005) Virus-glycopolymer conjugates by copper(I) catalysis of atom transfer radical polymerization and azide-alkyne cycloaddition. *Chem Commun (Camb)*, 4315-7.

(15) Sen Gupta, S., Kuzelka, J., Singh, P., Lewis, W. G., Manchester, M., and Finn, M. G. (2005) Accelerated bioorthogonal conjugation: a practical method for the

ligation of diverse functional molecules to a polyvalent virus scaffold. *Bioconjug Chem 16*, 1572-9.

(16) Hou, S., Sun, X. L., Dong, C. M., and Chaikof, E. L. (2004) Facile synthesis of chain-end functionalized glycopolymers for site-specific bioconjugation. *Bioconjug Chem 15*, 954-9.

(17) Vazquez-Dorbatt, V., and Maynard, H. D. (2006) Biotinylated glycopolymers synthesized by atom transfer radical polymerization. *Biomacromolecules 7*, 2297-302.

(18) Lele, B. S., Murata, H., Matyjaszewski, K., and Russell, A. J. (2005) Synthesis of uniform protein-polymer conjugates. *Biomacromolecules 6*, 3380-7.

(19) De, P., Li, M., Gondi, S. R., and Sumerlin, B. S. (2008) Temperature-regulated activity of responsive polymer-protein conjugates prepared by grafting-from via RAFT polymerization. *J Am Chem Soc 130*, 11288-9.

(20) Bontempo, D., Heredia, K. L., Fish, B. A., and Maynard, H. D. (2004) Cysteine-reactive polymers synthesized by atom transfer radical polymerization for conjugation to proteins. *J Am Chem Soc 126*, 15372-3.

(21) Bontempo, D., and Maynard, H. D. (2005) Streptavidin as a Macroinitiator for Polymerization: In Situ Protein-Polymer Conjugate Formation. *Journal of the American Chemical Society 127*, 6508-6509.

(22) Geng, J., Mantovani, G., Tao, L., Nicolas, J., Chen, G., Wallis, R., Mitchell, D. A., Johnson, B. R., Evans, S. D., and Haddleton, D. M. (2007) Site-directed conjugation of "clicked" glycopolymers to form glycoprotein mimics: binding to

mammalian lectin and induction of immunological function. *J Am Chem Soc 129*, 15156-63.

(23) Law, K.-Y. (1993) Organic photoconductive materials: recent trends and developments. *Chemical Reviews 93*, 449-486.

(24) Fabian, J., Nakazumi, H., and Matsuoka, M. (1992) Near-infrared absorbing dyes. *Chemical Review 92*, 1197-1226.

(25) Mishra, A., Behera, R. K., Behera, P. K., Mishra, B. K., and Behera, G. B. (2000) Cyanines during the 1990s: A Review. *Chem Rev 100*, 1973-2012.

(26) Zhao, W., and Carreira, E. M. (2005) Conformationally restricted aza-bodipy: a highly fluorescent, stable, near-infrared-absorbing dye. *Angew Chem Int Ed Engl 44*, 1677-9.

(27) Patonay, G., Salon, J., Sowell, J., and Strekowski, L. (2004) Noncovalent labeling of biomolecules with red and near- infrared dyes. *Molecules 9*, 40-9.

(28) Tung, C. H. (2004) Fluorescent peptide probes for in vivo diagnostic imaging. *Biopolymers 76*, 391-403.

(29) Zaheer, A., Lenkinski, R. E., Mahmood, A., Jones, A. G., Cantley, L. C., and Frangioni, J. V. (2001) In vivo near-infrared fluorescence imaging of osteoblastic activity. *Nat Biotechnol 19*, 1148-54.

(30) Wang, J.-S., and Matyjaszewski, K. (1995) Controlled/"living" radical polymerization. atom transfer radical polymerization in the presence of transition-metal complexes. *Journal of the American Chemical Society 117*, 5614-5615.

(31) Shi, W., Dolai, S., Averick, S., Fernando, S. S., Saltos, J. A., L'Amoreaux, W., Banerjee, P., and Raja, K. (2009) A General Methodology Toward Drug/Dye

Incorporated Living Copolymer-Protein Hybrids: (NIRF Dye-Glucose) Copolymer-Avidin/BSA Conjugates as Prototypes. *Bioconjug Chem*, 1595–1601.

(32) Luxenhofer, R., and Jordan, R. (2006) Click Chemistry with Poly(2-oxazoline)s. . *Macromolecules 39*, 3509-3516.

CHAPTER III

Synthesis and Applications of Drug/Dye Incorporated Copolymer-Protein Hybrids.

1. INTRODUCTION

The synthesis of well-defined polymer-protein/peptide hybrids is a rich and newly emerging field of research. These hybrid materials have potential applications in medical, biopharmaceutical and other life science areas (*1-5*). Modification or attachment of synthetic polymers with proteins is beneficial for both *in vivo* and *in vitro* applications. Polymer modification of proteins can induce increased biocompatibility, lower immune response, increase in *in vivo* stability, and delayed clearance by the reticuloendothelial system (*6*). Polymer attachment can provide cryoprotection for low-temperature sensitive proteins. Surface modification by polymers can also effectively mask the intrinsic characteristics of the surface preventing nonspecific protein adsorption (*6*). Although polymer modification of proteins, especially PEGylation, has proved to be effective, the enzymatic and in vivo activity of the modified protein essentially depend on number, length, and architecture (linear, branched, or dendrimeric) of the polymer chains as well as on the polymer attachment site (*7-11*). Particularly, the polymer attachment can lead to significant loss of biological activity if the polymer is nonspecifically attached to the active center. A significant loss of biological activity was observed when commercially available polydisperse polymers with various degrees of functionality were used towards these hybrid materials (*12*). The use of polydisperse polymers often resulted in introduction of heterogeneity in the resulting hybrid with multiple PEG conjugation or protein crosslinking (*13*). FDA approval requires precisely defined conjugates especially for medical or pharmaceutical applications (*14*). Therefore, a significant challenge is still present in the form of designing the protein-polymer conjugates and also optimization is required for each biomolecule (especially considering the size, function, tertiary

structure, and the availability of the specific functionality on the biomoelcule) (*15*). To overcome this, several strategies like the control of chemical conditions such as use of precise protein-to-polymer ratios, use of controlled polymerization methods as well as the development of site-specific conjugation methods has been reported (*15, 16*).

For example, the Maynard group (*17-20*), Francis group (*21-24*), and others (*25-28*) have demonstrated several elegant approaches using controlled radical polymerization methods such as atom transfer radical polymerization (ATRP) and reversible addition-fragmentation chain transfer (RAFT) for synthesizing well-defined protein–polymer conjugates and controlling the protein behavior in the resulting hybrids. An extensive review by Haddleton and co-workers covers recent work describing the attachment of living synthetic polymers to peptides and proteins (*2*); (a) A "grafting to" approach which involves the reaction between a preformed synthetic polymer and a protein: Poly methacryloxy ethyl glucoside with a fluorescein alkyne chain end has been synthesized and attached to the cowpea mosaic virus (CPMV) via the azide-alkyne triazole forming "click" bioconjugation reaction, there are other examples of this strategy (*29, 30*) (b) The "grafting from" approach: where the peptide/protein acts as a macro-initiator and the polymer chain grows from the macroinitator: the use of streptavidin as a macroinitiator for the polymerization of *N*-isopropylacrylamide (NIPAM) and poly(ethylene glycol) methyl ether methacrylate (PEGMA) and other similar reports demonstrate this strategy (*31, 32*). (c) The "grafting through" method: where peptide macromonomers are polymerized, for example Val-Pro-Gly-Val-Gly (VPGVG) methacrylate was polymerized via ATRP to produce poly (VPGVG methacrylate) homopolymer (*33*).

On the other hand, perhaps, the most widely used site-specific conjugation strategy uses Michael-type addition reactions between thiols of cysteine residues and maleimide- or vinyl sulfone-functionalized semitelechelic polymers. The success of this conjugation technique relies on the relatively low-natural abundance of cysteine residue on proteins (1.7% of all amino acids in globular proteins) (*34*), mild reaction conditions in water, and high reactivity rates of Michael-type addition reactions minimizing any side reactions. Other chemoselective reactions were also developed based on the Staudinger ligation (*35-37*) or click chemistry reactions (*38-40*) as a gateway to site specifically modify proteins. In particular, the Huisgen [3+2] azide-alkyne cycloaddition reaction (*38*) or widely known as 'click' reaction is highly specific, can be carried out in aqueous medium, and is fully bio-orthogonal (nonreactive to other amino acids present) without any side reactions (*15*).

The synthesis of copolymer-protein/peptide hybrid materials has been so far restricted to a few monomers such as carbohydrate, PEG acrylates/methacrylates and *N*-isopropyl acrylamide (*2, 41*). The fact that a wide range of acrylates/methacrylates cannot be freely used to produce copolymers via free radical polymerization arises from the difference in reactivity and solubility between monomers: for instance, the preparation of a copolymer containing a monosaccharide derived acrylate (hydrophilic) and taxol acrylate (hydrophobic) would be very challenging. The acrylate derivatives of many biologically active molecules/imaging agents such as curcumin could be synthesized but cannot be polymerized via free radical polymerization methods because the molecules are radical scavengers (*42*). The imaging efficacy and pharmacokinetics of many imaging agents and therapeutic drug candidates will be improved considerably if a general

synthetic technology for using them to produce water soluble and/or biocompatible polymer-protein hybrids is developed.

Our approach towards these conjugates involves three steps: (1) the synthesis of well-defined living polymers containing reactive chain-end and functional side-chain pendant groups in which the chain end and side chain possesses orthogonal reactivity, (2) the attachment of a number of water soluble, biocompatible moieties and imaging/therapeutic agents to the functional polymer side chains, and (3) attachment of the polymers (via the reactive polymer chain end) with proteins to produce the final bioconjugates. A general synthetic methodology to produce copolymers with a large number of copies of imaging agent/therapeutic agent and hydrophilic/biocompatible moieties attached in brush polymer architecture with a single reactive chain end are described in the previous chapter. Here we present the synthesis of protein-copolymer hybrids by attaching the reactive chain ends of the polymers to proteins via 'biotin-avidin' interaction or bioorthogonal 'click' reaction. In these novel hybrids a large number of imaging agent/drug units will be present thereby producing biomaterials with potentially amplified detection/therapeutic capabilities which was also investigated in the current work.

2. MATERIALS AND METHODS

2.1. General Information

Reagent-grade acetone, HPLC grade tetrahydrofuran, methylene chloride, N,N-dimethylformamide, dimethylsulfoxide, methanol, ethylacetate, *tert*-butanol were obtained from either Sigma-Aldrich or Fisher Scientific and used without further purification. 1,1,4,7,7-pentamethyldiethylenetriamine (PMDETA), copper (II) sulfate pentahydrate, glutaric anhydride, *N*-hydroxysuccinimide, *tris*-(2-carboxyethyl)phosphine (TCEP), potassium iodide, propargylamine, lithium hydroxide, sodium ascorbate, bovine serum albumin (BSA) and horse spleen apoferritin (HSF) were obtained from Sigma-Aldrich. 1-Ethyl-3-(3-dimethyllaminopropyl)carbodiimide hydrochloride (EDC.HCl), Tris salt and Avidin were obtained from Pierce Biotechnology. NIRF-Dye (ADS832WS) was obtained from American Dye Source, Inc. Streptavidin coated 96-Well Plates were obtained from Sigma. Anhydrous sodium sulfate, sodium bicarbonate and sodium azide were purchased from Fisher Scientific. Column chromatographic separations were performed using silica gel (Fisher) with a particle size of 0.040-0.063 mm. NHS-PEG-N_3 bisfunctional linker was purchased from Quanta BioDesign, Inc. Nuclear magnetic resonance (NMR) spectra were recorded on Oxford NMR 600 or 200 (600 MHz or 200 MHz) spectrometers. Mass spectra (ESI-MS) were recorded using an Agilent LC/MS mass spectrometer. Bruker Daltonics- microflex™ series-MALDI-TOF MS instrument equipped with FlexAnalysis software was used to record the MS of proteins (samples were prepared by mixing the protein with Sinapinic acid (matrix) in apporx. 1:10 molar ratio). FPLC analysis was performed using an AKTA explorer from GE Biosciences. The fluorescence spectras were obtained on JobinYvon Horiba FluoroMax-3 instrument.

Sodium dodecylsulfate-polyacrylamide gel electrophoresis (SDS-PAGE) apparatus, prepacked gels, marker, and necessary buffers were obtained from PAGEgel Inc. The Near Infrared images were taken using Odyssey imaging system (LI-COR, Lincoln, NE). Confocal microscopy was performed on a Leica SP2 AOBS confocal microscope using a 633 nm laser. Tris-(benzyltriazolylmethyl)amine (TBTA) was a generous gift from Dr. K. Barry Sharpless.

2.2. Synthetic Protocols

2.2.1. Comparison of UV-VIS-NIR spectrum and Fluorescence Spectroscopy of NIRF dye and copolymer 18.

NIRF dye (2.8 mg) was dissolved in 10 ml of deionized water to prepare a stock solution of 3 μM. Azide terminated poly(NIRF dye)-poly(glucose) copolymer **18** (11.7 mg; 5 dye molecule per polymer chain) was dissolved in 10 ml of deionized water to prepare a solution of 0.3 μM of effective dye concentration. The stock solution of NIRF dye was further diluted to 0.3 μM. The UV-VIS-NIR spectra were obtained on an Agilent Technologies 845x UV-Vis System using deionized water as blank. The fluorescence spectra of both the dye and the dye-incorporated copolymer **18** were obtained on JobinYvon Horiba FluoroMax-3 instrument using the solutions containing 0.3 μM effective dye concentration.

2.2.2. Conjugation of Biotin Terminated copolymer and Avidin.

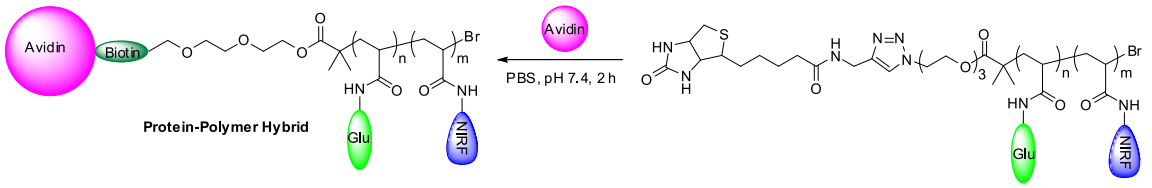

Avidin (1 mg) was dissolved in 0.25 mL of PBS buffer, pH 7.4. biotinylated poly(NIRF dye)-poly(glucose) copolymer **15** (5.5 mg) was dissolved in 0.65 ml PBS buffer, and slowly added. After 1.5 h at room temperature, the solution was extensively dialyzed using a 50 KDa MWCO membrane in deionized water, and the modified protein was analyzed by fast protein liquid chromatography (FPLC) and SDS-PAGE.

FPLC Characterization

The polymer-avidin reaction mixture (1 mL, dialyzed) was injected into AKTA Purifier FPLC chromatography system equipped with a HiPrep Sephacryl S200 26/10 (GE Healthcare) size exclusion column running through PBS buffer (pH 7.4). The flow rate was maintained at 1 mL/min and the purified samples were collected by an automated collection system.

SDS-PAGE

SDS-PAGE was performed by forming a complex of avidin with the polymer **15**, and then avidin alone as a control. First a mixture of avidin with the polymer in the ratio of 1:20 was incubated in PBS overnight on a rocking platform at 4 ºC, then the samples were heated and loaded onto 10-20% PAGEgel SDS Cassette Gel 17-Well. The avidin,

and the avidin-polymer hybrid were visualized using Odyssey imaging system (LI-COR, Lincoln, NE) in the NIR at 800 nm, then detected after protein staining with coomassie.

2.2.3. Synthesis of 5-oxo-5-(prop-2-ynylamino)pentanoic acid

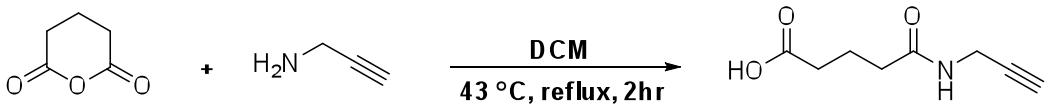

Glutaric anhydride (2.34 g, 0.2 mmol) was dissolved in 100 ml dry DCM in a round bottom flask and degassed with Ar. Propargyl amine (1.4 ml, 20 mmol) was added and the reaction mixture was refluxed at 43 ^{o}C for 2 hours and then stirred at room temperature for 2 hours. The solvent was evaporated and the crude product was purified by column chromatography using 95:5 CH_2Cl_2/ MeOH. Yield: 75%. ^{1}H NMR ($CDCl_3$, 200 MHz) δ (ppm): 1.67-1.76 (m, 2H), 2.09-2.26 (m, 4H), 2.38-2.41 (m, 1H), 3.75-3.76 (d, 2H).

2.2.4. Synthesis of 2,5-dioxopyrrolidin-1-yl-5-oxo-5-(prop-2-ynylamino)pentanoate (NHS-Alkyne)

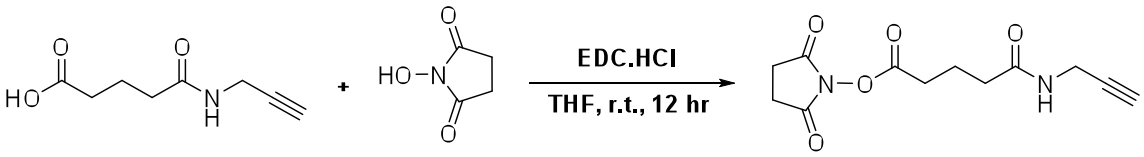

N-Hydroxy succinimide (0.93 g, 8.05 mmol), 5-oxo-5-(prop-2-ynylamino)pentanoic acid (1.01 g, 6 mmol) and EDC.HCl (1.22 g, 6.4 mmol) were dissolved in 50 ml of THF in a round bottom flask and degassed with Ar. The mixture

was stirred at room temperature for 12 hrs and then the solvent was evaporated. Further the crude reaction mixture was dissolved in DCM and washed thoroughly with water, saturated $NaHCO_3$, and brine. The organic layer was collected and dried over Na_2SO_4 and finally the solvent was evaporated to produce the product as white powder. Yield: 71 %. ^1H NMR ($CDCl_3$, 300 MHz) δ (ppm): 2.12-2.19 (m, 2H), 2.23-2.25 (t, 1H), 2.34-2.38 (t, 2H), 2.69-2.75 (m, 2H), 2.89 (s, 4H), 4.06-4.89 (m, 2H), 6.22 (bs, 1H).

2.2.5. Synthesis of Alkyne modified BSA

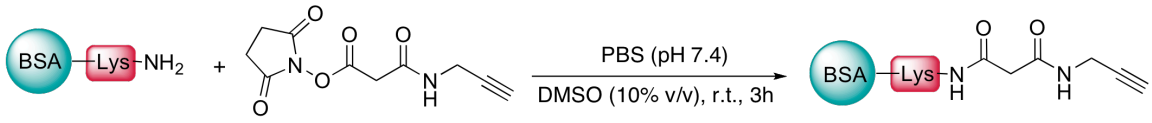

BSA (5mg, 5mg/ml in PBS, pH 7.4) was incubated with NHS-Azide (5mg in 100 µl DMSO, 10 eq to each modifiable lysine group) at room temperature for 3 h and then dialyzed against 0.1 M Tris buffer, pH 8.0 for 48 h to remove excess of azide linker. The dialyzed product was characterized via FPLC and used for further bioconjugation.

2.2.6. Synthesis of Protein-Polymer Conjugate; BSA-"clicked"-poly(NIRF dye)-poly(glucose) copolymer

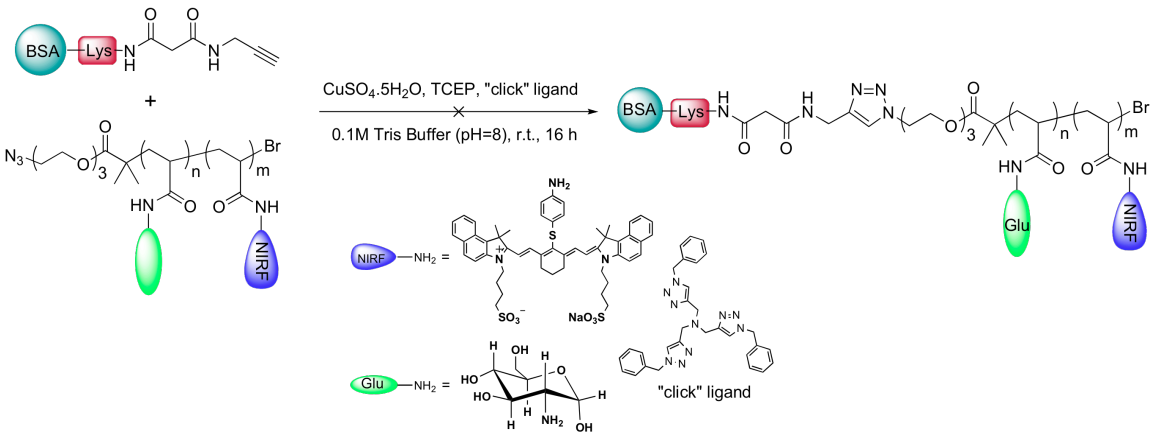

BSA-alkyne (5 mg, approx. 1.5 μmol in alkyne) was incubated with alkyne-poly(NIRF dye)-poly(glucose) copolymer (20 mg, 1 μmol) in Tris buffer (1800 μL, 0.1 M, pH 8) in the presence of TCEP (4 mM), "click" ligand (4 mM, dissolved in 200 μL if DMF) and copper sulfate (2mM) for 16 h at 4 ^{o}C. The ligand was added before the addition of copper sulfate. The reaction mixture was then dialyzed using Spectra Por 6 dialysis membrane (MWCO 50 KDAa) in PBS pH 7.4 for 48 h to remove excess of Copper and ligand. The conjugate was further characterized via Fast Protein Liquid Chromatographic system (Akta Purifier, Amarsham Biosciences) using HiPrep 26/10 Sephacryl S-200HR (GE Healthcare) size-exclusion column in PBS pH 7.4 as eluent buffer. The conjugate was also characterized via SDS PAGE.

2.2.7. Synthesis of Methyl-5-azido valerate

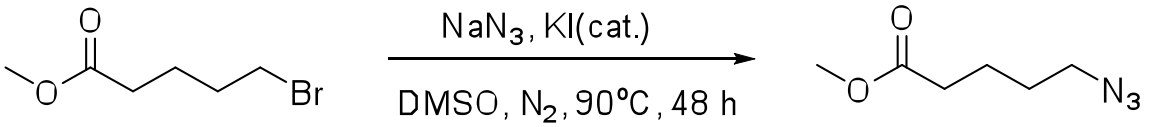

Methyl-5-bromovalerate (2.18 ml, 15.38 mmol) and Sodium azide (10 g, 10 eq) were dissolved in 20 ml DMSO in a round bottom flask and a pinch of KI was added. The mixture was stirred at 90 ^{o}C under N_2 atmosphere for 48 h. The reaction was cooled, diluted with water and extracted with hexanes. Organic layers were combined and dried over anhydrous Na_2SO_4. Solvent was evaporated to yield oily liquid. Yield: 2.2 g (91%); ^{1}H NMR (600 MHz, $CDCl_3$) δ (ppm): 1.56-1.59 (m, 2H; CH_2), 1.65-1.67 (m, 2H; CH_2),

2.30 (t, J =12 Hz, 2H; CH_2), 3.24 (t, J =12 Hz, 2H; CH_2), 3.62 (s, 3H; CH_3); ^{13}C NMR (150 MHz, $CDCl_3$) δ (ppm): 18.0, 24.2, 29.3, 47.0, 47.5, 169.5.

2.2.8. Synthesis of 5-Azido valeric acid

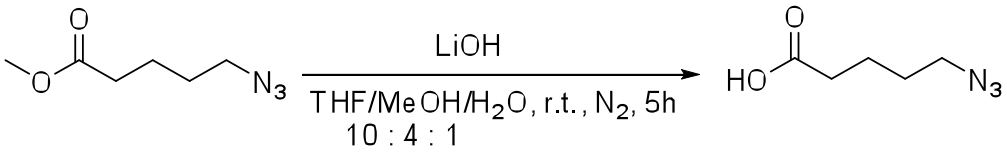

Methyl-5-azido valerate (2g, 12.73 mmol) was dissolved in 150 ml THF/MeOH/H_2O (10:4:1) mixture and LiOH (3.05 g, 10 eq) was added. The mixture was stirred at room temperature for 5h. The reaction was stopped and acidified to pH 2 with H_2SO_4 and extracted with ethyl acetate. Organic layers were combined, dried over anhydrous Na_2SO_4, and finally the solvent was evaporated to yield oily product. Yield: 1.1 g (60%); ^1H NMR (600 MHz, $CDCl_3$) δ (ppm): 1.25 (t, J = 12 Hz, 1H), 1.64-1.67 (m, 2H; CH_2), 1.70-1.73 (m, 2H; CH_2), 2.40 (t, J =11 Hz, 2H; CH_2), 3.30 (t, J =11 Hz, 2H; CH_2); ^{13}C NMR (150 MHz, $CDCl_3$) δ (ppm): 15.5, 23.2, 29.5, 34.9, 52.4, 180.8.

2.2.9. Synthesis of NHS-Azide

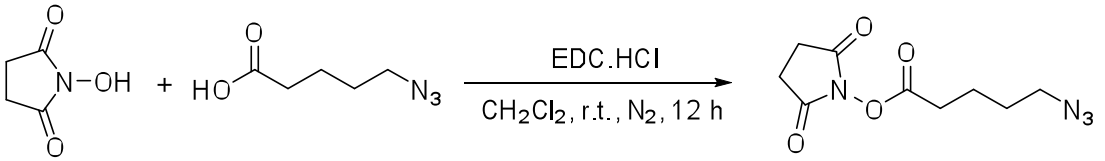

5-Azidovaleric acid (0.8 g, 5.6 mmol) and EDC.HCl (1.61 g, 1.5 mmol) were dissolved in 10 ml dry DCM and *N*-Hydroxysuccinimide (0.65 g, 1.01 mmol) was added. The reaction was stirred at room temperature under N_2 atmosphere for 12h. The reaction was stopped, diluted with water and extracted with EtOAc. The organic layers were

combined and washed with brine and dried over anhydrous Na_2SO_4. Finally the solvent was evaporated to yield sticky white product. Yield: 1.2 g (90%); ^{1}H NMR (600 MHz, $CDCl_3$) δ (ppm): 1.68-1.71 (m, 2H; CH_2), 1.80-1.84 (m, 2H; CH_2), 2.64 (t, J =12 Hz, 2H; CH_2), 2.81 (s, 4H; CH_2), 3.32 (t, J =11 Hz, 2H; CH_2); ^{13}C NMR (150 MHz, $CDCl_3$) δ (ppm): 17.8, 21.6, 23.9, 26.4, 46.8, 164.2, 165.1;

2.2.10. Synthesis of Azide modified BSA

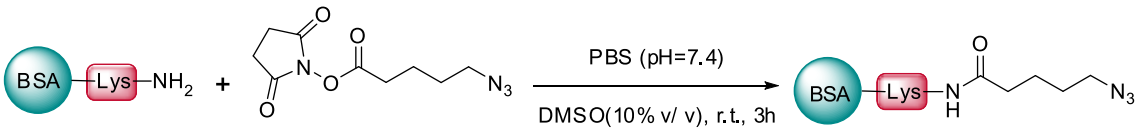

BSA (5 mg, 5 mg/ml in PBS, pH 7.4) was incubated with NHS-Azide (5 mg in 100 µl DMSO, 10 eq to each modifiable lysine group) at room temperature for 3 h and then dialyzed using 10KDAa MWCO membrane against 0.1 M Tris buffer, pH 8.0 for 48 h to remove excess of azide linker. The dialyzed product was characterized via FPLC and MALDI-TOF and used for further bioconjugation.

MALDI-TOF

Samples were prepared by mixing the protein samples with sinapinic acid as matrix in 10:1 molar ratio. Protein samples were prepared in PBS and sinapinic acid was dissolved in THF and then placed on to the sample grid and dried over vacuum, then exposed to laser beam. Molecular weights were determined using a Time of Flight detector.

2.2.11. Synthesis of Protein-Polymer Conjugate; BSA-"clicked"-poly(NIRF dye)-poly(glucose) copolymer

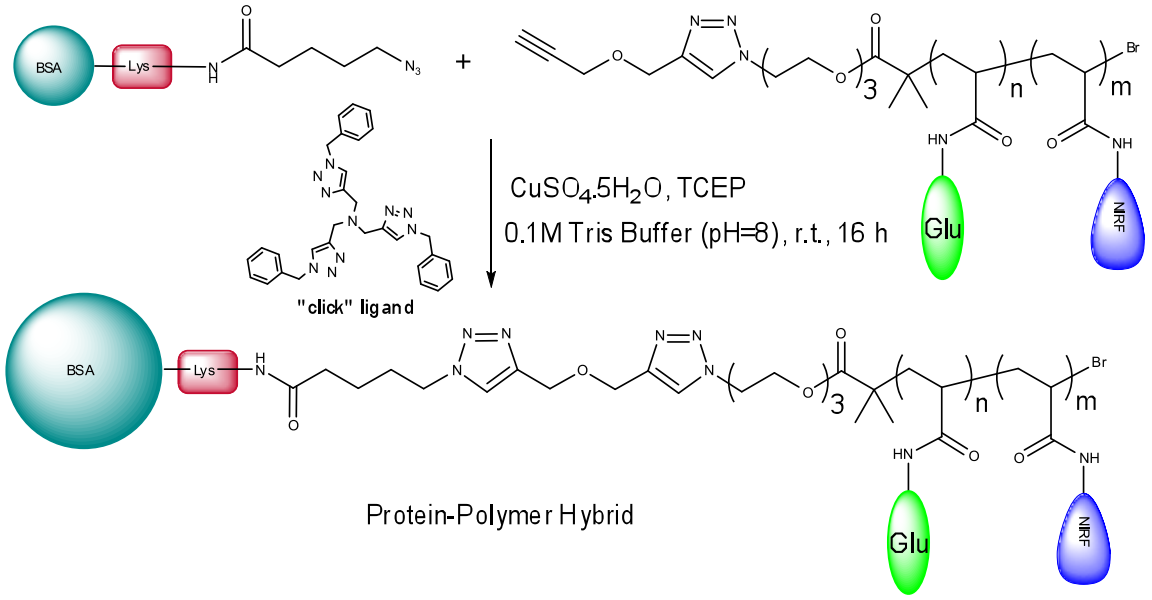

BSA-azide (5 mg, approx. 1.5 µmol in azide) was incubated with alkyne-poly(NIRF dye)-poly(glucose) copolymer (20 mg, 1 µmol) in Tris buffer (1800 µL, 0.1 M, pH 8) in the presence of TCEP (4 mM), "click" ligand TBTA (4 mM, dissolved in 200 µL if DMF) and copper sulfate (2 mM) for 16 h at 4 ^{o}C. The ligand was added before the addition of copper sulfate. The reaction mixture was then dialyzed using Spectra Por 6 dialysis membrane (MWCO 50KDa) in PBS pH 7.4 for 48 h to remove excess of Copper and ligand.

FPLC

The conjugate was further characterized via Fast Protein Liquid Chromatographic system (Akta Purifier, Amarsham Biosciences) using HiPrep 26/10 Sephacryl S-200HR (GE Healthcare) size-exclusion column in PBS pH 7.4 as eluent buffer.

SDS PAGE

SDS-PAGE was performed with BSA-polymer conjugate and alkyne-terminated poly(NIRF dye)-poly(glucose) copolymer, azide modified BSA as controls using a 10-20% PAGEgel SDS Cassette Gel. To confirm that the copolymer was indeed chemically bonded to the protein, the mixture of copolymer and modified BSA was incubated at 4 ^{o}C for 16h in the same ratio but without the "click" reagents and dialyzed the mixture with a 50 KDa MWCO membrane. The gel cassette was visualized using Odyssey imaging system (LI-COR, Lincoln, NE) in the NIR at 800 nm, prior to protein staining with coomassie.

2.2.12. Synthesis of Azide modified apoferritin.

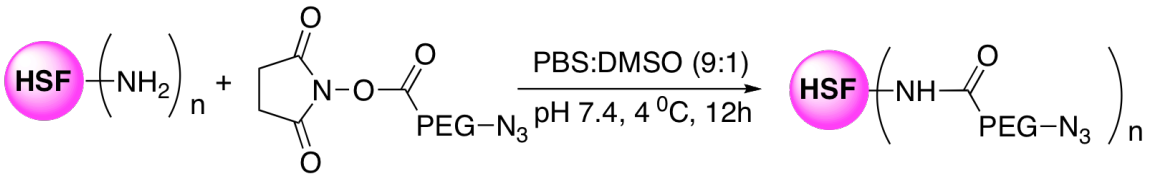

Horse Spleen Apoferritin (HSF) (purchased from Sigma) (50 mg, 0.1 µmol) was diluted in 1.7 ml of PBS (pH= 7.4). A solution of N_3-PEG-NHS (obtained from Quanta BioDesign) (1.5 mg, 2.6 µmol, ~ 25 eq of per HSF molecule; please note that there are 24 sub units and ~4 Lysine groups per HSF molecule) in 300 µL DMSO was added drop-wise while stirring to the HSF solution. The mixture was agitated on a rocker at 4 ^{o}C for 12h. The mixture was dialyzed using a cellulose membrane of MWCO 10KDa with constant flow of PBS (pH= 7.4) for 12 h. The dialyzed HSF-N_3 was used for bioconjugation without further purification.

2.2.13. Conjugation of NIRF copolymer to azide modified apoferritin.

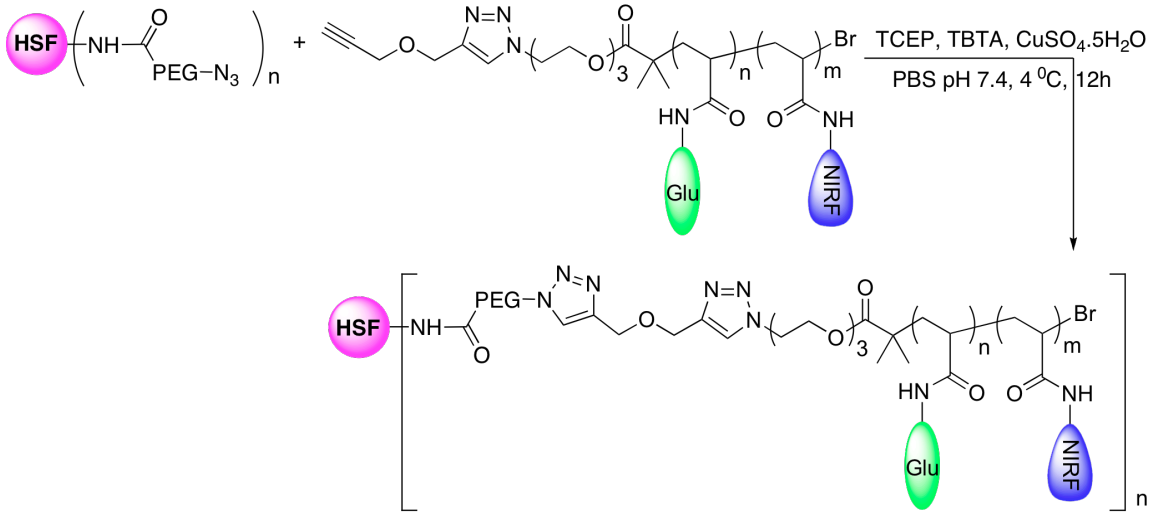

Alkyne terminated poly(NIRF)-poly(glucose) copolymer (50 mg, 2.5 µmol) was dissolved in PBS (pH= 7.4) solution containing HSF-N_3 (50 mg, 0.1 µmol). Freshly prepared solutions of TCEP (4 mM in PBS), TBTA (4 mM in DMSO), $CuSO_4.5H_2O$ (4 mM in PBS) was added respectively while stirring to the previous mixture. The dark colored solution was then allowed to react at 4 ^oC for 12h on a temperature-controlled agitator. The reaction mixture was dialyzed using a 50KDa MWCO membrane against PBS pH 7.4 for 24 h. The dialyzed product was characterized via FPLC techniques.

FPLC

The polymer-HSF reaction mixture (1 mL, dialyzed) was injected into Akta Purifier FPLC chromatography system equipped with a HiPrep Sephacryl S200 26/10 (GE Healthcare) size exclusion column running through PBS buffer (pH 7.4). The flow rate was maintained at 1 mL/min and the purified samples were collected by an automated collection system.

2.2.14. Multi-well Plate based assay.

Control poly(NIRF dye)-poly(glucose) copolymer, biotin terminated poly(acrylic acid)-poly (NIRF Dye) polymer **16**, and biotin terminated poly(NIRF dye)-poly(glucose) copolymer **15**. All samples were prepared at a starting effective molar dye concentration of 0.2 mM in PBS (pH=7.4), then each of the three samples were successively diluted ten-fold to final concentrations of 0.02, 2.0 x 10^{-3}, 2.0 x 10^{-4} mM. 50 µl of each solution was then added to the wells, and incubated overnight at 4 ^{o}C. Then the wells were washed four times with PBS containing 0.05% Tween-20. Finally, the wells were then visualized using the Odyssey imaging system (LI-COR, Lincoln, NE) at 800 nm.

2.2.15. Imaging Retinal Epithelial Cells.

Retinal pigment epithelial cells were divided onto four wells, and then allowed to grow for three days with regular feeding; the cells were then fixed using 2% PFA, then rinsed three times for five minutes each using PBS (pH=7.4). The nonspecific binding sites were then blocked using a blocking buffer and incubated for overnight. The blocking buffer was then removed, and well (**a**) only was incubated with the primary antibody, and incubated for overnight at 4 ^{o}C. The primary antibody was then rinsed three times five minutes each, and then the secondary antibody was added to wells (**a** & **b**), and incubated for overnight at 4 ^{o}C. Rinsing was performed for the excess secondary antibody using the same technique used for the primary antibody, then 500 µl of Avidin (1 mg/ml) was added to each of wells (**a**,**b** & **c**) and incubate for overnight at 4 ºC, and excess of avidin was washed off with PBS (pH=7.4) three times five minutes each. Finally 500 µl

of biotinylated poly(NIRF dye)-poly(glucose) copolymer (0.1 mg/ml) was added to each of the wells (**a**,**b**,**c** & **d**) and incubated for two hours at 37 ºC at a controlled temperature chamber. Excess polymer was washed off using PBS (pH=7.4) three times five minutes each, fresh PBS was then added to the wells and scanned using Odyssey imaging system (LI-COR, Lincoln, NE) with detection in the NIR region at 800 nm.

Blocking solution:

4% Normal goat serum (NGS)

2% BSA

0.05% Tween 20

Antibody dilution buffer:

2% NGS

1% BSA

0.05% Tween 20

50% blocking buffer in PBS was used to prepare the Antibody Dilution Buffer

Preparation of Antibodies:

Primary antibody: (2B- α5 Rabbit polyclonal IgG)

1: 200 preparation of the antibody in 2% ADB without Tween (not to permeate the cells).

Secondary antibody: (GtxRb secondary Lot: 0507003644)

1:200 preparartion of the antibody in 2% ADB without Tween (not to permeate the cells).

2.2.16. Protein-polymer hybrid in non-invasive imaging in mice.

Each of two female, six months old mice were injected with 200 µl of the NIRF dye, and the biotin terminated poly(NIRF dye)-poly(glucose) copolymer (0.2 mM effective dye concentration in both cases) via the tail vein. Each mouse was then anaesthetized using mixture of 15 µL Xylezene mixed with 54 µL Ketamine to reach a dose of 10 mg/kg body weight of Xylezene, and 90 mg/kg bodyweight of Ketamine per mouse, and then scanned using a Odyssey scanner (Near IR) at wavelength 800 nm. To investigate the extent of fluorescence, and the extent of catabolism of the polymer the mice were scanned after one hour and four hours. Another female six months old mouse (control mouse) was anaesthetized with the same anesthetic mixture and then scanned to eliminate background fluorescence.

2.2.17. HSF-polymer uptake by cells

Prior to imaging we applied the Apoferritin-polymer conjugate (0.2 mg/ml) to the breast cancer cell line BT549 and incubated for 24 hrs at 37 ^{0}C. The cells were then imaged on a Leica SP2 AOBS confocal microscope on reflected light mode using a 633 nm laser; the image provided is an overlay of the fluorescent (red; NIRF) and reflected light channels. For controls cells, the gain and offset of the fluorescent channel were identical to those in which the bioconjugate was imaged.

A control experiment was also conducted where the same cell line was incubated for the same time frame with apoferritin and the cells were imaged according to the above mentioned protocol.

3. RESULTS AND DISCUSSIONS

3.1. UV and Fluorescence Study.

We have investigated the absorbance and the fluorescence emission profiles for the NIRF dye (ADS832WS) and the poly(NIRF dye)-poly(glucose) copolymer **18** (**Figure 3.1**). The copolymer **18** had superior solubility in water compared to the dye molecule. As a result higher absorbance values were observed in the case of the polymer sample even though both the solutions contained the same effective dye concentration of 0.3 μM (**Figure 3.1A**). A red shift of 19 nm (from 747 nm to 766 nm) in the absorbance maxima (λ_{max}) of the dye was also observed. Although the fluorescence emission intensity of copolymer **18** was higher than the dye as expected, the dye displayed larger Stokes shift (79 nm) compared to copolymer **18** (63 nm) (**Figure 3.1B**).

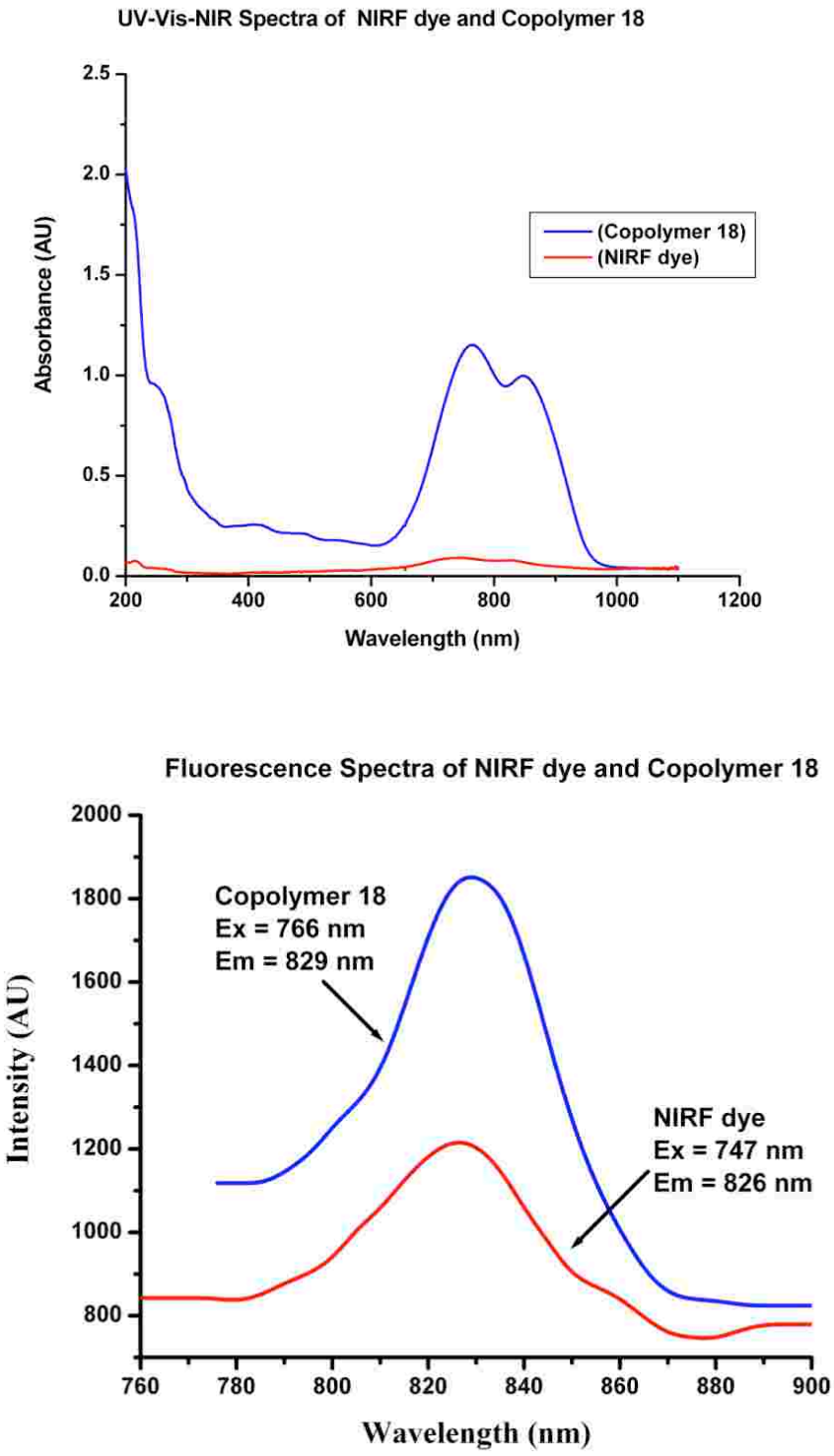

Figure 3.1. UV/Vis/NIR absorption spectra (**top**) and Fluorescence emission spectra (**bottom**) of NIRF copolymer **18** (blue line), NIRF dye (red line) in water at 25 ^{o}C. The effective dye concentrations in both the cases are identical (0.3 μM).

3.2. Polymer-Protein Hybrids via Biotin-Avidin Interaction.

The copolymer-protein hybrid **20** was synthesized by incubating the copolymer **15** with avidin. The formation of a conjugate was indicated by higher molecular weight bands in SDS PAGE; the conjugate band which glowed when imaged using a NIRF imager was also visible following Coomassie staining indicating the presence of both polymer and protein at the same ordinate (**Figure 3.2B)**. The formation of the conjugate was further confirmed via size exclusion Fast Protein Liquid Chromatography (FPLC) where the conjugate **20** eluted earlier (due to its higher molecular weight) in comparison to the synthetic polymer **15** and the control avidin sample (**Figure 3.2A**). A multi wavelength detector was used to monitor the elution of conjugate and polymer from the size exclusion column.

Scheme 3.1. Schematic representation of synthesizing protein-polymer hybrids via biotin-avidin interaction.

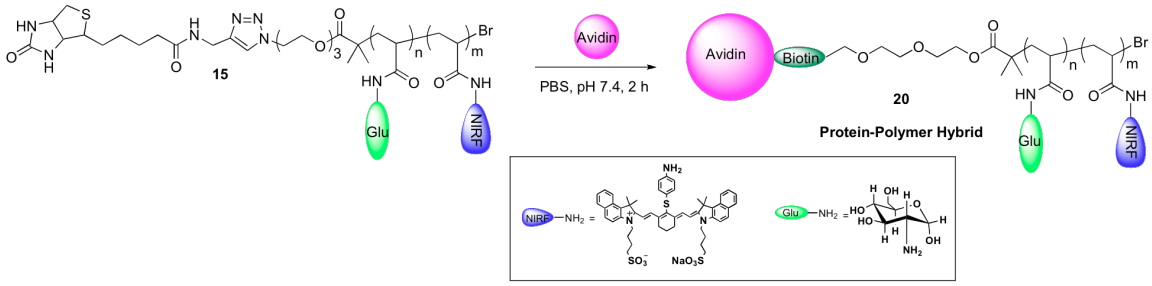

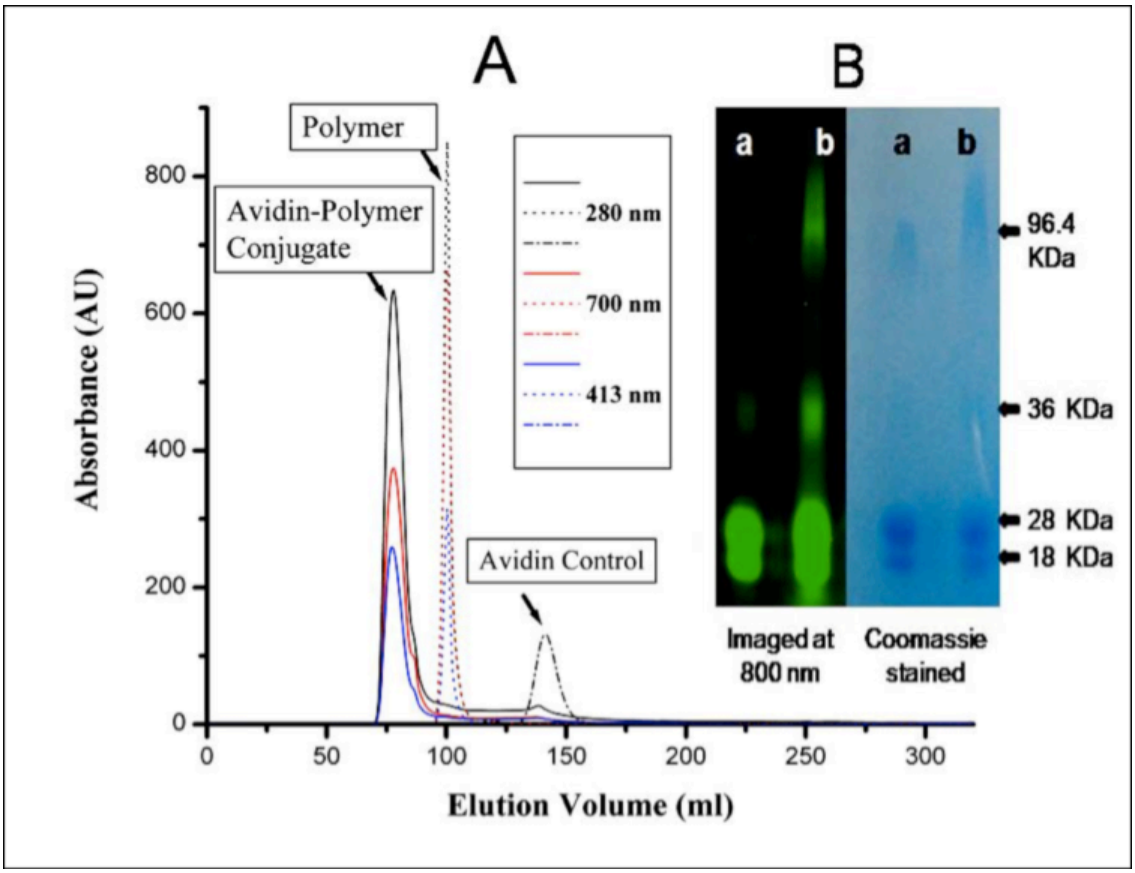

Figure 3.2. A. Size-exclusion FPLC (Hiprep 26/60^{TM} Sephacryl^{TM} S-200 HR column) of avidin (dashed line), copolymer **15** (dotted line), and conjugate **20** (solid line). **B**. SDS-PAGE of avidin (lane **a**) and conjugate **20** (lane **b**).

3.3. Polymer-Protein Hybrids via "click" reaction.

In the second synthetic methodology (**Scheme 3.2**) BSA was modified by reacting the surface lysine groups with NHS-Alkyne **21** or NHS-Azide **22** hetero-bifunctional linkers to produce either alkyne-labeled BSA or azide-labled BSA respectively.

Scheme 3.2. Synthetic routes to protein-polymer hybrids via 'click' chemistry.

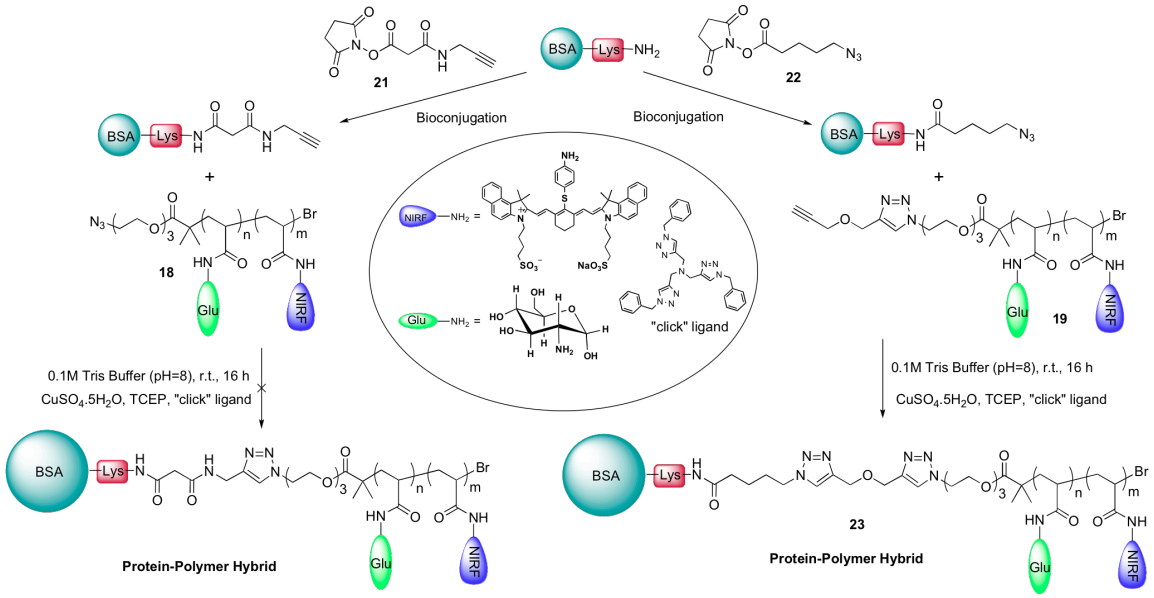

MALDI-TOF method was used to estimate the average number of surface lysine residue modifications of the BSA (please note that BSA contains ~60 lysine groups). Results indicate that on an average BSA was modified with ~35 alkyne or ~45 azide groups (**Figure 3.3**). The copolymer **18** with reactive azide chain-end was incubated with alkyne-modified BSA under "click" bioconjugation conditions (*29*) but unfortunately without any success (lack of reaction confirmed via SDS-PAGE). Earlier literature reports support the reduced/lack of reactivity of alkyne modified proteins in "click" bioconjugation reactions (*43*). To circumvent the above mentioned problem copolymer

18 was reacted with a large excess of di-propargyl ether under "click" condition to convert the azide-terminated copolymer to an alkyne-terminated poly (NIRF dye)-poly(glucose) copolymer **19**. The absence of the azide peak (~2100 cm^{-1}) in the FT-IR spectra confirmed the conversion of all the azide-end groups to alkyne. The incubation of azide-linker modified BSA with alkyne terminated copolymer **19** under 'click' bioconjugation condition finally produced the desired polymer-protein hybrid **23**. The formation of the conjugate was confirmed via FPLC (**Figure 3.4**) and SDS-PAGE (**Figure 3.5**).

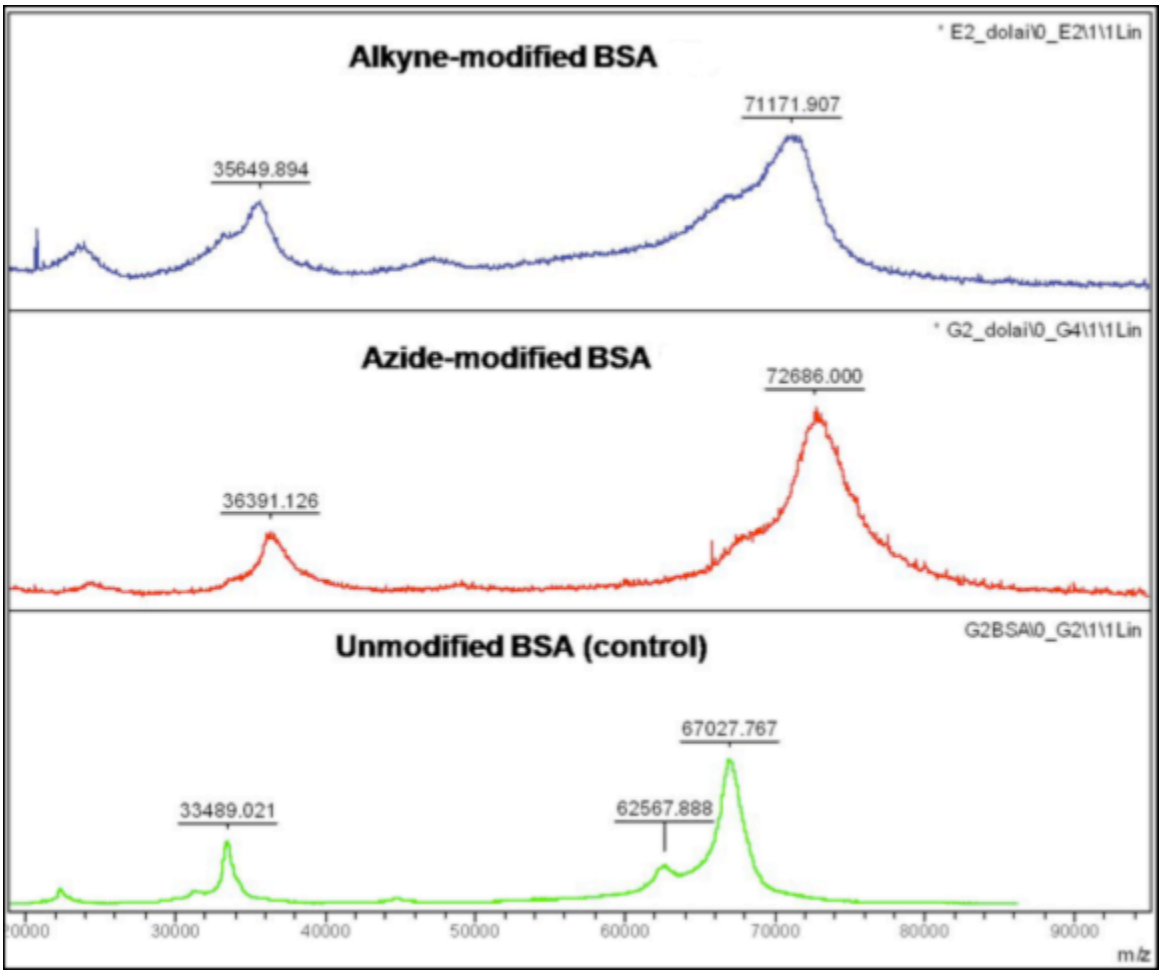

Figure 3.3. MALDI-TOF Data comparison of alkyne modified BSA (blue line), azide modified BSA (red line), unmodified BSA (green line).

The conjugate **23** eluted earlier than both the copolymer **19** and azide-modified BSA in the FPLC experiment. The unmodified BSA (control) eluted at the same volume as the modified BSA; hence it was not shown in the chromatogram. The SDS-PAGE gels were consistent with the FPLC results, the bands which glowed at 800 nm (lanes 4 & 8) also appeared when stained with Coomassie (but the control lanes 6 & 10 did not glow at 800 nm). This confirmed the presence of both protein and the polymer at the same ordinate in the conjugate samples. To confirm that the copolymer **19** was indeed chemically bonded to the protein, we incubated the mixture of copolymer **19** and azide-modified BSA in the same ratio but without the "click" reagents and dialyzed the mixture with a 50 KDa MWCO membrane; in this case no higher molecular weight conjugate bands were observed (lane 6).

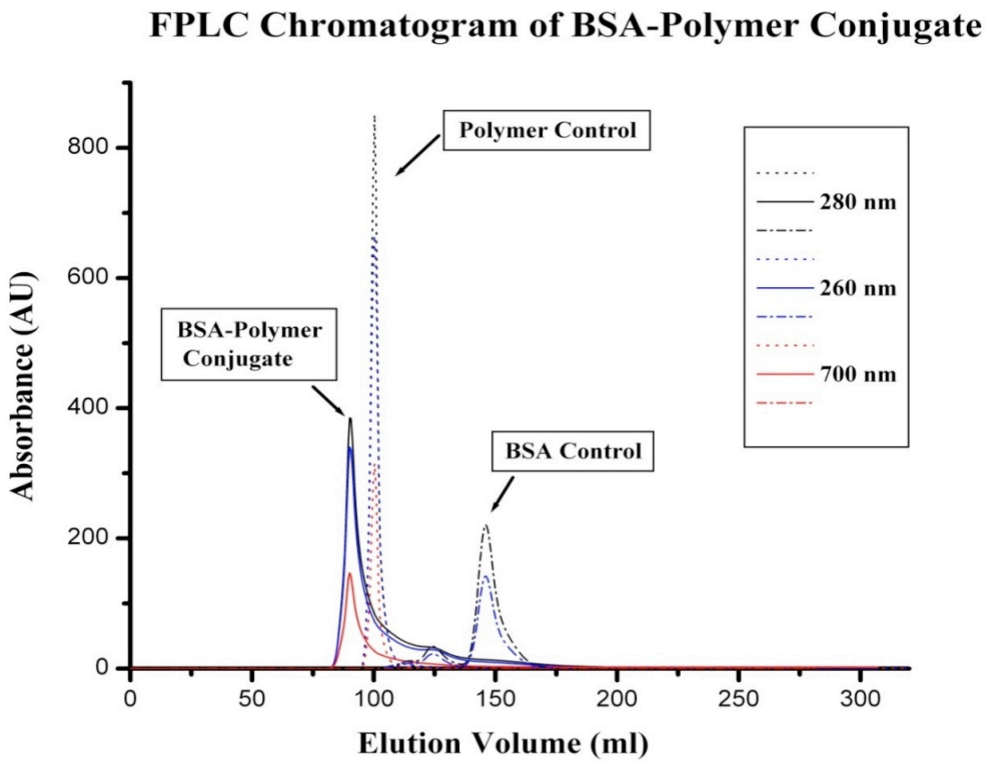

Figure 3.4. Size-exclusion FPLC (Hiprep 26/60^{TM} Sephacryl^{TM} S-200 HR column) of azide modified BSA (dashed line), copolymer **19** (dotted line), and conjugate **23** (solid line).

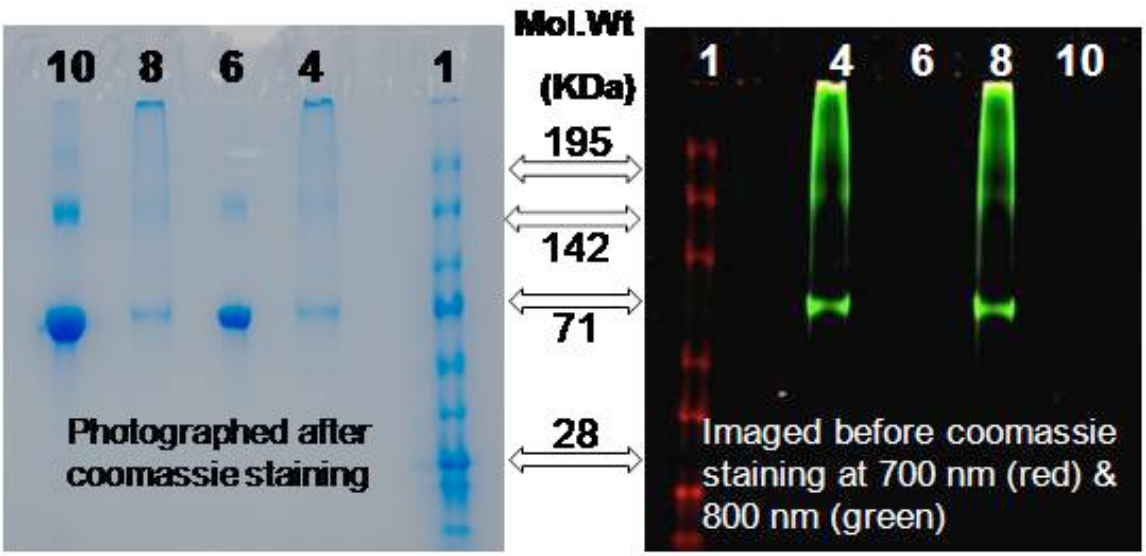

Figure 3.5. SDS-PAGE of conjugate **23** (lane 4&8), mixture of azide modified BSA & copolymer **19** without "click" reagents (lane 6) and unmodified BSA (lane 10).

3.4. Bionanoparticle-polymer conjugate via 'click' reaction

In another synthetic methodology, (**Scheme 3.3**) Horse Spleen Apoferritin (HSF) was modified by reacting the surface lysine groups with NHS-PEG-Azide (Quanta BioDesign, Inc.) hetero-bifunctional linker to generate azide-labled HSF. Apoferritin is a biomacromolecular assembly composed of 24 subunits with four chemically addressable lysine residues per subunit. The copolymer **19** with reactive alkyne chain-end was incubated with azide-modified HSF **24** under "click" bioconjugation conditions finally produced the desired bio-nanoparticle-polymer hybrid **25**. The formation of the conjugate was confirmed via FPLC (**Figure 3.6**).

Scheme 3.3. Synthetic scheme describing bionanoparticle-polymer hybrids.

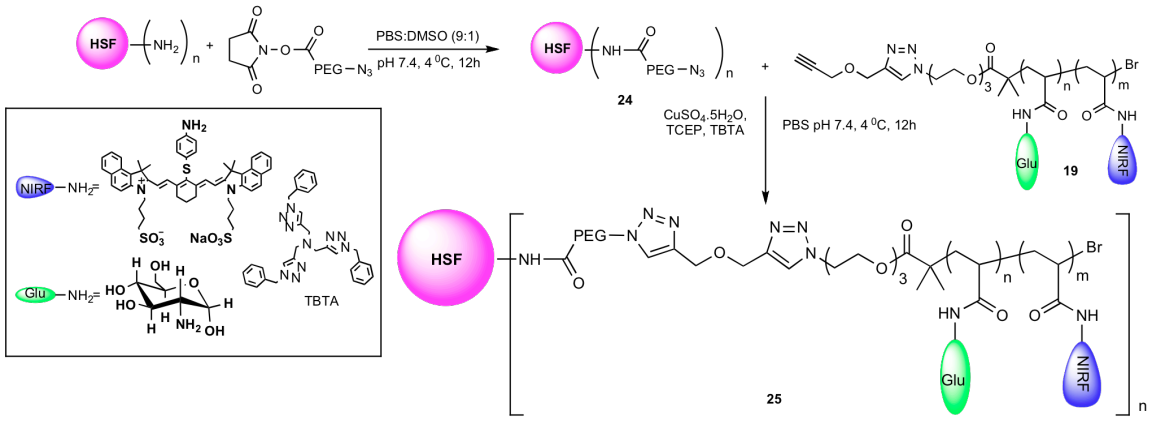

The FPLC chromatogram of HSF (control) and conjugate **25** (**Figure 3.6**) confirms the formation of the conjugate. The conjugate **25** eluted earlier than HSF when injected into a HiPrep Sephacryl S200 26/10 (GE Healthcare) size exclusion column running through PBS buffer (pH 7.4) with a flow rate of 1 mL/min. The azide-modified HSF **24** (control) eluted almost at the same volume as the unmodified HSF; hence it was not shown in the chromatogram. Three wavelengths were used to monitor the elution of

protein (260 nm, 280 nm) and copolymer (700 nm). The presence of the peaks at 260 nm, 280 nm and 700 nm at the same elution volume in the FPLC chromatogram confirms the formation of conjugate where as in case of HSF (control) peak at 700 nm (NIRF dye) is absent. Fractions were collected using an automated collection system. Purified fractions were collected and used for uptake of the conjugate by cells experiments.

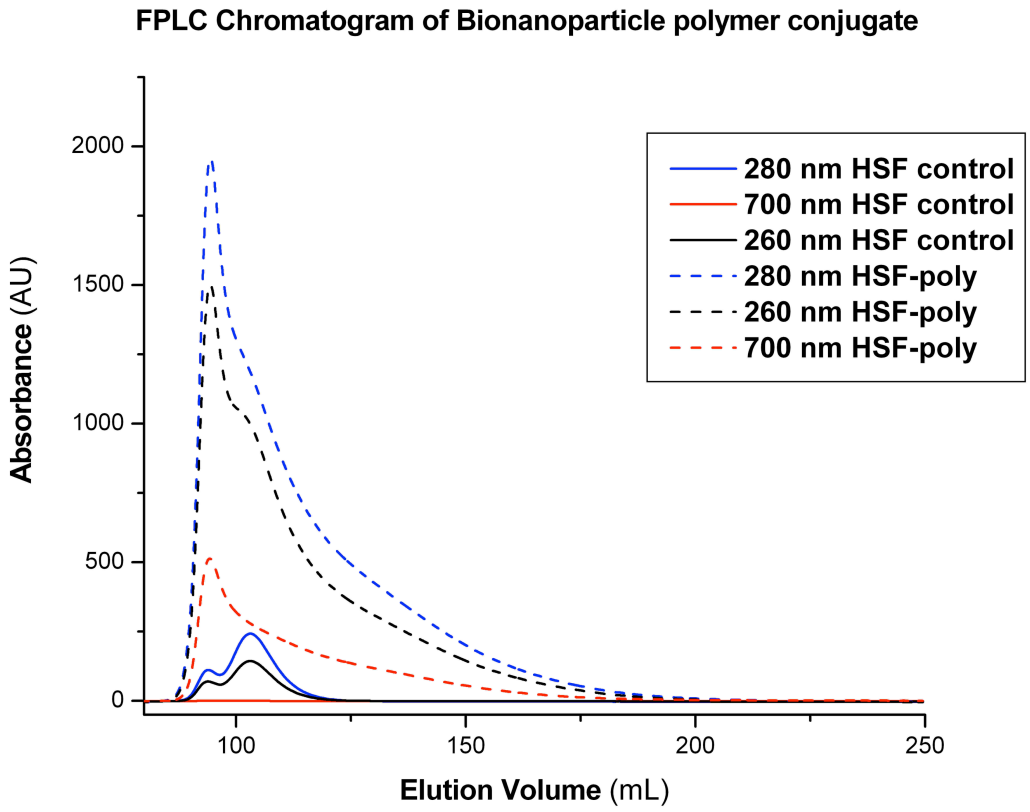

Figure 3.6. FPLC chromatogram of HSF (control) and poly(NIRF dye)-poly(glucose) copolymer decorated HSF **25**. (Dolai, S.; Debnath, S.; Sun, Chong, S.; Fata, J. and Raja, K. unpublisded data)

3.5. Applications

3.5.1. Multiwell Plate Binding Assay

Immobilization of the synthesized biotinylated neoglycopolymer was performed on streptavidin coated multiwell plates where the plates were incubated with a 10 fold serial dilution of (a) non-biotinylated poly(NIRF dye)-poly(glucose) copolymer control (b) polymer **16** and (c) copolymer **15**. The wells were washed with PBS buffer to avoid non-specific binding and scanned using an NIRF imaging system; see **Figure 3.7**. The result indicated that the control polymer did not bind to the plates (low fluorescence intensity) whereas the biotin terminated polymers remained bound to the streptavidin coated wells thereby resulting in higher fluorescence intensity. In the case of **15**, the fluorescence intensity was significantly higher than **16** presumably because of the superior water/buffer solubility of **15**. The resulting immobilized neoglycopolymers can interact with complementary cell surface receptors/lectins (*44*). Hence, one can potentially create a convenient platform to study carbohydrate-receptor interactions; by varying the carbohydrates in the polymer and by using dye modified lectins/cell receptors which are Fluorescence Resonance Energy Transfer (FRET) (*45*) partners for the NIRF dye on the polymers, a range of lectins /cell receptor interactions can be explored.

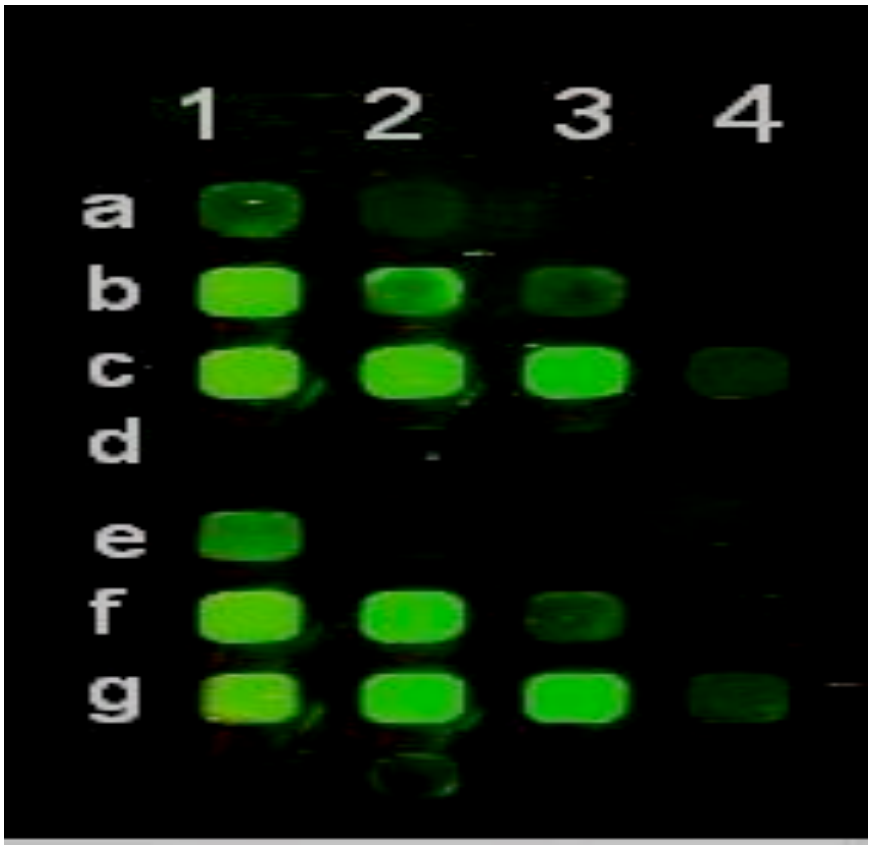

Figure 3.7. Streptavidin coated multiwell plates treated with non-biotinylated copolymer control (a&e), polymer **16** (b&f) and copolymer **15** (c&g).

3.5.2. *In Vitro* Imaging Study

The utility of copolymer **15** in *in vitro* imaging cells was also evaluated using retinal pigment epithelial cells. The cells were fixed and treated with primary antibody (2B-α5 Rabbit polyclonal IgG), biotinylated secondary antibody, avidin and poly(NIRF dye)-poly(glucose) copolymer **15** (**Figure 3.8**). Slide **a** was incubated with primary, secondary antibodies, avidin, and the copolymer **15**, in slide **b** the primary antibody was omitted, in slide **c** the primary and secondary antibodies were omitted, in slide **d** the primary, secondary antibodies and avidin were omitted prior to the copolymer **15** treatment step. Slides **b**, **c** and **d** serve as controls. The results indicate that only slide **a**

showed maximum fluorescence, while control slides show minimal fluorescence. The specificity of the biotin chain-end towards avidin is evident from the decreased fluorescence in the slide **d**. This also indicates the accessibility of the chain end of the copolymers towards bioconjugations.

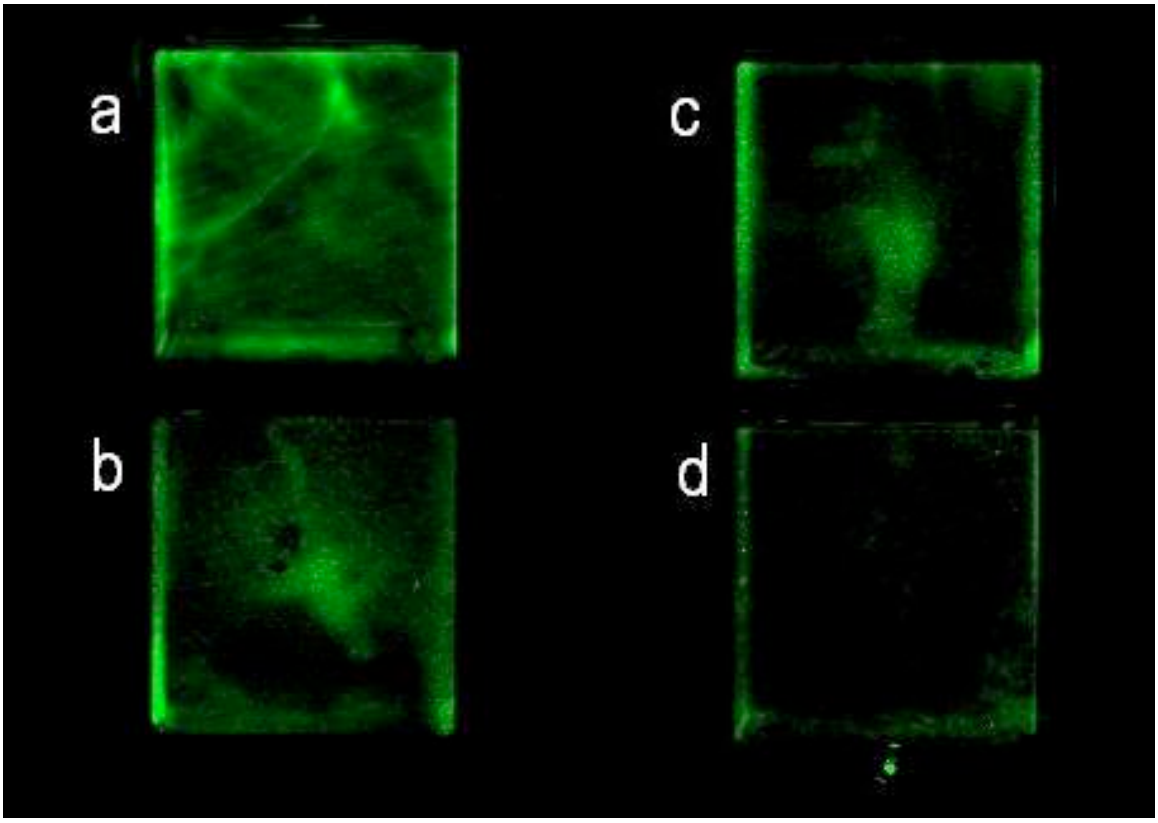

Figure 3.8. Fixed retinal pigment epithelial cells (ARPE-19) labeled using copolymer **15.** Slide **a** was incubated with primary, secondary antibody, avidin and copolymer **15** and imaged. Primary antibody was omitted in slide **b**, in slide **c** the primary and secondary antibodies were omitted, in slide **d** the primary, secondary antibodies and avidin were omitted prior to the copolymer **15** treatment step.

3.5.3. *In Vivo* Imaging Study

Copolymer **15** also showed considerable promise in non-invasive *in vivo* imaging of mice: mice injected with the polymer could be imaged more efficiently than mice injected with the small molecule NIRF-NH_2 dye (**Figure 3.9A-E**; please note that since

the mice were not shaved only the body parts without hair of mice were clearly visible). The polymer is superior for imaging mice compared to the low molecular weight dye probably because of the superior solubility of poly(NIRF dye)-poly(glucose) copolymer **15** in water/blood/serum compared to the dye and because it is presumably not cleared from the blood rapidly via kidney filtration.

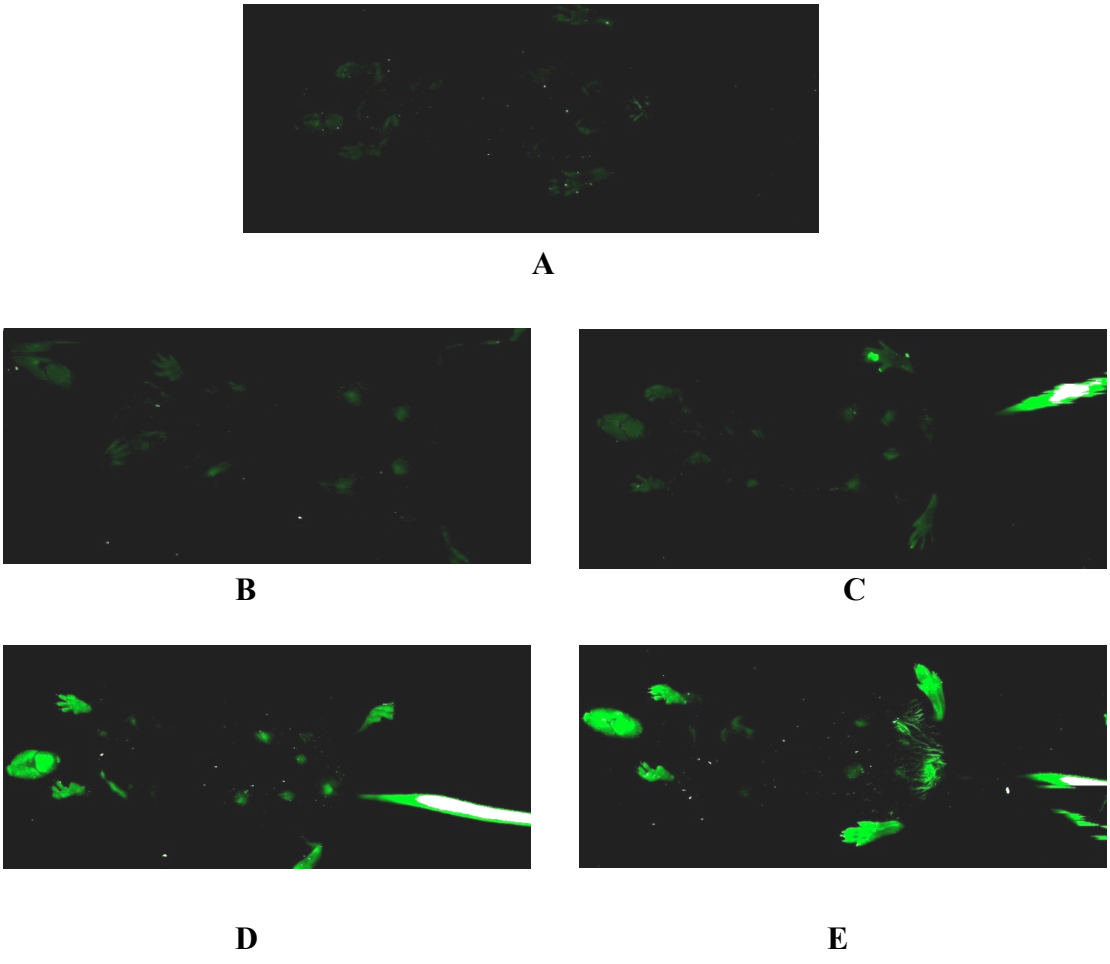

Figure 3.9. In vivo Imaging with NIRF dye incorporated copolymer. **A.** The control mouse without an imaging agent. **B** & **C.** Mouse scanned 1h and 4hs after tail-vein injection with the NIRF dye respectively. **D** & **E.** Mouse scanned 1h and 4hs after tail-vein injection with the copolymer **15** respectively. All the images were scanned using an odyssey NIRF imager at 800 nm.

3.5.4. Cell Uptake Study

Prior to imaging we applied the Apoferritin-polymer conjugate **25** (0.2 mg/ml) to the breast cancer cell line BT549. Cells were imaged using reflected light mode on a Leica SP2 AOBS confocal microscope using a 633 nm laser; the image provided is an overlay of the fluorescent (red; NIRF) and reflected light channels (**Figure 3.10**). For controls cells, the gain and offset of the fluorescent channel were identical to those in which the bioconjugate was imaged (**Figure 3.10**).

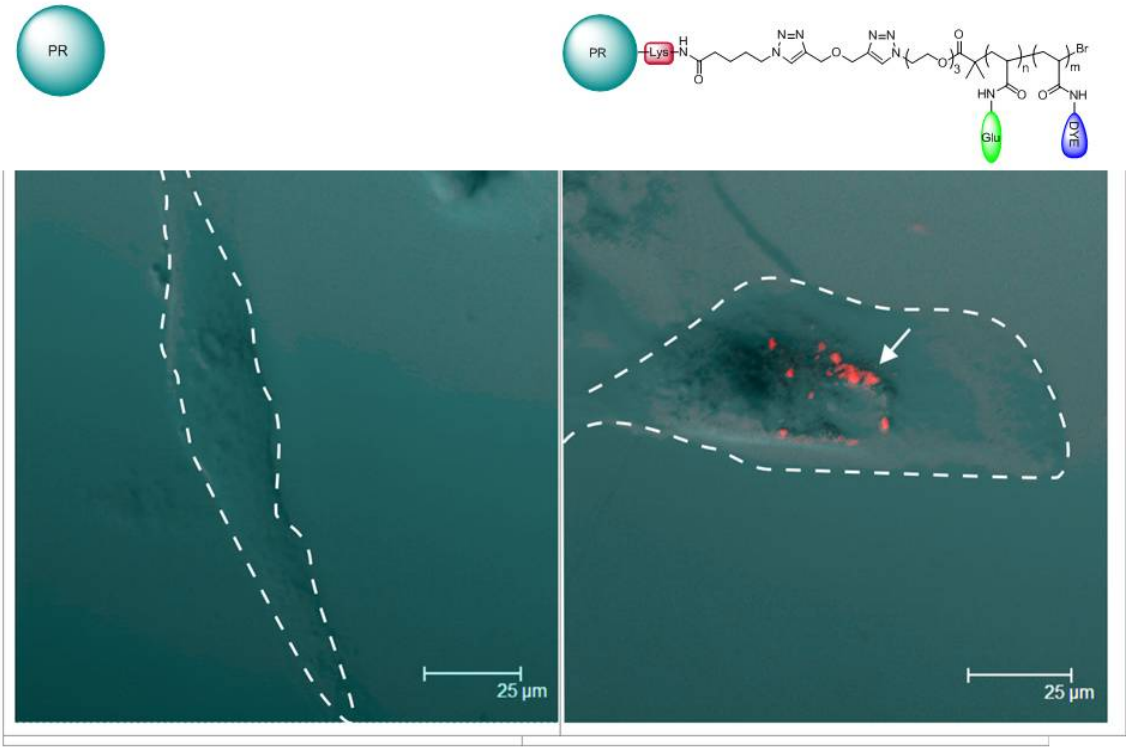

Figure 3.10. (Right panel) Uptake of Apoferritin-polymer bioconjugates into BT549 breast cancer cells. Arrow points to internalized and compartmentalized bioconjugate after a 24 hour incubation. Control cell (left panel) lacks the NIRF dye and exhibits no fluorescence.
(Dolai, S.; Debnath, S.; Sun, Chong, S.; Fata, J. and Raja, K. unpublisded data)

It can be seen from the above figure the cells treated with the HSF-polymer conjugate show fluorescence due to the presence of NIRF dye in the copolymer.

Whereas, the control cells lack of copolymer containing NIRF dye hence, exhibits no fluorescence. We hypothesized that the glucose units decorated on our Apoferritin conjugate would promote its binding and uptake into cells. Glucose is unable to freely diffuse across the cell membrane and instead enters the cell primarily through passive facilitated diffusion through integral membrane glucose transporters (GLUTs). We are currently working on a series of protein-polymer hybrids containing either both of NIRF dye and Glucose or only NIRF dye which will allow us to pinpoint the mechanism of cell uptake and also help us to develop a new technology towards cell imaging.

4. CONCLUSION

In conclusion, we have successfully synthesized several protein-synthetic polymer hybrids via either physical interaction or chemical bonding. In this study we have certainly overcome two fundamental limitations in the synthesis of bioconjugates: (a) the basic restriction in the diversity of copolymers which can be synthesized for producing bioconjugates and (b) the limitation that only a small number of dyes/drug molecules can be attached per protein molecule. After synthesizing a series of water-soluble copolymers containing reactive chain-end (biotin/azide/alkyne) and NIRF dye and glucose moieties in brush architecture via ATRP which possessed enhanced optical properties compared to their monomeric counterparts, we have conjugated these copolymers to Avidin, Bovine serum albumin (BSA), and Horse spleen apoferritin (HSF). The biotin-terminated poly(NIRF dye)-(glucose) was conjugated to Avidin via 'biotin-avidin' interaction and the formation of conjugate was confirmed using FPLC and SDS-PAGE experiments. After the conjugation of azide-terminated copolymer with alkyne modified BSA was unsuccessful, we decided to use a alkyne-terminated copolymer and azide modified protein instead. The alkyne-terminated poly(NIRF dye)-(glucose) was successfully 'clicked' to BSA and confirmed the formation via FPLC and SDS-PAGE. With the success of 'click' bioconjugation we extended our way by making a HSF-copolymer conjugate. Next, we evaluated the possible applications of the synthesized copolymers and also the protein-synthetic polymer hybrids. The copolymers were successfully immobilized for potential multiwell plate based assay experiments. The resulting immobilized neoglycopolymers can interact with complementary cell surface

receptors/lectins and a convenient platform to study carbohydrate-receptor interactions can be created; by varying the carbohydrates in the polymer and by using dye modified lectins/cell receptors which are Fluorescence Resonance Energy Transfer partners for the NIRF dye on the polymers, a range of lectin /cell receptor interactions can be explored. The synthesized copolymers were utilized for *in vivo* imaging; mice injected with the polymer could be imaged more efficiently than mice injected with the small molecule NIRF-NH_2 dye probably because of the superior solubility of copolymers in water/blood/serum compared to the dye and also presumably not cleared from the blood rapidly via kidney filtration. The utility of the copolymer in *in vitro* imaging cells was also evaluated using retinal pigment epithelial cells. The results indicate the accessibility of the chain end of the copolymers towards bioconjugations. The HSF-copolymer conjugate helped to indentify the possibility of using protein-polymer hybrids in cell imaging and identify the cell uptake process. We are currently exploiting this general synthetic methodology to produce a range of bioactive copolymers and protein/antibody-copolymer conjugates for applications ranging from tissue specific imaging to targeted drug delivery.

5. SPECTRAL CHARACTERIZATION DATA (^{1}H NMR and ^{13}C NMR)

^{1}H NMR

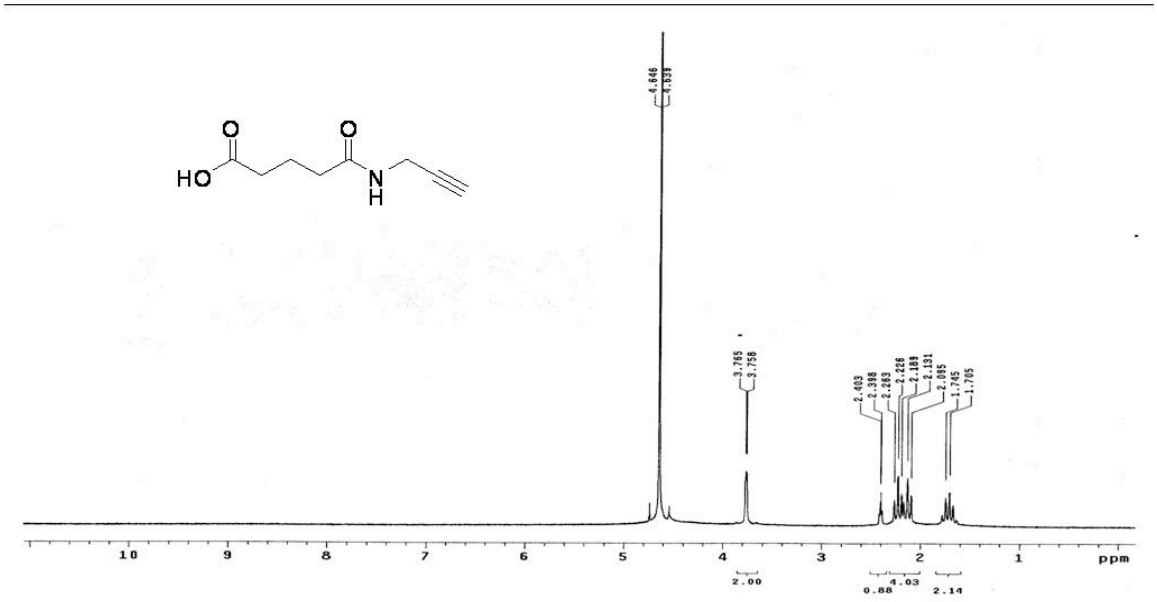

^{1}H NMR

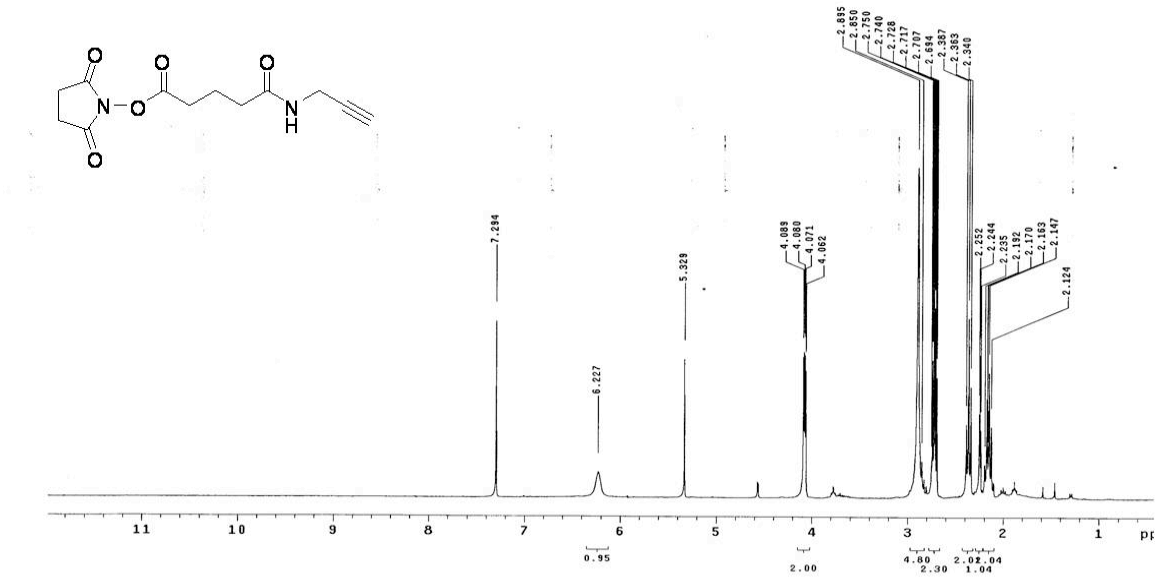

^{1}H NMR

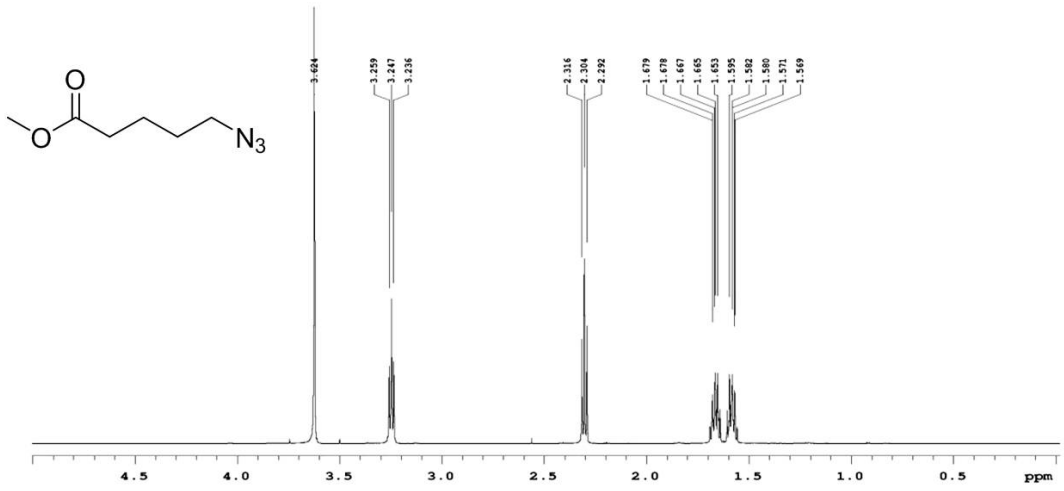

^{13}C NMR

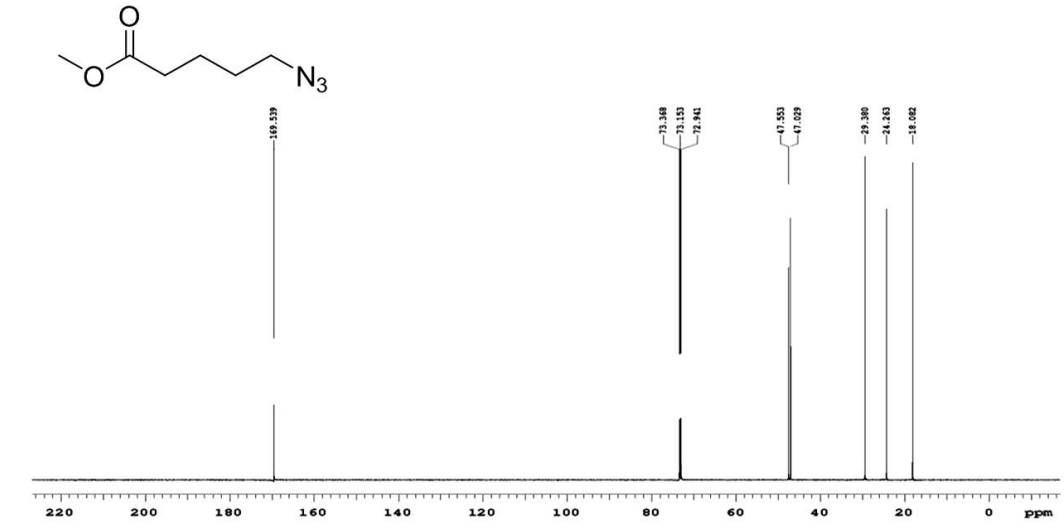

^{1}H NMR

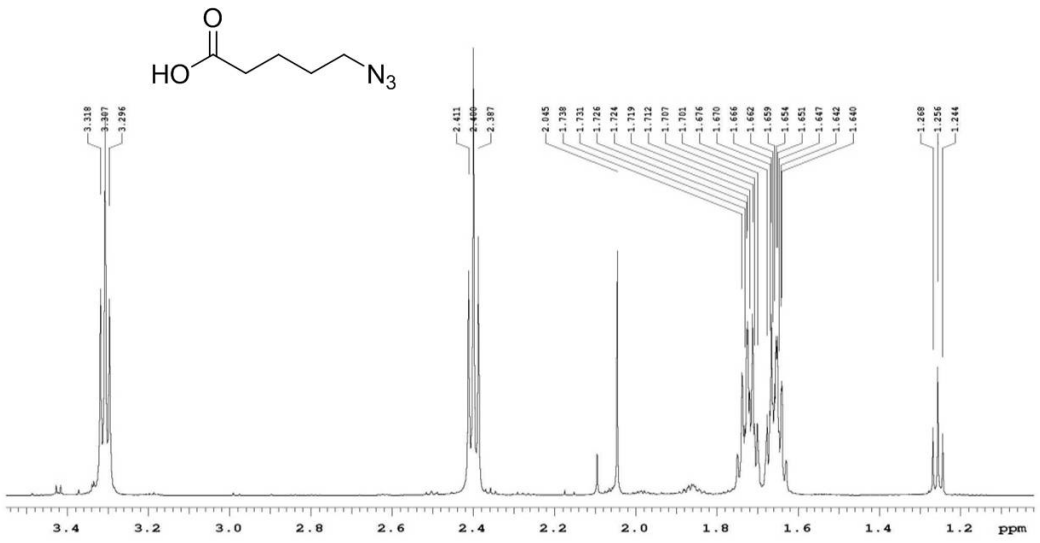

^{13}C NMR

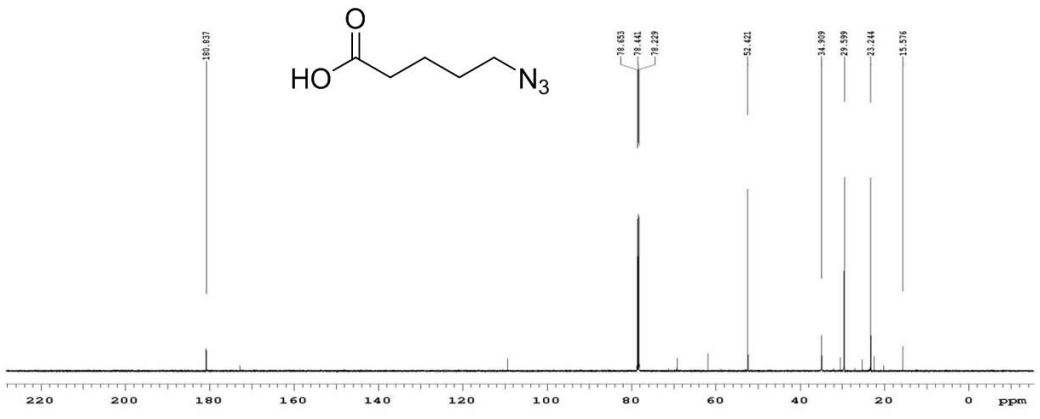

^{1}H NMR

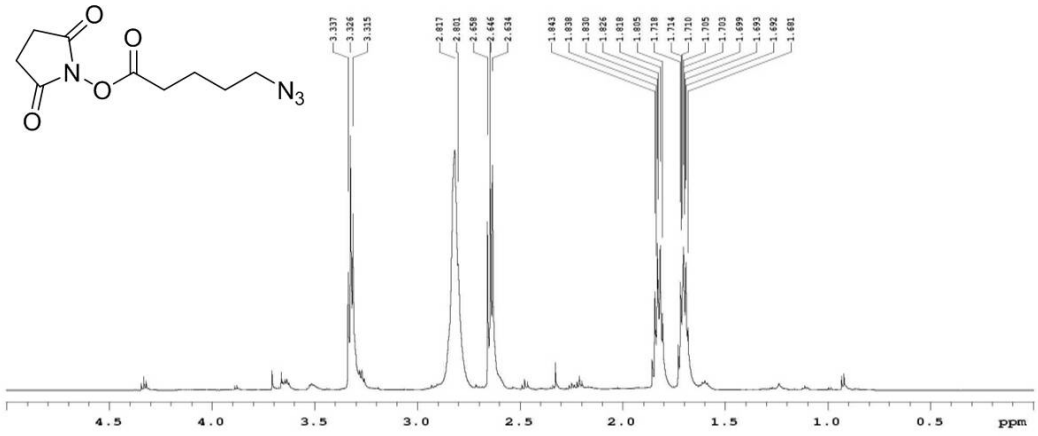

^{13}C NMR

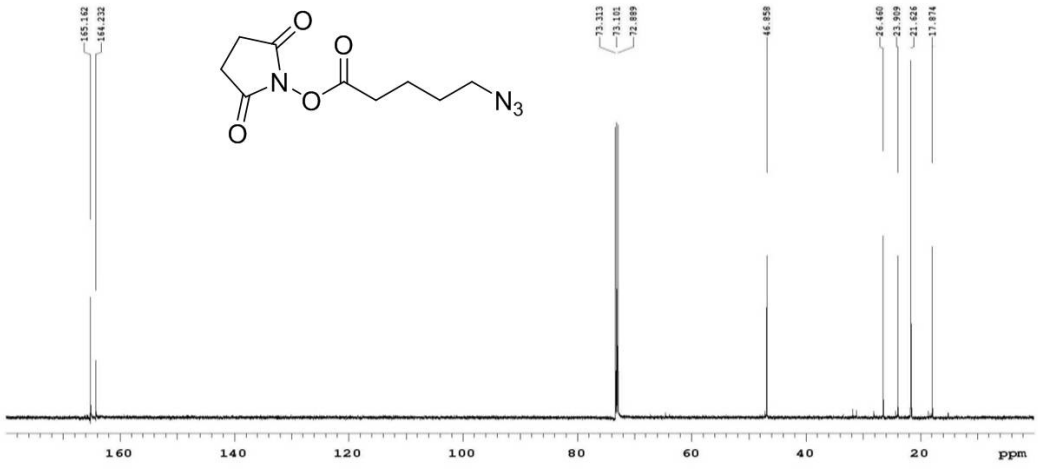

6. REFERENCES

(1) Harris, J. M. (1992) *Poly (ethylene glycol) chemistry; Biotechnical and Biomedical Applications.*, Plenum Press, New York.

(2) Nicolas, J., Mantovani, G., and Haddleton, D. M. (2007) Living Radical Polymerization as a Tool for the Synthesis of Polymer-Protein/Peptide Bioconjugates. *Macromol. Rapid Commun. 28*, 1083-1111.

(3) Raja, K. S., Dolai, S., Shi, W., and Wang, Q. (2009) in *Dekker Encyclopedia of Nanoscience and Nanotechnology, Second Edition* (Schwarz, J. A., Contescu, C. I., and Putyera, K., Eds.) pp 386-396, Taylor and Francis Group.

(4) Vriezema, D. M., Comellas Aragones, M., Elemans, J. A., Cornelissen, J. J., Rowan, A. E., and Nolte, R. J. (2005) Self-assembled nanoreactors. *Chem Rev 105*, 1445-89.

(5) Douglas, T., and Young, M. (2006) Viruses: making friends with old foes. *Science 312*, 873-5.

(6) Klok, H.-A. (2009) Peptide/Protein-Synthetic Polymer Conjugates: Quo Vadis. *Macromolecules 42*, 7990-8000.

(7) Miyamoto, M., Naka, K., Shiozaki, M., Chujo, Y., and Saegusa, T. (1990) Preparation and enzymic activity of poly[(N-acylimino)ethylene]-modified catalase. *Macromolecules 23*, 3201-3205.

(8) Bailon, P., and Won, C.-Y. (2009) PEG-modified biopharmaceuticals. *Expert Opinion on Drug Delivery 6*, 1-16.

(9) Kozlowski, A., and Harris, J. M. (2001) Improvements in protein PEGylation: pegylated interferons for treatment of hepatitis C. *J Control Release 72*, 217-24.

(10) Chapman, A. P., Antoniw, P., Spitali, M., West, S., Stephens, S., and King, D. J. (1999) Therapeutic antibody fragments with prolonged in vivo half-lives. *Nat Biotechnol 17*, 780-3.

(11) Rajender, R., K., Modi, M. W., and Pedder, S. (2002) Use of peginterferon alfa-2a (40 KD) (Pegasys) for the treatment of hepatitis C. *Advanced Drug Delivery Reviews 54*, 571-586.

(12) Kitamura, K., Takahashi, T., Yamaguchi, T., Noguchi, A., Takashina, K., Tsurumi, H., Inagake, M., Toyokuni, T., and Hakomori, S. (1991) Chemical engineering of the monoclonal antibody A7 by polyethylene glycol for targeting cancer chemotherapy. *Cancer Res 51*, 4310-5.

(13) Pedley, R. B., Boden, J. A., Boden, R., Begent, R. H., Turner, A., Haines, A. M., and King, D. J. (1994) The potential for enhanced tumour localisation by poly(ethylene glycol) modification of anti-CEA antibody. *Br J Cancer 70*, 1126-30.

(14) Veronese, F. M., and Pasut, G. (2005) PEGylation, successful approach to drug delivery. *Drug Discov Today 10*, 1451-8.

(15) Krishna, O. D., and Kiick, K. L. (2010) Protein- and peptide-modified synthetic polymeric biomaterials. *Biopolymers 94*, 32-48.

(16) Kochendoerfer, G. G., Chen, S. Y., Mao, F., Cressman, S., Traviglia, S., Shao, H., Hunter, C. L., Low, D. W., Cagle, E. N., Carnevali, M., Gueriguian, V., Keogh, P. J., Porter, H., Stratton, S. M., Wiedeke, M. C., Wilken, J., Tang, J., Levy, J. J., Miranda, L. P., Crnogorac, M. M., Kalbag, S., Botti, P., Schindler-Horvat, J., Savatski, L., Adamson, J. W., Kung, A., Kent, S. B., and Bradburne, J. A. (2003)

Design and chemical synthesis of a homogeneous polymer-modified erythropoiesis protein. *Science 299*, 884-7.

(17) Tao, L., Kaddis, C. S., Loo, R. R. O., Grover, G. N., Loo, J. A., and Maynard, H. D. (2009) Synthetic approach to homodimeric protein-polymer conjugates. *Chemical Communications 16*, 2148-2150.

(18) Maynard, H. D., Heredia, K. L., Li, R. C., Parra, D. P., and Vazquez-Dorbatt, V. (2007) Thermoresponsive biohybrid materials synthesized by ATRP. *Journal of Materials Chemistry 17*, 4015-4017.

(19) Heredia, K. L., and Maynard, H. D. (2007) Synthesis of protein-polymer conjugates. *Org Biomol Chem 5*, 45-53.

(20) Bontempo, D., Heredia, K. L., Fish, B. A., and Maynard, H. D. (2004) Cysteine-reactive polymers synthesized by atom transfer radical polymerization for conjugation to proteins. *J Am Chem Soc 126*, 15372-3.

(21) Romanini, D. W., and Francis, M. B. (2008) Attachment of peptide building blocks to proteins through tyrosine bioconjugation. *Bioconjugate chemistry 19*, 153-157.

(22) Gilmore, J. M., Scheck, R. A., Esser-Kahn, A. P., Joshi, N. S., and Francis, M. B. (2006) N-terminal protein modification through a biomimetic transamination reaction. *Angewandte Chemie, International Edition 45*, 5307-5311.

(23) Esser-Kahn, A. P., and Francis, M. B. (2008) Protein-cross-linked polymeric materials through site-selective bio-conjugation. *Angewandte Chemie, International Edition 47*, 3751-3754.

(24) Carrico, Z. M., Romanini, D. W., Mehl, R. A., and Francis, M. B. (2008) Oxidative coupling of peptides to a virus capsid containing unnatural amino acids. *Chem Commun (Camb)*, 1205-7.

(25) Kulkarni, S., Schilli, C., Grin, B., Muller, A. H., Hoffman, A. S., and Stayton, P. S. (2006) Controlling the aggregation of conjugates of streptavidin with smart block copolymers prepared via the RAFT copolymerization technique. *Biomacromolecules 7*, 2736-41.

(26) Boyer, C., Bulmus, V., Liu, J., Davis, T. P., Stenzel, M. H., and Barner-Kowollik, C. (2007) Well-defined protein-polymer conjugates via in situ RAFT polymerization. *J Am Chem Soc 129*, 7145-54.

(27) Tao, L., Mantovani, G., Lecolley, F., and Haddleton, D. M. (2004) Alpha-aldehyde terminally functional methacrylic polymers from living radical polymerization: application in protein conjugation "pegylation". *J Am Chem Soc 126*, 13220-1.

(28) Qi, K., Ma, Q., Remsen, E. E., Clark, C. G., Jr., and Wooley, K. L. (2004) Determination of the bioavailability of biotin conjugated onto shell cross-linked (SCK) nanoparticles. *J Am Chem Soc 126*, 6599-607.

(29) Sen Gupta, S., Raja, K. S., Kaltgrad, E., Strable, E., and Finn, M. G. (2005) Virus-glycopolymer conjugates by copper(I) catalysis of atom transfer radical polymerization and azide-alkyne cycloaddition. *Chem Commun (Camb)*, 4315-7.

(30) Hou, S., Sun, X. L., Dong, C. M., and Chaikof, E. L. (2004) Facile synthesis of chain-end functionalized glycopolymers for site-specific bioconjugation. *Bioconjug Chem 15*, 954-9.

(31) Bontempo, D., and Maynard, H. D. (2005) Streptavidin as a macroinitiator for polymerization: in situ protein-polymer conjugate formation. *Journal of the American Chemical Society 127*, 6508-6509.

(32) Lele, B. S., Murata, H., Matyjaszewski, K., and Russell, A. J. (2005) Synthesis of uniform protein-polymer conjugates. *Biomacromolecules 6*, 3380-7.

(33) Ayres, L., Vos, M. R. J., Adams, P. J. H. M., Shklyarevskiy, I. O., and Van Hest, J. C. M. (2003) Elastin-Based Side-Chain Polymers Synthesized by ATRP. *Macromolecules 36*, 5967-5973.

(34) Klok, H.-A. (2005) Biological-synthetic hybrid block copolymers: Combining the best from two worlds. *Journal of Polymer Science, Part A: Polymer Chemistry 43*, 1-17.

(35) Kohn, M., and Breinbauer, R. (2004) The Staudinger ligation-a gift to chemical biology. *Angew Chem Int Ed Engl 43*, 3106-16.

(36) Saxon, E., and Bertozzi, C. R. (2000) Cell surface engineering by a modified Staudinger reaction. *Science 287*, 2007-10.

(37) Kiick, K. L., Saxon, E., Tirrell, D. A., and Bertozzi, C. R. (2002) Incorporation of azides into recombinant proteins for chemoselective modification by the Staudinger ligation. *Proceedings of the National Academy of Sciences of the United States of America 99*, 19-24.

(38) Rostovtsev, V. V., Green, L. G., Fokin, V. V., and Sharpless, K. B. (2002) A stepwise huisgen cycloaddition process: copper(I)-catalyzed regioselective "ligation" of azides and terminal alkynes. *Angew Chem Int Ed Engl 41*, 2596-9.

(39) Link, A. J., and Tirrell, D. A. (2003) Cell surface labeling of Escherichia coli via copper(I)-catalyzed [3+2] cycloaddition. *J Am Chem Soc 125*, 11164-5.

(40) Deiters, A., Cropp, T. A., Summerer, D., Mukherji, M., and Schultz, P. G. (2004) Site-specific PEGylation of proteins containing unnatural amino acids. *Bioorg Med Chem Lett 14*, 5743-5.

(41) Nicolas, J., Khoshdel, E., and Haddleton, D. M. (2007) Bioconjugation onto biological surfaces with fluorescently labeled polymers. *Chem Commun (Camb)*, 1722-4.

(42) Shi, W., Dolai, S., Rizk, S., Hussain, A., Tariq, H., Averick, S., L'Amoreaux, W., El ldrissi, A., Banerjee, P., and Raja, K. (2007) Synthesis of monofunctional curcumin derivatives, clicked curcumin dimer, and a PAMAM dendrimer curcumin conjugate for therapeutic applications. *Org Lett 9*, 5461-4.

(43) Sen Gupta, S., Kuzelka, J., Singh, P., Lewis, W. G., Manchester, M., and Finn, M. G. (2005) Accelerated bioorthogonal conjugation: a practical method for the ligation of diverse functional molecules to a polyvalent virus scaffold. *Bioconjug Chem 16*, 1572-9.

(44) Kiessling, L. L., Gestwicki, J. E., and Strong, L. E. (2006) Synthetic multivalent ligands as probes of signal transduction. *Angew. Chem. Int. Ed. 45*, 2348-2368.

(45) Andrews, D. L. (2008) Mechanistic principles and applications of resonance energy transfer. *Can. J. Chem. 86*, 855-870.

CHAPTER IV

Synthesis of Novel Functional Curcumin Derivatives.

1. INTRODUCTION

Curcuma longa is used as a spice in South Asian cooking, as a cosmetic and in the ancient Ayurvedic system of medicine (*1*). Turmeric or Haldi is the dried powdered rhizome derived from the plant. Curcuminoids constitute around 5% of most turmeric preparations and can be readily isolated from the plant (*2*). There has recently been tremendous interest in curcumin, [(1*E*, 6*E*)-1, 7-bis (4-hydroxy-3-methoxyphenyl) hepta-1,6-diene 3,5-dione] the primary active ingredient in turmeric, because it has been shown to have antioxidant (*2, 3*), anticancer (*4, 5*), anti-inflammatory (*6*), anti-Alzheimer's disease activity (*7*) and antibiotic activity (*8*). Curcumin works on many biological pathways, it is a potent NF-κβ inhibitor, via this key receptor many down stream targets are modulated including gene products involved in blocking apoptosis (Bcl-2, Bcl-xL, XIAP), angiogenesis (VEGF) and metastasis (adhesion molecules) (*2, 9*). Curcumin has been shown to reduce pathology in AD mouse models overproducing Aβ (*7*). Curcumin appears to have multiple neuroprotective mechanisms including inhibition of inflammation, suppression of Aβ production, reduction of reactive oxygen species by chelating metals, inhibition of stress pathways and induction of heat shock proteins (*10*). Curcumin is an excellent candidate for developing a green drug because (a) Turmeric has been used as a spice and in Ayurvedic formulations for centuries which implies that it is non-toxic and is generally regarded as safe by the FDA (b) It can be isolated from Curcuma *longa* in reasonable yields and is inexpensive. (c) It has a relatively simple chemical structure which lends itself to efficient chemical manipulation. The safety of curcumin has been established in recent clinical trials, in a trial conducted in Taiwan volunteers were fed 8 g of curcumin orally with no toxic side effects, only 1.77 μM

concentration of curcumin was detected in the plasma; this is most probably because of the fact that curcumin is relatively hydrophobic with poor water solubility (*11, 12*).

The glucuronidation of curcumin *in vivo* is another possible reason for the observation of very low plasma levels of the compound (*13*). Commercial formulations such as Supercurcumin with Bioperine ® are a combination of curcumin and piperine from black pepper. It has been shown that the glucuridination of curcumin is suppressed by piperine: in a study it was shown that in humans a dose of 2 g curcumin alone resulted in serum levels of curcumin which were undetectable, concomitant administration of piperine 20 mg increased the bioavailability of curcumin by 2000% (*14*). It should be noted that this synergy between black pepper and turmeric has been exploited in Ayurvedic formulations and in Indian cooking for centuries for example Mahasudarshan is an example of an Ayurvedic formulation which contains both turmeric and black pepper, Pav Bhaji Masala (a spice mix) manufactured by Everest Inc. contains both turmeric and black pepper.

Nanoparticles formed by random copolymers of N-vinyl-2-pyrrolidone-N-isopropyl acryl amide poly(ethylene glycol) monoacrylate have been loaded with curcumin to produce a water soluble formulation " Nanocurcumin"(*15*). Nanocurcumin particles were ~50 nm in size, bioefficacy of this construct was comparable to curcumin in *in vitro* assays using pancreatic cancer cell lines (NF-κβ inhibition, induction of apoptosis and down regulation of pro inflammatory cytokines); *in vivo* studies have not been reported by the authors yet. Solid lipid nanoparticles ~450 nm size incorporating up to 70% w/w curcumin have been prepared using a microemulsion technique (*16*). Lyophilized solid lipid nanoparticles were stable over six months, they were employed in

a topical cosmetic formulation which significantly reduced skin wrinkles, improved skin moisture and the firmness, elasticity, and viscoelasticity of the skin of the volunteers. It must be noted that turmeric is a widely used cosmetic, for example Vicco ®. A colorless hydrogenated derivative of curcumin, tetrahydrocurcumin is also used as a cosmeceutical for example Anew® manufactured by Avon.

Liposomal formulations of curcumin have been developed. DMPC (1,2-Dimyristoyl-sn-glycero-3-phosphocholine) and DMPG (1,2-dimyristoyl-sn-glycero-3-phospho-rac-1-glycerol) loaded curcumin liposomes have been evaluated both *in vitro* and *in vivo* in the mouse model (*17*). The activity of liposomal curcumin was comparable to or better than that of free curcumin at equimolar concentrations, it down-regulated NF-κβ, suppressed cell proliferation, and induced apoptosis of human pancreatic cells in vitro. In vivo liposomal curcumin suppressed pancreatic carcinoma growth in murin xenograft models and inhibited tumor angiogenesis. There are other reports of liposomal curcumin formulations (*18*). A curcumin-phospholipid complex has recently been reported, the complex has better hepatoprotective activity compared to free curcumin (*19*). Bovine serum albumin and Chitosan have been employed to encapsulate curcumin to produce biodegradable microspheres (*20*). Curcumin has been solubilized using polymeric micelles, the formulation has been evaluated in the mouse model: it was shown via an HPLC assay that the micellar formulation increased the half-life of curcumin 162-fold compared to unformulated curcumin and that it increased the volume of distribution by 70-fold (*21*).

The chemical modification of 'green drug candidates' using few efficient reactions to produce derivatives with optimized bioefficacy and pharmacokinetics is

another route to green drugs (*22*). Curcumin is an excellent model system to explore this concept because of its simple structure, therapeutic promise and ready availability from commercially grown Curcumin *longa*. Curcuminoids (1,7-diaryl-1,6-heptadiene-3,5-diones) bind several metal ions, through keto-enol tautomerization of the β-diketonate moiety to form metallocomplexes. Vanadyl curcumin was recently reported, it was several-fold more potent than curcumin as an inhibitor of synoviocyte proliferation which is a measure of anti-arthritic potential (*23*). The Vanadyl complex was also more effective than curcumin in inhibiting mouse lymphoma cell growth. A five-coordinate curcumin–gold complex, $Au(cur)_2Cl$ has been synthesized (*24*). The curcumin gold complex was shown to be more effective than curcumin in reducing "paw swelling" using a rat model for arthritis. Curcumin-copper complexes have also been prepared, $Cu(curcumin)_2$ complexes were more cytotoxic in cultured L929 cells than uncomplexed curcumin, a significant reduction in solid tumor volume was observed in tumor-bearing mice treated with this complex (*25*). Curcumin copper complexes also serve as excellent superoxide dismutase mimics and are potent free radical scavengers (*26*). It has been shown that the curcumin-manganese complex Mn(cur)(OAc) has protective effects in a transient ischemia mouse model of neuronal damage (*27*). Curcumin derivatives with glycine and uridine have been synthesized (*8*). Uridine is part of the bacterial genome and glycine is part of bacterial cell walls, these derivatives were shown to be more effective than curcumin against several multi-resistant Gram positive and Gram negative bacteria. The minimum inhibitory concentration (MIC) against *Streptococcus pyogenes* was impressive 1.88 μM, MIC of the commercial antibiotic Amoxyclav against this strain was 7 μM. These derivatives were effective against β-Lactamase producing micro-organisms,

they are promising drug candidates to combat the problem of antibiotic resistance.

The development of a synthetic methodology to produce curcumin derivatives with water solublizing groups including synthetic polymers and targeting proteins can potentially enhance the therapeutic efficacy of curcumin. A general synthetic technology to produce monofunctional curcumin derivatives in which one of the phenolic groups of curcumin was chemically modified with reactive groups was recently developed by our group (*5*). The approach involved direct one/two step covalent modification of curcumin to produce the mono-functional derivatives (azide, alkyne, carboxylic acid, alcohol, amine, NHS and acrylate) in good yields. The synthesis of small molecule mono-functional curcumin derivatives afforded two advantages: (a) the presence of at least one free phenolic group is necessary for the biological activity of many antioxidants like curcumin. It was found that mono-functional derivatives of curcumin retain their ability to bind and dissociate amyloid fibrils in vitro (*5, 28*) (b) conjugates produced by using mono-functional derivatives produce soluble products in high yields whereas bifunctional derivatives would result in insoluble cross-linked products. A curcumin dimer in which two curcumin moieties were connected via a PEG spacer was synthesized the copper catalyzed azide-alkyne “click” reaction.

2. MATERIALS AND METHODS

2.1. General Information

Reagent-grade acetone, HPLC grade tetrahydrofuran, methylene chloride, N,N-dimethylformamide were used without further purification. Solvents used for reactions were purified using *pure solv*^{TM} system. Curcumin was obtained from Acros Organics. Copper (II) Sulfate and sodium ascorbate were purchased from Sigma. O-(2-Aminoethyl)-O'-(2-azidoethyl)-pentaethylene glycol (amino-PEG-azide) obtained from Sigma Chemicals was ~90% pure and was used as it is. G4 Cystamine core PAMAM dendrimer was purchased from Dendritic Nanotechnologies. Aβ1-40 peptide and human heart tissue slides containing intercellular amyloid were purchased from Sigma. Silica gel 60 F 254 plates for thin-layer chromatography (TLC) were purchased from Fisher Scientific. Column chromatographic separations were performed using silica gel (Fisher) with a particle size of 0.040-0.063 mm. Nuclear magnetic resonance (NMR) spectra were recorded on Oxford NMR 600 (600 MHz) spectrometer. Mass spectra (ES-MS) were recorded using an Agilent LC/MS and a Time of Flight (TOF) mass spectrometer. UV-visible spectra were recorded using a ChemStation Rev. A.10.01 from Agilent Technologies. FPLC analysis was performed using an AKTA explorer from GE Biosciences. TEM images were recorded using a Phillips CM 100 microscope. The heart amyloid slides were imaged using a Leica DMLP polarized light microscope under crossed polarizers.

2.2. Synthetic Protocols : Mono-functional Curcumin Derivatives

2.2.1. Synthesis of 5-(4-((1*E*,6*E*)-7-(4-hydroxy-3-methoxyphenyl)-3,5-dioxohepta-1,6-dienyl)-2-methoxyphenoxy)-5-oxopentanoic acid; Curcumin mono-carboxylic acid.

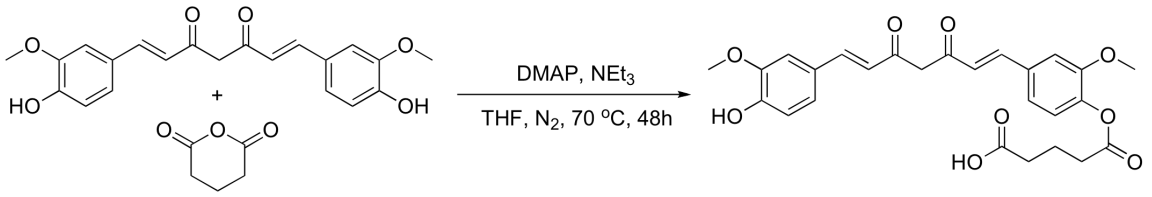

To a solution of 2.01 g (5.46 mmol) of curcumin, and 112 mg (0.92 mmol) of DMAP in 100 ml THF was added 1.33 ml (9.55 mmol) of Et_3N. 0.685 g (6 mmol) of glutaric anhydride (95%) in 5 mL THF was added slowly drop-wise to the curcumin solution. The mixture was stirred and refluxed under argon atmosphere overnight. THF was removed under vacuum, 55 mL EtOAc was added, followed by the addition of 15 mL of 1M HCL, the mixture was stirred for 10 minutes. The organic phase was separated and extracted with EtOAc three times; the solvent was removed and dried. The product was purified via column chromatography, eluting with CH_2Cl_2:MeOH, 95:5. Yield: 69 %. ^{1}HNMR ($CDCl_3$), δ (ppm): 2.10-2.12 (t, 2H); 2.56-2.58 (t, 2H); 2.69-2.72 (t, 2H); 3.87 (s, 3H); 3.94 (s,3H); 5.83 (s, 2H); 6.48-6.57 (t, 2H); 6.48-6.57 (m, 1H); 6.94-7.16 (m, 5H); 7.59-7.62 (d, 2H). ^{13}C NMR ($CDCl_3$), δ (ppm): 19.87; 32.65; 55.70; 101.48; 109.73; 111.23; 114.91; 120.83; 121.42; 123.02; 124.03; 127.22; 133.76; 133.90; 139.25; 141.06; 146.89; 148.09; 151.09; 170.85; 177.24; 181.59; 184.51. MS (ESI) *calcd.* for $C_{26}H_{26}O_9$: 482.48; found: 483.2 $[M+H]^+$.

2.2.2. Synthesis of (1*E*,6*E*)-1-(4-hydroxy-3-methoxyphenyl)-7-(3-methoxy-4-(prop-2-ynyloxy)phenyl)hepta-1,6 diene-3,5-dione; Curcumin mono-alkyne.

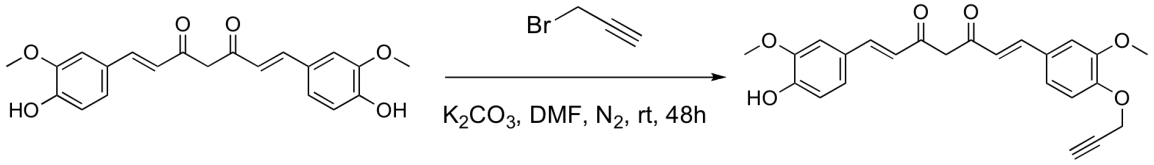

Curcumin (5 g, 13.57 mmol) and K_2CO_3 (1.88 g, 13.62 mmol) were added to 60 mL DMF followed by 1.62 g (13.61 mmol) of propargyl bromide. The mixture was stirred at room temperature under N_2 for 49 h, H_2O was added to the mixture and the solvent was removed under vacuum. The product was purified by column chromatography, eluting with CH_2Cl_2:hexane 50:50. Yield: 47%. ^{1}H NMR ($CDCl_3$), δ (ppm): 2.54 (s, 1H); 3.94 (d, 6H); 4.81 (d, 2H); 5.82 (d, 1H); 5.93 (d, 1H); 6.47-6.52 (t, 2H); 6.93-7.15 (m, 6H); 7.59-7.61 (d, 2H). ^{13}CNMR ($CDCl_3$), δ (ppm): 30.73; 30.77; 31.38; 31.40; 36.50; 55.70; 55.72; 55.76, 56.35; 101.44; 109.97; 110.01; 110.30; 113.39; 113.40; 115.14; 115.17; 121.22; 121.27; 121.94; 122.00; 122.25; 122.30; 122.85; 122.86; 127.13; 127.18; 128.93; 139.90; 139.92; 140.83; 140.86; 147.23; 148.33; 148.40; 148.46; 149.44; 162.74; 162.80; 182.57; 183.73. MS (ESI) *calcd.* for $C_{24}H_{22}O_6$: 406.43; found: 407.2 $[M+H]^+$, 445.2 $[M^+ + K]$.

2.2.3. Synthesis of 4-((1*E*,6*E*)-7-(4-hydroxy-3-methoxyphenyl)-3,5-dioxohepta-1,6-dienyl)-2-methoxyphenyl 1-azido-22-oxo-3,6,9,12,15,18-hexaoxa-21-azahexacosan-26-oate; Curcumin mono-azide.

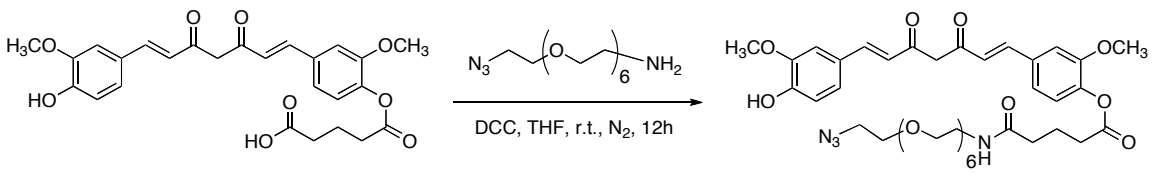

To a solution of 158 mg (0.45 mmol) of curcumin mono-carboxylic acid in 3 mL dry THF at room temperature was added 206 mg (0.427 mmol) of *O*-(2-Aminoethyl)-*O'*-(2-azidoethyl)-pentaethylene glycol and 96 mg (0.47 mmol) of 1,3-dicyclohexylcarbodiimide. The mixture was stirred at 25 ^{o}C overnight under N_2 atmosphere. The reaction mixture was then diluted with 10 mL of ethyl acetate, filtered to remove the urea by-product, and the organic solvent was removed using a vacuum pump. The reaction mixture was dissolved in methylene chloride and washed with water. The organic phase was separated and dried using a vacuum pump. The sample was purified via column chromatography, eluting with CH_2Cl_2:MeOH, 95:5. Yield: 29%. ^{1}H NMR ($CDCl_3$), δ (ppm): 1.79 (bs, 2H); 2.35-2.37 (t, 2H); 2.65-2.68 (t, 2H); 3.62-3.66 (m, 28H); 3.87 (s, 3H); 3.95 (s, 3H); 6.40 (s, 1H); 6.48-6.57 (m, 2H); 6.93-6.94 (d, 1H); 7.05-7.16 (m, 6H); 7.60-7.61 (m, 2H). ^{13}CNMR ($CDCl_3$), δ (ppm): 29.63; 33.03; 35.04; 39.16; 50.57; 55.80; 55.87; 69.94; 70.37; 70.41; 70.45; 70.50; 70.54; 70.57; 101.53; 109.65; 109.66; 111.28; 114.89; 114.91; 120.93; 122.99; 123.20; 127.33; 133.95; 141.03; 146.88; 148.09; 151.20; 171.06; 172.24; 181.64; 184.49. ESI-MS (*calcd.* for $C_{40}H_{54}N_4O_{14}$ 814.36), found: 837.38 [M^+ +Na], 853.35 [M^+ + K].

2.2.4. Synthesis of (1*E*,6*E*)-1-(4-hydroxy-3-methoxyphenyl)-7-(4-((1-(2-(2-(2-hydroxyethoxy)ethoxy)ethyl)-1H-1,2,3-triazol-4-yl)methoxy)-3-methoxyphenyl)hepta-1,6-diene-3,5-dione; Curcumin mono-alcohol.

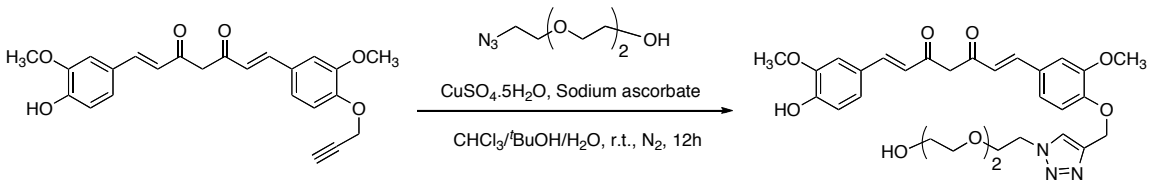

To a stirred solution of Curcumin mono-alkyne (63 mg, 0.16 mmol) and 2-(2-(2-azidoethoxy)ethoxy)ethanol (46 mg, 0.26 mmol) in ^{t}BuOH (1.1 mL) and $CHCl_3$ (0.3 mL) was added a prepared solution of $CuSO_4.5H_2O$ (8 mg, 0.03 mmol) and sodium ascorbate (13 mg, 0.07 mmol) in H_2O (1.3 mL). After vigorous stirring overnight the solvent was removed under vacuum. The mixture was dissolved in $CHCl_3$, washed with H_2O and the organic phase was separated, dried over Na_2SO_4 and evaporated. Purification was performed by column chromatography, eluting with CH_2Cl_2:MeOH 98:2. Yield: 26%. ^{1}HNMR (600 MHz; $CDCl_3$), δ (ppm): 3.55-3.60 (m, 8H); 3.72-3.72 (t, 3H); 3.87-3.94 (m, 8H); 4.54-4.55 (t, 2H); 5.80 (s, 1H); 6.07 (s, 1H); 6.46-6.50 (dd, 2H); 6.92-6.94 (d, 1H); 7.05-7.12 (m, 5H); 7.56-7.60 (q, 2H); 7.92 (s, 1H).). ^{13}C NMR (150 MHz; $CDCl_3$), δ (ppm): 29.66; 50.24; 55.92; 61.65; 62.76; 69.24; 70.14;70.44; 72.36; 101.29; 109.58;110.24; 113.46; 114.83; 122.24. ESI-MS *calcd.* for $C_{30}H_{35}N_3O_9$: 581.61; found: 582.3 $[M+H]^+$, 604.3 $[M^+ +Na]$, 620.3 $[M^+ + K]$.

2.2.5. Synthesis of (1*E*,6*E*)-1-(4-((1-(2-(2-(2-(2-aminoethoxy)ethoxy)ethoxy)ethyl)-1*H*-1,2,3-triazol-4-yl)methoxy)-3-methoxyphenyl)-7-(4-hydroxy-3-methoxyphenyl)hepta-1,6-diene-3,5-dione; Curcumin mono-amine.

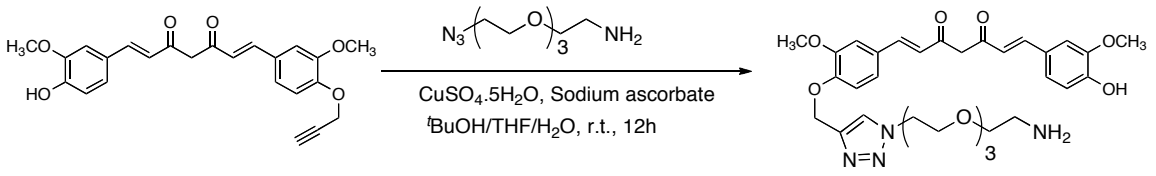

Curcumin mono-alkyne (100 mg, 0.245 mmol) and N_3-PEG-NH_2 (48 μL, 0.245 mmol) were dissolved in 4 mL equal mixtutres of ^{t}BuOH and THF. Freshly prepared

solutions of $CuSO_4.5H_2O$ and sodium ascorbate in water were added to the reaction mixture. Final concentrations of $CuSO_4.5H_2O$ and sodium ascorbate were kept at 4 mM. The mixture was stirred for 12h at room temperature. Once the reaction was stopped, solvent was evaporated and finally the dark brown colored product was isolated via column chromatography using Chloroform: Methanol (90:10 v/v). Yield: 120 mg (78%). ^{1}H NMR (600 MHz, $CDCl_3$), δ (ppm): 3.36-3.88 (m), 4.51-4.52 (t), 5.27 (s), 5.77 (s), 6.44 (t), 6.87 (d), 7.01-7.06 (m), 5.52-7.56 (q), 7.83 (s). ^{13}C NMR (150 MHz, $CDCl_3$), δ (ppm): 50.28, 50.63, 55.82, 55.88, 62.79, 68.10, 69.33, 69.98, 70.12, 70.21, 70.36, 70.46, 70.48, 70.56, 70.59, 70.63, 101.24, 109.87, 110.36, 113.60, 115.25, 121.36, 122.18, 122.29, 122.97, 124.37, 127.12, 128.69, 128.75, 130.84, 139.97, 140.81, 143.41, 147.33, 148.67, 149.51, 149.54, 182.66, 183.70. ESI-MS *calcd.* for $C_{32}H_{40}N_4O_9$: 624.28; found: 625.6 $[M+H]^+$, 647.5 $[M^+ +Na]$.

2.2.6. Synthesis of 2,5-dioxocyclopentyl 4-((1*E*,6*E*)-7-(4-hydroxy-3-methoxyphenyl)-3,5-dioxohepta-1,6-dienyl)-2-methoxyphenyl glutarate; Curcumin mono-NHS.

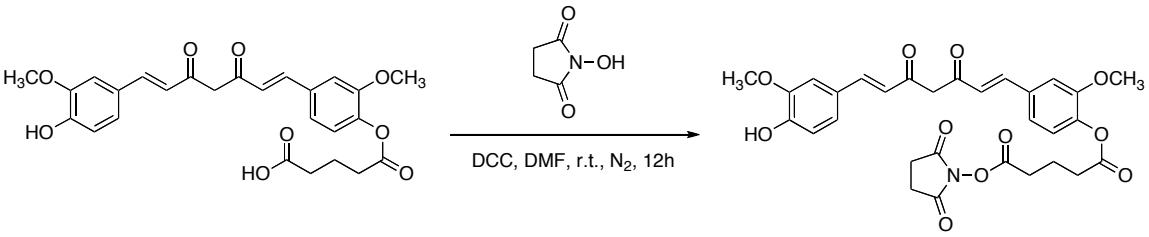

Curcumin mono-carboxylic acid (500 mg, 1.04 mmol) and *N*-hydroxysuccinimide (120 mg, 1.04 mmol) were dissolved in 10 ml dry-DMF in a 50 ml r.b. Stirred for 15 mins and then ice-cold solution of DCC (309 mg, 1.5 mmol) in 5 ml dry-DMF was added drop-wise. The mixture was degassed with N_2 and stirred at room temperature for 12h.

Formed carbohexyl urea was filtered off and solvent was evaporated and the product was isolated precipitating from excess of ether. The crude product was finally purified via column chromatography using Chloroform: Methanol (98:2). Yield: 465 mg (77.5 %).[1]HNMR (600 MHz; $CDCl_3$), δ (ppm): 1.11-1.15 (t), 1.23-1.33 (t), 1.57-1.59 (d), 1.67-1.69 (m), 1.90-1.91 (t), 2.15-2.19 (m), 2.65-2.94 (m), 2.41 (s), 3.79-3.90 (m), 5.82-5.85 (d), 6.48-6.58 (m), 6.89-6.91 (d), 6.03-7.15 (m), 7.54-7.61 (m), 8.0 (s). ^{13}C NMR (150 MHz; $CDCl_3$), δ (ppm): 19.92, 20.28, 24.83, 25.33, 25.50, 25.57, 29.78, 32.40, 32.78, 33.66, 49.33, 55.07, 55.80, 55.83, 101.55, 101.84, 111.38, 111.42, 114.54, 120.95, 121.07, 121.62, 123.06, 123.15, 124.22, 127.42, 133.06, 134.10, 133.94, 141.02, 141.15, 141.23, 146.97, 148.17, 151.22, 151.24, 151.29, 151.32, 157.63, 166.11, 169.12, 169.21, 170.42, 170.85, 172.20, 181.74, 183.11, 184.80. ESI-MS *calcd.* for $C_{30}H_{29}NO_{11}$: 579.17; found: 580.3 $[M+H]^+$, 578.5 $[M-H]^-$.

2.2.7. Synthesis of 4-((1*E*,6*E*)-7-(4-hydroxy-3-methoxyphenyl)-3,5-dioxohepta-1,6-dienyl)-2-methoxyphenyl 1-(4-((4-((1*E*,6*E*)-7-(4-hydroxy-3-methoxyphenyl)-3,5-dioxohepta-1,6-dienyl)-2-methoxyphenoxy)methyl)-1H-1,2,3-triazol-1-yl)-22-oxo-3,6,9,12,15,18-hexaoxa-21-azahexacosan-26-oate. Curcumin dimmer.

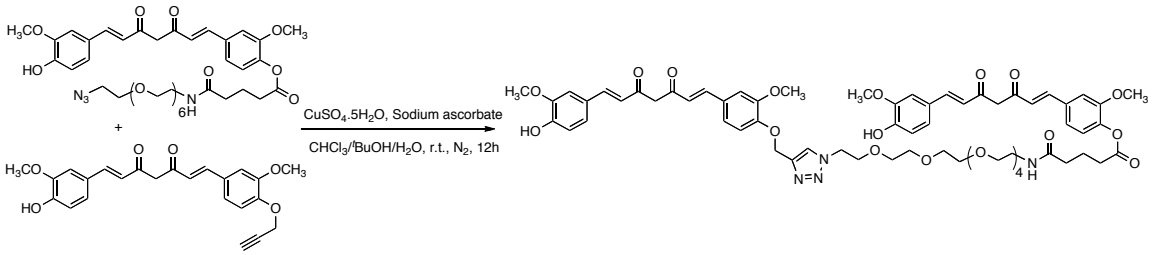

The above molecule was synthesized by dissolving 30 mg (0.037 mmol) of Curcumin mono-azide and 25.3 mg (0.062 mmol) of Curcumin mono-alkyne in a mixture of 0.55 mL ^{t}BuOH and 0.15 mL chloroform. Sodium ascorbate (4.7 mg, 0.0237 mmol)

and $CuSO_4.5H_2O$ (2.2 mg, 0.008 mmol) were dissolved in 0.6 mL of deionized water and added to the reaction mixture. The mixture was stirred for overnight at room temperature under N_2 atmosphere. After removing the solvents the crude product was dissolved in $CHCl_3$ and washed thoroughly with water. Purification was performed by column chromatography, eluting with CH_2Cl_2:MeOH 98:2. Yield: 41%. ^{1}H NMR ($CDCl_3$), δ (ppm): 1.97-1.99 (t, 2H); 2.27-2.29 (t, 2H); 2.47-2.49 (t, 2H); 3.41-3.42 (t, 2H); 3.53-3.63 (m, 26H); 3.86-3.95 (m, 12H); 4.54-4.55 (d, 4H); 5.33 (s, 2H); 6.55-6.56 (bd, 4H); 6.94-7.11 (bm, 12H); 7.59 (s, 4H); 7.87 (s, 1H).). ^{13}CNMR ($CDCl_3$), δ (ppm): 20.92; 21.22; 24.69; 25.24; 26.02; 30.70; 32.44; 34.97; 35.07; 39.10; 39.12; 50.20; 50.22; 55.77; 62.59; 69.21; 69.23; 69.63; 69.75; 70.03; 70.28; 70.33; 70.36; 101.24; 101.25; 109.59; 109.60; 109.61; 109.63; 109.64; 110.08; 110.09; 110.11; 110.13; 111.22; 111.23; 113.30; 113.33; 113.36; 113.38; 113.39; 114.90; 120.86; 121.43; 122.00; 122.10; 122.16; 122.23; 122.83; 122.95; 123.12; 124.07; 124.08; 124.43; 127.21; 127.31; 128.48; 133.88; 139.15; 140.02; 140.09; 140.09; 140.64; 141.11; 143.24; 146.88; 146.90; 148.00; 148.12; 149.38; 149.39; 149.41; 149.47; 149.49; 149.50; 151.10; 153.96; 172.23; 172.97; 181.54; 182.73; 183.48; 184.49. ESI-MS (*calcd.* for $C_{64}H_{76}N_4O_{20}$ 1220.51), found: 1243.52 [M^++Na], 1259.47 [M^++K].

2.2.8. Synthesis of (2*R*,4*S*,5*R*)-2-(acetoxymethyl)-6-(2-(2-(2-(4-((4-((1*E*,6*E*)-7-(4-hydroxy-3-methoxyphenyl)-3,5-dioxohepta-1,6-dienyl)-2-methoxyphenoxy)methyl)-1*H*-1,2,3-triazol-1-yl)ethoxy)ethoxy)ethoxy)tetrahydro-2*H*-pyran-3,4,5-triyl triacetate; Sweet-curcumin (protected).

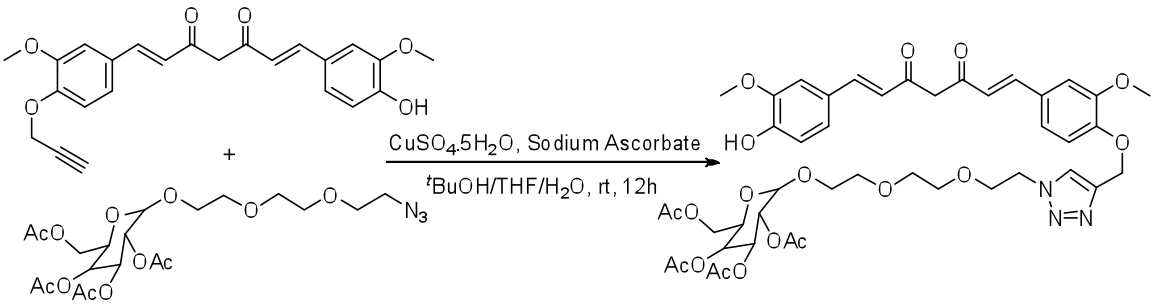

Curcumin mono-alkyne (500 mg, 1.23 mmol) was dissolved in 2 mL of THF and added to 2mL of *t*-BuOH containing commercially available acetal-protected Azido-Galactose derivative [2-[2-(2-Azidoethoxy)ethoxy]ethyl-2,3,4,6-Tetra-O-acetyl-D-galactopyranoside] (625 mg, 1.23 mmol) in a round bottom flask (r.b.). Fresh solutions of $CuSO_4.5H_2O$ (76 mg, 0.3 mmol) and Sodium Ascorbate (90 mg, 0.45 mmol) were prepared separately in 1 mL of milipore water. Sodium Ascorbate solution was added to the r.b. followed by $CuSO_4$ solution and stirred for 12 hours. The reaction was stopped and the solvent was removed by evaporation. The crude product was extracted from water-chloroform mixture. The organic layer was dried over anhydrous $NaSO_4$ and solvent was evaporated. Finally the product was purified via column chromatography using Chloroform: Ethyl acetate (90:10) mixture to yield orange solid. Yield: 785 mg (70%). ^{1}H NMR ($CDCl_3$, 600 MHz): δ(ppm) 1.93 (s, 3H),1.97-1.99 (d, 6H), 2.08 (s, 3H),

3.52-3.56 (m, 7H), 3.64-3.66 (m, 1H), 3.81-3.90 (m, 10H), 4.04-4.11 (m, 3H), 4.46-4.50 (m, 3H), 4.95-4.97 (dd, 1H), 5.13-5.16 (m, 1H), 5.25-5.28 (m, 2H),5.32 (m, 1H),5.76 (s, 1H), 6.41-6.45 (m, 2H), 6.86-6.88 (d, 1H), 6.99-7.07 (m, 4H), 7.51-7.54 (m, 2H), 7.80 (s, 1H); ^{13}C NMR ($CDCl_3$, 150 MHz): δ(ppm):20.48, 20.54, 20.56, 20.65, 50.23, 55.82, 55.84, 61.09, 62.77, 66.92, 68.69, 69.04, 69.28, 70.07, 70.45, 70.47, 70.53, 70.75, 101.18, 101.23, 109.61, 110.30, 113.57, 114.84, 121.59, 122.15, 122.24, 122.84, 124.25, 139.99, 140.61, 143.39, 146.82, 147.93, 149.50, 149.51, 169.33, 170.04, 170.13, 170.28, 182.73, 183.52.; ESI-MS: for $C_{44}H_{53}N_3O_{18}$; calculated-911.33.; observed-912.3 $[M+H]^+$.

2.2.9. Synthesis of (1*E*,6*E*)-1-(4-hydroxy-3-methoxyphenyl)-7-(3-methoxy-4-((1-(2-(2-(2-((3*R*,4*S*,6*R*)-3,4,5-trihydroxy-6-(hydroxymethyl)tetrahydro-2*H*-pyran-2-yloxy)ethoxy)ethoxy)ethyl)-1*H*-1,2,3-triazol-4-yl)methoxy)phenyl)hepta-1,6-diene-3,5-dione; Sweet-curcumin.

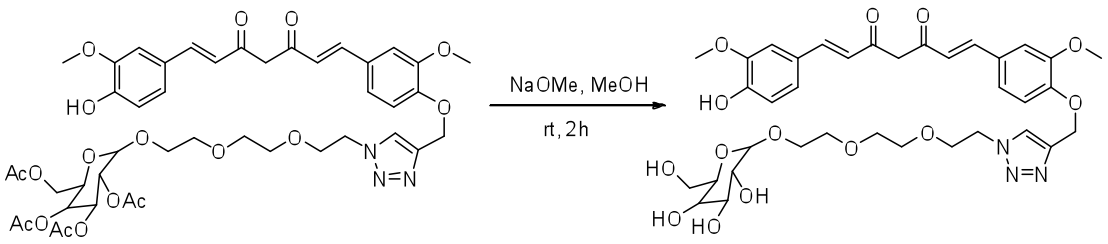

Protected curcumin-"clicked"-galactose (90 mg, 0.098 mmol) was dissolved in 3 mL of 0.3 M NaOMe in anhydrous MeOH. The mixture was stirred at room temperature for 2 hours. The pH of the solution was neutralized to pH=7 using Amberlite15 ion exchange resin and the color of the solution became light yellow from dark orange. The solution was filtered and the solvent was removed.Finally the crude product was purified

via column chromatography using $CHCl_3$:MeOH (95:5) to yield a dark yellow solid.Yield: 55 mg (76 %). ^{1}H NMR (CD_3OD, 600 MHz): δ(ppm) 3.01(s, 4H), 3.09-3.13 (m, 2H), 3.17-3.19 (m, 2H), 3.25 (s, 4H), 3.27-3.29(m, 2H), 3.32-3.42 (m, 3H), 3.47-3.52(d, 2H), 3.54-3.57 (m, 6H), 3.62-3.64(m, 1H), 3.86-3.87 (d, 1H), 4.25-4.27 (t, 2H), 4.91 (s, 2H), 6.28-6.35 (m, 2H), 6.48-6.49 (d, 1H), 6.76-6.91(m, 4H), 7.22-7.25 (dd, 2H), 7.80 (s, 1H); ^{13}C NMR ($CDCl_3$, 150 MHz): δ(ppm) 49.84, 51.48, 56.48, 56.53, 62.54, 62.79, 63.34, 69.59, 70.30, 71.09, 71.31, 71.37, 71.41, 72.50, 74.89, 76.66, 105.03, 111.79, 112.08, 115.35, 116.59, 123.55, 124.19, 126.57, 128.54, 130.50, 131.21, 141.30, 142.37, 144.47, 149.40, 150.50, 151.06, 151.37, 183.92, 185.37. ESI-MS: for $C_{36}H_{45}N_3O_{14}$; calculated-743.29; observed-744.3 $[M+H]^+$.

2.2.10. Synthesis of 4-((1*E*,6*E*)-7-(4-hydroxy-3-methoxyphenyl)-3,5-dioxohepta-1,6-dienyl)-2-methoxyphenyl ((3a*S*,5*S*,5a*R*,8a*R*,8b*S*)-2,2,7,7-tetramethyltetrahydro-3a*H*-bis[1,3]dioxolo[4,5-*b*:4',5'-*d*]pyran-5-yl)methyl glutarate; Curcumin mono-Galactose (protected).

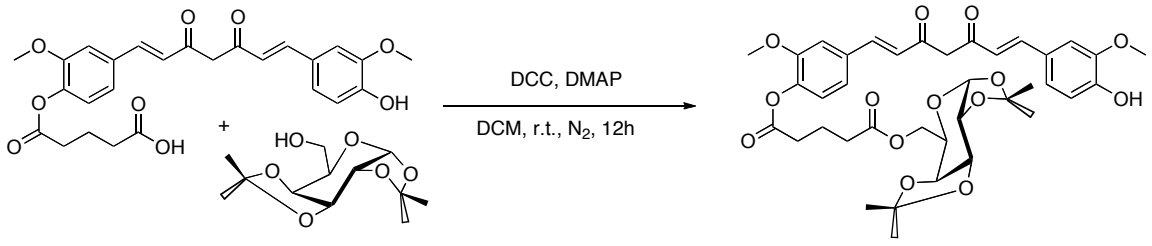

Curcumin mono-carboxylic acid (1g, 2.07 mmol), 1,2:3,4-Di-O-isopropylidene-D-galactopyranose (97%) (535 mg, 2.05 mmol) and 4-Dimethylaminopyridine (12.5 mg, 0.10 mmol) were dissolved in 10 mL dry DCM and cooled to 0 ^oC. 1,3-

Dicyclohexylcarbodiimide (640 mg, 3.10 mmol) in 5 mL dry DCM was added drop-wise to the reaction mixture while stirring. Formed Dicyclohexyl urea was filtered off after stirring the reaction mixture at room temperature under N_2 atmosphere for 12 hrs. The crude product was finally purified via column chromatography using $CHCl_3$:EtOAc (95:5) as eluent. The product was isolated as orange powder. Yield: 1.195 g (80 %). ^{1}H NMR (600 MHz, $CDCl_3$), δ (ppm): 1.17-1.33 (m); 1.45 (s); 1.50 (s); 1.52 (s); 1.54-1.57 (m); 1.67-1.74 (m); 1.90-1.91 (m); 2.20-2.24 (p); 2.51-2.54 (t); 2.66-2.68 (t); 2.76-2.79 (t); 3.17-3.20 (m); 3.46-3.48 (m); 3.71-3.76 (m); 3.83 (s); 3.84 (s); 3.87 (s); 3.92 (s), 4.26-4.27 (d); 4.32-4.33 (m); 4.60-4.61 (d); 5.55-5.56 (d); 5.82-5.85 (m); 6.54-6.57 (d); 6.90-6.91 (d); 7.03-7.14 (m); 7.59-7.62 (d). ^{13}C NMR (150 MHz, $CDCl_3$), δ (ppm): 20.09, 20.20, 24.25, 24.44, 24.90, 25.56, 25.89, 25.91, 25.96, 25.99, 26.24, 32.78, 32.95, 33.10, 33.90, 49.14, 55.85, 55.91, 62.35, 63.31, 63.48, 65.86, 65.93, 68.02, 70.40, 70.54, 70.66, 70.73, 70.98, 71.02, 71.60, 96.25, 96.27, 101.14, 101.48, 108.65, 108.73, 109.45, 109.60, 109.62, 111.36, 114.84, 120.92, 121.69, 122.84, 123.02, 123.19, 124.19, 127.46, 127.60, 140.53, 141.15, 146.80, 147.89, 151.30, 156.76, 170.82, 172.80, 183.23. MS (ESI) *calcd.* for $C_{38}H_{44}O_{14}$: 724.27; found: 723.5 $[M-H]^-$.

2.2.11. Synthesis of 4-((1*E*,6*E*)-7-(4-hydroxy-3-methoxyphenyl)-3,5-dioxohepta-1,6-dienyl)-2-methoxyphenyl methacrylate; Curcumin mono-acrylate.

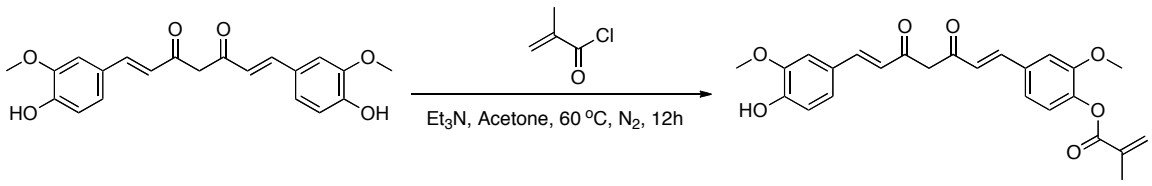

To an ice-cold solution of curcumin (500 mg, 1.35 mmol) in 25 mL dry acetone, NEt_3 (275 μL, 2 mmol) was added drop-wise. A solution of methacryloyl chloride (170 mg, 1.62 mmol) in 20 mL icy-cold acetone was added to the curcumin solution drop-wise via a syringe. This mixture was stirred at 0 ^oC under N_2 atmosphere for ~90 mins. Further the reaction mixture was refluxed at 60 ^oC for overnight. The reaction was stopped, solvent was evaporated and the crude mixture was dissolved in DCM. The product was further purified via column chromatography eluting with DCM: hexanes (90:10). Yield: 104 mg (38%). ^1H NMR (600 MHz, $CDCl_3$), δ (ppm): 2.07 (s), 3.87 (s), 3.94 (s), 5.78 (s), 5.83 (s), 6.37 (s), 6.48-6.57 (m), 6.93-6.94 (d), 7.05-7.16 (m), 7.59-7.62 (d). ^{13}C NMR (150 MHz, $CDCl_3$), δ (ppm): 18.42, 55.91, 55.94, 101.53, 109.58, 111.43, 114.01, 120.96, 121.72, 123.01, 123.28, 124.11, 127.51, 127.57, 133.93, 136.36, 139.46, 141.07, 141.40, 146.75, 147.94, 151.50, 165.21, 181.84, 184.43.

2.2.12. Synthesis of 4-((1*E*,6*E*)-7-(4-hydroxy-3-methoxyphenyl)-3,5-dioxohepta-1,6-dienyl)-2-methoxyphenyl 2-(*tert*-butoxycarbonylamino)acetate; Curcumin mono Glycine-Boc

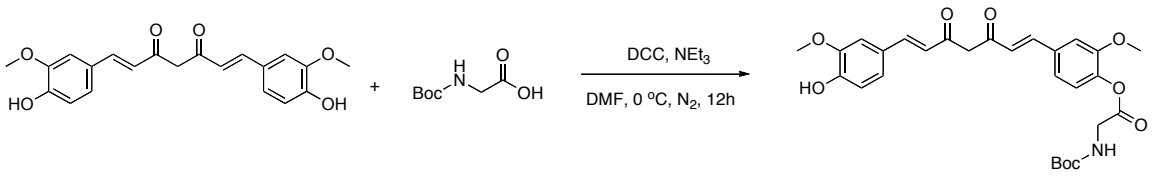

Curcumin (200 mg, 0.54 mmol), Glycine-Boc (114 mg, 0.65 mmol) and DMAP (17 mg, 0.14 mmol) were dissolved in 10 mL dry DCM and placed under ice bath in a r.b. flask. 225 μL of NEt3 was added to the mixture under positive flow of nitrogen gas. Separately, DCC (134 mg, 0.65 mmol) in 5 mL of DCM cooled under ice bath was added to the

mixture dropwise. The resulting reaction mixture was stirred under nitrogen overnight. Dicyclohexyl urea was filtered off and the crude product was isolated after washing the reaction mixture with water, saturated $NaHCO_3$ and brine. Organic layer was isolated, dried over anhydrous Na_2SO_4, and solvent was evaporated under vacuum. The crude product was purified via column chromatography using $CHCl_3$: MeOH (98:2) as eluent to produce dark orange product. Yield: 160 mg (56%). ^{1}H MNR (600 MHz, $CDCl_3$) δ (ppm): 1.25-1.94 (m), 3.47-3.49 (t), 3.86 (m), 4.14-4.15 (d), 5. 79 (s), 6.04 (s), 6.46-6.48 (d), 6.92-6.93 (t), 7.04 (s), 7.10-7.13 (t), 7.57-7.61 (m), 8.01 (s). ^{13}C NMR (150 MHz, $CDCl_3$) δ (ppm): 24.93, 25.60, 29.70, 31.47, 33.93, 36.52, 49.17, 55.96, 101.19, 109.67, 114. 88, 121.73, 122.89, 127.65, 140.57, 146.85, 147.93, 162.59, 183.28. ESI-MS: calcultd. for $C_{28}H_{31}NO_9$ m/z = 525.20; observed 521.1 $[M-4H]^-$.

2.3. Synthetic Protocols: Di-functional Curcumin Derivatives

2.3.1. Synthesis of 5,5'-(4,4'-((1*E*,6*E*)-3,5-dioxohepta-1,6-diene-1,7-diyl)bis(2-methoxy-4,1-phenylene))bis(oxy)bis(5-oxopentanoic acid); Curcumin di-carboxylic acid.

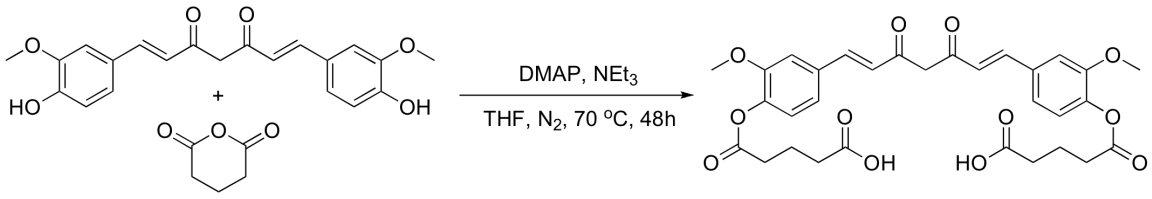

To a solution of 4 g (10.86 mmol) of curcumin, and 330 mg (2.71 mmol) of DMAP in 140 ml THF was added 3.78 ml (27.15 mmol) of Et_3N. 2.73 g (23.88 mmol) of

glutaric anhydride (95%) in 10 mL THF was added slowly dropwise to the curcumin solution. The mixture was stirred and refluxed under N_2 atmosphere for 48 hrs. THF was removed under vacuum, redissoved in 100 mL $CHCl_3$ and washed with 100 mL 0.1 N HCl followed by water (3x50 mL) and brine (3x50 mL). The organic layer was separated and dried over anhydrous Na_2SO_4. The product was purified via column chromatography, eluting with $CHCl_3$:EtOAc (95:5) and isolated as dark yellow powder. Yield: 69 %. ^{1}H NMR (600 MHz, $CDCl_3$), δ (ppm): 2.07-2.10 (t, 4H); 2.53-2.55 (t, 4H); 2.67-2.69 (t, 4H); 3.84 (s, 6H); 5.82 (s, 2H); 6.51-6.54 (d, 2H); 7.02-7.13 (m, 6H); 7.57-7.59 (d, 2H). ^{13}C NMR (150 MHz, $CDCl_3$), δ (ppm): 19.87; 32.65; 55.70; 101.48; 109.73; 111.23; 114.91; 120.83; 121.42; 123.02; 124.03; 127.22; 133.76; 133.90; 139.25; 141.06; 146.89; 148.09; 151.09; 170.85; 177.24; 181.59; 184.51. MS (ESI) *calcd.* for $C_{31}H_{32}O_{12}$: 596.19; found: 597.4 $[M+H]^+$.

2.3.2. Synthesis of (4,4')-((1*E*,6*E*)-3,5-dioxohepta-1,6-diene-1,7-diyl)bis(2-methoxy-4,1-phenylene) bis(((3a*S*,5*S*,5a*R*,8a*R*,8b*S*)-2,2,7,7-tetramethyltetrahydro-3a*H*-bis[1,3]dioxolo[4,5-*b*:4',5'-*d*]pyran-5-yl)methyl) diglutarate; Curcumin di-galactose (protected).

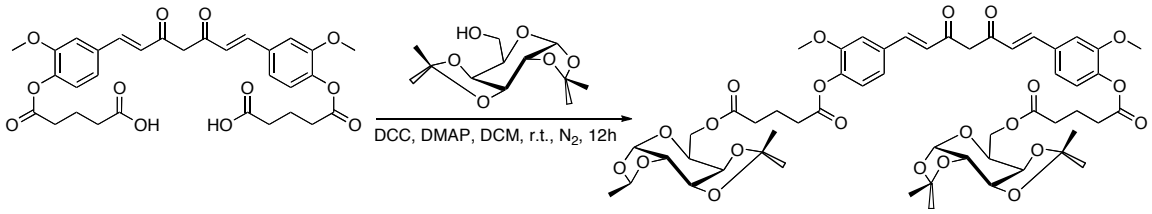

Curcumin di-carboxylic acid (1g, 1.67 mmol), 1,2:3,4-Di-O-isopropylidene-D-galactopyranose (97%) (690 mg, 2.65 mmol) and 4-Dimethylaminopyridine (12.5 mg, 0.10 mmol) were dissolved in 10 mL dry DCM and cooled to 0 ^{o}C. 1,3-

Dicyclohexylcarbodiimide (860 mg, 4.16 mmol) in 5 mL dry DCM was added drop-wise to the reaction mixture while stirring. Formed di-cyclohexyl urea was filtered off after stirring the reaction mixture at room temperature under N_2 atmosphere for 12 hrs. The crude product was finally purified via column chromatography using $CHCl_3$:EtOAc (95:5) as eluent. The product was isolated as dark orange powder. Yield: 1.31 g (72 %). ^{1}H NMR (600 MHz, $CDCl_3$), δ (ppm): 1.15-1.34 (m); 1.43 (s); 1.48 (s); 1.50 (s); 1.52-1.55 (m); 1.69-1.71 (m); 1.88-1.89 (m); 2.04-2.09 (p); 2.18-2.23 (p); 2.38-2.40 (t); 2.49-2.52 (t); 2.64-2.66 (t); 2.75-2.77 (t); 3.14-3.19 (m); 3.84-3.85 (d); 4.17-4.32 (m); 4.57-4.60 (m); 5.11-5.12 (d); 5.83 (s); 5.52-6.55 (dd); 7.02-7.14 (m); 7.57-7.60 (dd). ^{13}C NMR (150 MHz, $CDCl_3$), δ (ppm): 14.22; 20.26; 24.49; 24.97; 25.98; 26.01; 33.01; 33.98; 34.94; 55.90; 60.40; 63.53; 65.98; 70.44; 70.72; 71.07; 96.32; 108.78; 109.67; 121.08; 122.15; 123.25; 124.24; 129.24; 133.92; 139.98; 141.33; 151.37; 170.82; 172.80; 183.10. MS (ESI) *calcd.* for $C_{55}H_{68}O_{22}$: 1080.42; found: 1079.3 $[M-H]^-$.

2.3.3. Synthesis of (1*E*,6*E*)-1,7-bis(3-methoxy-4-(prop-2-ynyloxy)phenyl)hepta-1,6-diene-3,5-dione; Curcumin di-alkyne.

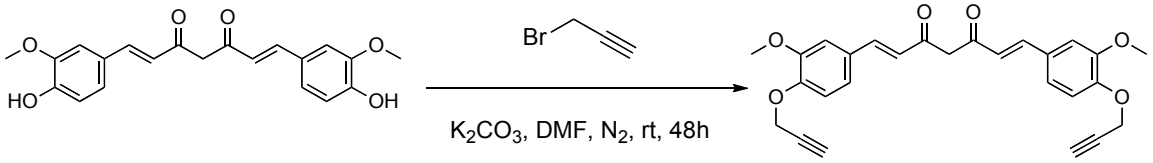

Curcumin (2 g, 5.43 mmol) and K_2CO_3 (1.52 g, 11.0 mmol) were added to 50 mL DMF followed by 1.62 g (13.61 mmol) of propargyl bromide. The mixture was stirred at room temperature under N_2 for 48 h, H_2O was added to the mixture and the solvent was removed under vacuum. The product was purified by column chromatography, eluting with $CHCl_3$:hexane 90:10. Yield: 1.78 g (74%). ^{1}H NMR (600 MHz, $CDCl_3$), δ (ppm):

2.47 (s, 2H); 3.84 (s, 6H); 4.71-4.74 (m, 4H); 6.42-6.44 (d, 2H); 6.95-7.07 (m, 6H); 7.51-7.53 (d, 2H). ^{13}C NMR (150 MHz, $CDCl_3$), δ (ppm): 55.91, 56.07, 56.58, 101.43, 110.37, 113.78, 122.05, 122.51, 129.17, 148.65, 149.60, 183.18. MS (ESI): calculated for $C_{27}H_{24}O_6$: 444.16; found: 445.1 $[M+H]^+$, 483.0 $[M+K]^+$.

2.3.4. Synthesis of (2*R*,4*R*,5*R*)-2-(acetoxymethyl)-6-(2-(2-(2-(4-((2-methoxy-4-((1*E*,6*E*)-7-(3-methoxy-4-((1-(2-(2-(2-((3*R*,4*R*,5*R*,6*S*)-3,4,5-triacetoxy-6-(acetoxymethyl)tetrahydro-2*H*-pyran-2-yloxy)ethoxy)ethoxy)ethyl)-1*H*-1,2,3-triazol-4-yl)methoxy)phenyl)-3,5-dioxohepta-1,6-dienyl)phenoxy)methyl)-1*H*-1,2,3-triazol-1-yl)ethoxy)ethoxy)ethoxy)tetrahydro-2*H*-pyran-3,4,5-triyl triacetate; Curcumin 'clicked' di-galactose (protected).

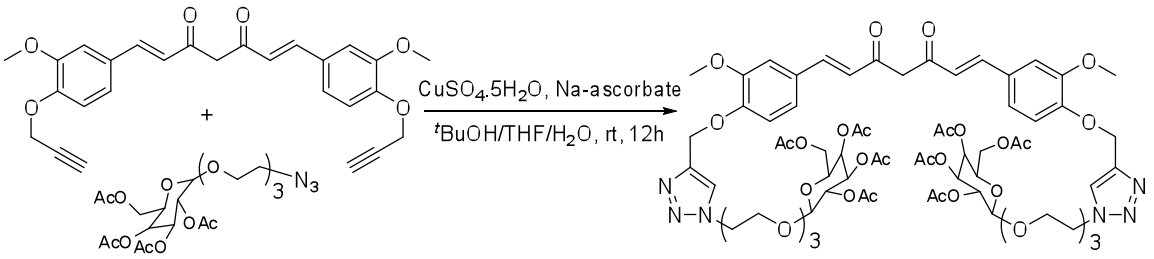

Curcumin di-alkyne (500 mg, 1.12 mmol) was dissolved in 2 mL of THF and added to 2mL of *t*-BuOH containing commercially available acetal-protected Azido-Galactose derivative [2-[2-(2-Azidoethoxy)ethoxy]ethyl-2,3,4,6-Tetra-O-acetyl-D-galactopyranoside] (1.14 g, 2.25 mmol) in a round bottom flask (r.b.). Fresh solutions of $CuSO_4.5H_2O$ (100 mg, 0.4 mmol) and Sodium Ascorbate (90 mg, 0.45 mmol) were prepared separately in 1 mL of milipore water. Sodium Ascorbate solution was added to the r.b. followed by $CuSO_4$ solution and stirred for 12 hours. The reaction was stopped and the solvent was removed by evaporation. The crude product was extracted from

water-chloroform mixture. The organic layer was dried over anhydrous $NaSO_4$ and solvent was evaporated. Finally the product was purified via column chromatography using Chloroform: Ethyl acetate (90:10) mixture to yield orange solid. Yield: 978 mg (60%). ^{1}H NMR ($CDCl_3$, 600 MHz): δ(ppm) 1.93 (s, 6H), 1.97-1.98 (d, 12H), 2.08 (s, 6H), 3.50-3.56 (m, 12H), 3.64-3.65 (m, 2H), 3.81-3.90 (m, 14H), 4.04-4.12 (m, 6H), 4.46-4.50 (m, 6H), 4.94-4.97 (dd, 2H), 5.12-5.15 (m, 2H), 5.25-5.28 (m, 4H), 5.32 (d, 2H), 5.77 (s, 1H), 6.43-6.46 (d, 2H), 7.02-7.06 (m, 4H), 7.52-7.54 (d, 2H), 7.80 (s, 2H); ^{13}C NMR ($CDCl_3$, 150 MHz): δ(ppm): 20.57, 20.63, 20.65, 20.73, 50.32, 55.92, 61.17, 62.89, 66.99, 68.77, 69.11, 69.37, 70.17, 70.54, 70.56, 70.62, 70.82, 101.31, 110.38, 113.66, 122.30, 122.34, 124.30, 128.70, 140.23, 143.49, 149.61, 149.62, 169.40, 170.12, 170.21, 170.36, 183.17.; ESI-MS: for $C_{67}H_{86}N_6O_{30}$; calculated-1454.54; observed-1455.2 $[M+H]^+$, 738.3 $[M+Na]^{2+}$.

2.3.5. Synthesis of (1*E*,6*E*)-1-(3-methoxy-4-((1-(2-(2-(2-((3*R*,4*S*,6*R*)-3,4,5-trihydroxy-6-(hydroxymethyl)tetrahydro-2*H*-pyran-2-yloxy)ethoxy)ethoxy)ethyl)-1*H*-1,2,3-triazol-4-yl)methoxy)phenyl)-7-(3-methoxy-4-((1-(2-(2-(2-((3*S*,4*R*,6*S*)-3,4,5-trihydroxy-6-(hydroxymethyl)tetrahydro-2*H*-pyran-2-yloxy)ethoxy)ethoxy)ethyl)-1*H*-1,2,3-triazol-4-yl)methoxy)phenyl)hepta-1,6-diene-3,5-dione; Curcumin 'clicked' di-galactose.

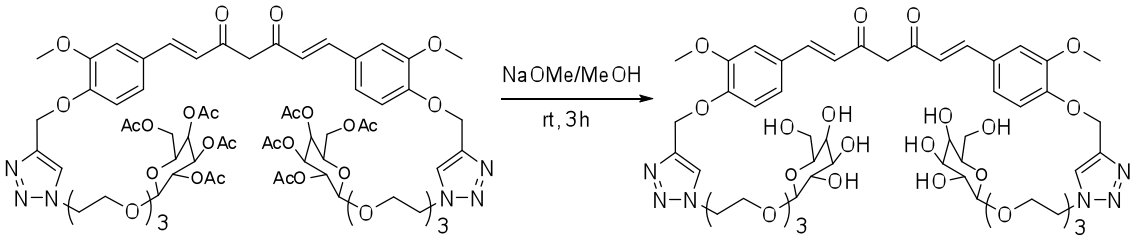

Protected curcumin-"clicked"-di-galactose (100 mg, 0.069 mmol) was dissolved in 3 mL of 0.3 M NaOMe in anhydrous MeOH. The mixture was stirred for 3 hours at room temperature. The pH of the solution was neutralized to pH=7 using Amberlite15 ion exchange resin and the color of the solution became light yellow from dark orange. The solution was filtered and the solvent was removed. Finally, the crude product was purified via column chromatography using $CHCl_3$:MeOH (95:5) to yield a dark yellow-orange solid. Yield: 66 mg (85 %). ^{1}H NMR (CD_3OD, 600 MHz): δ(ppm) 3.52 (s, 4H), 2.65 (s, 4H),3.01 (s, 1H), 3.09-3.13 (m, 4H), 3.17-3.22 (m, 2H), 3.25-3.29 (m, 12H), 3.26-3.41 (m, 6H), 3.46-3.51 (m, 2H), 3.53-3.56 (m, 6H), 3.62-3.63 (m, 2H), 3.85-3.87 (d, 2H), 4.26-4.50 (t, 4H), 4.91 (s, 2H), 6.33-6.36 (d, 2H), 6.78-6.91(m, 4H), 7.57-7.59 (d, 2H), 7.64 (s, 1H), 7.80 (s, 2H); ^{13}C NMR ($CDCl_3$, 150 MHz): δ(ppm) 30.22, 35.52, 49.72, 55.12, 61.12, 61.93, 68.17, 68.86, 69.97, 71.08, 73.47, 75.25, 103.63, 110.66, 113.97, 114.52, 122.24, 125.16, 129.02, 140.23, 143.04, 149.72, 149.98, 163.43. ESI-MS: for $C_{51}H_{70}N_6O_{22}$; calculated-1118.45; observed-1119.4 $[M+H]^+$, 560.4 $[M+2H]^{2+}$.

3. RESULTS AND DISCUSSIONS

3.1. Synthesis of novel functional and water-soluble Curcumin derivatives

In this part we present a convenient route to synthesize functional curcumin derivatives via the synthesis of novel mono-functional curcumin derivatives in which one of the phenolic groups of curcumin has been chemically modified with either reactive groups (azide, alkyne, carboxylic acid, alcohol, amine, NHS and acrylate) (**Schemes 4.1-4.3**) or water solubilizing moiety (sugar) (**Schemes 4.4, 4.5**). The synthesis of mono-functional curcumin derivatives affords two advantages: (a) The presence of at least one free phenolic group is necessary for the biological activity of many antioxidants like curcumin (*5*) (b) Bioconjugation and polymer modifications using mono-functional derivatives produce soluble conjugates in high yields whereas bi-functional derivatives would result in insoluble cross-linked products (*29*). We have also synthesized a 'clicked' curcumin-dimer possessing two phenolic-OH groups like in parent compound curcumin (**Scheme 4.6**). To increase the solubility of curcumin conjugates we have also synthesized surcumin di-sugar either via 'click' reaction or esterification (**Scheme 4.7**).

3.2. Mono-Functional Curcumin Derivatives

3.2.1. Synthesis of Curcumin mono-carboxylic acid based derivatives

To synthesize Curcumin mono carboxylic acid **1a**, curcumin was refluxed with glutaric anhydride in presence of *N,N*-dimethyl amino pyridine in THF at 70 ^{0}C under inert atmosphere for 48h. The formation of the product was confirmed via ^{1}H NMR and ESI-MS; peaks at 2.10- 2.71 ppm originating from $-CH_2$ moieties in glutaric acid and m/z signal at 483.2 $[M+H]^+$. The overall yield of the reaction was ~70%. The curcumin mono-COOH **1a** was further reacted with commercially available *O*-(2-Aminoethyl)-*O'*-(2-azidoethyl)-pentaethylene glycol following amidation chemistry in presence of DCC, which forms very reactive *O*-acylisourea, intermediate which can be viewed as a carboxylic ester with an activated leaving group. The *O*-acylisourea finally reacts with amines to give the desired amide. The product **1b** was characterized using NMR and ESI-MS techniques. Presence of m/z 837.38 $[M^+$+Na] peak confirms the formation of adduct. The compound **1b** bears a reactive azide group that could be reacted preferentially with alkyne group in triazole forming [3+2] cycloaddition reaction. Previously synthesized curcumin-COOH **1a** was next reacted with *N*-hydroxy succinimide using DCC chemistry at room temperature in DMF to yield curcumin mono-NHS **1c**. The synthesis was confirmed via NMR techniques as well as ESI-MS (m/z 578.5 $[M-H]^-$). The fairly stable but reactive-NHS ester could be used to conjugate with lysine residues of proteins (e.g BSA, antibody) to produce biologically relevant curcumin adducts. In fact, curcumin mono-NHS was successfully loaded onto antibodies and the conjugate was found to be very useful to treat tumors (discussed in the next chapter).

Scheme 4.1. Schematic route to synthesize Curcumin mono-carboxylic acid, mono-NHS and mono-azide.

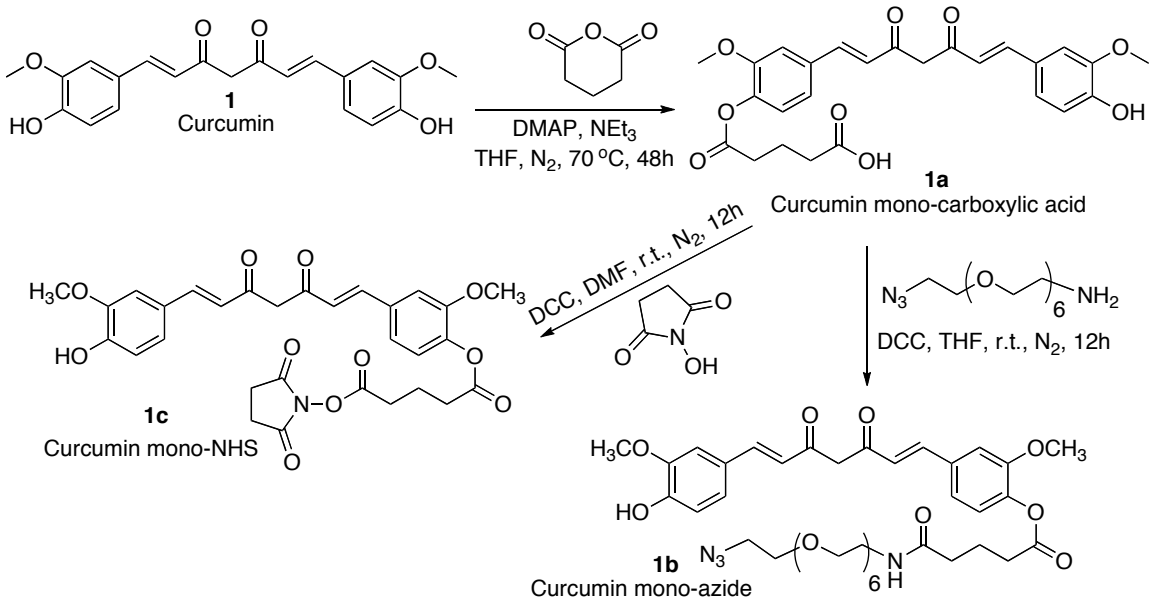

3.2.2. Synthesis of Curcumin mono-alkyne based derivatives

The mono-alkyne derivative of curcumin **2a** was prepared using propargyl bromide and potassium carbonate at room temperature. A peak at 2.54 ppm originating from C≡C-H in the ^{1}H NMR and ESI-MS m/z 407.2 $[M+H]^+$ confirms the successful synthesis although the yield was a bit lower ~47%. The alkyne functionality is a very useful handle to connect curcumin with other bis-functional reagents via 'click' chemistry to yield other functional curcumin derivatives. For example, when Curcumin mono-alkyne **2a** was reacted with 2-(2-(2-azidoethoxy)ethoxy)ethanol following 'click' reaction conditions in presence of copper sulfate pentahydrate and sodium ascorbate at room temperature in equal mixtures of chloroform, *tert*-butanol and water, end-alcohol functionalized curcumin **2c** was produced . The triazole C-H peak at 7.92 ppm in ^{1}H NMR spectra as well as ESI-MS m/z 582.3 $[M+H]^+$ confirmed the successful synthesis. The alcohol functionality of curcumin mono-alcohol **2b** could be used as a mechanical

handle to connect curcumin with other compatible functionalities or moieties. In another process, curcumin mono-alkyne was 'clicked' with commercially available azido-PEG-amine bis-functional linker which yielded curcumin mono-amine (**Scheme 4.2**). The peak arising from the triazole proton at 7.83 ppm in the ^{1}H NMR spectrum and presence of m/z peak at 625.6 $[M+H]^{+}$ confirmed the actual synthesis. This particular compound was found to be in part water soluble. If we increase the PEG block in the azido-PEG-amine part we can eventually make curcumin water soluble. The amine group could be a useful handle to produce curcumin incorporated water soluble polymers reacting with reactive chain-ended polyacrylic acid and finally producing curcumin incorporated protein-polymer hybrids. These type of hybrids might be useful for detection and therapeutic applications.

Scheme 4.2. Schematic representation to synthesize Curcumin- mono-alkyne, mono-alcohol, and mono-amine.

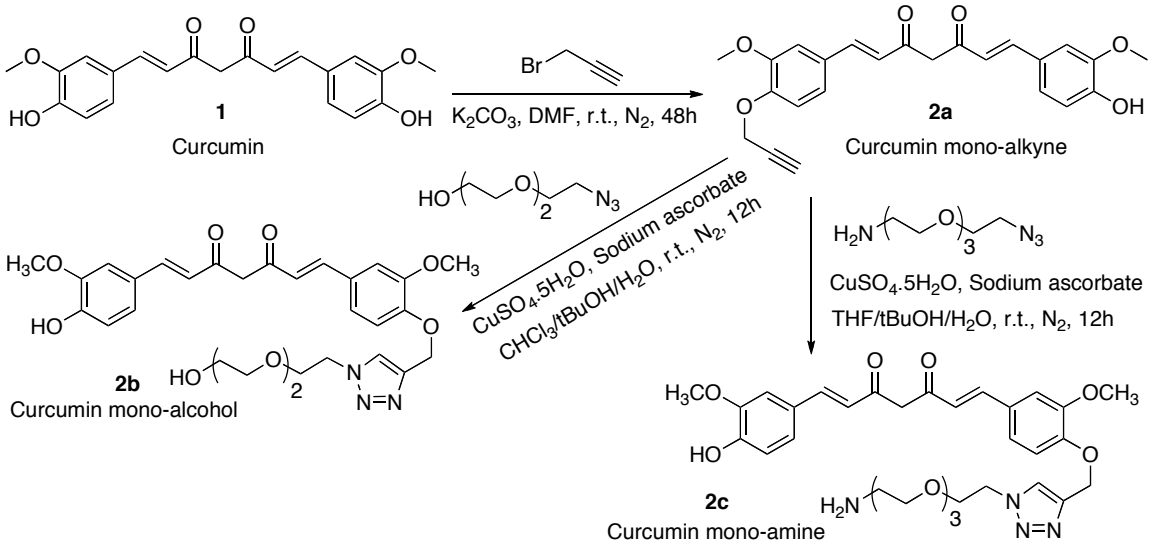

3.2.3. Other mono-functional derivatives: Curcumin mono-acrylate and Curcumin mono-Glycine

Using the very handy phenolic-OH groups of curcumin an acrylate verivative was produced when curcumin was reacted with methacryloyl chloride in presence of weak base NEt3 in acetone. The formation of curcumin mono-acrylate **3a** was confirmed via NMR techniques. The synthesis of an acrylate derivative of such a biologically relevant compound (Curcumin) could be possible but could not be polymerized via free radical polymerization methods to obtain a polymer containing this biologically active molecules/imaging agent as it acts as radical scavenger (*30*). Please note that, this radical scavenging property of curcumin makes it a well renowned Anti-oxidant (*5*). Again, using the phenolic-OH group as chemical handle, curcumin was further reacted with Boc-protected Glycine. The synthesized Curcumin mono-Gly-Boc **3b** was characterized via NMR techniques and ESI-MS (m/z found 521.1 $[M-4H]^-$). The deprotection of Boc-group leads to amine-functionalized curcumin. Curcumin mono-Glycine **3c** could be conjugated with reactive chain-ended poly(acrylic acid) with the help of amide chemistry to generate curcumin containing polymer. The water-soluble curcumin incorporated copolymers could then be implanted on to the surface of various proteins (e.g. anibody, BSA, protein A, apoferritin, protein G etc.) to construct biologically relevant and active protein-polymer hybrids. These kinds of hybrids materials could find great opportunities in modern medicinal chemistry as imaging and therapeutic agents.

Scheme 4.3. Scheme to synthesize Curcumin mono-Glycine and Curcumin mono-acrylate.

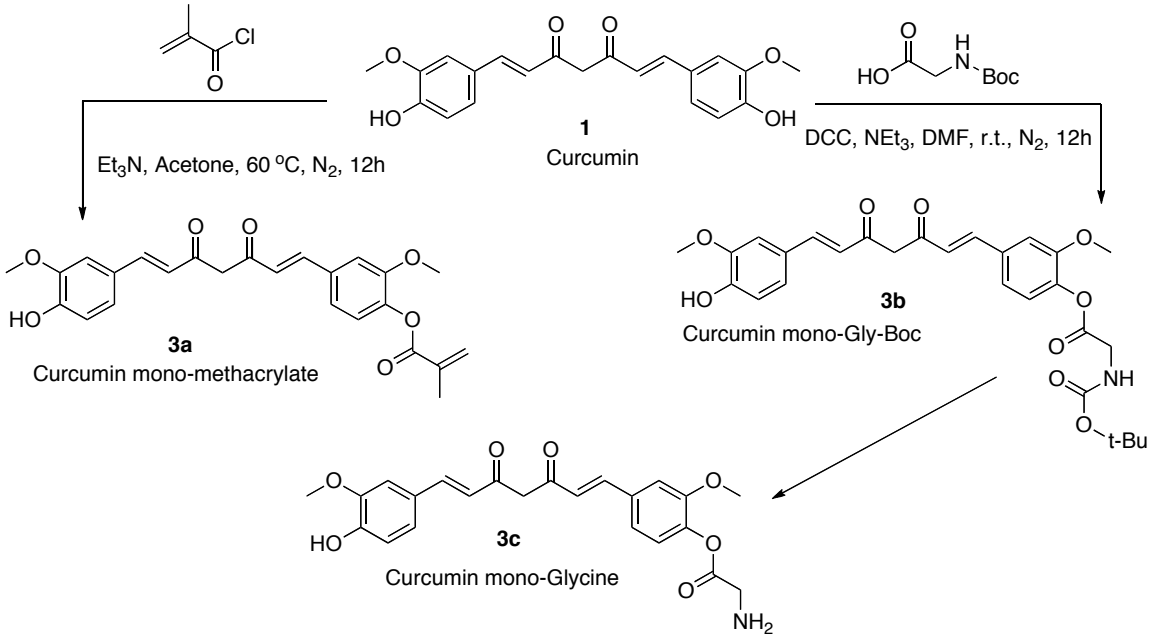

3.2.4. Synthesis of Curcumin sugar conjugate based upon Curcumin mono-alkyne and Curcumin mono-carboxylic acid

Although several mono-functional derivatives were synthesized, we could not yet get a water soluble adduct of curcumin. Hence, we decided to incorporate a sugar moiety onto curcumin. The reason behind this concept was such that sugars are nontoxic, biocompatible and very much hydrophilic as well as it could probably make such a hydrophilic molecule (curcumin) water soluble. Towards this goal we reacted previously synthesized curcumin mono-alkyne **2a** with commercially available 2-[2-(2-Azidoethoxy)ethoxy]ethyl-2,3,4,6-Tetra-O-acetyl-D-galactopyranoside (acetal-protected galactose azide) under 'click' reaction conditions in presence of copper sulfate pentahydrate and sodium ascorbate in equivolume moxtures of THF, *tert*-butanol and water at room temperature. Acetal-protected galactose was employed due to the solubility

mismatch of sugars and **2a** in organic solvents. The 8.1 ppm peak (triazole proton) in the ^{1}H NMR and ESI-MS data M/z = 912.3 confirms the conjugation of curcumin with sugar. Completely water soluble curcumin-sugar conjugate (sweet curcumin) **4b** was obtained when acetal-protected sweet curcumin **4a** was treated with 3M sodium methoxide (NaOMe) in methanol for 2h at room temperature. The resulting mixture was neutralized using Amberlite15 ion-exchange resin. The final purified product was obtained when confirmed via NMR and ESI-MS techniques. The absence of peaks at 2.22-2.38 ppm in ^{1}H NMR, 20.48-20.65 ppm in ^{13}C NMR and along with the presence of a peak at M/z = 744.3 in ESI-MS confirmed the complete deprotection of the galactose. The synthesized freely water soluble sweet curcumin showed immense promise in disaggregating and probably redissolving Amyloid- plaques thought to be responsible for Alzheimer's disease (AD). This will be discussed in details in next chapter.

Scheme 4.4. Synthetic scheme for Curcumin 'clicked' mono-galactose.

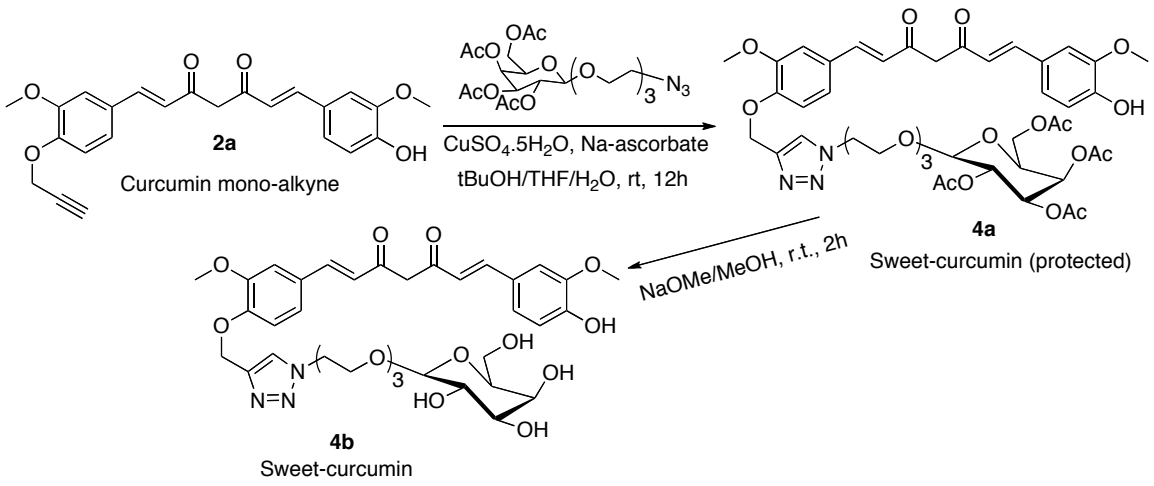

While it was very interesting to synthesize such an important molecule that contained both biologically important moieties in the same adduct, it is worthy to note that the both components (curcumin and galactose) were connected through an ether

linkage which is enzymatically stable. Further, we have decided to connect the both moieties via an ester or amide linkage so that it could be cleaved under enzymatic conditions releasing curcumin. Our point was the molecule should be water/serum soluble, biocompatible, nontoxic and could easily penetrate the cell walls. It should be noted that the carcinogenic cells (e. g. malignant tumor cells) are very hungry and want to reproduce in a faster rate. As the sugars are needed for their survival our strategy might be helpful destroying these types of cells. As the curcumin sugar conjugate is being accumulated in carcinogenic cells the enzyme might break the amide or ester linkage and eventually freeing the curcumin which can preferentially destroy the faulty cells. Keeping this hypothesis in mind we have synthesized another curcumin sugar conjugate where both moieties are connected via ester linkage. To do so, we have reacted previously synthesized curcumin mono-carboxylic acid derivative **1a** with commercially available 1,2:3,4-Di-O-isopropylidene-D-galactopyranose (ketal-protected galactose) in presence of DCC and DMAP in dichloromethane. Ketal-protected galactose was chosen over acetal-protected one as the deprotection reaction condition for the later would also cleave the ester linkage between curcumin and galactose. Where as, ketal-protection could be removed in presence of ester linkage. Formation of the ketal-protected curcumin mono-galactose was observed in the ^{1}H NMR spectrum (peaks at 1.17-1.33 ppm originating from the ketal $-CH_3$ groups and ESI-MS (m/z = 723.5 $[M-H]^-$).

Scheme 4.5. Schematic synthesis of Curcumin mono-galactose.

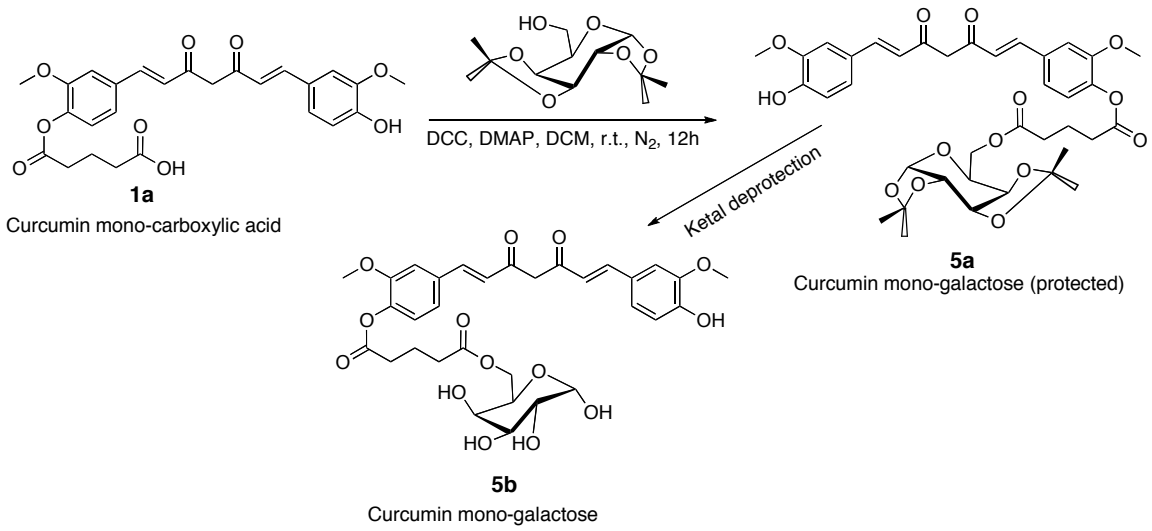

3.2.5. Synthesis of Curcumin-'clicked'-dimer

Another approach was to mimic the curcumin structure in terms of the free phenolic-OH groups which is very important for it's biological activity. Hence, we have synthesized a curcumin-dimer **6** by 'click'-ing curcumin mono-alkyne **2a** with curcumin mono-azide in presence of copper sulfate pentahydrate and sodium ascorbate. The structure was characterized via ^{1}H NMR and ESI-MS. The peak at 7.87 ppm responsible for the triazole proton and m/z 1243.52 [M^{+}+Na] confirmed the formation of adducts. The long oligoethylene glycol bridging unit in between two curcumin moieties help to solubilize to some extent in aqueous media and gives its unique properties of selectively destroying human neurotumor cells *in vitro* via apoptosis which could be found in details in the very next chapter.

Scheme 4.6. Schematic design to synthesize Curcumin-dimer via 'click' reaction.

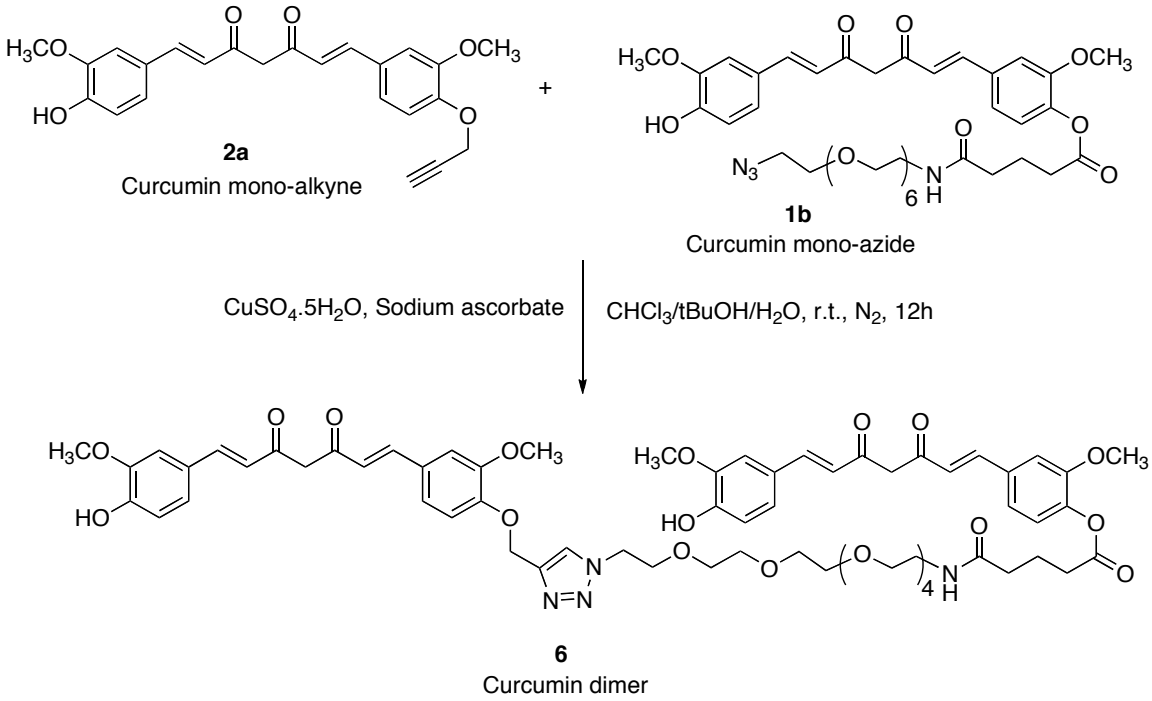

3.3. Di-functional Curcumin derivatives

3.3.1. Synthesis of Curcumin di-alkyne and 'clicked' di-galactose

To screen the effect of addition of sugar moieties on the hydrophobic curcumin, we synthesized curcumin di-sugar or in other words curcumin 'clicked' di-galactose according to **Scheme 4.7**. In order to get up to curcumin di-sugar we had to synthesize curcumin di-alkyne **7a**. Curcumin was etherified with propargyl bromide and the product was characterized using NMR and ESI-MS techniques. Curcumin di-alkyne was next reacted with acetal-protected galactose azide in presence of 'click' reagents at room temperature. The product **7b** was isolated and confirmed via ^{1}H NMR peak at 7.80 ppm originating from triazole proton as well as using ESI-MS where m/z was observed at

1455.2 $[M+H]^+$. Finally the acetal-protected curcumin 'clicked' di-galactose **7b** was treated with 3M NaOMe in methanol for 3h at room temperature. The pH of the resulting solution was neutralized by the usage of Amberlite 15 ion-exchange resin. The isolated product was examined using NMR and ESI-MS methods. The absence of peaks at 1.93-2.08 ppm (acetal $-CH_3$'s) in ^1H NMR spectrum and 20-22 ppm in ^{13}C NMR spectrum responsible for acetal-carbons along with these presence of peak value of m/z at 560.4 $[M+2H]^{2+}$ confirmed the formation of product.

3.3.2. Synthesis of Curcumin di-carboxylic acid and di-galactose

Via another approach mostly similar to synthesis of curcumin mono-galactose we have prepared curcumin di-galactose where two sugar units are connected via ester linkage to curcumin. At first, we have synthesized curcumin di-carboxylic acid **8a** in accordance with **Scheme 4.7** where curcumin was reacted with glutaric anhydride in 1:2 molar ratio. NMR and ESI-MS techniques were used to characterize the compound. ^1H NMR spectra showed the presence of peaks originating from the glutaric acid moiety; 2.07-2.69 ppm along with aromatic peaks of curcumin at 7.02-7.59 ppm. ESI-MS was used to determine the m/z which came out to be 597.4 $[M+H]^+$. Next, **8a** was attached to ketal-protected galactose via esterification method using DCC and DMAP. The product **8b** was isolated and characterized via NMR and ESI-MS. Peaks responsible for ketal $-CH_3$'s was found at 1.15-1.34 ppm and aromatic peaks of curcumin at 7.02-7.60 ppm. ESI-MS calculated m/z was 1080.42 and experimental value was found to be 1079.3 $[M-H]^-$. We are still working on the deprotection reaction which could yield curcumin di-galactose **8c**.

Scheme 4.7. Schematic route to synthesize di-functional curcumin derivatives.

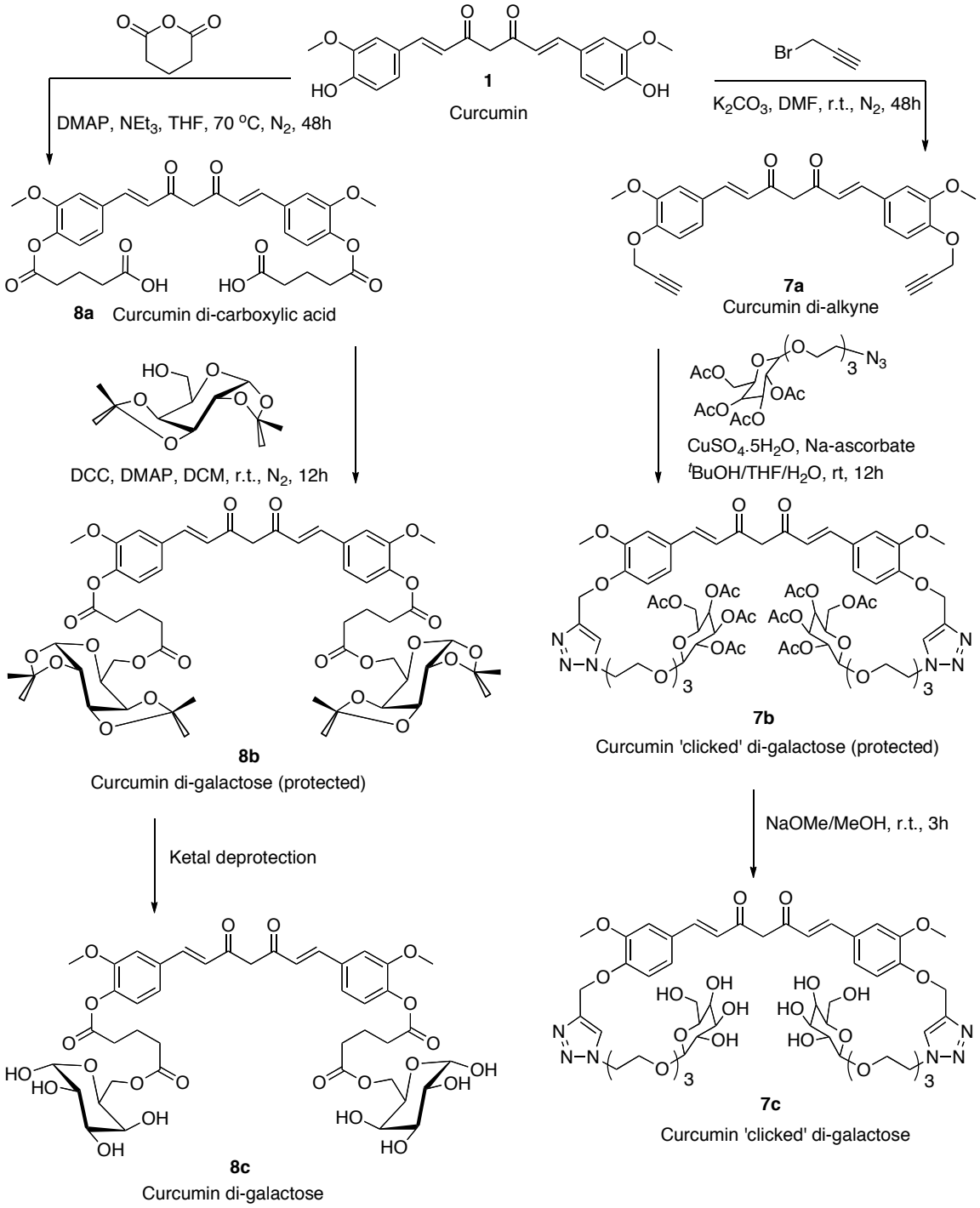

4. CONCLUSION

In conclusion, we have successfully synthesized and properly characterized several mono-functional and few di-functional derivatives. Using the phenolic-OH as a chemical handle following simple one-two step processes, all the derivatives were synthesized. We have tried to minimize the chemical manipulation on the curcumin molecule itself so that the derivatized curcumin would still retain its biological activities. We have started our work synthesizing curcumin mono-carboxylic acid and mono-alkyne. Using these as origin, via chemical manipulation, we have modified the carboxylic acid group to -NHS and azide, whereas the alkyne group was modified to alcohol and amine. We have also synthesized curcumin mono-acrylate, mono-glycine as well as a curcumin-dimer which displayed same numbers of phenolic-OH as the parent compound. In order to produce nontoxic, biocompatible and completely water soluble adduct of curcumin, we have successfully conjugated sugar moieties on to the curcumin via either esterification or 'click' bioconjugation reaction. We have also synthesized several bis-functional derivatives using both the phenolic-OH groups of curcumin; curcumin di-alkyne, di-carboxylic acid, di-galactose and 'clicked' di-galactose. All these chemically reactive functional derivatives could further be used to form variety of other adducts or conjugates via proper chemical manipulation and synthetic methods, e.g. curcumin-dendrimer conjugate, curcumin-antibody conjugate, curcumin-incorporated polymers etc. Most of these synthesized derivatives were found to retain the biological activities of curcumin and some with amplified efficacy. For example, curcumin mono-carboxylic acid was found be to more effective dissociating amyloid plaques compared to curcumin. On the other hand sweet curcumin have shown to disintegrate the amyloid plaques in nano-molar

concentrations. It was also found to be ~1000 times more powerful antioxidant than curcumin. On the other hand curcumin dimer was found to be as effective as curcumin to selectively destroy the human neuro tumor cells. The derivatives have also showed promising results when used as imaging agents. Most of the applications are described in the next chapter. Finally, to the best of my knowledge this is the first study describing a general methodology for preparing reactive functional curcumin derivatives.

5. SPECTRAL CHARACTERIZATION DATA (^{1}H NMR, ^{13}C NMR AND ESI-MS)

Curcumin mono-carboxylic acid.

^{1}H NMR

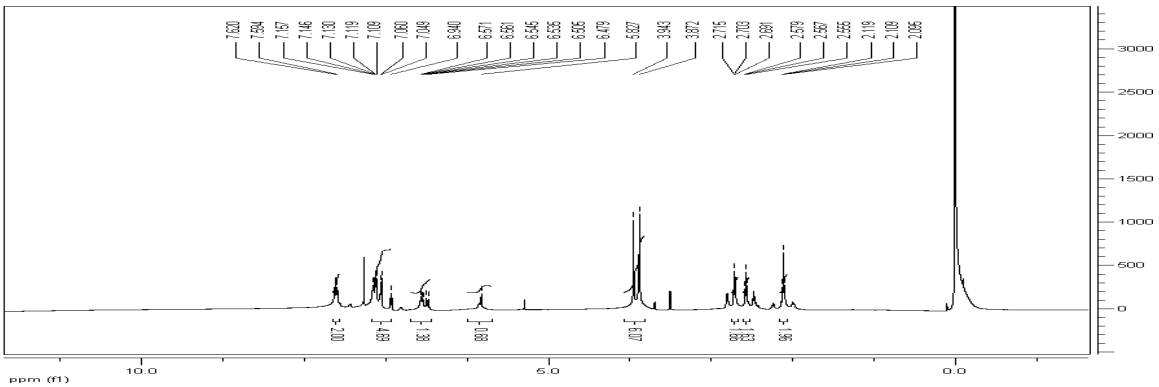

^{13}C NMR

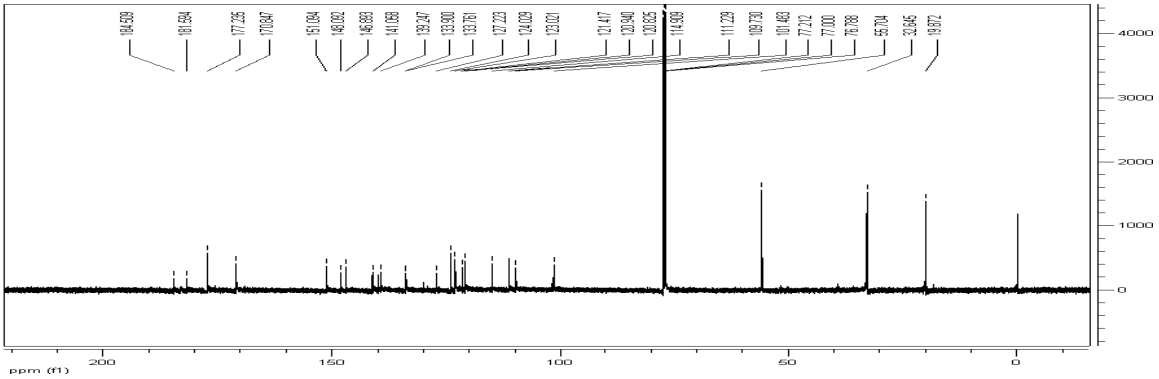

ESI-MS

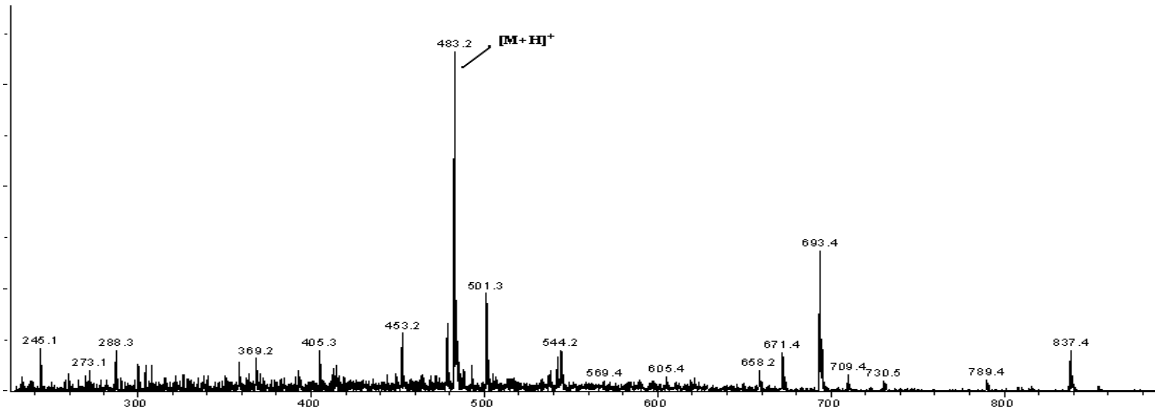

Curcumin mono-alkyne.

^{1}H NMR

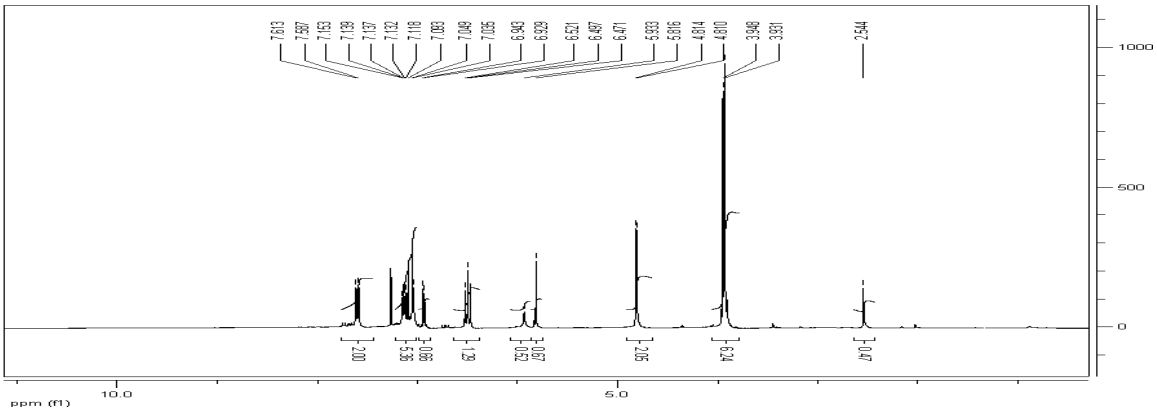

^{13}C NMR

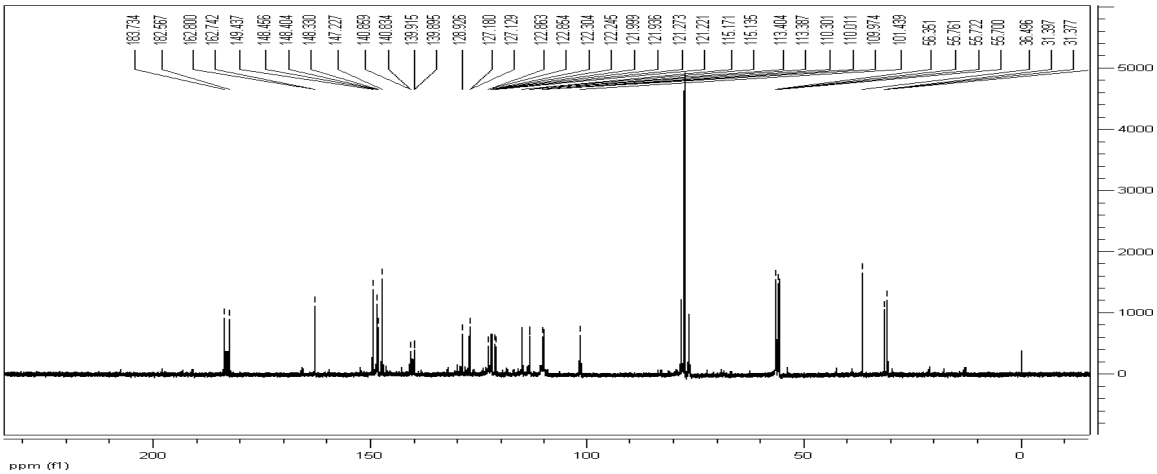

ESI-MS

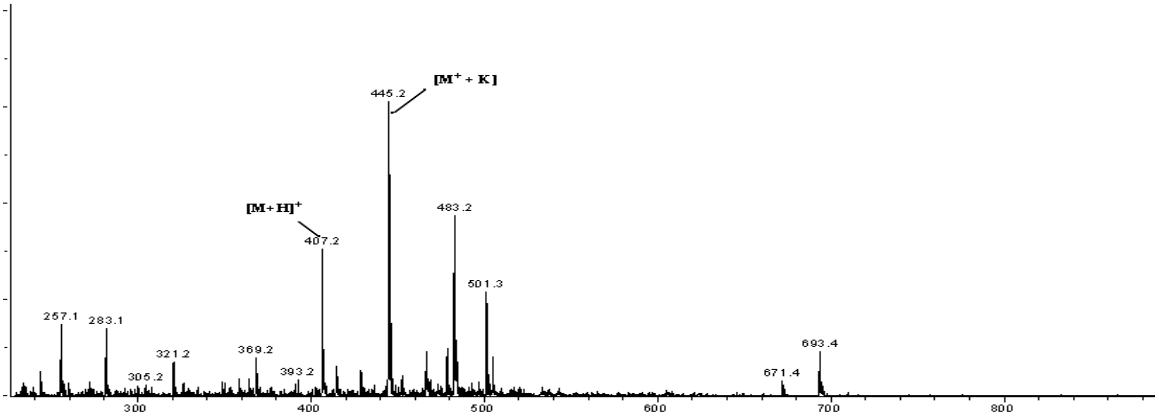

Curcumin mono-azide.

^{1}H NMR

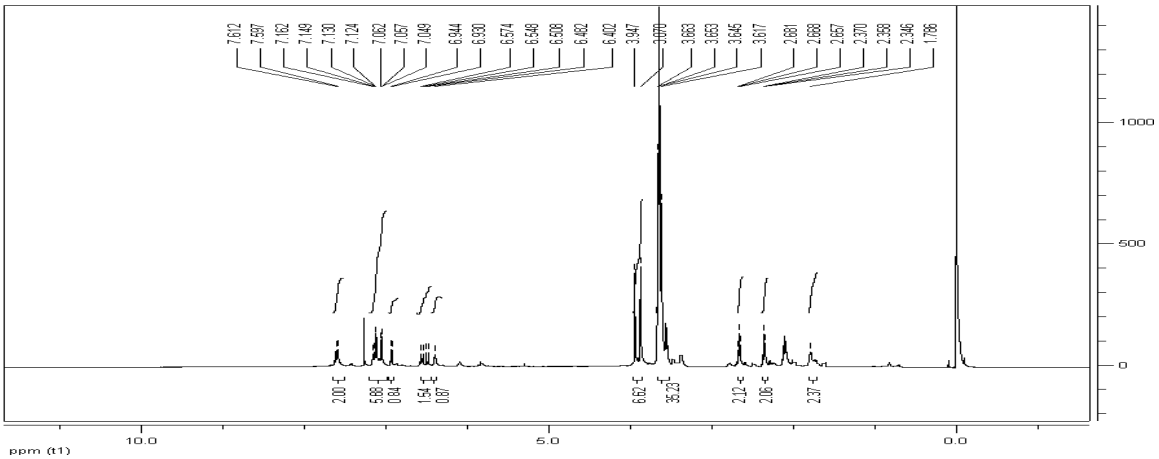

^{13}C NMR

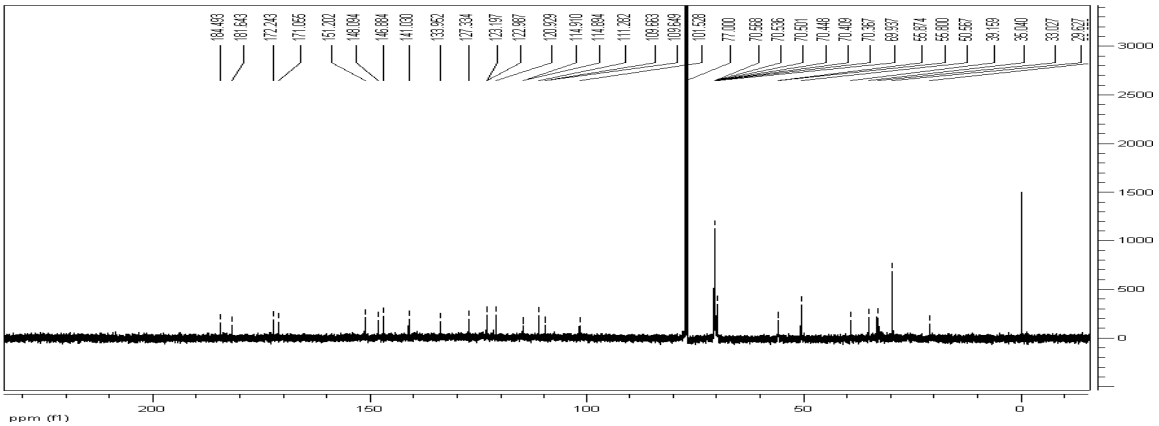

ESI-MS

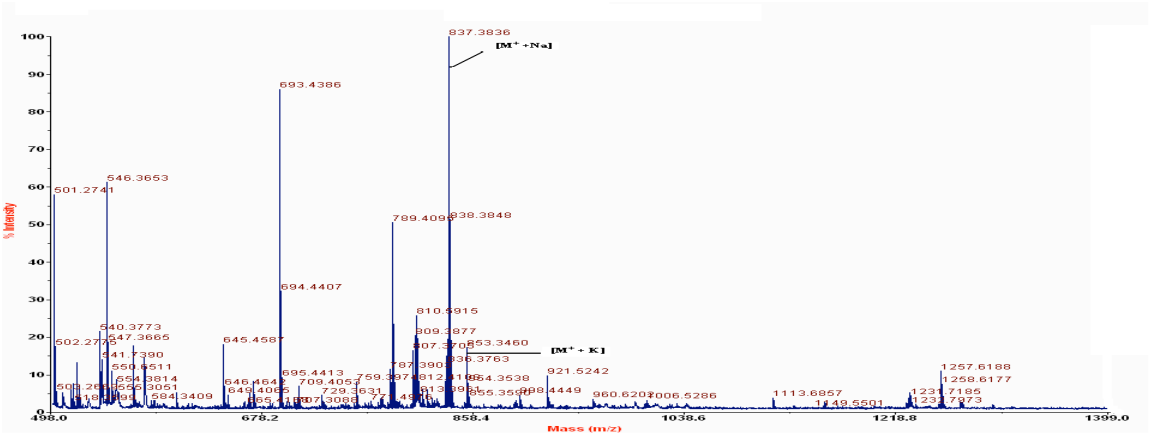

Curcumin mono-alcohol

^{1}H NMR

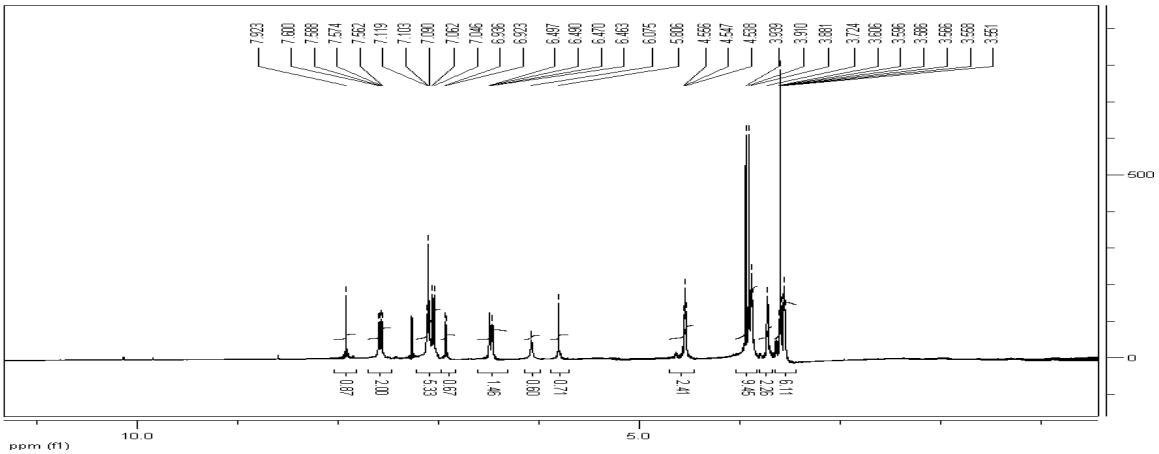

^{13}C NMR

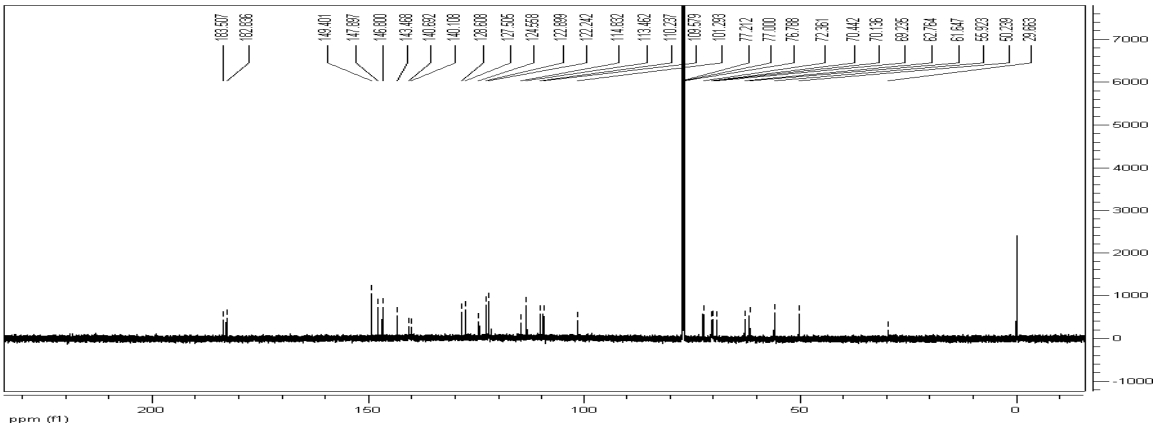

ESI-MS

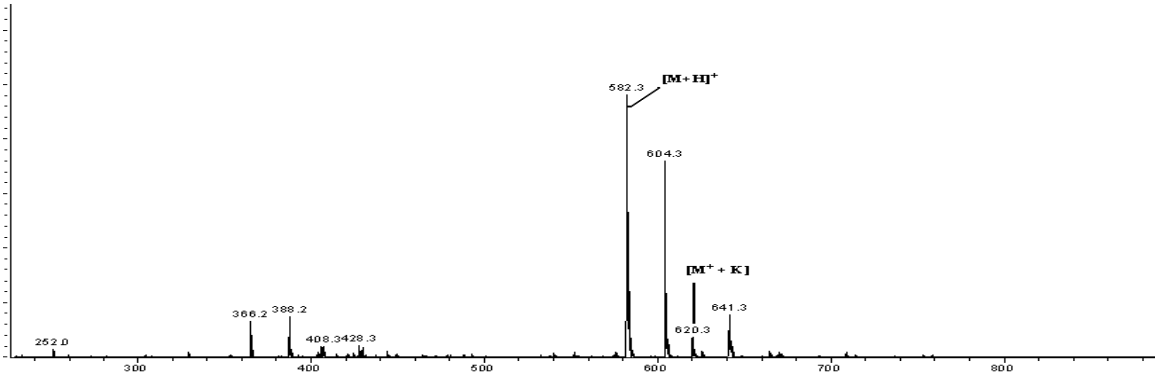

Curcumin mono-amine

^{1}H NMR

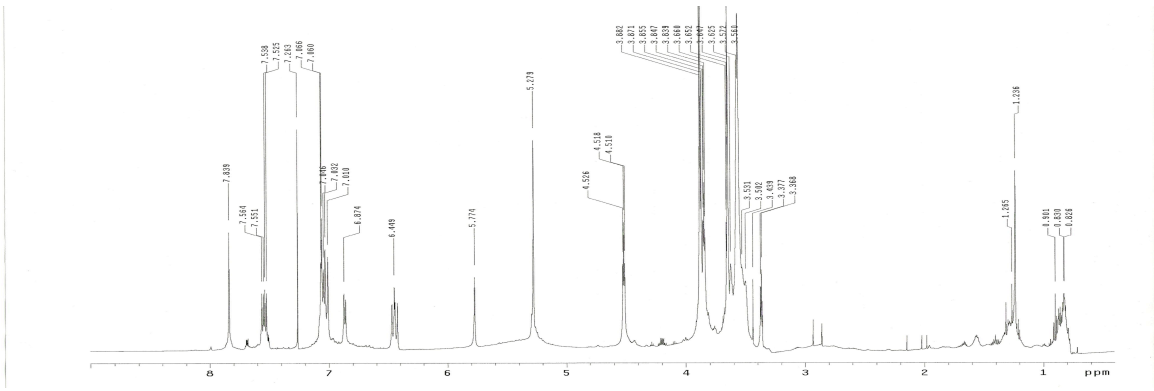

^{13}C NMR

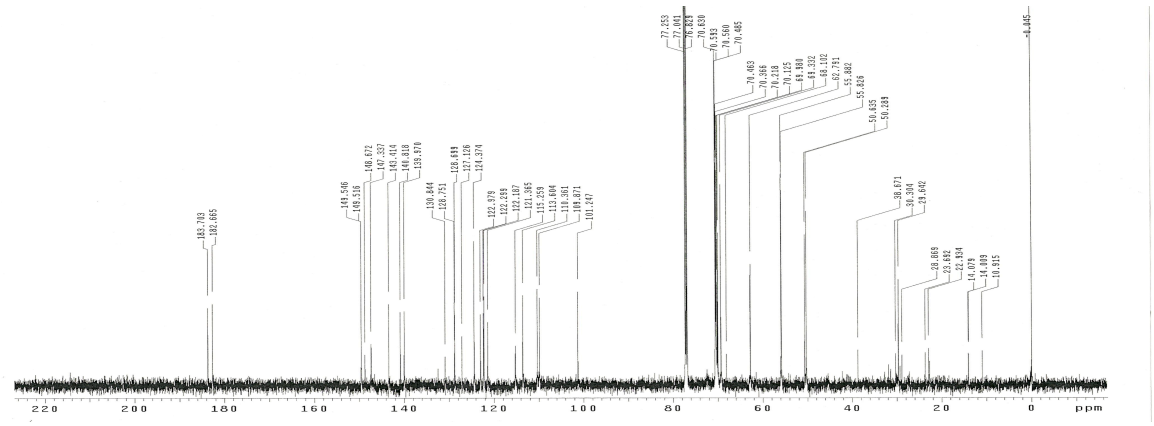

ESI-MS

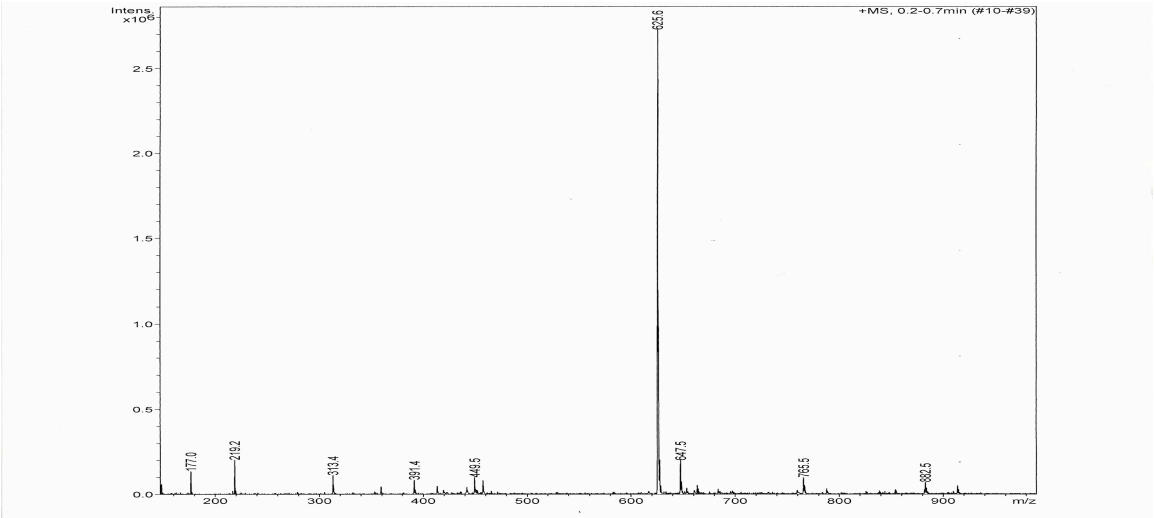

Curcumin mono-NHS.

^{1}H NMR

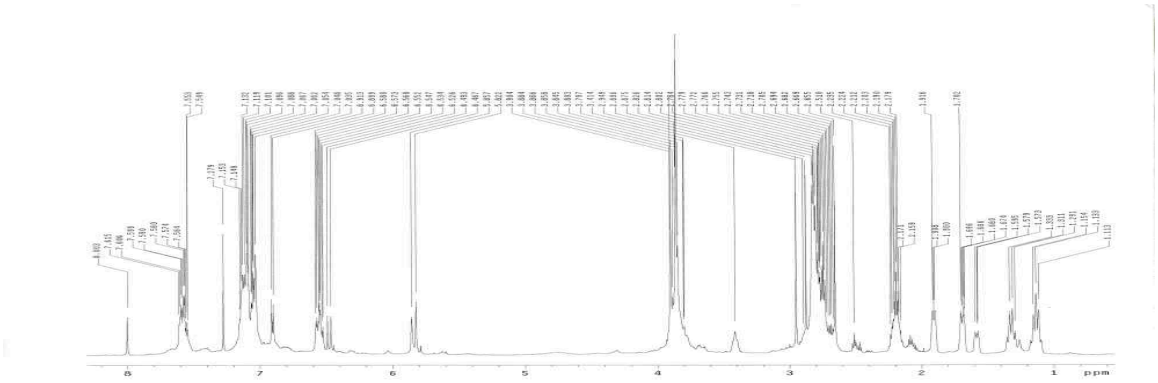

^{13}C NMR

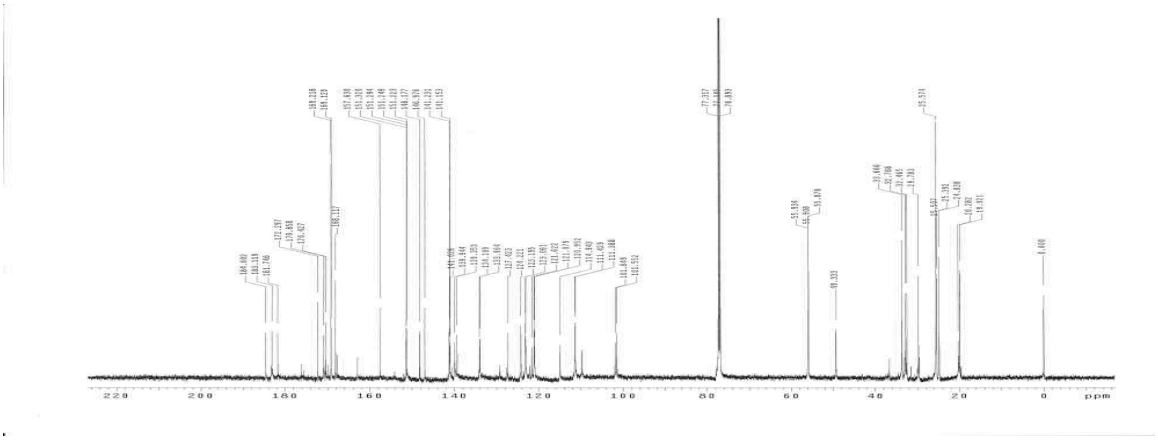

ESI-MS

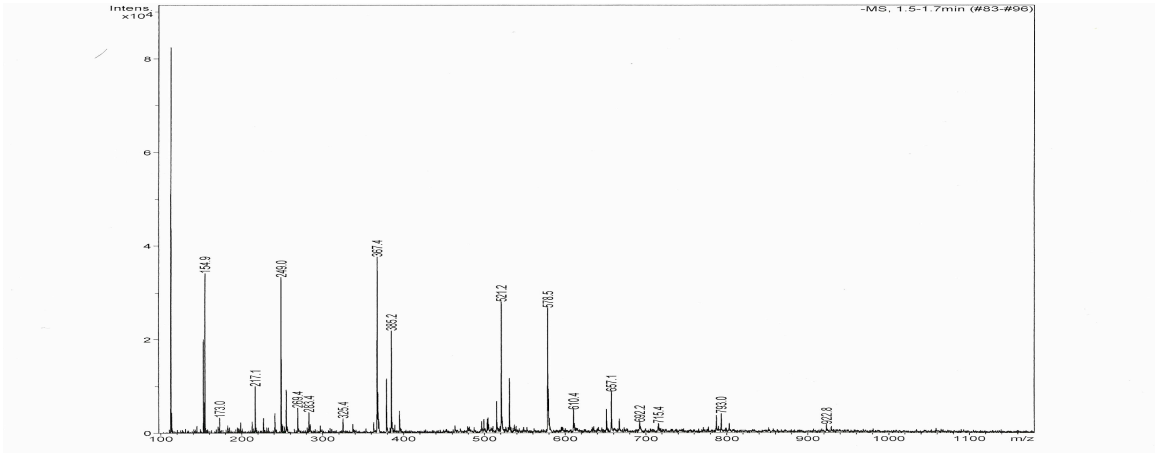

Curcumin dimmer.

^{1}H NMR

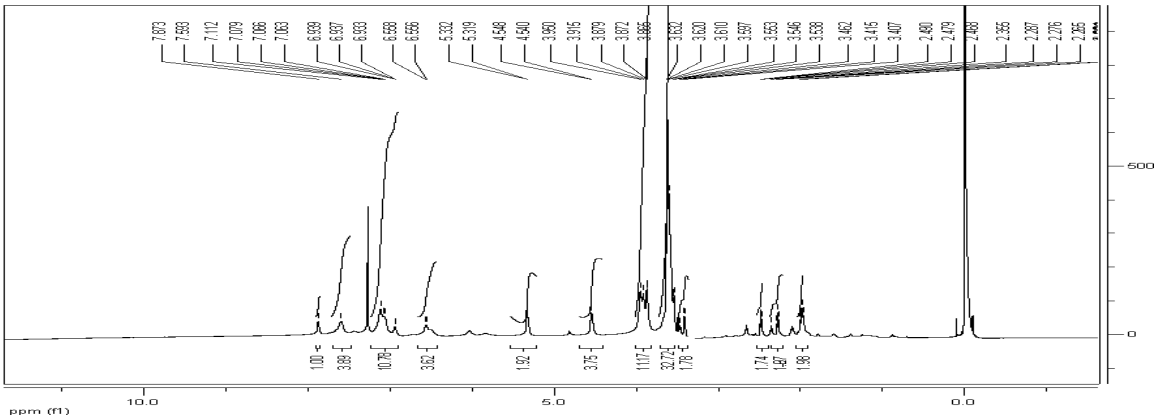

^{13}C NMR

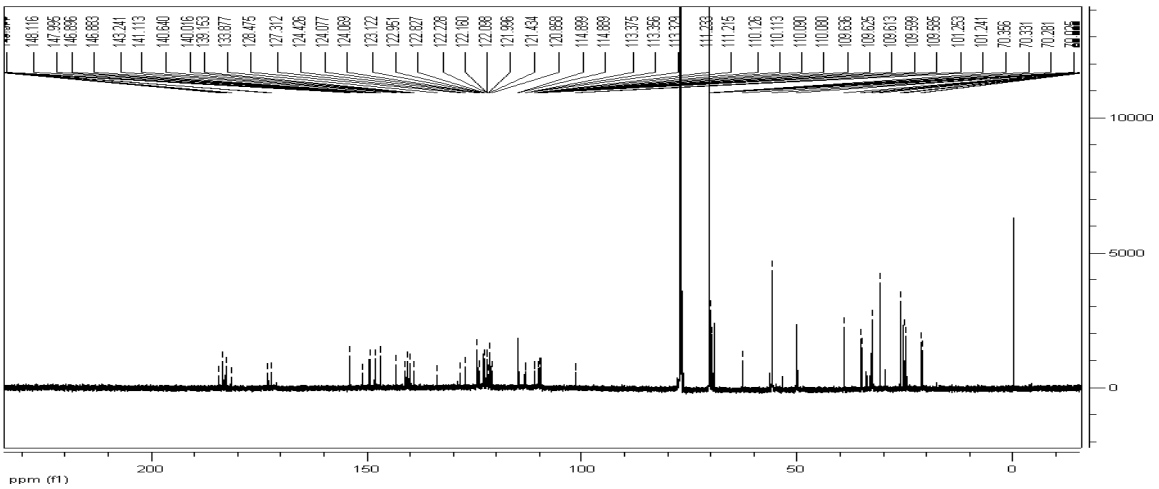

ESI-MS

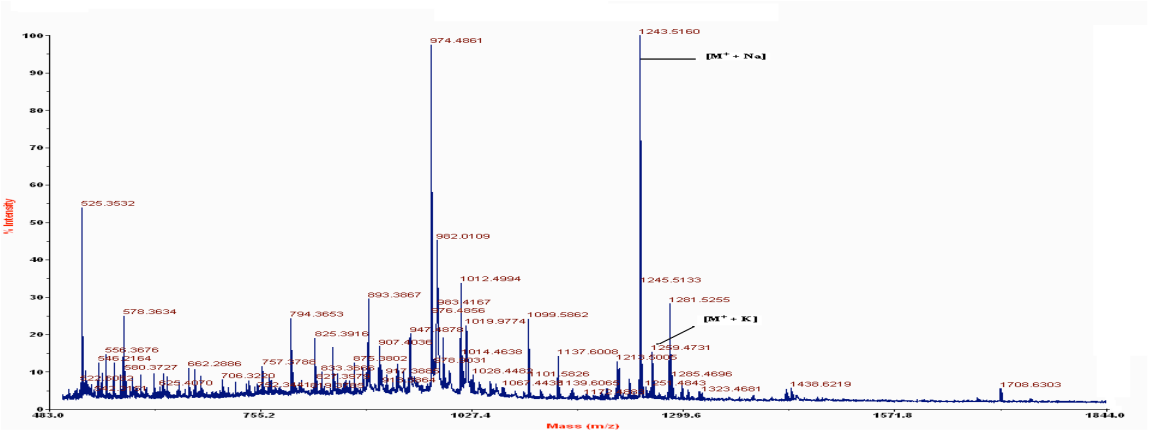

Sweet-curcumin (protected)

^{1}H NMR

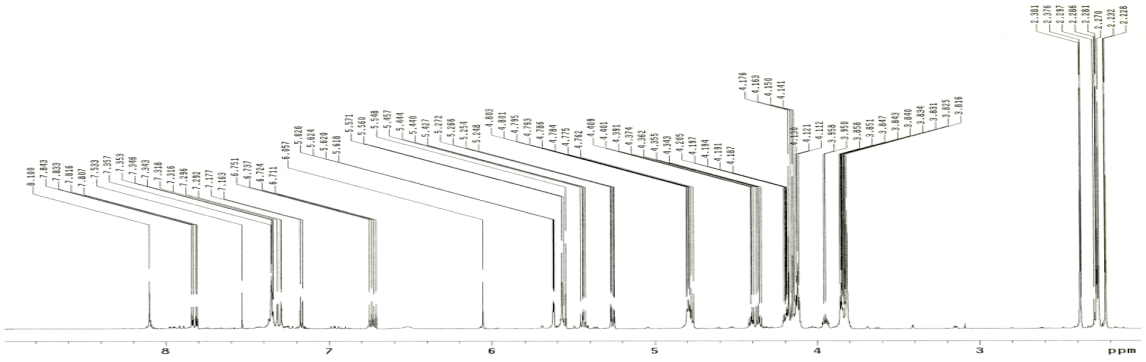

^{13}C NMR

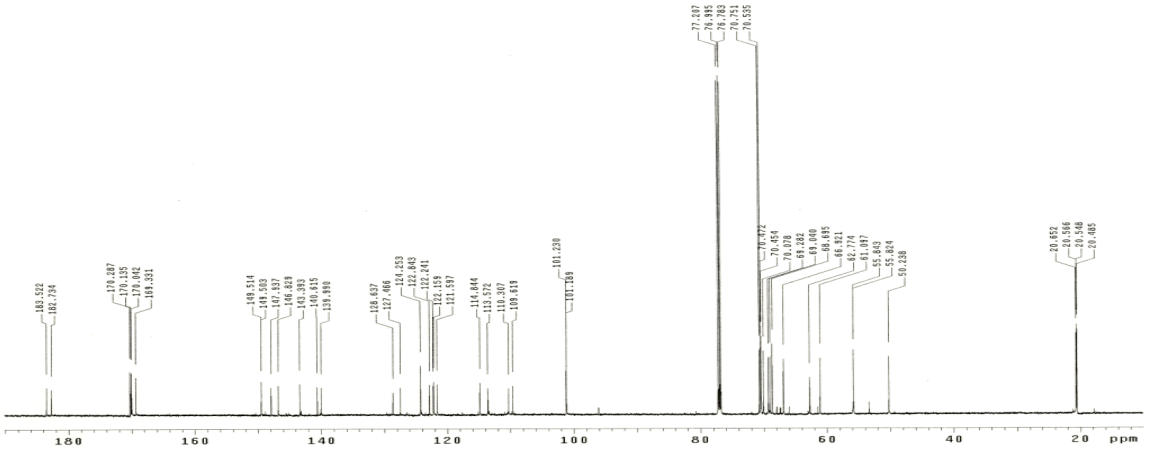

ESI-MS

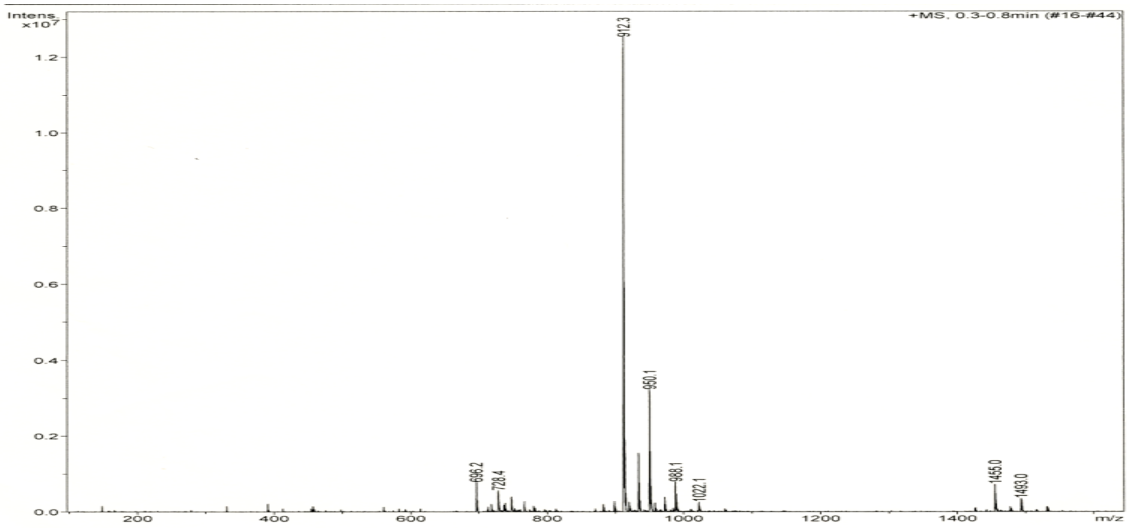

Sweet-curcumin.

^{1}H NMR

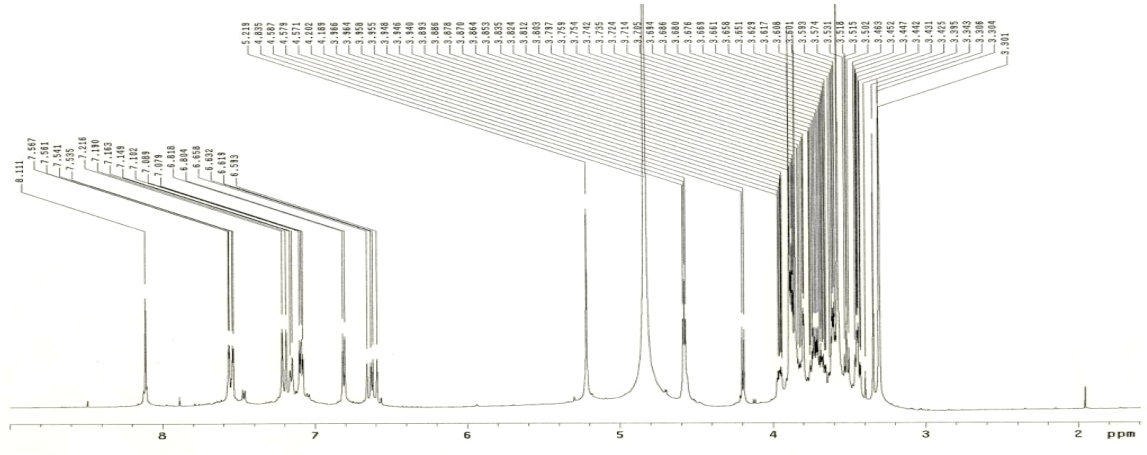

^{13}C NMR

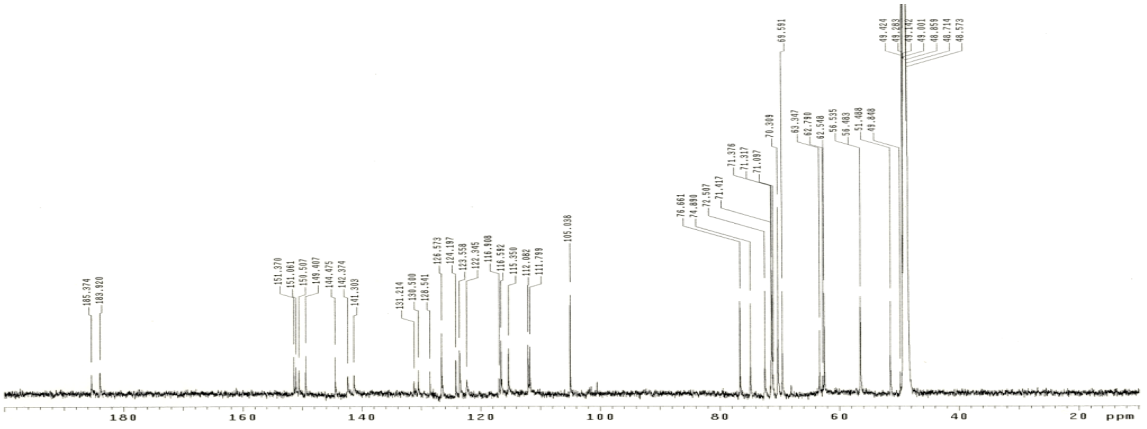

ESI-MS

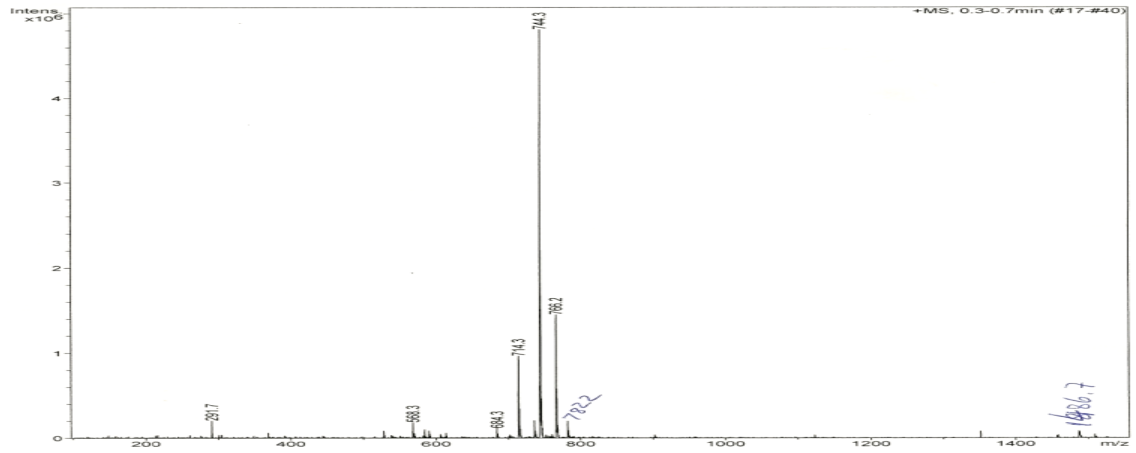

Curcumin mono-Galactose (protected)

^{1}H NMR

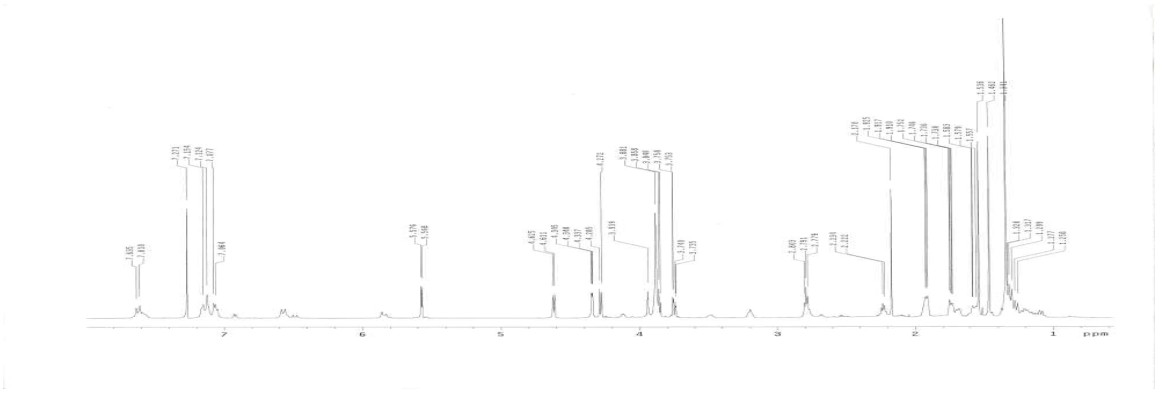

^{13}C NMR

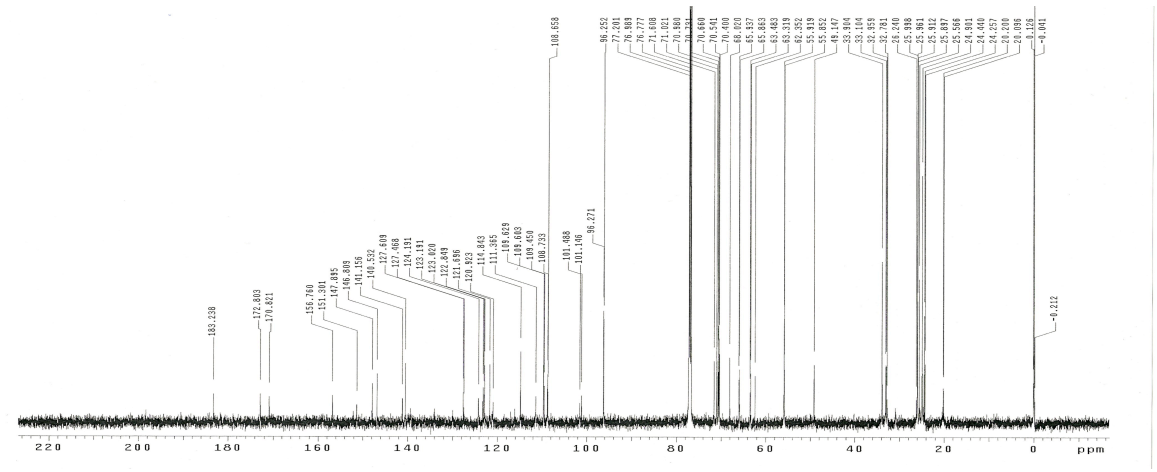

ESI-MS

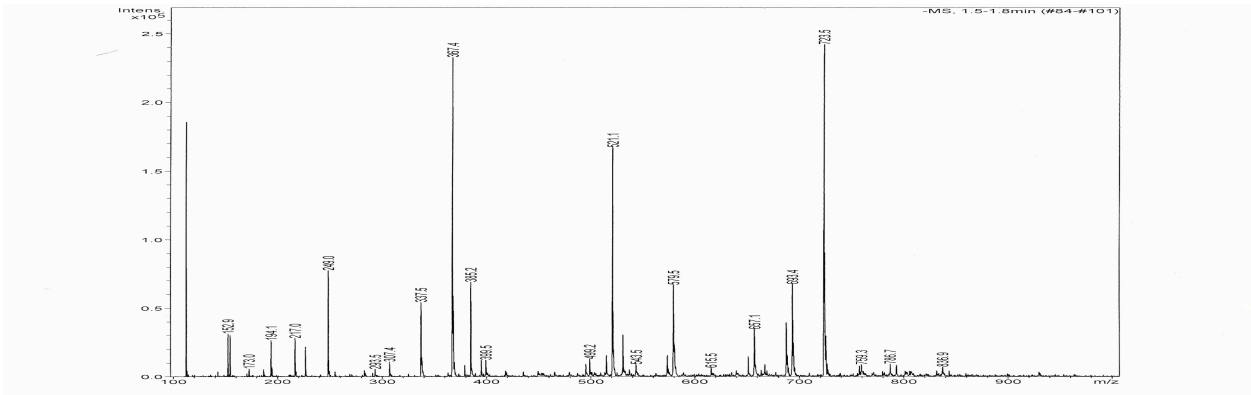

Curcumin mono-acrylate

^{1}H NMR

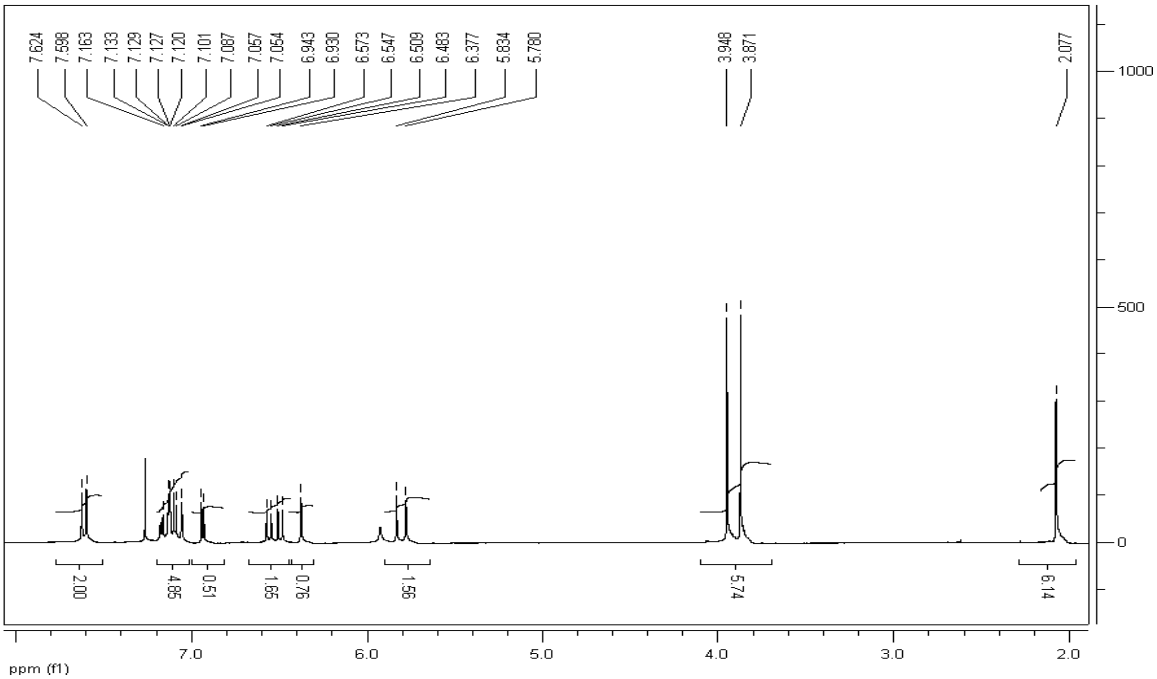

^{13}C NMR

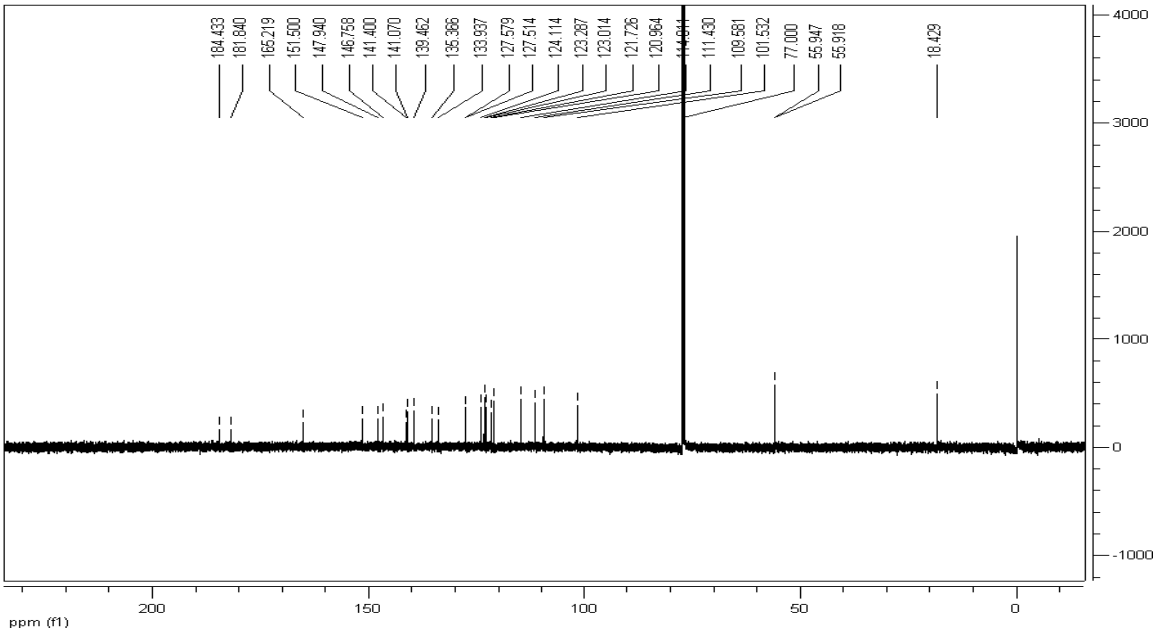

Curcumin mono-Glycine-Boc

^{1}H NMR

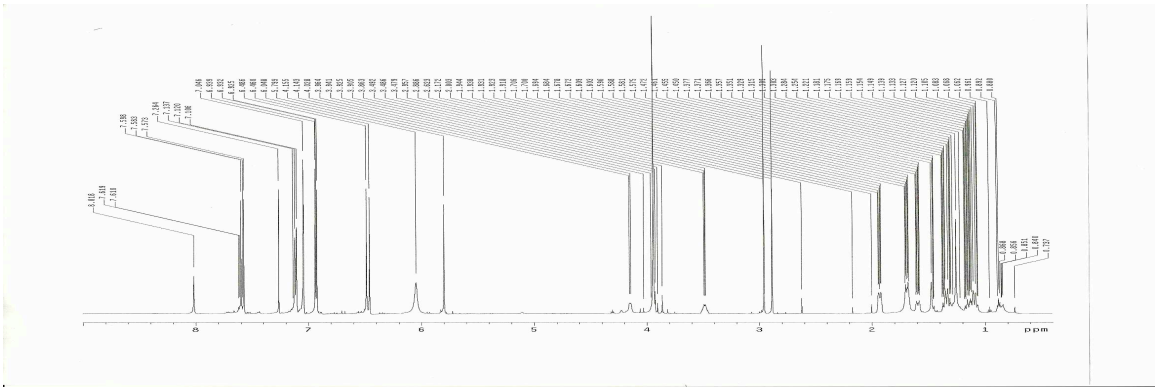

^{13}C NMR

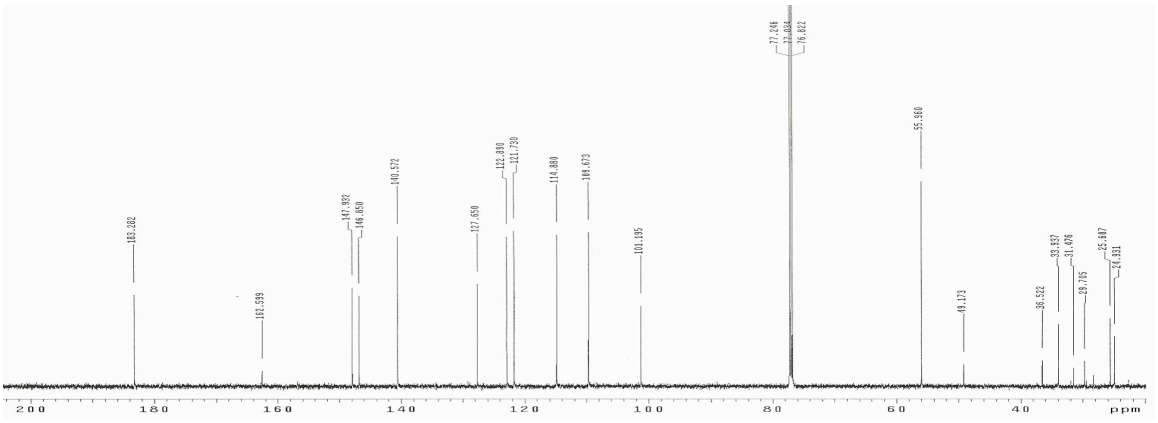

ESI-MS

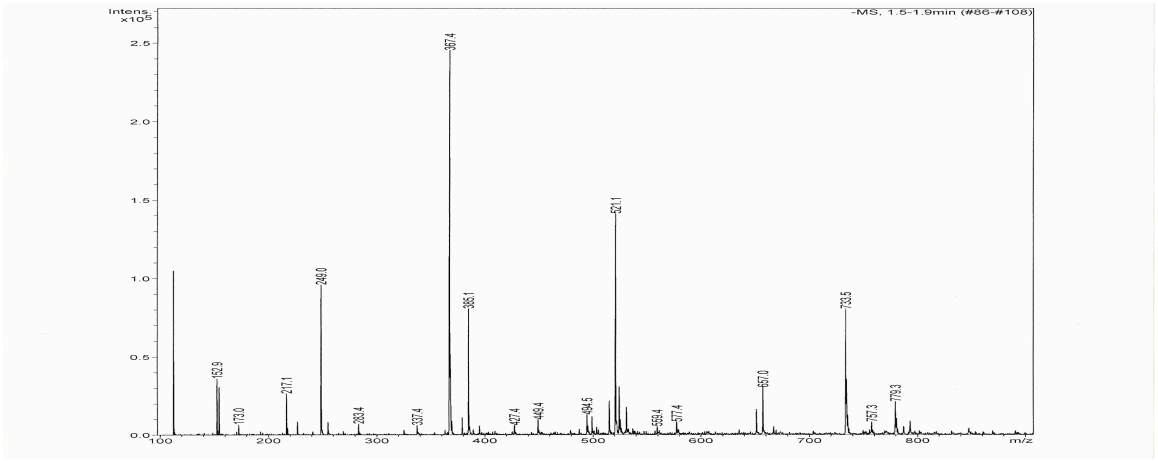

Curcumin di-carboxylic acid.

^{1}H NMR

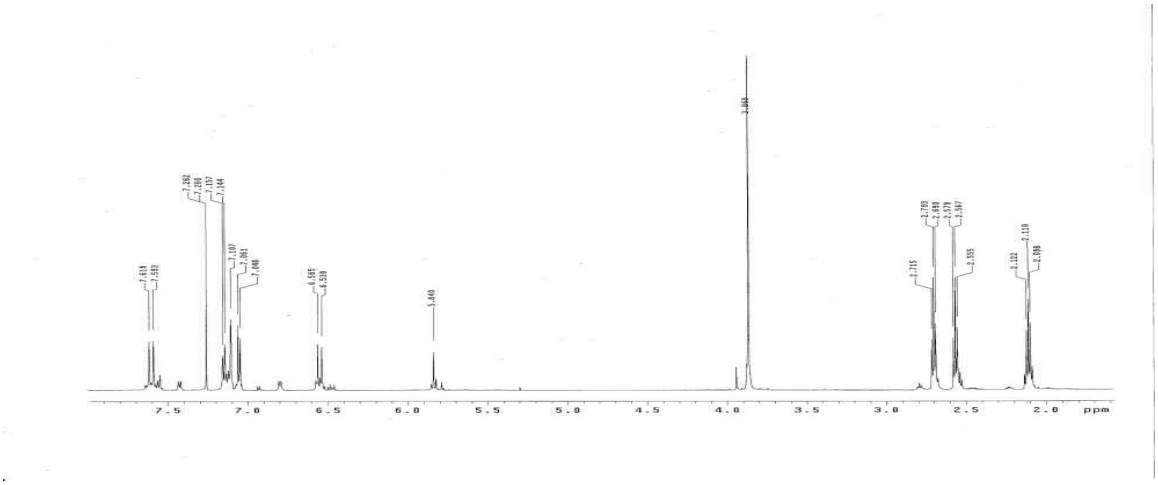

^{13}C NMR

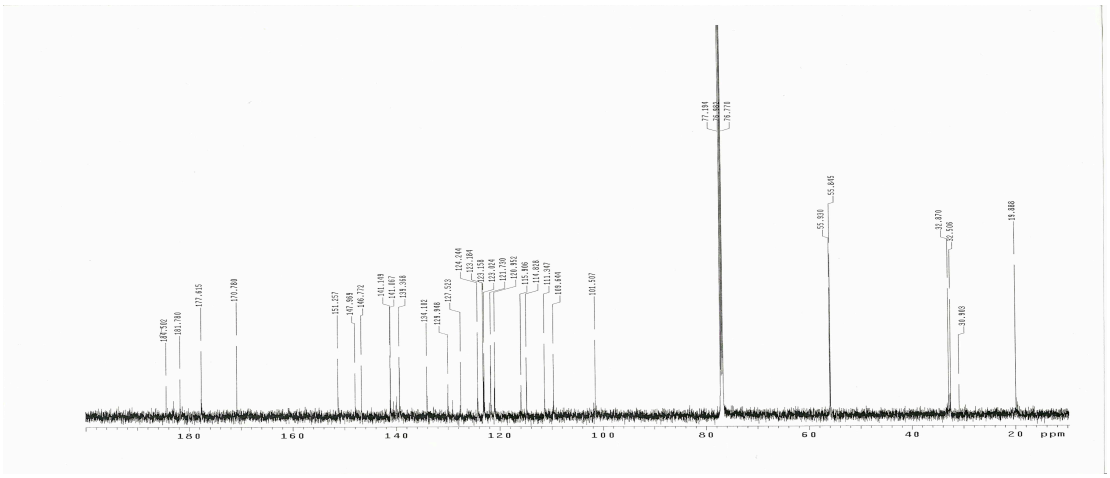

ESI-MS

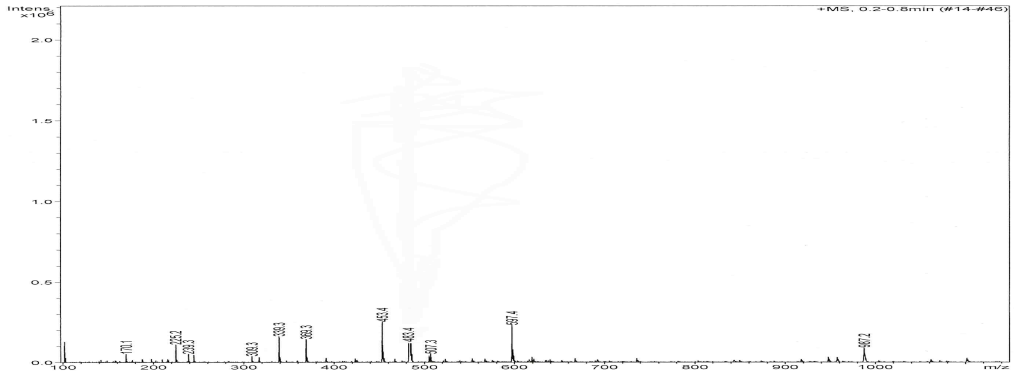

Curcumin di-galactose (protected).

^{1}H NMR

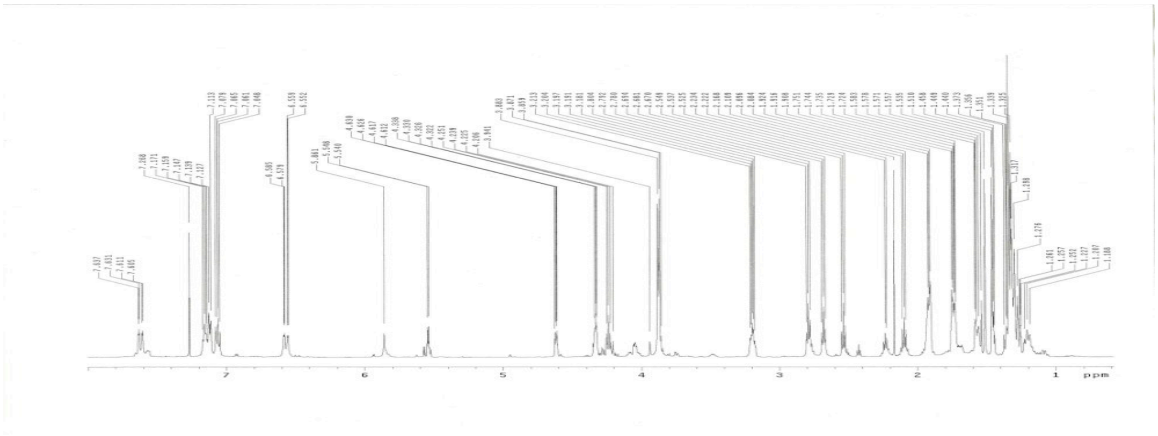

^{13}C NMR

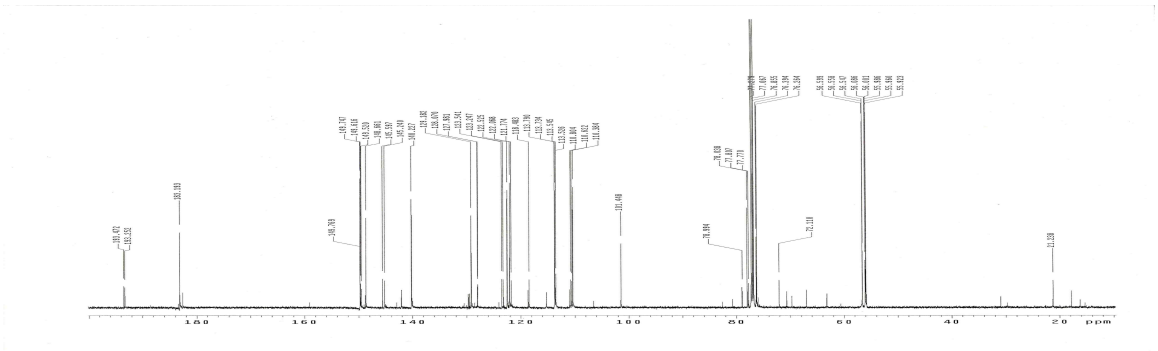

ESI-MS

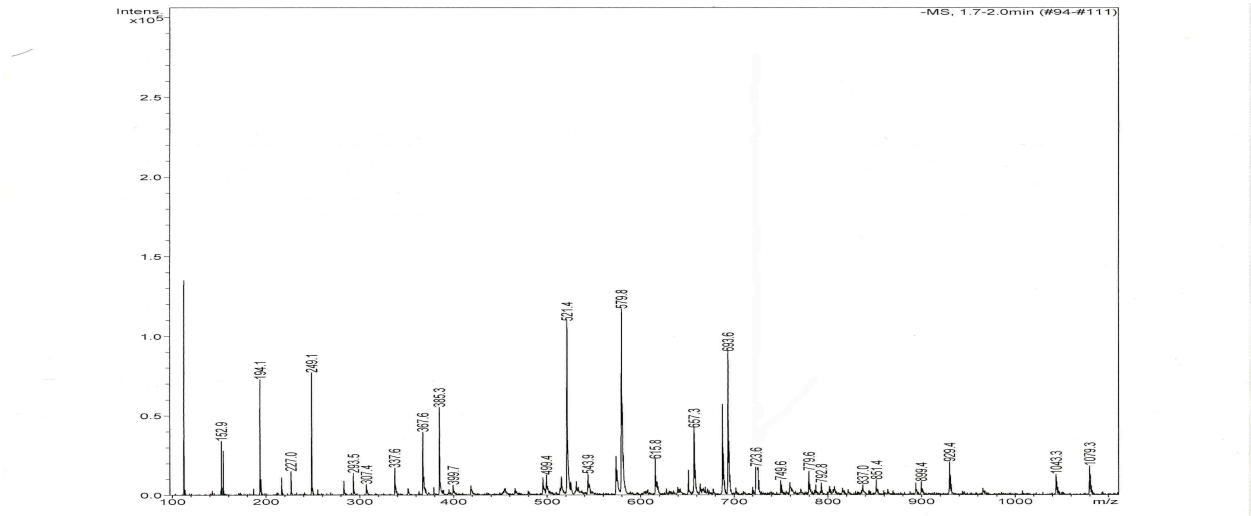

Curcumin di-alkyne.

^{1}H NMR

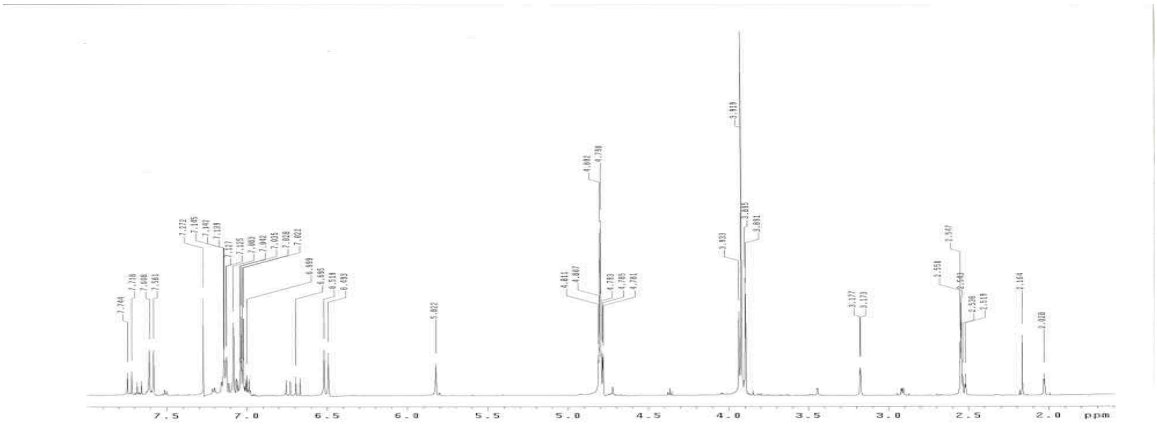

^{13}C NMR

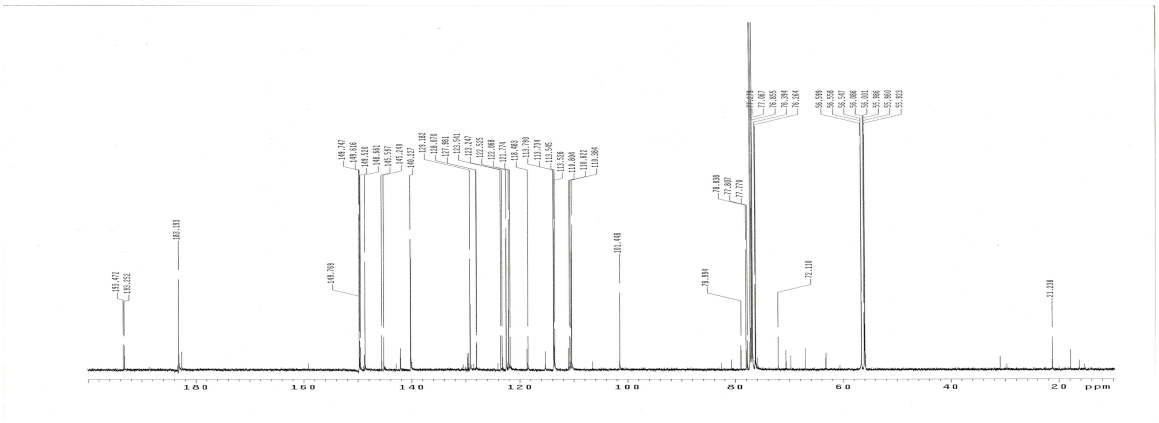

ESI-MS

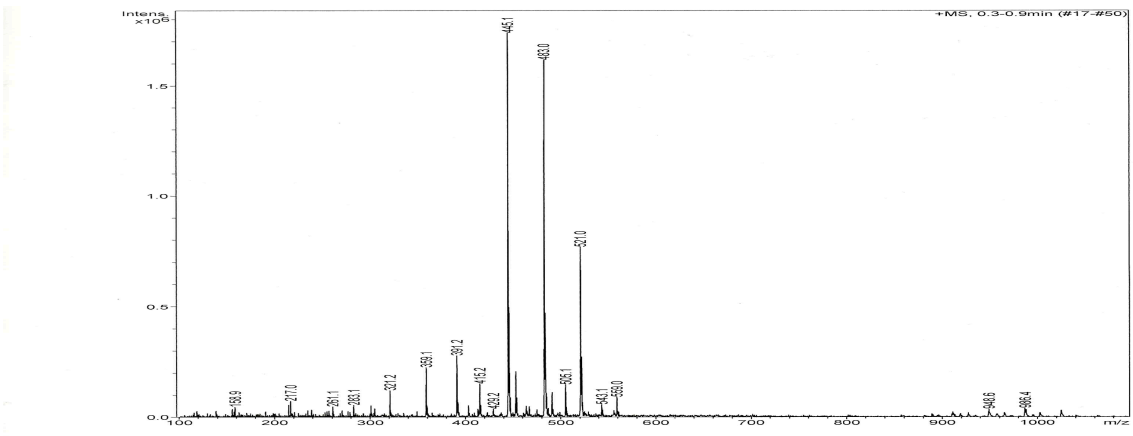

Curcumin 'clicked' di-galactose (protected).

^{1}H NMR

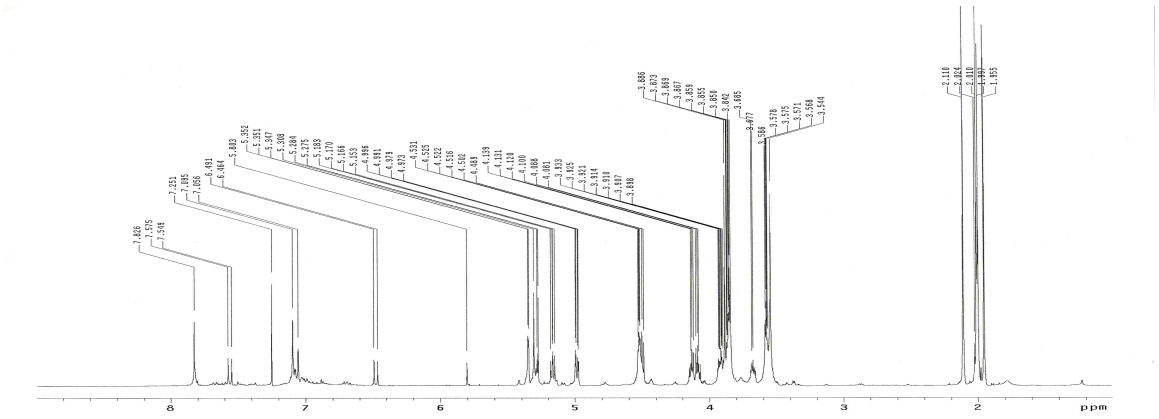

^{13}C NMR

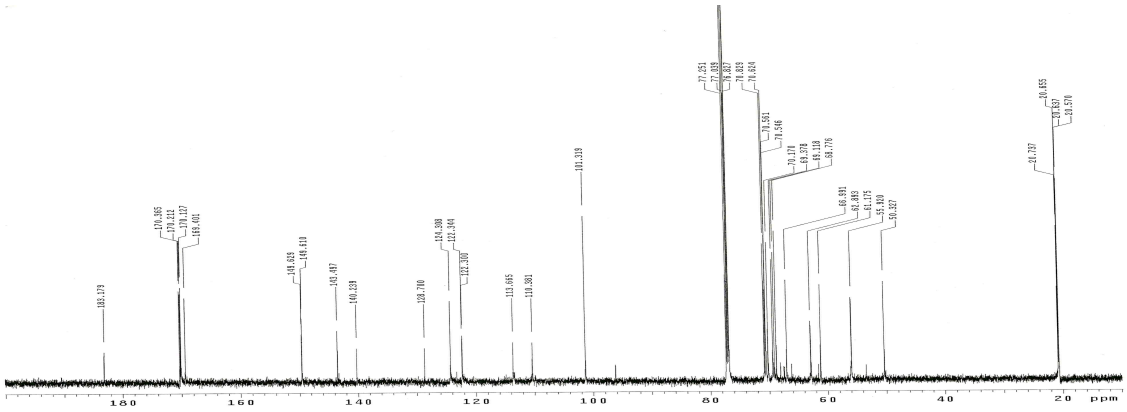

ESI-MS

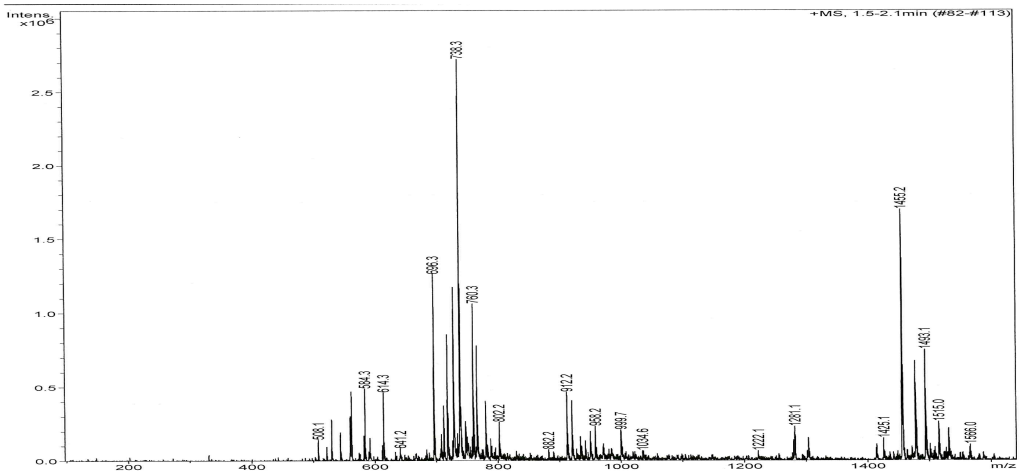

Curcumin 'clicked' di-galactose.

^{1}H NMR

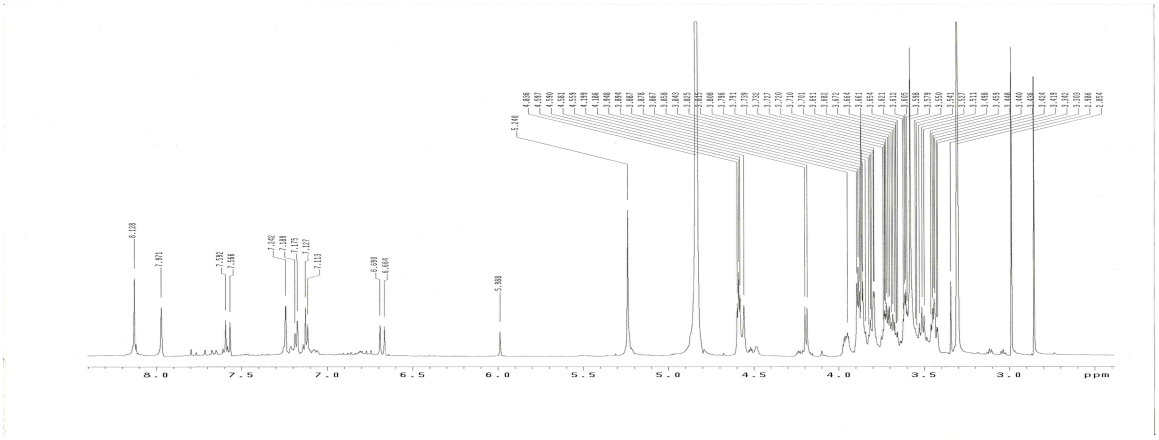

^{13}C NMR

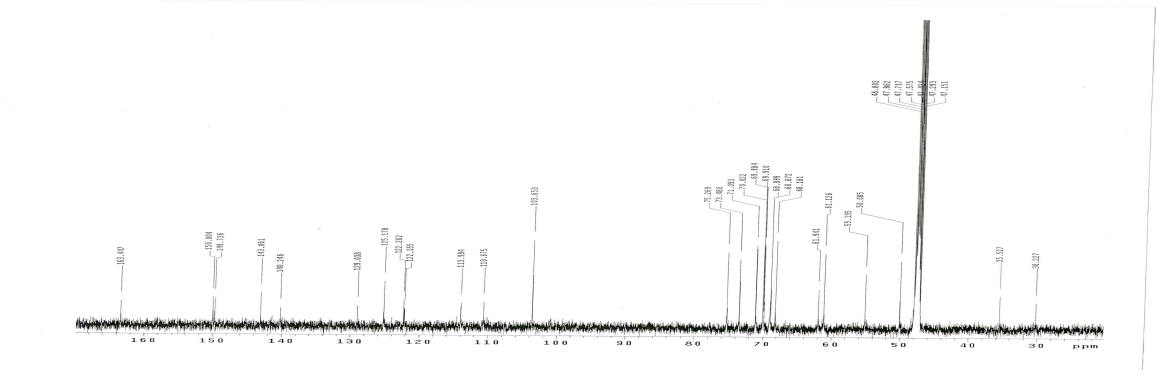

ESI-MS

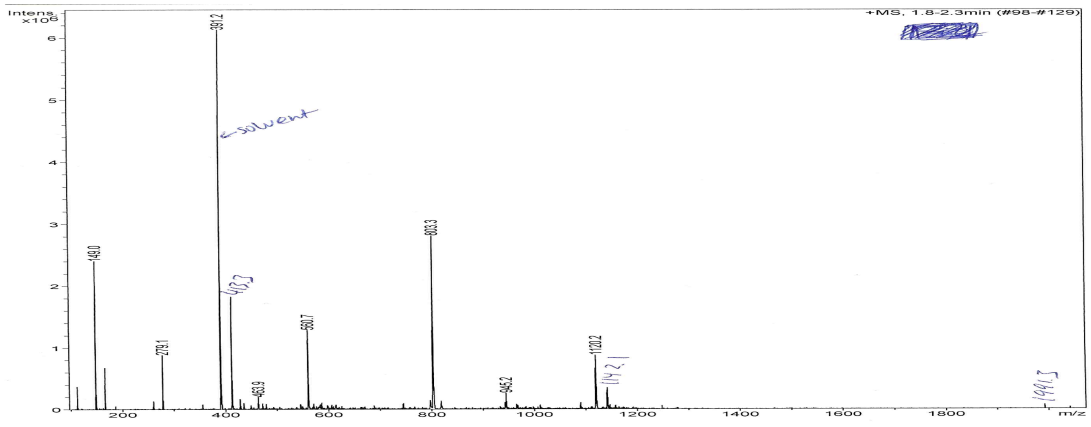

6. REFERENCES

(1) Chattopadhyay, I., Biswas, K., Bandyopadhyay, U., and Banerjee, R. K. (2004) Turmeric and curcumin: Biological actions and medicinal applications. *Current Science 87*, 44-53.

(2) Strimpakos, A. S., and Sharma, R. A. (2008) Curcumin: preventive and therapeutic properties in laboratory studies and clinical trials. *Antioxid Redox Signal 10*, 511-45.

(3) Aggarwal, B. B., and Shishodia, S. (2006) Molecular targets of dietary agents for prevention and therapy of cancer. *Biochem Pharmacol 71*, 1397-421.

(4) Leyon, P. V., and Kuttan, G. (2003) Studies on the role of some synthetic curcuminoid derivatives in the inhibition of tumour specific angiogenesis. *J Exp Clin Cancer Res 22*, 77-83.

(5) Shi, W., Dolai, S., Rizk, S., Hussain, A., Tariq, H., Averick, S., L'Amoreaux, W., El ldrissi, A., Banerjee, P., and Raja, K. (2007) Synthesis of monofunctional curcumin derivatives, clicked curcumin dimer, and a PAMAM dendrimer curcumin conjugate for therapeutic applications. *Org Lett 9*, 5461-4.

(6) Nurfinal, A. N., Reksohadiprodjo, M. S., Timmerman, H., Jenie, U. A., Sugiyant, D., and van der Goot, H. (1997) Synthesis of some symmetrical curcumin derivatives and their antiinflammatory activity. *European Journal of Medicinal Chemistry 32*, 321-328.

(7) Yang, F., Lim, G. P., Begum, A. N., Ubeda, O. J., Simmons, M. R., Ambegaokar, S. S., Chen, P. P., Kayed, R., Glabe, C. G., Frautschy, S. A., and Cole, G. M.

(2005) Curcumin inhibits formation of amyloid beta oligomers and fibrils, binds plaques, and reduces amyloid in vivo. *J Biol Chem 280*, 5892-901.

(8) Kumar, S., Narain, U., Tripathi, S., and Misra, K. (2001) Syntheses of Curcumin Bioconjugates and Study of Their Antibacterial Activities against beta-Lactamase-Producing Microorganisms. *Bioconjug Chem 12*, 464-9.

(9) Shishodia, S., Amin, H. M., Lai, R., and Aggarwal, B. B. (2005) Curcumin (diferuloylmethane) inhibits constitutive NF-kappaB activation, induces G1/S arrest, suppresses proliferation, and induces apoptosis in mantle cell lymphoma. *Biochem Pharmacol 70*, 700-13.

(10) Cole, G. M., Teter, B., and Frautschy, S. A. (2007) Neuroprotective effects of curcumin. *Adv Exp Med Biol 595*, 197-212.

(11) Cheng, A. L., Hsu, C. H., Lin, J. K., Hsu, M. M., Ho, Y. F., Shen, T. S., Ko, J. Y., Lin, J. T., Lin, B. R., Ming-Shiang, W., Yu, H. S., Jee, S. H., Chen, G. S., Chen, T. M., Chen, C. A., Lai, M. K., Pu, Y. S., Pan, M. H., Wang, Y. J., Tsai, C. C., and Hsieh, C. Y. (2001) Phase I clinical trial of curcumin, a chemopreventive agent, in patients with high-risk or pre-malignant lesions. *Anticancer Res 21*, 2895-900.

(12) Anand, P., Kunnumakkara, A. B., Newman, R. A., and Aggarwal, B. B. (2007) Bioavailability of curcumin: problems and promises. *Mol Pharm 4*, 807-18.

(13) Pfeiffer, E., Hoehle, S. I., Walch, S. G., Riess, A., Solyom, A. M., and Metzler, M. (2007) Curcuminoids form reactive glucuronides in vitro. *J Agric Food Chem 55*, 538-44.

(14) Shoba, G., Joy, D., Joseph, T., Majeed, M., Rajendran, R., and Srinivas, P. S. (1998) Influence of piperine on the pharmacokinetics of curcumin in animals and human volunteers. *Planta Med 64*, 353-6.

(15) Ryu, E. K., Choe, Y. S., Lee, K. H., Choi, Y., and Kim, B. T. (2006) Curcumin and dehydrozingerone derivatives: synthesis, radiolabeling, and evaluation for beta-amyloid plaque imaging. *J Med Chem 49*, 6111-9.

(16) Bisht, S., Feldmann, G., Soni, S., Ravi, R., Karikar, C., and Maitra, A. (2007) Polymeric nanoparticle-encapsulated curcumin ("nanocurcumin"): a novel strategy for human cancer therapy. *J Nanobiotechnology 5*, 3.

(17) Tiyaboonchai, W., Tungpradit, W., and Plianbangchang, P. (2007) Formulation and characterization of curcuminoids loaded solid lipid nanoparticles. *Int J Pharm 337*, 299-306.

(18) Li, L., Braiteh, F. S., and Kurzrock, R. (2005) Liposome-encapsulated curcumin: in vitro and in vivo effects on proliferation, apoptosis, signaling, and angiogenesis. *Cancer 104*, 1322-31.

(19) Li, L., Ahmed, B., Mehta, K., and Kurzrock, R. (2007) Liposomal curcumin with and without oxaliplatin: effects on cell growth, apoptosis, and angiogenesis in colorectal cancer. *Mol Cancer Ther 6*, 1276-82.

(20) Maiti, K., Mukherjee, K., Gantait, A., Saha, B. P., and Mukherjee, P. K. (2007) Curcumin-phospholipid complex: Preparation, therapeutic evaluation and pharmacokinetic study in rats. *Int J Pharm 330*, 155-63.

(21) Kumar, V., Lewis, S. A., Mutalik, S., Shenoy, D. B., Venkatesh, and Udupa, N. (2002) Biodegradable microspheres of curcumin for treatment of inflammation. *Indian J Physiol Pharmacol 46*, 209-17.

(22) Raja, K. S., Balambika, R., Dolai, S., and Shi, W. (2009) The concept of a green drug, curcumin and it's derivatives as a model system. *Mini-Reviews in Organic Chemistry 6*, 152-158.

(23) Mosley, C. A., Liotta, D. C., and Snyder, J. P. (2007) Highly active anticancer curcumin analogues. *Adv Exp Med Biol 595*, 77-103.

(24) Thompson, K. H., Bohmerle, K., Polishchuk, E., Martins, C., Toleikis, P., Tse, J., Yuen, V., McNeill, J. H., and Orvig, C. (2004) Complementary inhibition of synoviocyte, smooth muscle cell or mouse lymphoma cell proliferation by a vanadyl curcumin complex compared to curcumin alone. *J Inorg Biochem 98*, 2063-70.

(25) Sharma, K. K., Chandra, S., and Basu, D. K. (1987) Synthesis and antiarthritic study of a new orally active diferuloylmethane (curcumin) gold complex. *Inorganica Chimica Acta 135*, 47-48.

(26) Krishnankutty, K., and Venugopalan, P. (1998) Metal chelates of curcuminoids. *Synthesis and Reactivity in Inorganic and Metal-Organic Chemistry 28*, 1313-1325.

(27) Barik, A., Mishra, B., Kunwar, A., Kadam, R. M., Shen, L., Dutta, S., Padhye, S., Satpati, A. K., Zhang, H. Y., and Priyadarsini, K. I. (2007) Comparative study of copper(II)-curcumin complexes as superoxide dismutase mimics and free radical scavengers. *European Journal of Medicinal Chemistry 42*, 431-439.

(28) Vajragupta, O., Boonchoong, P., Watanabe, H., Tohda, M., Kummasud, N., and Sumanont, Y. (2003) Manganese complexes of curcumin and its derivatives: evaluation for the radical scavenging ability and neuroprotective activity. *Free Radic Biol Med 35*, 1632-44.

(29) Hermanson, G. T. (1996) *Bioconjugate Techniques*, Academic Press, San Diego, California.

(30) Shi, W., Dolai, S., Averick, S., Fernando, S. S., Saltos, J. A., L'Amoreaux, W., Banerjee, P., and Raja, K. (2009) A General Methodology Toward Drug/Dye Incorporated Living Copolymer-Protein Hybrids: (NIRF Dye-Glucose) Copolymer-Avidin/BSA Conjugates as Prototypes. *Bioconjug Chem*, 1595–1601.

CHAPTER V

Imaging and Therapeutic Applications of Curcumin Derivatives.

1. INTRODUCTION

Curcumin, a yellow pigment isolated from the root of ginger-like plant, *Curcuma longa* rhizomes, was widely used as food additives or spices for many years (*1, 2*). It has been found in the last few decades that curcumin possesses broad biological activities such as anticancer (*1-3*); antioxidant, anti-inflammatory (*4*) and potent anti-Alzheimer's disease activity (*5*) and anti-HIV protease activity (*6*). Curcumin is currently being used in human clinical trails both to treat cancer and Alzheimer's disease (*7*). Curcumin and other curcuminoids including demethoxy curcumin (DC) and tetrahydrocurcumin (THC) were known as potent inhibitors of angiogenesis. Extensive studies on structural-activity relationship of curcuminiods have revealed that these biological activities are derived from the phenol group and the α,β-diketone moiety.

One of the major limitations of using curcumin as a drug is its poor water and plasma solubility: even doses as high as 8 g of curcumin per day to human result in an average peak serum concentration of ~ 1.77 μM (*7*). The development of synthetic methods to attach curcumin to water soluble polymers and targeting proteins would considerably enhance the therapeutic potential of curcumin by enhancing bioavailability and by improving pharmacokinetics. Curcumin, [(1E,6E)-1,7-bis(4-hydroxy-3-methoxyphenyl)hepta-1,6-diene 3,5-dione] has two phenolic groups, which can be used as covalent handles for chemical modification. Many curcumin analogs, which have been reported in literature are symmetric in which both the phenolic groups have been blocked (*4*), thus severely diminishing its bioactivity.

Alzheimer's disease (AD) involves amyloid-β (Aβ) accumulation, oxidative damage, and inflammation, and risk is reduced with increased antioxidant and anti-

inflammatory substance consumption (*5*). Curcumin was found to possess potent anti-inflammatory and antioxidant activities and can suppress oxidative damage, inflammation, cognitive deficits, and amyloid accumulation. Since the molecular structure of curcumin suggested potential Aβ binding, Yang et al. have investigated its effect on Aβ aggregation and found that under aggregating conditions in vitro, curcumin inhibited aggregation (IC_{50} = 0.8 μM) as well as disaggregated fibrillar Aβ40 (IC_{50} = 1 μM), indicating favorable stoichiometry for inhibition. Curcumin was found to be a better Aβ40 aggregation inhibitor than ibuprofen and naproxen, and also prevented Aβ42 oligomer formation between 0.1 and 1.0 μM. In vivo studies showed that peripherally injected curcumin into aged Tg mice crossed the blood-brain barrier and bound plaques (*5*). When fed to aged Tg2576 mice with advanced amyloid accumulation, curcumin was found to label plaques and also reduced amyloid levels and plaque burden. As, curcumin directly binds to small amyloid species to block aggregation and fibril formation in vitro and as well as in vivo, curcumin is currently being used in clinical trials to prevent or treat Alzheimer's disease.

Although curcumin has shown a wide range of pharmacological activities, its anticancer properties have attracted much of interests. Despite being challenged by some researchers (*8-11*), the most accepted theory of cancer ("somatic mutation theory of cancer") considers that this disease is caused by DNA alterations (*12*). Several in vivo studies have revealed that curcumin can protect DNA from damage induced by different carcinogens (*13, 14*). It is widely accepted that the formation of a malignant tumor requires that tumor cells acquire several capabilities (the so-called 'hallmarks of cancer'), such as apoptosis resistance, increased angiogenesis, or capacity of invasion and

metastasis (*15*). The formation of a cancer requires that tumor cells develop apoptosis resistance, and it has been observed that curcumin can produce a mild but yet significant activation of apoptosis in vivo (*16, 17*). Malignant tumors are known to activate angiogenesis (the generation of new blood vessels), and several reports have shown that curcumin can inhibit angiogenesis in vivo (*18, 19*). Recent research has established that the activation of the nuclear factor kappa β (NF-κβ) is a crucial event both in inflammation and cancer (*20*). Many recent reports have shown that curcumin is an efficient NF-κβ inhibitor (*21, 22*). Accumulating evidence suggests that reactive oxygen species (ROS) play a key role in carcinogenesis (*23-25*). Antioxidant agents prevent or reduce excessive cellular levels of ROS and, therefore, play a protective role in cancer development. Curcumin being an excellent antioxidant, is very effective controlling the cellular levels of ROS and suppressing carcinogenesis (*14*). In vitro studies have clearly established that curcumin-induced cancer cell death occurs in a dose and time-dependent manner (*14*). Cancer cells do not undergo apoptosis in the presence of curcumin unless this dietary agent is at concentrations of approximately 5-50 μM during several hours. These concentrations of curcumin are not achieved outside the gastrointestinal tract through the oral route. Intravenous (i.v.) infusion seems to be an appropriate route of administration to overcome the low oral bioavailability and extensive metabolism of curcumin in the human body. But when thought in terms of solubility of curcumin in water/blood/serum, makes the i.v. method impossible to work with unless water soluble, nontoxic, bio-available derivatives or conjugates of curcumin are synthesized.

Surgery and radiotherapy are generally used when a tumor is localized to a certain tissue, but chemotherapy is needed when metastasis has occurred. Despite extensive

research, most anticancer drugs have nonspecific toxicity. By targeting the cell cycle and thereby killing rapidly proliferating cells, they do not explicitly discriminate between healthy and tumor tissues and only gain a limited selectivity for malignant cells. Such cytotoxic drugs have a narrow therapeutic window, which limits their efficacy and results in severe side effects. Due to a lack of selectivity, drug concentrations that would eradicate the tumor often can not be used. In addition, tumors can develop resistance against anticancer drugs after prolonged treatment. Therefore, achieving improved tumor selectivity through targeting of cytotoxic drugs to the cancer cells is needed.

A promising approach to achieving a more selective treatment is targeted prodrug therapy (*26*). Antibody-drug conjugates (ADCs) are ideal candidates for such prodrugs. ADCs are monoclonal antibodies (mAbs) linked to cell-killing drugs. Thanks to their high binding specificity for tumor-specific antigens, mAbs can be used as vehicles to target cell-killing payloads to tumor cells. Unique or over expressed, tumor-specific antigens can be found in a wide range of human tumor cells (*27*). Some mAbs have the ability to recognize and specifically bind to these tumor-associated antigens. They can be used as single agents for the treatment of cancer through binding to cancer-cell-specific antigens and induction of an immunological response against the target cancer cell (*28*). However, therapeutic efficacy is often limited by the extent to which the antibody leads to cell death. Monoclonal antibodies are extremely discriminating for their targets but sometimes therapeutically ineffective on their own. The insufficient efficiency of most naked mAbs in cancer therapy has been circumvented by arming the immunoglobulin with radioactive isotopes (*29*) or cytotoxic drugs (*30-32*), yielding highly specific ADCs.

Synthesis of such a adduct comprising of anti-carcinogenic curcumin and mAb would be very exciting and worthy.

Dendritic polymers are arguably the most spectacular example of a synthetic polyvalent scaffold. Dendrimers have potential applications in diverse areas ranging from material science to nanomedicine (*33*). Due to the observed extraordinary structure control and nanoscale dimensions for dendrimers, it is obvious to find extensive use of it as globular protein mimics (*33, 34*). Based upon their systematic size scaling properties as well as their hydrophilic/hydrodynamic behavior (*35, 36*) often, dendrimers are referred as "artificial proteins" (*33, 37, 38*). In recent years, dendrimers have also find its applications in site-isolation mimicry of proteins (*39, 40*), enzyme-like catalysis (*41*), drug delivery (*37*), surface engineering (*42*), and light harvesting (*35, 43*) hybridization with fullerenes (*44*) or single strand DNA's (*45*) to produce a wide variety of nanoscale sizes, shapes, containers and scaffolding. The commercial applications of dendrimer as globular protein replacements for gene transfection (i.e. Superfect®, Qiagen, Inc.) (*46, 47*), immunodiagnostics (i.e., Status®, Dade-Behring) (*48, 49*), as a nanopharmaceutical for the prevention of HIV (i.e., Vivagel®; Starpharma Ltd.) (*50*) are well established. It might be very useful if curcumin could be conjugated to water soluble dendrimers as it can act as polyphenol. Higher molecular weight plant polyphenols have been shown to possess physiological properties such as antioxidant or anticancer properties compared to their low molecular weight analogs (*51-54*). This kind of curcumin adduct with dendrimer might behave differently from a small molecule like free curcumin *in vivo*; and exibit the EPR (Enhanced Permeability and Retention) effect which in turn may give rise to a superior anticancer drug.

2. MATERIALS AND METHODS

2.1. General Information

All solvents and chemicals were purchased either from Fisher Scientific, Acros Organics or Sigma Aldrich and used as received. Human heart tissues containing intercellular amyloid, Amyloid-beta fragments1-40 and 25-35 were purchased from Sigma. Cystamine-core G4 PAMAM dendrimer was obtained from Dendritic Nanotechnologies. Sephadex LH20 size-exclusion gel was ordered from GE Healthcare. Carbon coated grids for TEM (200 mesh) were obtained from Electron Microscopy Sciences and TEM was performed using FEI Tecnai Spirit instrument equipped with AMT CCD camera at College of Staten Island's Advanced Imaging Facility. UV-Vis spectroscopy was performed on Agilant Technologies UV ChemStation Rev. A.10.01. FPLC analysis was performed using an AKTA explorer from GE Biosciences. Nuclear magnetic resonance (NMR) spectra were recorded on Oxford NMR 600 or 200 (600 MHz or 200 MHz) spectrometers.

2.2. Antioxdant potentiality assay by linoleic acid peroxidation method.

Using the Thiocyanide assay method (Jayaprakasha, et al. *Food Chem.,* **2006**, *98*, 720-724), antioxdant potentiality was carried out with Curcumin **1**, curcumin mono-carboxylic acid **1a**, curcumin mono-alkyne **2a**, and sweet-curcumin **4b**. 0.28 gm of linoleic acid, 0.28 gm of tween 40 as emulsifier and 50 ml of phosphate buffer (0.2 M, pH 7) were used to prepare a linoleic acid emulsion. The curcumin derivatives (5 mg of each) were dissolved in three different solvent mixtures; water, 80% (v/v) water-ethanol, ethanol and vortexed. These solutions were centrifuged to eliminate any undissolved

residue. 0.5 ml of each one of them was pipetted out into different test-tubes. Then 2.5 ml of linoleic acid emulsion was added to each one of them followed by the addition of 2.5 ml of phosphate buffer. All the tubes were incubated at 37 °C for 7 days. The mixture prepared as above without test sample was the control one. At the regular interval of 24 hours, 0.1 ml of the aliquots were drawn out of the incubation mixture and mixed with 5 ml of 75% ethanol, 0.1 ml of 30 % ammonium thiocyanate and 0.1 ml of 20 mM ferrous chloride in 3.5 % HCl. The tubes were allowed to stand in room temperature for 3 minutes. UV-Vis Spectrophotometric analysis was performed at 500 nm. All the tests were carried out in duplicate and averaged. Using the recorded absorbances the Anti-Oxidant Potential (AOP) were calculated according to the following equation.

Anoxidant activity = [1-(increase in absorbance of the sample/increase in absorbance of control)]*100

2.3. Solubility Comparison between Curcumin and Sweet-curcumin.

The improved solubility of the sweet-curcumin **4b** was confirmed via the following procedure using a UV-Vis spectrometer: 7.5 mg (0.01 mmol) of SC **4b** was vortexed in 1 ml of deionized water in an eppendorf ™ tube to create a stock solution. A control sample was also prepared by adding 3.7 mg (0.01 mmol) of curcumin in 1 ml of water in an eppendorf ™ tube and vortexed. Both the samples were centrifuged at 13,000 RPM for 2 min to eliminate any undissolved amount. 100 μL of the SC **4b** solution was added to 900 μL of deionized water and thoroughly mixed. The UV-Vis absorbance of the diluted SC and the stock curcumin solution were recorded. It is evident from the UV spectra that the SC **4b** (~0.2 mM in water, calculated from a previously determined molar

extinction coefficient) has vastly improved solubility relative to curcumin (0.0 mM in water). It should be noted that the solubility study outlined above measures the direct solubility of the compounds in water and closely models "real life" conditions, in contrast to other experiments in which the compounds are first dissolved in other solvents followed by dilution in water.

2.4. Human Heart Tissue Staining using Curcumin mono-carboxylic acid.

Human heart tissues containing intercellular amyloid were purchased from Sigma. Congo red staining was done according to the "Benhold's" protocol. A 50 nM solution of **1a** (with respect to curcumin) in 0.1M TBS (pH =7.4) was freshly prepared. Slides were dipped in 75% ethanol for 10 min. The slides were then treated with 0.3% Triton X-100 and 0.1 M TBS (pH = 7.4) containing 3% BSA with 0.5% Tween 20 for 10 min each. The 50 nM solution of curcumin mono-carboxylic acid was applied to the slides for 1 h at 37 °C in a humidified chamber. Sections were washed in TBS three times, rinsed once in distilled water, and cover slipped with fluorescent mounting medium. The slides were imaged using a polarized light microscope.

2.5. Degradation of Amyloid-β plaques using Curcumin mono-carboxylic acid.

Human heart tissues containing intercellular amyloid were purchased from Sigma. Congo red staining was done according to the "Benhold's" protocol. A 50 nM solution of **1a** (with respect to curcumin) in 0.1M TBS (pH =7.4) was freshly prepared. Slides were dipped in 75% ethanol for 10 min. The slides were then treated with 0.3% Triton X-100

and 0.1 M TBS (pH = 7.4) containing 3% BSA with 0.5% Tween 20 for 10 min each. The 50 nM solution of curcumin mono-carboxylic acid was applied to the slides for 1 h at 37 °C in a humidified chamber. Sections were washed in TBS three times, rinsed once in distilled water, and cover slipped with fluorescent mounting medium. The slides were imaged using a polarized light microscope.

Aβ 1-40 (100 μg/ml) was incuated for 3 days at 37 °C to generate fibrils in a 96 well plate (40 μL per well). On the 3rd day curcumin-COOH 1a or control buffer 0.1M TBS (pH = 7.4) was added to the preformed fibrils wells at a 1:1 volume ratio. The final concentration of the Aβ 1-40 was 50 μg/mL (11.6 μM) in both the curcumin-COOH treated sample and the control sample. The final concentration of curcumin-COOH was 8 μM. After the addition of the control buffer or curcumin-COOH to the fibrils, the plate was incubated for an additional 3 days at 37°C, and the TEM images and the UV spectra were recorded.

2.6. Dissolution of Amyloid-beta (Aβ) fragments by Sweet Curcumin at ultra-low concentrations.

2.6.1. Dissolution of Amyloid-β plaques.

Amyloid-beta (Aβ) fragment 25-35 (Sigma A-4559) was diluted in water to a stock of 1 mg/mL. 10 μM curcumin and sweet-curcumin stocks were also prepared in distilled water. Samples were prepared so that an equal volume of Aβ and the appropriate curcumin (sweet-curcumin or curcumin) were added in a 1:1 ratio so that the final concentration of the Aβ was 50 μg/mL and the curry was diluted to the desired molar concentration. Samples were incubated at 37˚C for 6 days. Aggregation of the protein

fragment was determined using transmission electron microscopy. 200 mesh carbon coated grids (Electron Microscopy Sciences) were used and prepared for negative staining by adding 5 μL of incubation mixture to the grid surface for one minute, followed by drying the grid with filter paper and contrasting with 5 μl of freshly filtered 2% phosphotungstic acid (pH =7.2) for one minute. Once grids were dry, examination was done using the FEI Tecnai Spirit at the College of Staten Island's Advanced Imaging Facility. Micrographs were captured using an AMT CCD camera.

2.6.2. Cell viability assay on normal brain cells using MTT.

2.6.2.1. Hippocampal slice Culture: Followed the procedure reported by Mehta, M. *et al*. *J. Neurochem.,* **2007,** *101*, 918-928.

Mouse pups of specific ages were anesthetized with ketamine (100 mg/kg) and decapitated. Under sterile conditions, the brains were isolated and then cut at 60^{o} angle from the longitudinal fissure at the top using a hippocampus- dissecting tool to expose the hippocampus. The hemispheres containing the hippocampi were then placed in modified Gey's balanced salt solution (mGBSS) at 4 ^{o}C for 30-40 minutes while bubbling a mixture of 95% O_2 and 5% CO_2. Individual hippocampi were isolated using dissection tool and then 400 μM thick transverse slices were prepared using a tissue chopper (Stoelting, Wood Dale, IL, USA). The slices were placed in ice coldmGBSS and inspected using a dissection microscope for the presence of uninterrupted bright transparent neuronal layers characteristic of the hippocampal structure. Only such slices were placed on Millicell CM filters (Millipore, Bedford, MA, USA). The filters were placed in a six well dish with 1 ml of medium in each well. The slices were kept on high

K^+ culture medium (25% horse serum, 50% Basal Essential Media- Eagles, 25% Eagle's Balanced Salt Solution (EBSS), 25 mM Na-HEPES, 1 mM Glutamine, 28 mM Glucose, pH 7.2) for the first two days. After incubation at 32 ^oC in a 5% CO_2 atmosphere, the culture medium was changed to physiological K^+ slice culture medium (20% dialyzed fetal bovine serum, 5% Basal Essential Media- Eagles, and EBSS modified to adjust the K^+ concentration to 2.66 mM). After 20% dialyzed serum treatment for two days and the slices were placed in 5% serum medium (same medium as above but with 5% serum) for two days.

2.6.2.2. MTT assay: MTT assay was performed according to Purkayastha, S. *et al*. *Brain Res.* **2009**, *1266*, 130-138.

Hippocampal slices from adult mice brain were cultured as described above. by Mehta et al (2007). After six days in vitro the slices were treated with different concentrations of the sweet-curcumin (i.e., 8 nM, 8 μM and 80 μM respectively) overnight along with the slices treated with the carrier as control.

After the treatment with sweet-curcumin, slices from each treatment group were placed in 400 μL PBS in one well of 48-well plate and then treated with 200 μL of MTT (5 mg/mL) per well with gentle mixing at 37 ^oC for 2hours. The slices were triturated to homogenize with the help of a micropipette. After that 800 μL of lysis buffer (20% SDS, 50% DMF) was added to each well and the plate was sealed and incubated overnight at 37 ^oC with gentle mixing. Now 100 μL mix from each well was taken in respective wells of a 96 well plate in triplicates and absorbance was measured at 570 nm using a plate reader. Results obtained were normalized to the total protein content and then expressed as percent carrier-treated samples.

2.7. Caspase-3 assay with Curcumin dimer.

SHSY5Y metastatic human neurotumor cells were grown in DMEM containing 10% fetal bovine serum. Two hours before drug treatment the medium was changed to neurobasal medium containing 2% B27. DMSO solutions of curcumin/dimer **6** were added followed by incubation for 16h at 37 ^{0}C. The effects of curcumin/dimer **6** were compared with appropriate DMSO controls.

General Protocol: The cells in a 96 well plate were plated with an approximate confluency of 40% for the day of the treatment. At least two hours before treating the cells with a drug, the medium was aspirated carefully from each well and 200 µl of B27 containing media (Neurobasal medium + 1%v/v penicillin-streptomycin + B27 supplement) was added to each well and then the drug was diluted to appropriate concentrations in the B27-containing medium (e.g. 500 µl, 250 µl, 100 µl, 50 µl, and 20 µl). In addition, the appropriate controls were also diluted in B27 containing media. The appropriate wells were treated with 50 µl of each concentration of the drug, and the plate was incubated for 16 h in a 37 ºC incubator. After the 16 h treatment, all kit components necessary for the experiment were warmed to room temperature. The substrate solution was prepared fresh for each experiment: Dithiothreitol (DTT) solution was prepared as follows: 40 µl of 1 M DTT (component E) was mixed with 1000 µl of assay buffer (component D). 1 µl of Caspase 3 substrate (component A) was diluted with 100 µl in the DTT solution (component E + component D). The reagents were mixed well, and 50 µl per well of Caspase-3 substrate solution was added. The reagents were allowed to completely mix by placing the plate on a plate shaker at 100 rpm for 60 minutes. The

fluorescence was measured by taking an end-point reading. The excitation wavelength was 485/20 nm and the emission wavelength was 528/20 nm. The sensitivity was set to 70. The results were plotted.

2.8. Synthesis and application of cystamine core G4 poly(amidoamine) dendrimer curcumin conjugate.

2.8.1. Synthetic protocol.

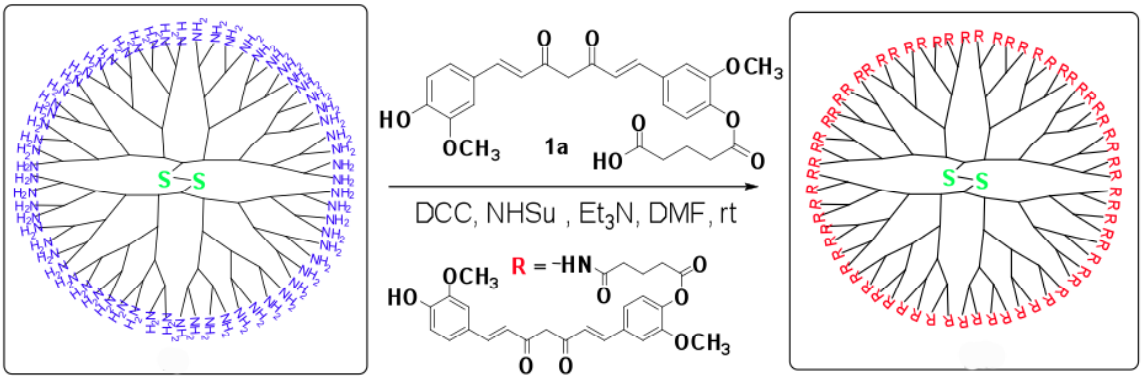

Curcumin mono-carboxylic acid **1a** (170 mg, 0.37 mmol), N-Hydroxysuccinimide (NHSu) (53 mg, 0.47 mmol) and 1,3-dicyclohexylcarbodiimide (DCC) (100 mg, 0.5 mmol) were dissolved in 3 mL DMF at 0 ^{o}C and stirred for 4 h. PAMAM G4 dendrimer (50 mg, 3.6 µmol) dissolved in DMSO (3 mL) and Et_3N (0.08 ml, 0.57 mmol) were added to the solution and stirred for 5 days at room temperature under N_2 atmosphere. The reaction mixture was added to 20 ml of MeOH-H_2O (50:50) mixture followed by centrifugation. The supernatant liquid was evaporated and the solid was dissolved in 20% MeOH-H_2O mixture and dialyzed extensively against 20% MeOH-H_2O using a 3500 MWCO membrane. The product was further purified using Sephadex^{TM} LH20 column with methanol as eluent. ^{1}H NMR (CD_3OD), δ (ppm): 1.24-1.27 (t); 1.85-1.88 (b); 1.91 (s); 2.14 (s); 2.22-2.24 (t); 2.35-2.38 (m); 2.64 (s); 3.11-3.15 (q); 3.29-3.30 (m); 3.64-

3.67 (m); 3.75-3.88 (br); 6.31-7.41 (br, m, Ar-H). ^{13}CNMR ($CDCl_3$), δ (ppm): 11.40; 14.39; 24.03; 24.96; 30.14; 31.63; 35.32; 36.22; 38.25; 40.19; 41.44; 69.12; 112.43; 118.66; 125.11; 125.19; 129.86; 132.40; 133.60; 169.34. The number of Curcumin units per dendrimer was calculated to be 37 from the ^{1}HNMR spectrum comparing the intensity of Ar-H (δ = 6.31-7.41 ppm) from **1a** with the -CONH-*CH_2*-*CH_2*-NHCO- protons from the dendrimer at δ = 3.11-3.15 ppm. FTIR (cm^{-1}): 3271, 1723, 1634, 1557, 1449, 1384, 1287, 1283, 1102, 748, 597, 472. C=O (R-CH=CH-*CO*-CH_2-*CO*-CH=CH-R arising from compound **1a**) stretching vibration was observed at 1723 cm^{-1}. =C-H (R-*CH=CH*-CO-CH_2-CO-*CH=CH*-R) stretching vibration was observed at 748 cm^{-1}.

2.8.2. FPLC experiment.

The PAMAM dendrimer standard, the control sample (non- covalent mixture of the dendrimer and the curcumin mono-carboxylic acid **1a**) and the dendrimer curcumin mono-carboxylic acid conjugate **9** was analyzed via FPLC using Hi-Prep™ 26/10 desalting column (GE Biosciences). 100 μL of sample solution in distilled water was injected using 0.1M Na_2CO_3 solution (pH = 9) as the running buffer.

2.8.3. Applications (<u>The following experiments were performed by Ms. Shawon Debnath in collaboration with our group and Dr. Fata's Group in CSI/CUNY</u>)

2.8.3.1. MTT assay protocol.

MTT system is a means of measuring the activity of living cells via mitochondrial dehydrogenase. The key component is [3-(4,5-dimethylthiazol-2yl)-2,5-diphenyl tetrazolium bromide] or MTT. Solution of MTT, dissolved in medium or balanced solutions without phenol red, are yellowish in color. Mitochondrial dehydragenase of

viable cells cleave the trtrazolium ring, yielding purple formazan crystals which are insoluble in aqueous solutions. The crystals are dissolved in acidic isopropanol. The resulting purple solution is spectrophotometrically measured. An increase or decrease in cell numbers result in concomitant change in the amount of formazon formed, indicating the degree of cytotoxicity caused by the treated material.

General Protocol: Cells (BT549) were plated in a 96-well plate at a density ranging from $20x10^3$ to $25x10^3$ cells/well. Cells were then incubated for 24 h at 37 ^{0}C in presence of 5% CO_2 until they are well flattened and distributed evenly in the plates. Following this, cells were washed and then treated with different concentrations (10, 20, 40, 60, 80 and 100 mM) drug dissolved in different media (H_2O or DMSO). Next, cells treated with drugs were further incubated for a definite period (24h) at 37 ^{0}C and in presence of 5% CO_2. MTT solution was then added to each well in an amount equal to 10% of the culture media volume. The MTT treated cells were then incubated for 2-4 hrs depending on the cell type and maximum cell densities away from light. After the incubation period, formazan crystals in each well was dissolved by adding an amount of MTT stabilization solution equal to the original culture media volume. Each well then was carefully mixed to give a homogeneous color by pipetting up and down several times. The plate was then covered with aluminum foil and put in a shaker for 15 mins. Absorbance of each well was measured at 690 nm and 570 nm. (High protein level may form a precipitate when MTT stabilization solution is added). The toxic effect of curcumin and its derivatives are found to be decreased in presence of serum, hence, the MTT assay was performed in absence of serum during drug treatment.

2.8.3.2. Uptake of the drugs by the cells.

Cells were plated at a density of $25x10^3$ cells/well in a 96-well plate and incubated for 24h in presence of 5 % CO_2 at 37 ^{0}C. Next the wells were washed two times with media before drug treatment step. Cells were treated with 5 μM of curcumin and dendrimer-curcumin conjugate **9** dissolved in either water or DMSO. The wells were further washed with basic media and then treated with original media. Fluorescence emission was taken of the wells at 485 nm and the value for the media was subtracted to ensure that the fluorescence observed was only because of the drug entrapped within the cells. The whole experiment was done in triplicates and averaged.

2.8.3.3. Caspase-3 Assay

The BT549 cells were seeded into the 8-well chamber at the density of 10,000 cells per wells and incubate in a humidified environment of 5% CO_2 at 37˚C overnight. The cells were exposed to the dendrimer-curcumin in DMSO/water and curcumin in DMSO/water with concentration of 10 μM respectively and incubate 24h. First of the all the cells were rinsed with PBS, and then the cells were fixed by formalin solution for 10 min. After washing with PBS three times (5 min each), the cells were blocked with 5% bovine serum 1 h and washed by 0.5% triton-x for 5 min and PBS twice (5 min each). After that, the sample was incubated with caspase-3 antibody (1:200 dilution) 1 h at room temperature. After being washed three times with PBS (5 min each), the samples were incubated with second antibody goat anti-rabbit IgG conjugated to Cy3^{TM} (1:10000 dilution) for 1 h at room temperature. After being washed in PBS three times (5 min each). The cells were incubated with the DAPI solution (0.6 mM) for 5 min. After washed with PBS three times (5 min each), the slides were mounted and examined in a

Leica confocal microscope. Digitized images of the fluorescent-antibody-stained cells were acquired and the intensity was quantified with software provided by Leica.

2.9. Synthesis of Curcumin-NHS Antibody adduct and its application. (The following experiments were performed by Ms. Phyllis Langone in collaboration with our group and Prof. Banerjee's group in CSI/CUNY)

2.9.1. Synthetic Protocol.

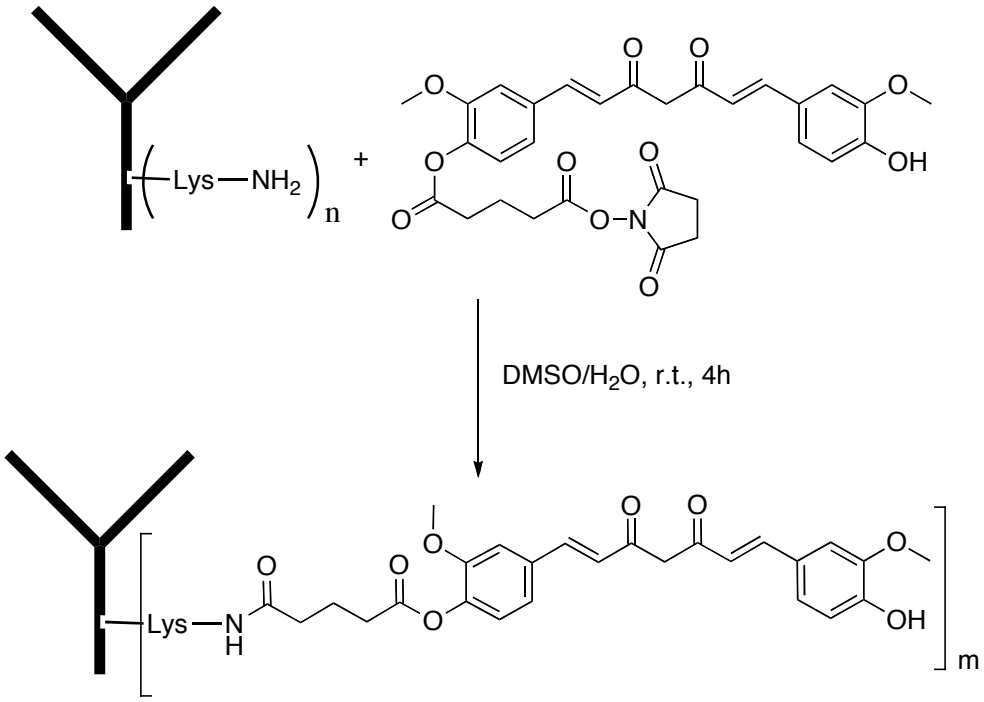

0.9 mg Curcumin mono-NHS **1c** was dissolved in 1 ml DMSO. For each 100 µl antibody (Santa Cruz CD68 #sc-9139 or Mel-CAM #sc-28667 for GL261 or B16F10 cells, respectively), 10 µl curcumin-NHS solution was added in increments while vortexing. Reactions were allowed to mix for 4 h at room temperature. The mol:mol ratio, antibody to curcumin, in the reaction is 1:100. The adducts were tagged with

DyLight fluors (633 or 594) using the instructions provided in the DyLight™ Microscale Antibody Labeling Kit (Thermo Scientific, IL).

2.9.2. Caspase 3/7 assay.

GL261 cells were incubated in a 96 well plate for 24 h at 37 ºC in a humidified 5% CO_2 incubator and then treated in triplicate with 166 nM curcumin-CD68 adduct or CD68 control. After additional 24 h incubation, cells were subjected to caspase 3/7 assay using the SensoLyte Homogeneous Rh110 Caspase-3/7 Assay Kit (AnaSpec, San Jose, CA). Fluorescence in each well was measured using a FLx 800 plate reader (Bio-Tek Instruments, Winooski, VT) set at 485/20 nm excitation and 528/20 emission. Results were analyzed with student's t-test (two-tailed distribution, two-sample unequal variance).

2.9.3. Determination of IC_{50} for Antibody-curcumin adduct.

Serial dilutions of curcumin adduct or Ab only in Neurobasal Medium (with 2% B27, 1% PS for B16F10 cells or with 2% B27, 4 mM glutamine or glutamax, and 2% PS for GL261 cells) were used to treat cancer cells (Ab=CD68 for GL261 cells; Ab=Mel-CAM/MUC18 for B16F10 cells). The IC_{50} was determined by plotting mean live cell counts against curcumin concentrations. The IC_{50} values obtained are as follows: 75 nM for B16F10 (24 h), 70 nM for GL261 (24 h). Results were analyzed with student's t-test (two-tailed distribution, two-sample unequal variance).

2.9.4. In vivo application of curcumin-Ab adduct

Implantation of cancer cells into mice: Mice were anaesthetized with a solution of xylazine and ketamine. Using aseptic conditions, cells were implanted into the right front brain [coordinates: with respect to the Bregma (in mm) AP=2.5; L= –1.1; D=1.5] at the

rate of 1 µl per minute using a stereotaxic set-up (KDS Model 310 plus infusion-withdrawal syringe pump) (Paxinos and Franklin, 2001). 5 x 10^5 GL261 glioblastoma cells were implanted. Wound area was then treated with an antiseptic solution and closed with suture clips. Mice were placed under a warming lamp to recover.

Drug treatments in mice: Drug injections took place days 13 and 15 (adduct containing 268 picomoles of curcumin on each day). Mice were prepared for surgery and immobilized in stereotaxic equipment as described previously. 5 µL PBS containing curcumin adduct (Curcumin-CD68) or control (CD68) was injected into the right front brain at the rate of 1 µL per minute. Mice were treated post-surgically as above.

3. RESULTS AND DISCUSSIONS

3.1. Antioxidant Potentiality Assay of Selective Curcumin Derivatives via Linoleic acid Peroxidation Method.

To assess whether the derivatization of curcumin has any effect on its antioxidant properties we have performed an antioxidant potential assay via linoleic acid peroxidation method. In this method capability of curcumin was compared with curcumin mono-carboxylic acid **1a**, curcumin mono-alkyne **2a** and sweet curcumin **4b**. Three different solvent systems were employed i.e. pure ethanol (100%), ethanol-water mixture (80:20 v/v) and pure water. In our experiment, it was found that absorbance of the control showed a steady increase for the first three days. On the fourth day the absorbance decreased followed by a steady decrease after120 hrs of incubation (**Figure 5.1**). The oxidation of linoleic acid generates linoleic acid hydroperoxides which generates the formation of secondary oxidation products. These oxidised species converts ferrous chloride to ferric chloride that on reaction with ammonium thiocyanate form ferric thiocyanate and results in blood red coloration. Here the peroxide formation becomes stagnant after 72 hrs which slows down the formation of ferric chloride and hence the absorbance value. When the absorbance values were plotted in terms of antioxidant potential (AOP) (**Figure 5.1**), it was observed that for the first two days the AOP increased and then decreased afterwards. It can be seen from the fig. 5.1 that curcumin, curcumin mono-carboxylic acid and curcumin mono-alkyne showed similar absorbance patterns in all types of solvent medium tested leading to almost comparable AOP through out the days. Where as sweet curcumin showed solvent dependence in absorbance and hence in AOP as well. It was found that sweet curcumin showed very strong AOP in

water media but negligible in ethanolic media through out the days and it was almost steady. It could be explained in terms of solubility of sweet curcumin in different solvent media. It was found that sweet curcumin **4b** was freely soluble in pure water but sparingly soluble in organic media. It could be seen clearly from fig. 5.2 that sweet curry showed very strong AOP in water compared to ethanol and ethanol-water mixtures. Hence, compound **4b** is a much better antioxidant than Curcumin **1** as well as other curcumin derivatives (**1a**, **2a**) in an aqueous medium which serves as a model for physiological conditions (plasma).

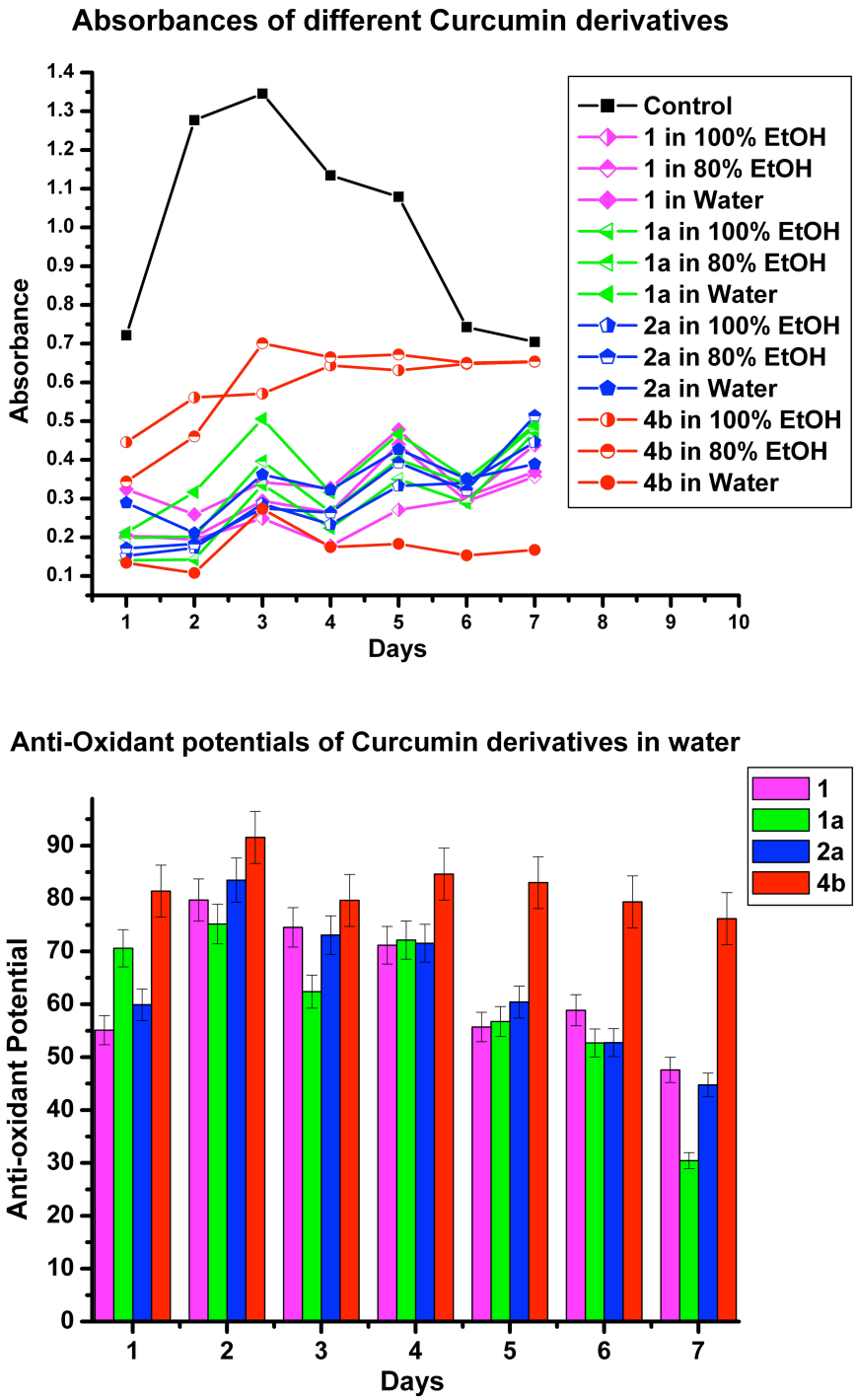

Figure 5.1. (Top) Absorbances of Curcumin **1**, Curcumin mono-carboxylic acid **1a**, Curcumin mono-alkyne **2a**, and Sweet curcumin **4b** in ethanol, water and ethanol-water mixture. (Bottom) Antioxidant potentials of the same in water.

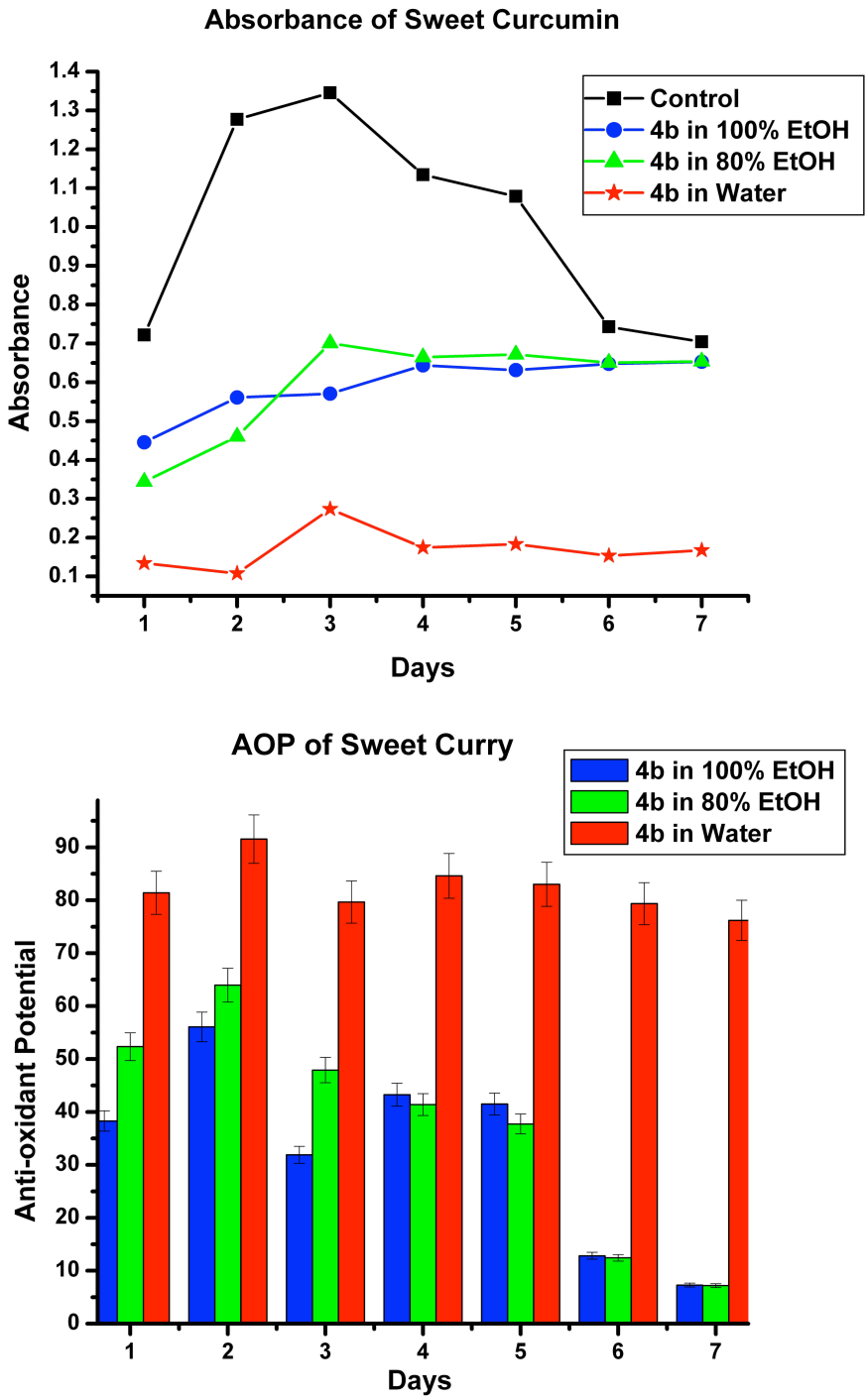

Figure 5.2. Comparison of absorbances and AOP of sweet curcumin **4b** in water, ethanol and ethanolic water.

(Dolai, S.; Averick, S.; Corbo, C.; Debnath, S.; Mogha, A.; Alonso, A.; Banerjee, P. and Raja, K. unpublished data).

3.2. Solubility Comparison Study of Curcumin and Sweet curcumin in water.

To prove the superior water solubility of Sweet curcumin **4b** compared to Curcumin **1** we conducted a simple UV-Vis analysis. Both curcumin and sweet-curcumin were dissolved in water, centrifuged, diluted and UV-Vis spectrum was taken. From the spectrum it is evident that sweet curcumin is more than 1000 times more soluble in water than curcumin. It should be noted that the solubility study outlined above measures the direct solubility of the compounds in water and closely models "real life" conditions, in contrast to other experiments in which the compounds are first dissolved in other solvents followed by dilution in water.

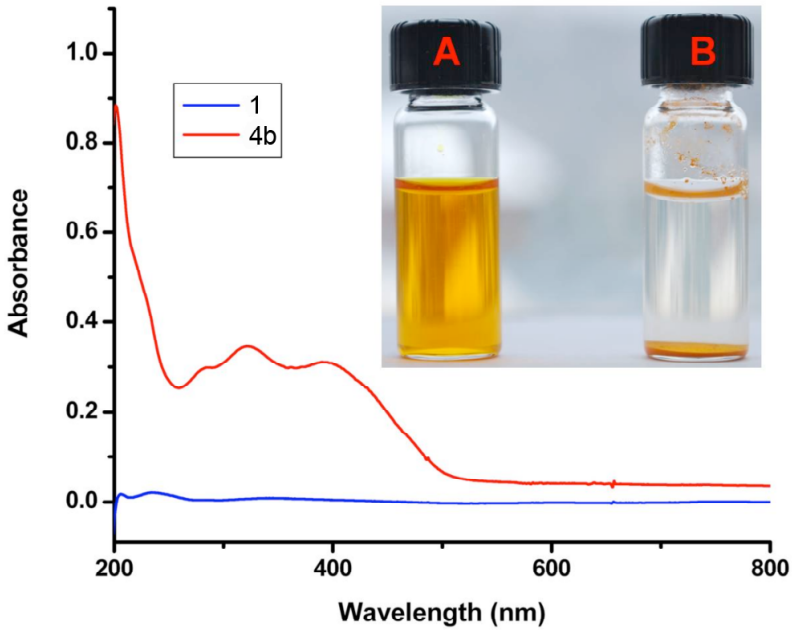

Figure 5.3. UV-Vis spectrometric comparison of solubility of curcumin **1** and sweet-curcumin **4b** in water. (A) curcumin in water (5 mg/mL), (B) sweet-curcumin in water (5 mg/mL).

(Dolai, S.; Averick, S.; Corbo, C.; Debnath, S.; Mogha, A.; Alonso, A.; Banerjee, P. and Raja, K. unpublished data).

3.3. Tissue Imaging with curcumin derivatives

Human heart tissue containing intercellular amyloid was stained with Congo Red (*55*) according to the "Benhold's" protocol (control sample) or with curcumin mono-carboxylic acid **1a** and imaged using a polarized light microscope; the images indicate that **1a** labels amyloid fibrils very effectively (**Figure 5.4**). Curcumin and its derivatives have the advantage that they can effectively label fibrils at a much lower concentration than Congo Red: 50 nM of **1a** compared to 0.014 M for Congo Red.

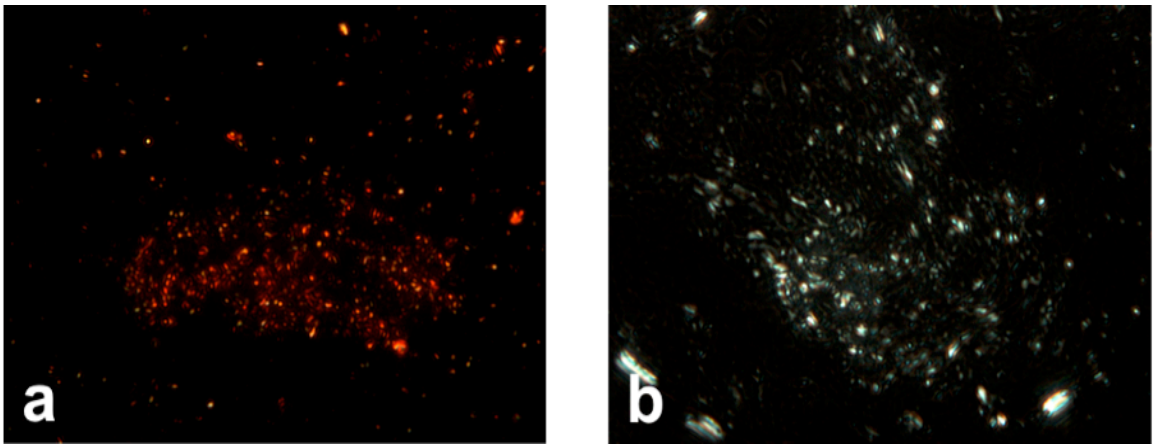

Figure 5.4. Human heart tissue containing intercellular amyloid stained using **a.** 0.014 M Congo Red (control sample) and **b.** 50 nM curcumin mono-carboxylic acid **1a** imaged using a polarized light microscope under cross polarizers.

3.4. Application of Curcumin Derivatives in Modulation of Amyloid-β Aggregates.

3.4.1. Curcumin mono-carboxylic acid

Curcumin binds and dissolves amyloid fibrils very effectively (*5*). Preliminary studies were carried out to assess whether the mono-functional curcumin derivatives retained the ability to bind and dissolve amyloid fibrils *in vitro*. The ability of **1a** to dissolve amyloid aggregates (fibrils) was also evaluated. In a typical experiment amyloid fibrils were formed by incubating Aβ 1-40 peptide. Either curcumin mono-carboxylic

acid **1a** or control buffer was added to the fibrils followed by visualization using Transmission Electron Microscopy that the curcumin derivatives are promising candidates for the dissolution of amyloid fibrils.

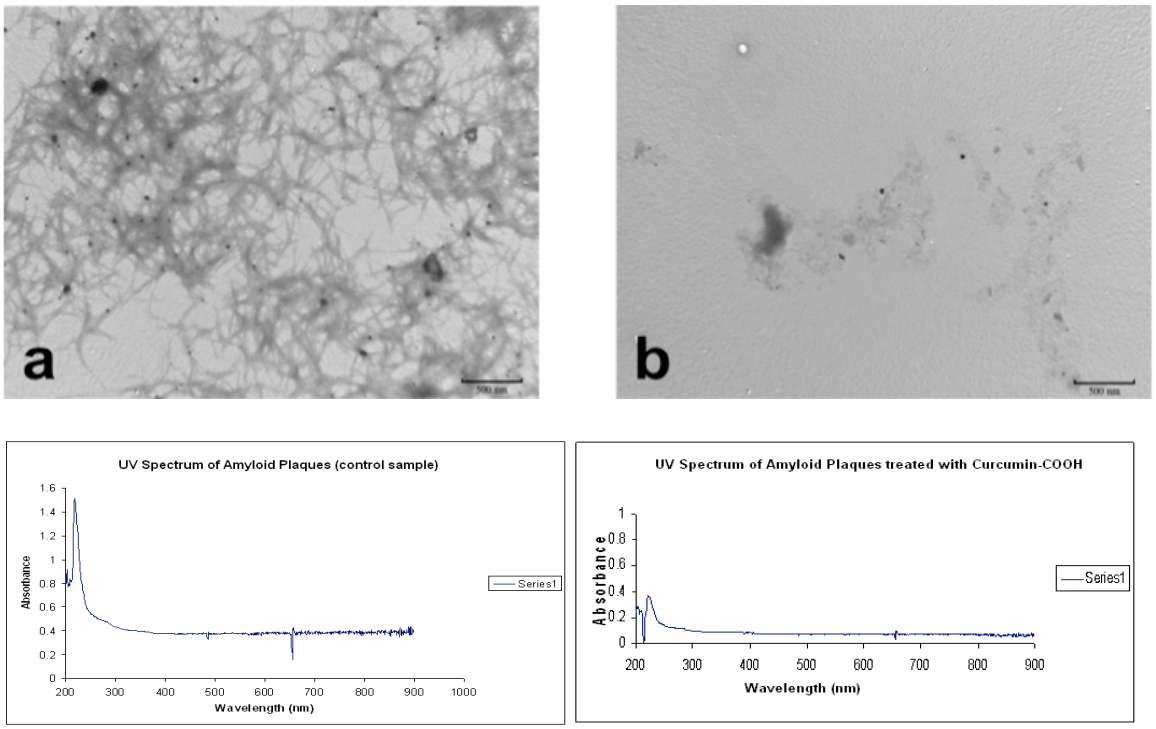

Figure 5.5. [Top] (slide **a**) Transmission electron micrograph of amyloid fibrils produced by incubating Aβ 1-40 for 6 days at 37 ^{o}C. (slide **b**) No fibrils are detected by TEM when amyloid fibrils produced by incubating Aβ 1-40 for 3 days was further incubated with **1a** (8 μM) for 3 days at 37 ^{o}C. The final Aβ 1-40 concentration is the same in both **a** and **b**. The scale bar for the TEM images is 500 nm.
[Bottom] (left panel) UV spectrum of amyloid plaques produced by incubating Aβ-40 for six days at 37 ^{o}C. (right panel) UV spectrum of amyloid plaques dissolved by incubation with Curcumin mono-carboxylic acid (8 μM) for three days at 37 ^{o}C.

The presence of fibrils in the control sample was marked by the significant increase in absorbance intensity throughout the UV-visible spectrum due to light scattering from the aggregated fibrils. The **1a** treated sample has significantly reduced absorbance intensity throughout the UV-visible spectrum due to dissolution of the fibrils by curcumin mono-carboxylic acid **1a**.

3.4.2. Sweet curcumin at Ultra-low Concentrations.

We also have studied sweet-curcumin's ability to dissolve Amyloid-beta plaques. Amyloidβeta (Aβeta) fragments 25-35 were incubated with different concentrations of either curcumin or sweet-curcumin at 37°C for 6 days. The aggregations of the plaques were determined via transmission electron microscopy (TEM) where the samples were negatively stained using phosphotungstic acid for better visualization. Surprisingly the sweet-curcumin inhibits the Aβ aggregation at very low concentrations compared to curcumin. Where the curcumin can barely inhibit aggregation at concentration of 8 μM, sweet-curcumin completely dissolutes amyloid plaques at concentrations as low as 8 nM. At higher concentrations (e.g. 8 μM, 0.8 μM) of sweet-curcumin the inhibition of aggregation is not as effective as 80 nM or 8 nM, but better than curcumin.

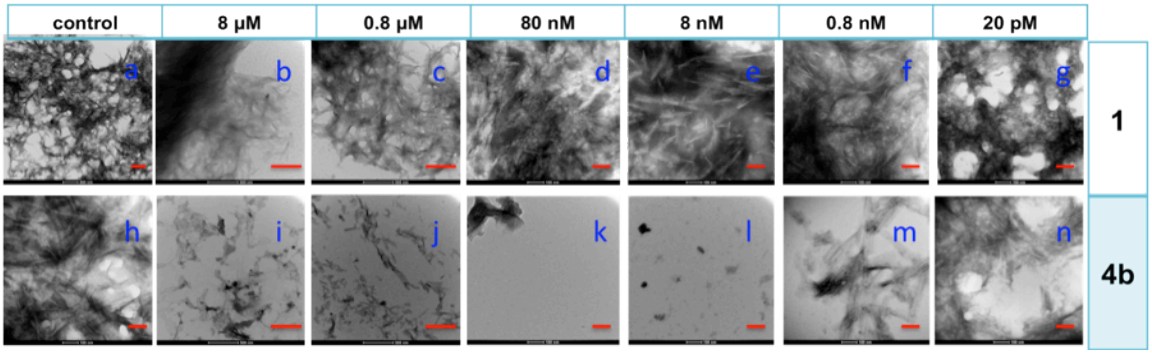

Figure 5.6. TEM micrographs of Amyloid plaques treated with different concentrations of (i) curcumin **1** [b-g], (ii) sweet-curcumin **4b** [i-n] and no reagent (control) [a, h]. The scale bars indicate 500 nm (a-c, i-j) and 100 nm (d-g, h, k-n) respectively.
(Dolai, S.; Averick, S.; Corbo, C.; Debnath, S.; Mogha, A.; Alonso, A.; Banerjee, P. and Raja, K. unpublished data).

To investigate the neuro-toxicity of the synthesized compound we performed MTT assay on cultured hippocampal slices of mouse-brain. The results of the MTT assay show that at low concentrations (i.e. 8 nM and 8 μM) the viability of the cells is near the

control samples but at a higher concentration (i.e., 80 μM) cell viability was a little higher than the control samples, which shows that the sweet-curcumin has no harmful effect on the normal brain tissue as long as viability is concerned. Hence, It could be concluded form the fig. 5.7 that sweet curry has no harmful effect on the normal brain cells at low concentrations, and at higher concentrations the cell viability among the brain cells is even better.

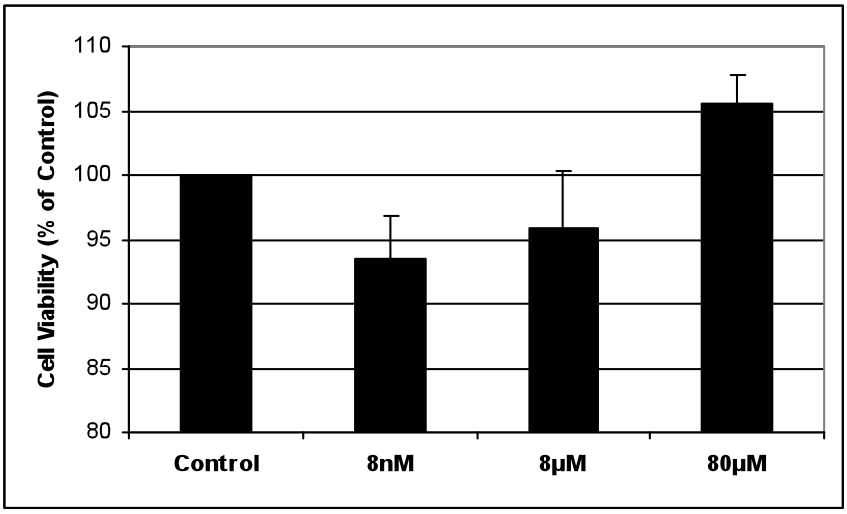

Figure 5.7. Cytotoxicity associated with sweet-curcumin on cultured hippocampal slices using a MTT assay. Cell viability (%) with 80 μM, 8 μM and 8 nM of sweet-curcumin **4b**.
(Dolai, S.; Averick, S.; Corbo, C.; Debnath, S.; Mogha, A.; Alonso, A.; Banerjee, P. and Raja, K. unpublished data).

3.5. Applications of Curcumin Derivatives in Cancer Treatment.

3.5.1. Efficacy of Curcumin dimer in eliminating Human Neurotumor cells.

The ability of the curcumin derivatives to eliminate SHSY5Y metastatic human neurotumor cells was evaluated using a Caspase-3 activation assay. The Curcumin dimer **6** was found to be the most selective derivative among water non-soluble derivatives. As could be seen from **Fig. 5.8** both curcumin and **6** show a concentration dependant caspase activation; at 500 μM curcumin is slightly better than the dimer in inducing cell apoptosis. The same assay was performed on healthy control neuronal cells at 500 μM concentration, curcumin induced considerable apoptosis whereas the dimer **6** induced only marginal apoptosis.

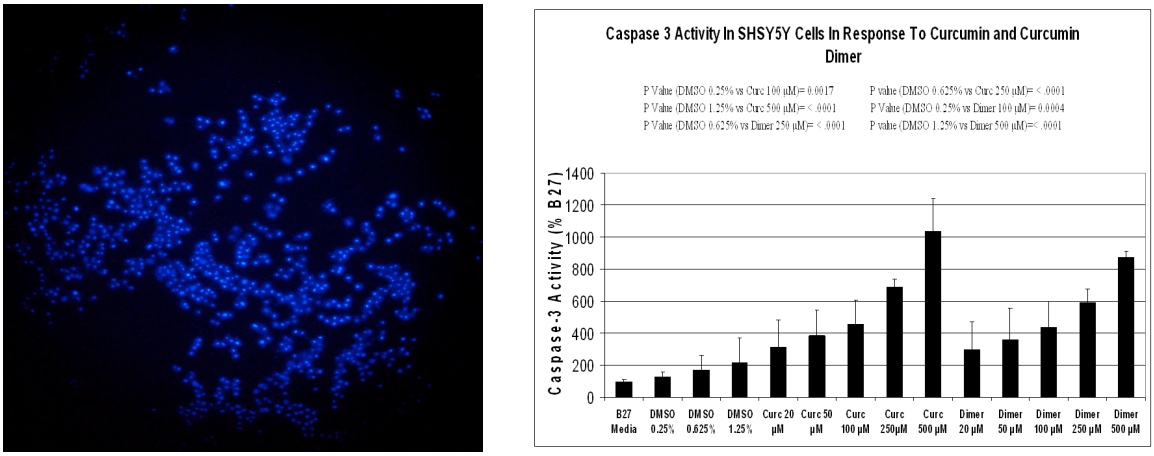

Figure 5.8. Caspase-3 activation assay of Curcumin mono-carboxylic acid **1a** and curcumin **1**.

3.5.2. Curcumin dendrimer Conjugate

3.5.2.1. Synthesis and Characterization of Dendrimer-curcumin conjugate.

In order to synthesize water soluble curcumin adduct, a generation 4 cystamine core Polyamidoamine dendrimer (from Dendritic Nanotechnologies [DNT]) was coupled to Curcumin monocarboxylic acid **1a** using EDC-HCl, HOBt in DMF to produce the conjugate **9**. The reaction mixture was added to excess MeOH-H_2O (1:1) followed by centrifugation. The supernatant liquid was evaporated and the resulting crude prodct was further purified by extensive dialysis (3500 MWCO dialysis membrane), 20% MeOH-H_20 was used for dialysis, the product was lyophilized. The curcumin-dendrimer conjugate **9** is freely soluble in water and the aqueous solution has the characteristic yellow color of curcumin (**Figure 5.9**). The conjugate was analyzed via ^{1}H NMR and FTIR. The NMR revealed that conjugation in deed proceeded as the appearance of aromatic peaks at δ= 7.16 –7.38 ppm. 20 % loading of the Curcumin mono-carboxylic acid was calculated from ^{1}H NMR spectra comparing with the intensity of Ar-H (δ = 7.22-7.62 ppm) from **1a** with the CH_2CO (δ =2.25 ppm) from the dendrimer. The FTIR spectra shows peaks at 1723 cm^{-1} and 748 cm^{-1} correspond to C=O and C=C-H stretching vibrations (R-CH=CH-CO-CH_2-CO-CH=CH-R from curcumin). The conjugate was also analyzed via FPLC using a Hi-Prep™ 26/10 size-exclusion column (GE Biosciences), 0.1 M Na_2CO_3 (pH = 9) was used as the running buffer, a peak which elutes at the same volume as the dendrimer with strong absorbance at 320 nm and 430 nm arising from curcumin was observed indicating that curcumin is for certain conjugated to the dendrimer. The possibility of non-covalent association of carboxylic acids with dendrimers was ruled out as in our case no curcumin mono-carboxylic acid **1a** was

released. Theoretically, any non-covalently associated carboxylic acid-dye would be released from the dendrimer in 0.1 (M) Na_2CO_3 solution (pH = 9) buffer due to ionization of the carboxylic acid.

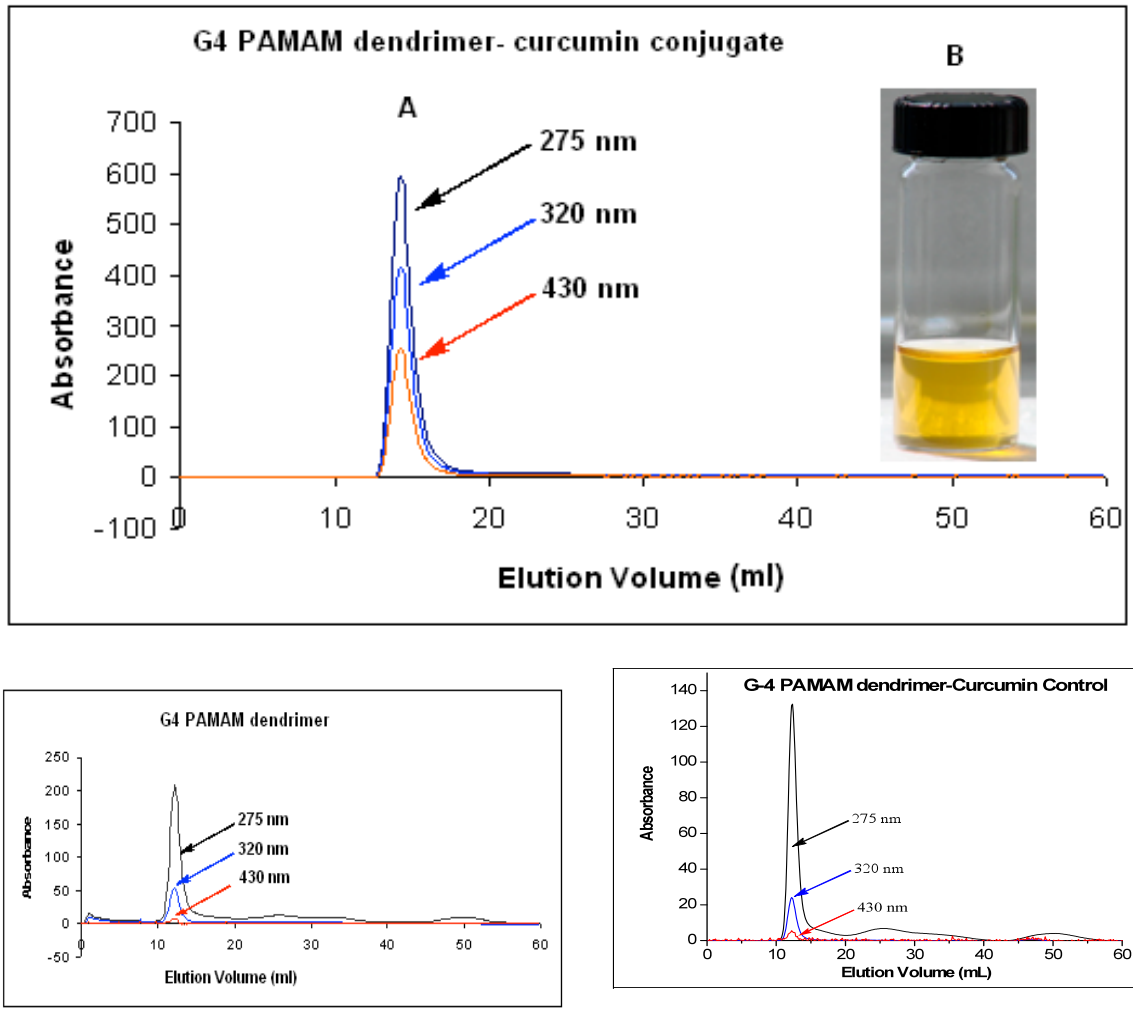

Figure 5.9. [Top] FPLC of G4 cystamine-core poly(amidoamine) dendrimer-curcumin conjugate sample **9**, using a Hi-Prep™ 26/10 desalting column, 0.1 M Na_2CO_3 solution (pH = 9) was used as the running buffer. [Bottom Left] FPLC of dendrimer (control). [Bottom Right] FPLC of control mixture of dendrimer and curcumin mono-carboxylic acid **1a**.

(Dolai, S.; Debnath, S.; Sun, C.; Fata, J. and Raja, K. unpublished data)

3.5.2.2. Solubility Comparison and Fluorescence Study.

To compare the solubility between curcumin **1** and dendrimer-curcumin conjugate **9** we have conducted a simple experiment. Both curcumin and dendrimer-curcumin conjugate were dissolved in DMSO and water and centrifuged. It is evident from the figure that only curcumin was insoluble in water whereas everything else were soluble in either water or DMSO.

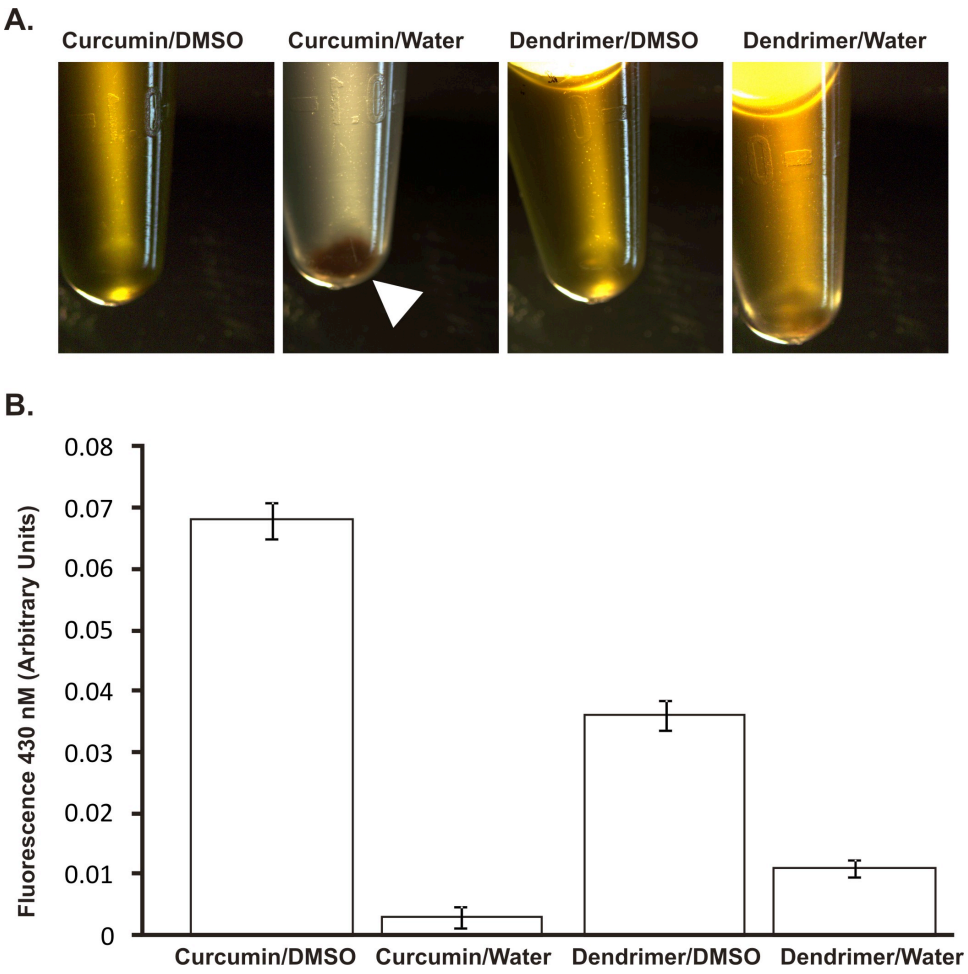

Figure 5.10. [Top] Pictures of curcumin and dendrimer-curcumin conjugates in different solvent media. [Bottom] Fluorescence intensity of curcumin and conjugate **9** in different systems.

(Dolai, S.; Debnath, S.; Sun, C.; Fata, J. and Raja, K. unpublished data).

3.5.2.3. Cell Uptake Study of Curcumin and Dendrimer-curcumin conjugate.

To investigate the possible uptake of curcumin and dendrimer-curcumin conjugate by cells, we incubated cultured BT549 cells with curcumin (dissolved in DMSO and water) and dendrimer-curcumin conjugate (in DMSO and water) for 40 mins. The pictures were captured using Zeiss Live Imager microscope under bright field and FITC. The above pictures showed that except curcumin in water everything else were taken up by the cells. Graphical representation of the fluorescence intensity showed the maximum value for cells treated with curcumin in DMSO followed by dendrimer-curcumin conjugate in DMSO and water. It could be misleading to our eyes form the above pictures that curcumin in DMSO penetrates the cells more compared to dendrimer-curcumin conjugate. To confirm that this effect is not really true we have performed a simple experiment where the fluorescence of these compounds in different media was measured (**Figure 5.10** bottom panel). It showed that curcumin dissolved in DMSO was itself highly fluorescent compared to dendrimer-curcumin conjugate in DMSO/water.

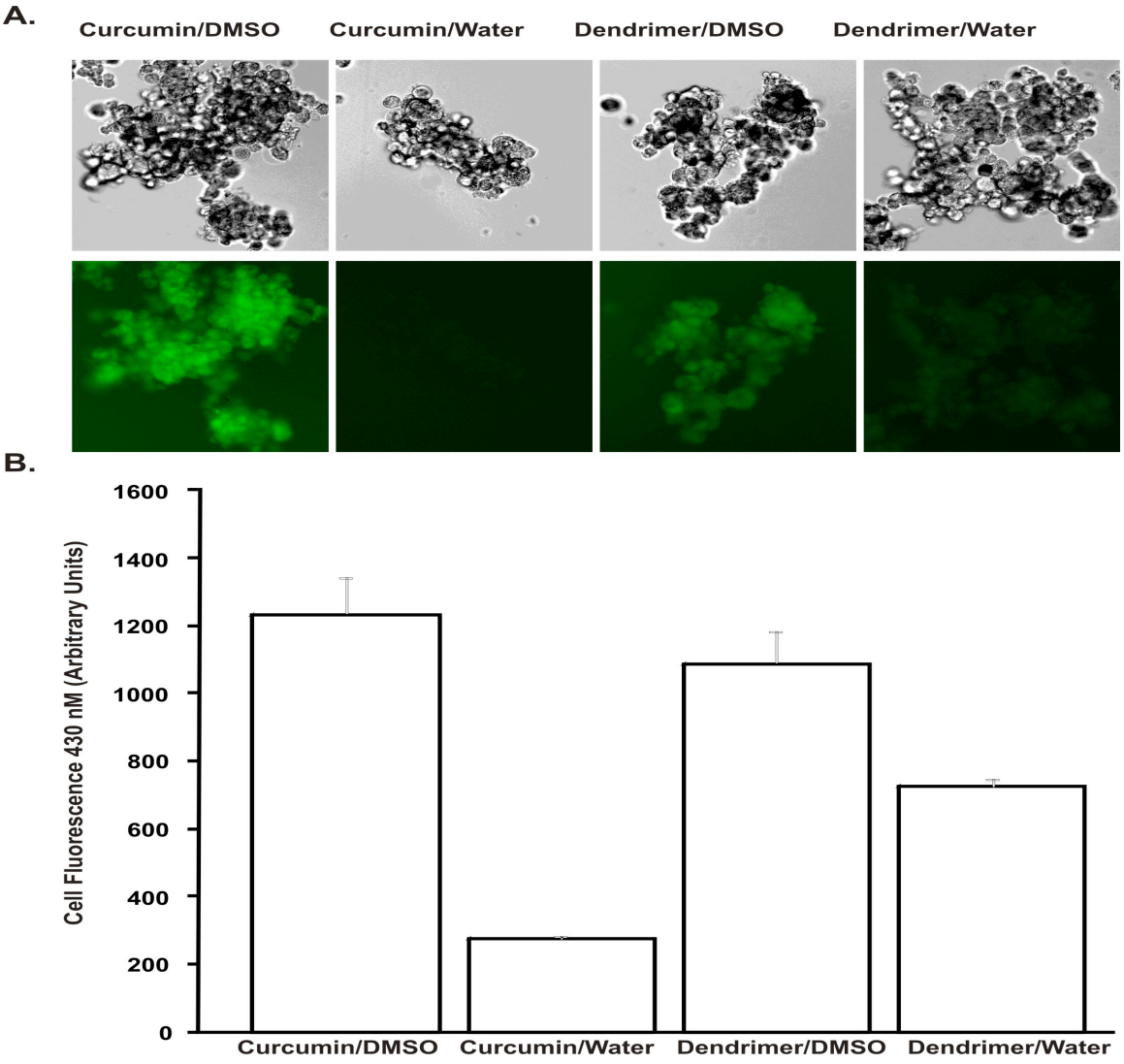

Figure 5.11. **A.** Uptake of curcumin and dendrimer-curcumin conjugate **9** by BT549 mammalian cancer cell line. Pictures were taken using bright field as well as FITC. **B.** Graphical interpretation of fluorescence intensity under different conditions.

(Dolai, S.; Debnath, S.; Sun, C.; Fata, J. and Raja, K. unpublished data)

3.5.2.4. Determination of IC_{50} value

The IC_{50} value of curcumin in DMSO was found to be 50 mM where as curcumin in water was completely ineffective to kill the cells. In case of dendrimer-curcumin conjugate in DMSO/water the IC_{50} value dropped to 20 mM, thus making it more potent anticancer drug candidate.

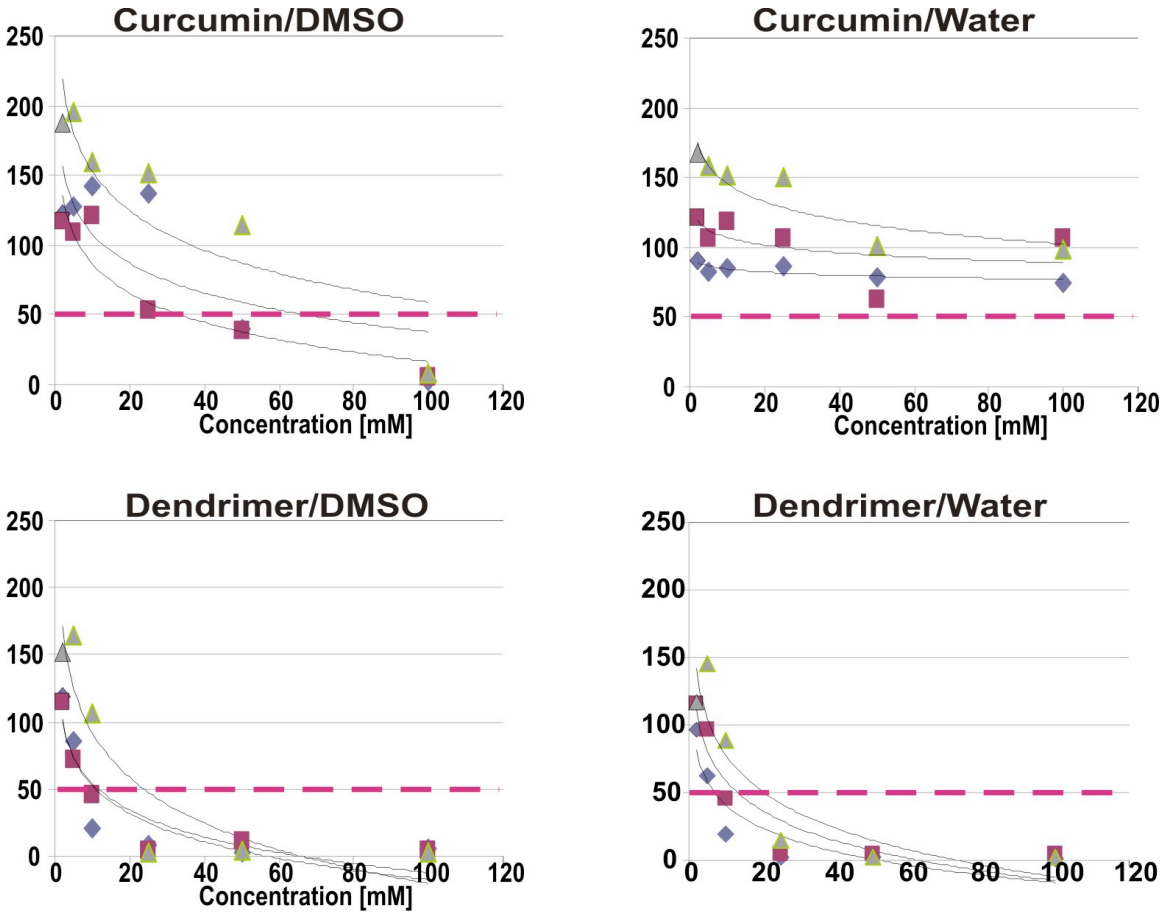

Figure 5.12. Mesurement of IC_{50} (Inhibitory Concentration 50%) using MTT assay.
(Dolai, S.; Debnath, S.; Sun, C.; Fata, J. and Raja, K. unpublished data)

3.5.2.5. Caspase-3 Activity Assay

Activation of Caspase-3 was detected using immuno-staining procedures. Except curcumin in water the other three show caspase-3 activation.

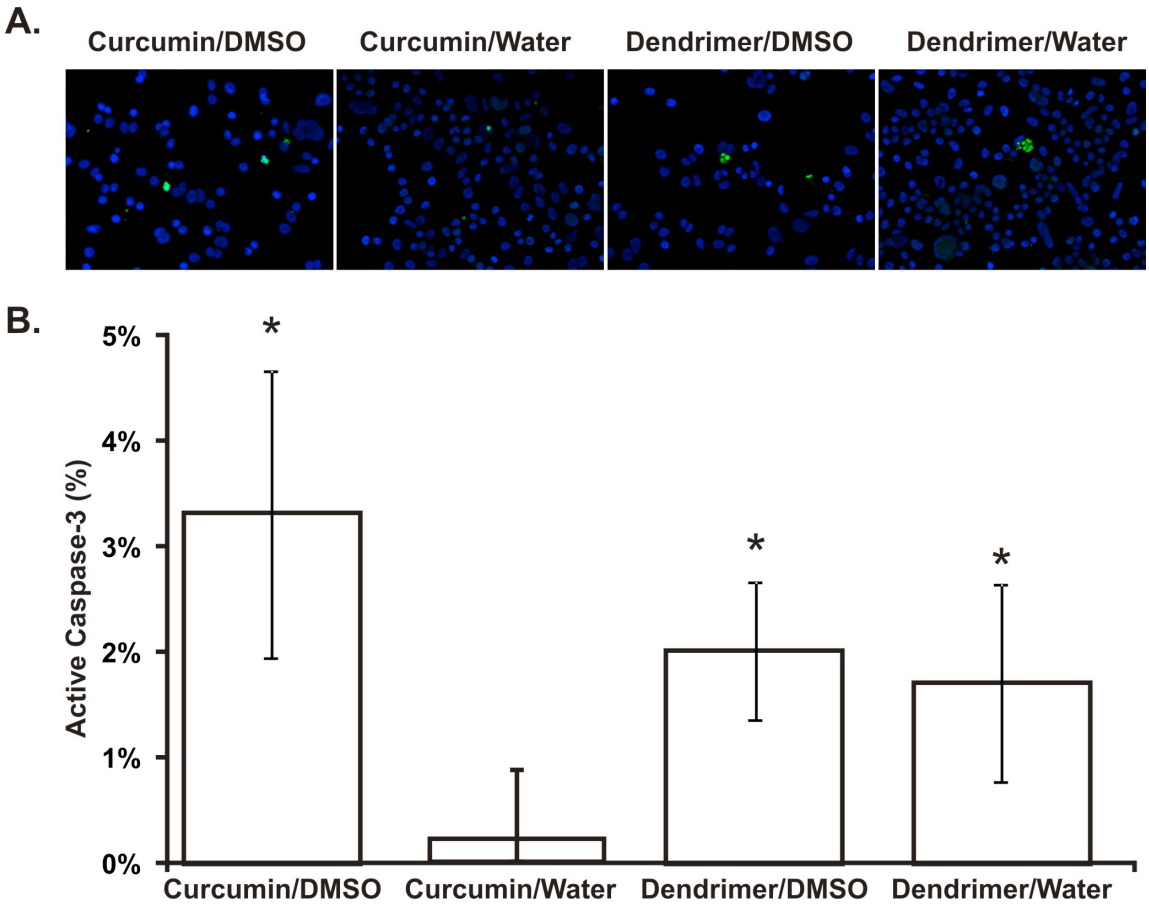

Figure 5.13. Inducing apoptosis by Caspase-3 activation in BT459 cells.
(Dolai, S.; Debnath, S.; Sun, C.; Fata, J. and Raja, K. unpublished data)

3.5.3. Curcumin Antibody Conjugate.

In order to make a targeted drug delivery vehicle we have conjugated curcumin to Antibody via NHS chemistry. Previously synthesized Curcumin mono-NHS **1c** was dissolved in DMSO and mixed with either Santa Cruz CD68 #sc-9139 or Mel-CAM #sc-28667 antibody following antibody: curcumin 1:100 mol/mol ratio and incubated with stirring for 4h at room temperature. Further the Antibody-curcumin adducts were tagged with DyLight fluors according to the procedure provided on DyLight™ Microscale Antibody Labeling Kit (Thermo Scientific, IL).

The formed adducts were applied in a caspase-3/7 activation assay following 24h incubation with GL261 glioblastoma cells or B16F10 melanoma cells. Compared to control CD68 treated cells, the Curcumin-CD68 treated cells showed a dramatic increase in caspase-3/7 activity (**Figure 5.14**).

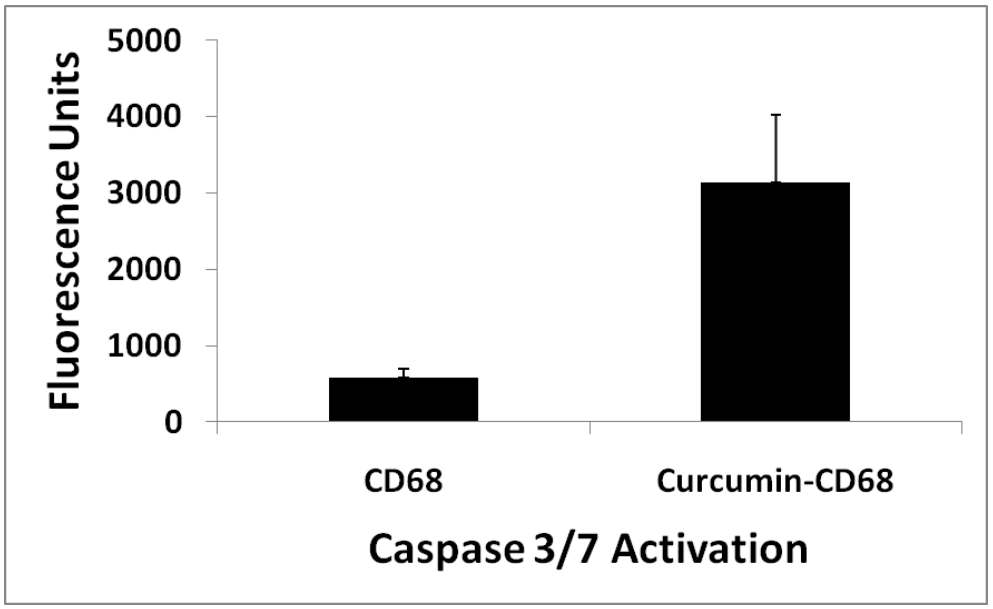

Figure 5.14. Arbitrary Fluorescence Units vs. Caspase 3/7 Activation in response to 24 h curcumin adduct or control treatment.

(Langone, P.; Curcio, G. M.; Dolai, S.; Raja, K. and Banerjee, P. unpublished data)

We have also determined the Inhibitory Concentration 50% (IC_{50}) values for the two curcumin-antibody adducts i.e. Curcumin-CD68 and Curcumin-Muc18 with respect to curcumin itself using GL261 glioblastoma cells and B16F10 melanoma cells respectively. From the fig. 5.15 it could be seen that curcumin eliminated B16F10 melanoma cells in micromolar range: IC_{50}=15μM; whereas curcumin-Muc18 conjugate eliminated the same cells in nanomolar range: IC_{50}=75 nM.

On the other hand in case of GL261 glioblastoma cells, free curcumin was found to be effective in the micromolar concentration IC_{50}=10 μM and antibody adduct Curcumin-CD68 was effective in nanomolar concentrations. Hence, it is evident that antibody-curcumin adducts are almost 1000 times more effective eliminating cancerous cells.

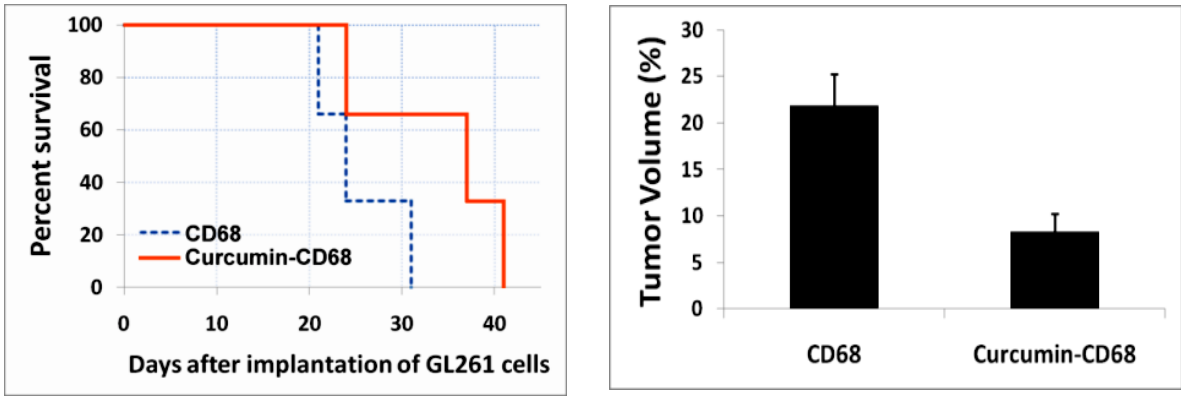

Figure 5.15. *In vivo* application of curcumin-antibody adduct. (Left) Survival chart for mice. (Right) Tumor volumes as a percent of total brain volume. The mean tumor volume difference for drug-treated vs. control mice is significant, p = 0.007924.

(Langone, P.; Curcio, G. M.; Dolai, S.; Raja, K. and Banerjee, P. unpublished data)

From the successful findings of *in vitro* studies we decided to move onto *in vivo* experiments. To do so, at first we have implanted the GL261 glioblastoma cells in the

mouse brain via intracranial implantation. It was found that the curcumin-CD68 antibody adduct not only causes a significant decrease in tumor size but also helps increase in survival of mice (**Figure 5.15**). It could be seen from the pictures of the mouse brain that ones treated with curcumin-CD68 conjugate were smaller in size and mice lived longer. The tumor volume decreased more than half the size of the original. The mice treated with curcumin-antibody lived almost 10 days longer than the control. We are currently working on the exact concentrations needed to completely destroy the tumor and giving the subjects a whole new life.

4. CONCLUSION

In conclusion, after the successful synthesis of mono-functional curcumin derivatives we embarked on the possible applications. Although the antioxidant efficiency of several derivatives were similar to that of curcumin, the freely water soluble curcumin sugar conjugate was found to be several times more antioxidant compared to curcumin. The curcumin sugar conjugate was ~1000 times more soluble in water compared to curcumin. The curcumin mono-carboxylic acid was able to stain and dissolute amyloid-beta plaques at a much lower concentrations compared to curcumin. In case of curcumin sugar conjugate, it was able to modulate the Aβ aggregation in nano molar concentrations compared to curcumin which is effective in micro-molar concentrations. The curcumin sugar conjugate was found to neuro-protective as well. The curcumin dimer which have the same numbers of free phenolic-OH as curcumin, was able to selectively destroy human neurotumor cells. The dendrimer-curcumin conjugate displaying curcumin in a polyvalent display was freely soluble in water and was effective towards BT459 mammalian cancer cells in nano molar concentrations. Towards the synthesis of targeted drug delivery module for curcumin, the synthesis of Antibody-curcumin adduct showed a great promise in destroying GL261 glioblastoma cells as well as B16F10 melanoma cells in nano molar concentrations compared to curcumin which is effective in micromolar concentrations. The in vivo studies indicated that mice treated with antibody-curcumin conjugate not only causes a significant decrease in tumor size but also helps increase in survival of mice.

5. SPECTRAL CHARACTERIZATION DATA (^{1}H NMR, ^{13}C NMR, FT-IR)

^{1}H NMR of compound **9**

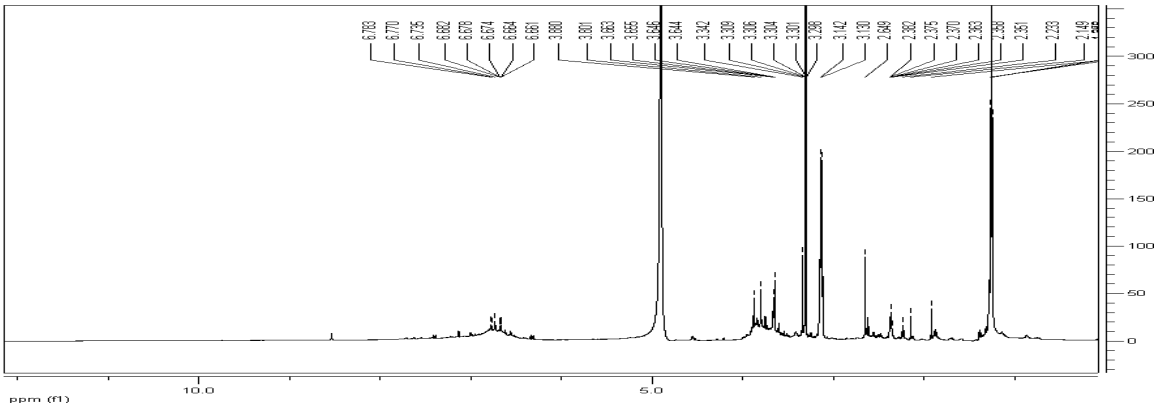

^{13}C NMR of compound **9**

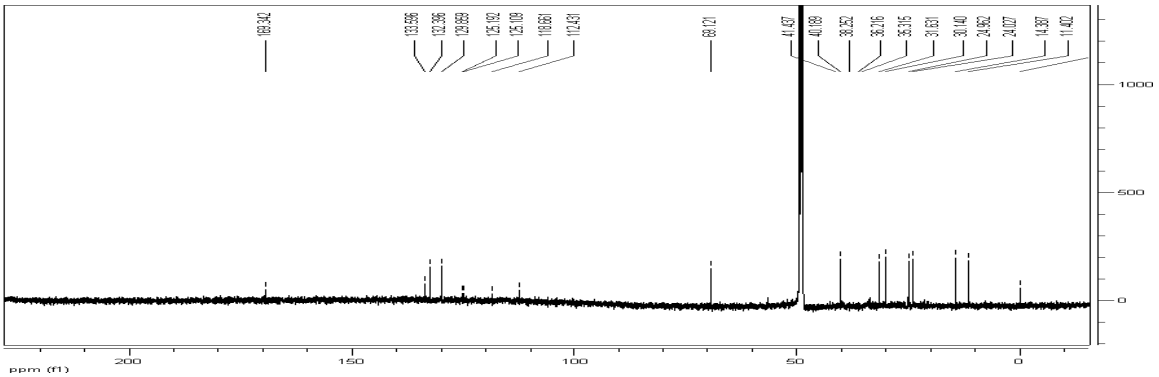

FT-IR of compound **9**

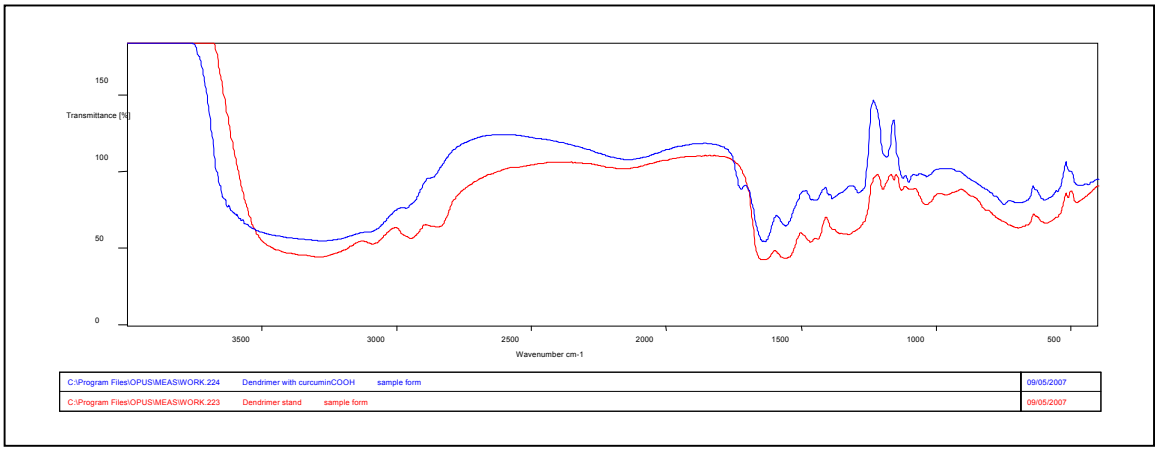

Dendrimer (red line) and Dendrimer-Curcumin conjugate **9** (blue line).

6. REFERENCES

(1) Chattopadhyay, I., Biswas, K., Bandyopadhyay, U., and Banerjee, R. K. (2004) Turmeric and curcumin: Biological actions and medicinal applications. *Current Science 87*, 44-53.

(2) Aggarwal, B. B., and Shishodia, S. (2006) Molecular targets of dietary agents for prevention and therapy of cancer. *Biochem Pharmacol 71*, 1397-421.

(3) Leyon, P. V., and Kuttan, G. (2003) Studies on the role of some synthetic curcuminoid derivatives in the inhibition of tumour specific angiogenesis. *J Exp Clin Cancer Res 22*, 77-83.

(4) Nurfinal, A. N., Reksohadiprodjo, M. S., Timmerman, H., Jenie, U. A., Sugiyant, D., and van der Goot, H. (1997) Synthesis of some symmetrical curcumin derivatives and their antiinflammatory activity. *European Journal of Medicinal Chemistry 32*, 321-328.

(5) Yang, F., Lim, G. P., Begum, A. N., Ubeda, O. J., Simmons, M. R., Ambegaokar, S. S., Chen, P. P., Kayed, R., Glabe, C. G., Frautschy, S. A., and Cole, G. M. (2005) Curcumin inhibits formation of amyloid beta oligomers and fibrils, binds plaques, and reduces amyloid in vivo. *J Biol Chem 280*, 5892-901.

(6) Mazumder, A., Neamati, N., Sunder, S., Schulz, J., Pertz, H., Eich, E., and Pommier, Y. (1997) Curcumin Analogs with Altered Potencies against HIV-1 Integrase as Probes for Biochemical Mechanisms of Drug Action. *Journal of Medicinal Chemistry 40*, 3057-3063.

(7) Cheng, A. L., Hsu, C. H., Lin, J. K., Hsu, M. M., Ho, Y. F., Shen, T. S., Ko, J. Y., Lin, J. T., Lin, B. R., Ming-Shiang, W., Yu, H. S., Jee, S. H., Chen, G. S., Chen,

T. M., Chen, C. A., Lai, M. K., Pu, Y. S., Pan, M. H., Wang, Y. J., Tsai, C. C., and Hsieh, C. Y. (2001) Phase I clinical trial of curcumin, a chemopreventive agent, in patients with high-risk or pre-malignant lesions. *Anticancer Res 21*, 2895-900.

(8) Folkman, J., Hahnfeldt, P., and Hlatky, L. (2000) Cancer: looking outside the genome. *Nat Rev Mol Cell Biol 1*, 76-9.

(9) Soto, A. M., and Sonnenschein, C. (2004) The somatic mutation theory of cancer: growing problems with the paradigm? *Bioessays 26*, 1097-107.

(10) Gibbs, W. W. (2003) Untangling the roots of cancer. *Sci Am 289*, 56-65.

(11) Prehn, R. T. (1994) Cancers beget mutations versus mutations beget cancers. *Cancer Res 54*, 5296-300.

(12) Vogelstein, B., and Kinzler, K. W. (2004) Cancer genes and the pathways they control. *Nature Medicine 10*, 789-799.

(13) Garcea, G., Berry, D. P., Jones, D. J. L., Singh, R., Dennison, A. R., Farmer, P. B., Sharma, R. A., Steward, W. P., and Gescher, A. J. (2005) Consumption of the Putative Chemopreventive Agent Curcumin by Cancer Patients: Assessment of Curcumin Levels in the Colorectum and their Pharmacodynamic Consequences. *Cancer Epidemiology, Biomarkers & Prevention 14*, 120-125.

(14) Lopez-Lazaro, M. (2008) Anticancer and carcinogenic properties of curcumin: considerations for its clinical development as a cancer chemopreventive and chemotherapeutic agent. *Molecular nutrition & food research 52*, S103-S127.

(15) Hanahan, D., and Weinberg, R. A. (2000) The hallmarks of cancer. *Cell 100*, 57-70.

(16) Samaha, H. S., Kelloff, G. J., Steele, V., Rao, V., and Reddy, B. S. (1997) Modulation of apoptosis by sulindac, curcumin, phenylethyl-3-methylcaffeate and 6-phenylhexyl isothiocyanate: apoptotic index as a biomarker in colon cancer chemoprevention and promotion. *Cancer Research 57*, 1301-1305.

(17) Volate, S. R., Davenport, D. M., Muga, S. J., and Wargovich, M. J. (2005) Modulation of aberrant crypt foci and apoptosis by dietary herbal supplements (quercetin, curcumin, silymarin, ginseng and rutin). *Carcinogenesis 26*, 1450-6.

(18) Li, L., Braiteh, F. S., and Kurzrock, R. (2005) Liposome-encapsulated curcumin: in vitro and in vivo effects on proliferation, apoptosis, signaling, and angiogenesis. *Cancer 104*, 1322-31.

(19) Li, L., Ahmed, B., Mehta, K., and Kurzrock, R. (2007) Liposomal curcumin with and without oxaliplatin: effects on cell growth, apoptosis, and angiogenesis in colorectal cancer. *Molecular Cancer Therapeutics 6*, 1276-1282.

(20) Karin, M. (2006) Nuclear factor-kappaB in cancer development and progression. *Nature 441*, 431-6.

(21) Chuang, S. E., Cheng, A. L., Lin, J. K., and Kuo, M. L. (2000) Inhibition by curcumin of diethylnitrosamine-induced hepatic hyperplasia, inflammation, cellular gene products and cell-cycle-related proteins in rats. *Food Chem Toxicol 38*, 991-5.

(22) Leclercq, I. A., Farrell, G. C., Sempoux, C., dela Pena, A., and Horsmans, Y. (2004) Curcumin inhibits NF-kappaB activation and reduces the severity of experimental steatohepatitis in mice. *J Hepatol 41*, 926-34.

(23) Klaunig, J. E., and Kamendulis, L. M. (2004) The role of oxidative stress in carcinogenesis. *Annu Rev Pharmacol Toxicol 44*, 239-67.

(24) Lopez-Lazaro, M. (2007) Excessive superoxide anion generation plays a key role in carcinogenesis. *Int J Cancer 120*, 1378-80.

(25) Lopez-Lazaro, M. (2007) Dual role of hydrogen peroxide in cancer: possible relevance to cancer chemoprevention and therapy. *Cancer Lett 252*, 1-8.

(26) Kratz, F., Muller, I. A., Ryppa, C., and Warnecke, A. (2008) Prodrug strategies in anticancer chemotherapy. *ChemMedChem 3*, 20-53.

(27) Panchal, R. G. (1998) Novel therapeutic strategies to selectively kill cancer cells. *Biochem Pharmacol 55*, 247-52.

(28) Zangemeister-Wittke, U. (2005) Antibodies for targeted cancer therapy -- technical aspects and clinical perspectives. *Pathobiology 72*, 279-86.

(29) Wu, A. M., and Senter, P. D. (2005) Arming antibodies: prospects and challenges for immunoconjugates. *Nat Biotechnol 23*, 1137-46.

(30) Ricart, A. D., and Tolcher, A. W. (2007) Technology insight: cytotoxic drug immunoconjugates for cancer therapy. *Nat Clin Pract Oncol 4*, 245-55.

(31) Senter, P. D. (2009) Potent antibody drug conjugates for cancer therapy. *Curr Opin Chem Biol 13*, 235-44.

(32) Carter, P. J., and Senter, P. D. (2008) Antibody-drug conjugates for cancer therapy. *Cancer J 14*, 154-69.

(33) Tomalia, D. A. (2003) *Handbook of Nanoscience, Engineering and Technology*, CRC Press, Boca Raton, FL.

(34) Tomalia, D. A., Huang, B., Swanson, D. R., Brothers, H. M., and Klimash, J. W. (2003) Structure control within poly(amidoamine) dendrimers: size, shape and regio-chemical mimicry of globular proteins. *Tetrahedron Letters 59*, 3799-3813.

(35) Zhang, C., and Tomalia, D. A. (2001) *Dendrimers and Other Dendritic Polymers*, Wiley, Chichester.

(36) Brothers, H. M., Piehler, L. T., and Tomalia, D. A. (1998) Slab-gel and capillary electrophoretic characterization of polyamidoamine dendrimers. *Journal of Chromatography, A 814*, 233-248.

(37) Esfand, R., and Tomalia, D. A. (2001) Poly(amidoamine) (PAMAM) dendrimers: from biomimicry to drug delivery and biomedical applications. *Drug Discovery Today 6*, 427-436.

(38) Tomalia, D. A., Brothers, H. M., 2nd, Piehler, L. T., Durst, H. D., and Swanson, D. R. (2002) Partial shell-filled core-shell tecto(dendrimers): a strategy to surface differentiated nano-clefts and cusps. *Proc Natl Acad Sci U S A 99*, 5081-7.

(39) Tomalia, D. A., Naylor, A. M., and Goddard, W. A., III. (1990) Starburst dendrimers: control of size, shape, surface chemistry, topology and flexibility in the conversion of atoms to macroscopic materials. *Angewandte Chemie, International Edition 102*, 119-157.

(40) Hecht, S., and Frechet, J. M. J. (2001) Dendritic encapsulation of function: applying nature's site isolation principle from biomimetics to materials science. *Angewandte Chemie, International Edition 40*, 74-91.

(41) Piotti, M. E., Rivera, F., Jr., Bond, R., Hawker, C. J., and Frechet, J. M. J. (1999) Synthesis and Catalytic Activity of Unimolecular Dendritic Reverse Micelles with

"Internal" Functional Groups. *Journal of the American Chemical Society 121*, 9471-9472.

(42) Tomalia, D. A., and Frechet, J. M. (2005) Introduction to "Dendrimers and dendritic polymers". *Progress in Polymer Science 30*, 217-219.

(43) Adronov, A., and Frechet, J. M. J. (2000) Light-harvesting dendrimers. *Chemical Communications 18*, 1701-1710.

(44) Jensen, A. W., Maru, B. S., Zhang, X., Mohanty, D. K., Fahlman, B. D., Swanson, D. R., and Tomalia, D. A. (2005) Preparation of fullerene-shell dendrimer-core nanoconjugates. *Nano Lett 5*, 1171-3.

(45) DeMattei, C. R., Huang, B., and Tomalia, D. A. (2004) Designed Dendrimer Syntheses by Self-Assembly of Single-Site, ssDNA Functionalized Dendrons. *Nano Letters 4*, 771-777.

(46) Kubasiak, L. A., and Tomalia, D. A. *Polymeric Gene Delivery Principles and Applications*, CRC Press, Boca Raton.

(47) Kim, T.-I., Seo, H. J., Choi, J. S., Jang, H.-S., Baek, J., Kim, K., and Park, J.-S. (2004) PAMAM-PEG-PAMAM: novel triblock copolymer as a biocompatible and efficient gene delivery carrier. *Biomacromolecules 5*, 2487-2492.

(48) Singh, P. (2001) *Dendrimers and Dendritic Polymers.*, Wiley, Chichester.

(49) Singh, P., Moll, F., III, Lin, S. H., and Ferzli, C. (1996) Starburst dendrimers: A novel matrix for multifunctional reagents in immunoassays. *Clinical Chemistry 42*, 1567-1569.

(50) Jiang, Y.-H., Emau, P., Cairns, J. S., Flanary, L., Morton, W. R., McCarthy, T. D., and Tsai, C.-C. (2005) SPL7013 gel as a topical microbicide for prevention of

vaginal transmission of SHIV89.6P in macaques. *AIDS Research and Human Retroviruses 21*, 207-213.

(51) Ihara, N., Schmitz, S., Kurisawa, M., Chung, J. E., Uyama, H., and Kobayashi, S. (2004) Amplification of inhibitory activity of catechin against disease-related enzymes by conjugation on poly(epsilon-lysine). *Biomacromolecules 5*, 1633-6.

(52) Ariga, T., and Hamano, M. (1990) Antioxidative properties of proanthocyanidins. Part II. radical scavenging action and its mode in procyanidins B-1 and B-3 from Azuki beans to peroxyl radicals. *Agricultural and Biological Chemistry 54*, 2499-2504.

(53) Saito, M., Hosoyama, H., Ariga, T., Kataoka, S., and Yamaji, N. (1998) Antiulcer Activity of Grape Seed Extract and Procyanidins. *Journal of Agricultural and Food Chemistry 46*, 1460-1464.

(54) Hagerman, A. E., Riedl, K. M., Jones, G. A., Sovik, K. N., Ritchard, N. T., Hartzfeld, P. W., and Riechel, T. L. (1998) High molecular weight plant polyphenolics (tannins) as biological antioxidants. *Journal of Agricultural and Food Chemistry 46*, 1887-1892.

(55) Puchtler, H., Sweat, F., and Levine, M. (1962) The binding of Congo red by amyloid. *Journal of Histochemistry and Cytochemistry 10*, 355-364.

BIBLIOGRAPHY

Chapter I

(1) Jatzkewitz, H. (1954) The incorporation of a physiologically active substance in a colloid blood plasma substitute. I. Incorporation of a mescaline-peptide into poly(vinylpyrrolidinone) (PVP). *Physiologische Chemie 297*, 149-156.

(2) Jatzkewitz, H. (1955) A peptamine (glycyl-L-leucylmescaline) bound to a colloidal blood plasma substitute (polyvinylpyrrolidone) as a new type of depot for a biologically active primary amine (mescaline). *Zeitschrift fuer Naturforschung 10*, 27-31.

(3) Abuchowski, A., Van Es, T., Palczuk, N. C., and Davis, F. F. (1977) Alteration of immunological properties of bovine serum albumin by covalent attachment of polyethylene glycol. *Journal of Biological Chemistry 252*, 3578-3581.

(4) Abuchowski, A., McCoy, J. R., Palczuk, N. C., van Es, T., and Davis, F. F. (1977) Effect of covalent attachment of polyethylene glycol on immunogenicity and circulating life of bovine liver catalase. *J Biol Chem 252*, 3582-6.

(5) Maeda, H., Takeshita, J., and Kanamaru, R. (1979) A lipophilic derivative of neocarzinostatin. A polymer conjugation of an antitumor protein antibiotic. *Int J Pept Protein Res 14*, 81-7.

(6) Maeda, H., Ueda, M., Morinaga, T., and Matsumoto, T. (1985) Conjugation of poly(styrene-co-maleic acid) derivatives to the antitumor protein neocarzinostatin: pronounced improvements in pharmacological properties. *J Med Chem 28*, 455-61.

(7) Matsumura, Y., and Maeda, H. (1986) A new concept for macromolecular therapeutics in cancer chemotherapy: mechanism of tumoritropic accumulation of proteins and the antitumor agent smancs. *Cancer Res 46*, 6387-92.

(8) Spach, G. R., Leonard; Loucheux, Marie H.; Parrod, Jacques. (1969) Synthesis of block copolymers in which one block is a polypeptide. *Journal of Polymer Science, Polymer Symposia 16*, 4705-4712.

(9) Reibel, L., Spach, G., and Dufour, C. (1973) Physicochemical study of trisequence copolymers, poly(gamma-benzyl-L-glutamate)-poly(ethylene oxide)-poly(gamma-benzyl-L-glutamate). Role of polydispersity in the determination of conformation of the molecules in dilute solution. *Biopolymers 12*, 2391-2408.

(10) Perly, B., Douy, A., and Gallot, B. (1974) Synthesis of the polybutadiene-poly(benzyl-L-glutamate) sequential copolymers and structural study of their mesophases. *Comptes Rendus des Seances de l'Academie des Sciences, Serie C: Sciences Chimiques 279*, 1109-1111.

(11) Perly, B., Douy, A., and Gallot, B. (1976) Block copolymers polybutadiene/poly(benzyl-L-glutamate) and polybutadiene/poly(N5-hydroxypropylglutamine). Preparation and structural study by x-ray and electron microscopy. *Makromolekulare Chemie 177*, 2569-2589.

(12) Yamashita, Y., Iwaya, Y., and Ito, K. (1975) Block copolymerization. 9. Polymerization of the NCA [N-carboxy anhydride] of methyl D-glutamate by telechelic polystyrene having glycyl groups as active chain ends. *Makromolekulare Chemie 176*, 1207-1216.

(13) Klok, H.-A. (2009) Peptide/Protein-Synthetic Polymer Conjugates: Quo Vadis. *Macromolecules 42*, 7990-8000.

(14) Deming, T. J. (1997) Polypeptide materials. New synthetic methods and applications. *Advanced Materials 9*, 299-311.

(15) Deming, T. J. (2000) Living polymerization of α-amino acid-N-carboxyanhydrides. *Journal of Polymer Science, Part A: Polymer Chemistry 38*, 3011-3018.

(16) Deming, T. J. (2006) Polypeptide and polypeptide hybrid copolymer synthesis via NCA polymerization. *Advances in Polymer Science 202*, 1-18.

(17) Kricheldorf, H. R. (2006) Polypeptides and 100 years of chemistry of α-amino acid N-carboxyanhydrides. *Angewandte Chemie, International Edition 45*, 5752-5784.

(18) Agut, W., Taton, D., and Lecommandoux, S. (2007) A Versatile Synthetic Approach to Polypeptide Based Rod-Coil Block Copolymers by Click Chemistry. *Macromolecules 40*, 5653-5661.

(19) Schatz, C., Louguet, S., Le Meins, J.-F., and Lecommandoux, S. (2009) Polysaccharide-block-polypeptide copolymer vesicles: towards synthetic viral capsids. *Angewandte Chemie, International Edition 48*, 2572-2575.

(20) Wang, K., Liang, L., Lin, S., and He, X. (2008) Synthesis of well-defined ABC triblock copolymers with polypeptide segments by ATRP and click reactions. *European Polymer Journal 44*, 3370-3376.

(21) Steig, S., Cornelius, F., Witte, P., Staal, B. B. P., Koning, C. E., Heise, A., and Menzel, H. (2005) Synthesis of polypeptide based rod-coil block copolymers. *Chemical Communications 43*, 5420-5422.

(22) Steig, S., Cornelius, F., Heise, A., Knoop, R. J. I., Habraken, G. J. M., Koning, C. E., and Menzel, H. (2007) Synthesis of rod-coil block copolymers using two controlled polymerization techniques. *Macromolecular Symposia 248*, 199-206.

(23) Knoop, R. J. I., Habraken, G. J. M., Gogibus, N., Steig, S., Menzel, H., Koning, C. E., and Heise, A. (2008) Synthesis of poly(benzyl glutamate-b-styrene) rod-coil block copolymers by dual initiation in one pot. *Journal of Polymer Science, Part A: Polymer Chemistry 46*, 3068-3077.

(24) Deming, T. J. (1997) Facile synthesis of block copolypeptides of defined architecture. *Nature 390*, 368-389.

(25) Deming, T. J. (1999) Cobalt and Iron Initiators for the Controlled Polymerization of α-Amino Acid-N-Carboxyanhydrides. *Macromolecules 32*, 4500-4502.

(26) Peng, Y.-L., Lai, S.-L., and Lin, C.-C. (2008) Preparation of Polypeptide via Living Polymerization of Z-Lys-NCA Initiated by Platinum Complexes. *Macromolecules 41*, 3455-3459.

(27) Fields, G. B., and Noble, R. L. (1990) Solid-phase peptide synthesis utilizing 9-fluorenylmethoxycarbonyl amino acids. *International Journal of Peptide & Protein Research 35*, 161-214.

(28) Chan, W. C., and White, P. D. (2000) *Fmoc Solid Phase Peptide Synthesis - A Practical Approach.*, Oxford University Press, New York.

(29) Gauthier, M. A., and Klok, H.-A. (2008) Peptide/protein-polymer conjugates: synthetic strategies and design concepts. *Chemical Communications 23*, 2591-2611.

(30) Parrish, B., Breitenkamp, R. B., and Emrick, T. (2005) PEG- and peptide-grafted aliphatic polyesters by click chemistry. *J Am Chem Soc 127*, 7404-10.

(31) Dirks, A. J., Van Berkel, S. S., Hatzakis, N. S., Opsteen, J. A., Van Delft, F. L., Cornelissen, J. J. L. M., Rowan, A. E., Van Hest, J. C. M., Rutjes, F. P. J. T., and Nolte, R. J. M. (2005) Preparation of biohybrid amphiphiles via the copper catalyzed Huisgen [3+2] dipolar cycloaddition reaction. *Chemical Communications 33*, 4172-4174.

(32) Lutz, J.-F., Boerner, H. G., and Weichenhan, K. (2006) Combining ATRP and "Click" Chemistry: a Promising Platform toward Functional Biocompatible Polymers and Polymer Bioconjugates. *Macromolecules 39*, 6376-6383.

(33) Lutz, J.-F., Boerner, H. G., and Weichenhan, K. (2007) Click Bioconjugation of a Well-Defined Synthetic Polymer and a Protein Transduction Domain. *Australian Journal of Chemistry 60*, 410-413.

(34) Shi, W., Dolai, S., Averick, S., Fernando, S. S., Saltos, J. A., L'Amoreaux, W., Banerjee, P., and Raja, K. (2009) A General Methodology Toward Drug/Dye Incorporated Living Copolymer-Protein Hybrids: (NIRF Dye-Glucose) Copolymer-Avidin/BSA Conjugates as Prototypes. *Bioconjug Chem*.

(35) Rosler, A., Klok, H. A., Hamley, I. W., Castelletto, V., and Mykhaylyk, O. O. (2003) Nanoscale structure of poly(ethylene glycol) hybrid block copolymers

containing amphiphilic beta-strand peptide sequences. *Biomacromolecules 4*, 859-63.

(36) Hentschel, J., Krause, E., and Borner, H. G. (2006) Switch-peptides to trigger the peptide guided assembly of poly(ethylene oxide)-peptide conjugates into tape structures. *J Am Chem Soc 128*, 7722-3.

(37) Burkoth, T. S., Benzinger, T. L. S., Jones, D. N. M., Hallenga, K., Meredith, S. C., and Lynn, D. G. (1998) C-Terminal PEG blocks the irreversible step in β-amyloid(10-35) fibrillogenesis. *Journal of the American Chemical Society 120*, 7655-7656.

(38) Burkoth, T. S., Benzinger, T. L. S., Urban, V., Lynn, D. G., Meredith, S. C., and Thiyagarajan, P. (1999) Self-Assembly of Aβ(10-35)-PEG Block Copolymer Fibrils. *Journal of the American Chemical Society 121*, 7429-7430.

(39) Becker, M. L., Liu, J., and Wooley, K. L. (2003) Peptide-polymer bioconjugates: hybrid block copolymers generated via living radical polymerizations from resin-supported peptides. *Chemical Communications 2*, 180-181.

(40) Mei, Y., Beers, K. L., Byrd, H. C., VanderHart, D. L., and Washburn, N. R. (2004) Solid-phase ATRP synthesis of peptide-polymer hybrids. *J Am Chem Soc 126*, 3472-6.

(41) Becker, M. L., Liu, J., and Wooley, K. L. (2005) Functionalized micellar assemblies prepared via block copolymers synthesized by living free radical polymerization upon peptide-loaded resins. *Biomacromolecules 6*, 220-8.

(42) Ding, H., Kopeckova, P., and Kopecek, J. (2007) Self-association properties of HPMA copolymers containing an amphipathic heptapeptide. *J Drug Target 15*, 465-74.

(43) Kasuya, Y., Lu, Z. R., Kopeckova, P., Minko, T., Tabibi, S. E., and Kopecek, J. (2001) Synthesis and characterization of HPMA copolymer-aminopropylgeldanamycin conjugates. *J Control Release 74*, 203-11.

(44) Maynard, H. D., Okada, S. Y., and Grubbs, R. H. (2000) Synthesis of Norbornenyl Polymers with Bioactive Oligopeptides by Ring-Opening Metathesis Polymerization. *Macromolecules 33*, 6239-6248.

(45) Breitenkamp, R. B., Ou, Z., Breitenkamp, K., Muthukumar, M., and Emrick, T. (2007) Synthesis and Characterization of Polyolefin-graft-oligopeptide Polyelectrolytes. *Macromolecules 40*, 7617-7624.

(46) Biagini, S. C. G., and Parry, A. L. (2007) Investigation into the ROMP copolymerization of peptide- and PEG-functionalized norbornene derivatives. *Journal of Polymer Science, Part A: Polymer Chemistry 45*, 3178-3190.

(47) Fernandez-Trillo, F., Dureault, A., Bayley, J. P. M., van Hest, J. C. M., Thies, J. C., Michon, T., Weberskirch, R., and Cameron, N. R. (2007) Elastin-Based Side-Chain Polymers: Improved Synthesis via RAFT and Stimulus Responsive Behavior. *Macromolecules 40*, 6094-6099.

(48) Ayres, L., Vos, M. R. J., Adams, P. J. H. M., Shklyarevskiy, I. O., and Van Hest, J. C. M. (2003) Elastin-Based Side-Chain Polymers Synthesized by ATRP. *Macromolecules 36*, 5967-5973.

(49) van Hest, J. C. M., and Tirrell, D. A. (2001) Protein-based materials, toward a new level of structural control. *Chemical Communications 19*, 1897-1904.

(50) Bailon, P., and Won, C.-Y. (2009) PEG-modified biopharmaceuticals. *Expert Opinion on Drug Delivery 6*, 1-16.

(51) Roberts, M. J., Bentley, M. D., and Harris, J. M. (2002) Chemistry for peptide and protein PEGylation. *Adv Drug Deliv Rev 54*, 459-76.

(52) Osada, K., and Kataoka, K. (2002) Drug and gene delivery based on supramolecular assembly of PEG-polypeptide hybrid block copolymers. *Advances in Polymer Science 202*, 113-153.

(53) Yokoyama, M., Kwon, G. S., Okano, T., Sakurai, Y., Seto, T., and Kataoka, K. (1992) Preparation of micelle-forming polymer-drug conjugates. *Bioconjugate Chemistry 3*, 295-301.

(54) Mitra, A., Nan, A., Papadimitriou, J. C., Ghandehari, H., and Line, B. R. (2006) Polymer-peptide conjugates for angiogenesis targeted tumor radiotherapy. *Nucl Med Biol 33*, 43-52.

(55) Rothenfluh, D. A., Bermudez, H., O'Neil, C. P., and Hubbell, J. A. (2008) Biofunctional polymer nanoparticles for intra-articular targeting and retention in cartilage. *Nat Mater 7*, 248-54.

(56) Lee, H., Jeong, J. H., and Park, T. G. (2001) A new gene delivery formulation of polyethylenimine/DNA complexes coated with PEG conjugated fusogenic peptide. *J Control Release 76*, 183-92.

(57) Kwon, E. J., Bergen, J. M., and Pun, S. H. (2008) Application of an HIV gp41-derived peptide for enhanced intracellular trafficking of synthetic gene and siRNA delivery vehicles. *Bioconjug Chem 19*, 920-7.

(58) Rathore, O., and Sogah, D. Y. (2001) Nanostructure Formation through β-Sheet Self-Assembly in Silk-Based Materials. *Macromolecules 34*, 1477-1486.

(59) Rathore, O., and Sogah, D. Y. (2001) Self-assembly of beta-sheets into nanostructures by poly(alanine) segments incorporated in multiblock copolymers inspired by spider silk. *J Am Chem Soc 123*, 5231-9.

(60) Hentschel, J., and Borner, H. G. (2009) Blendable peptide-polymer nanofibers to modulate mechanical properties of polymers. *Macromol Biosci 9*, 187-94.

(61) Wang, C., Stewart, R. J., and Kopecek, J. (1999) Hybrid hydrogels assembled from synthetic polymers and coiled-coil protein domains. *Nature 397*, 417-20.

(62) Yang, J., Xu, C., Kopeckova, P., and Kopecek, J. (2006) Hybrid hydrogels self-assembled from HPMA copolymers containing peptide grafts. *Macromol Biosci 6*, 201-9.

(63) Yang, J., Xu, C., Wang, C., and Kopecek, J. (2006) Refolding Hydrogels Self-Assembled from N-(2-Hydroxypropyl)methacrylamide Graft . *Biomacromolecules 7*, 1187-1195.

(64) Wu, K., Yang, J., Konak, C., Kopeckova, P., and Kopecek, J. (2008) Novel synthesis of HPMA copolymers containing peptide grafts and their self-assembly into hybrid hydrogels. *Macromolecular Chemistry and Physics 209*, 467-475.

(65) Jing, P., Rudra, J. S., Herr, A. B., and Collier, J. H. (2008) Self-assembling peptide-polymer hydrogels designed from the coiled coil region of fibrin. *Biomacromolecules 9*, 2438-46.

(66) Tzokova, N., Fernyhough, C. M., Topham, P. D., Sandon, N., Adams, D. J., Butler, M. F., Armes, S. P., and Ryan, A. J. (2009) Soft hydrogels from nanotubes of poly(ethylene oxide)-tetraphenylalanine conjugates prepared by click chemistry. *Langmuir 25*, 2479-85.

(67) Lutolf, M. P., Raeber, G. P., Zisch, A. H., Tirelli, N., and Hubbell, J. A. (2003) Cell-responsive synthetic hydrogels. *Advanced Materials 15*, 888-892.

(68) Lutolf, M. P., Weber, F. E., Schmoekel, H. G., Schense, J. C., Kohler, T., Muller, R., and Hubbell, J. A. (2003) Repair of bone defects using synthetic mimetics of collagenous extracellular matrices. *Nat Biotechnol 21*, 513-8.

(69) Wang, C., Kopecek, J., and Stewart, R. J. (2001) Hybrid hydrogels cross-linked by genetically engineered coiled-coil block proteins. *Biomacromolecules 2*, 912-20.

(70) Rizzi, S. C., and Hubbell, J. A. (2005) Recombinant protein-co-PEG networks as cell-adhesive and proteolytically degradable hydrogel matrixes. Part I: Development and physicochemical characteristics. *Biomacromolecules 6*, 1226-38.

(71) Rizzi, S. C., Ehrbar, M., Halstenberg, S., Raeber, G. P., Schmoekel, H. G., Hagenmuller, H., Muller, R., Weber, F. E., and Hubbell, J. A. (2006) Recombinant protein-co-PEG networks as cell-adhesive and proteolytically

degradable hydrogel matrixes. Part II: biofunctional characteristics. *Biomacromolecules 7*, 3019-29.

(72) Murphy, W. L., Dillmore, W. S., Modica, J., and Mrksich, M. (2007) Dynamic hydrogels: translating a protein conformational change into macroscopic motion. *Angew Chem Int Ed Engl 46*, 3066-9.

(73) Sui, Z., King, W. J., and Murphy, W. L. (2007) Dynamic materials based on a protein conformational change. *Advanced Materials 19*, 3377-3380.

(74) Sui, Z., King, W. J., and Murphy, W. L. (2008) Protein-based hydrogels with tunable dynamic responses. *Advanced Functional Materials 18*, 1824-1831.

(75) Yuan, W., Yang, J., Kopeckova, P., and Kopecek, J. (2008) Smart hydrogels containing adenylate kinase: translating substrate recognition into macroscopic motion. *J Am Chem Soc 130*, 15760-1.

(76) Kasparova, P., Antonietti, M., and Coelfen, H. (2004) Double hydrophilic block copolymers with switchable secondary structure as additives for crystallization control. *Colloids and Surfaces, A: Physicochemical and Engineering Aspects 250*, 153-162.

(77) Guo, X.-H., Yu, S.-H., and Cai, G.-B. (2006) Crystallization in a mixture of solvents by using a crystal modifier: morphology control in the synthesis of highly monodisperse CaCO3 microspheres. *Angewandte Chemie, International Edition 45*, 3977-3981.

(78) Guo, X.-H., Xu, A.-W., and Yu, S.-H. (2008) Crystallization of Calcium Carbonate Mineral with Hierarchical Structures in DMF Solution under Control of Poly(ethylene glycol)-b-poly(L-glutamic acid): Effects of Crystallization

Temperature and Polymer Concentration. *Crystal Growth & Design 8*, 1233-1242.

(79) Kessel, S., and Boerner, H. G. (2008) High rate silicification of peptide-polymer assemblies toward composite nanotapes. *Macromolecular Rapid Communications 29*, 419-424.

(80) Chen, G., and Hoffman, A. S. (1993) Preparation and properties of thermoreversible, phase-separating enzyme-oligo(N-isopropylacrylamide) conjugates. *Bioconjug Chem 4*, 509-14.

(81) Stayton, P. S., Shimoboji, T., Long, C., Chilkoti, A., Chen, G., Harris, J. M., and Hoffman, A. S. (1995) Control of protein-ligand recognition using a stimuli-responsive polymer. *Nature 378*, 472-4.

(82) Pennadam, S. S., Lavigne, M. D., Dutta, C. F., Firman, K., Mernagh, D., Gorecki, D. C., and Alexander, C. (2004) Control of a multisubunit DNA motor by a thermoresponsive polymer switch. *J Am Chem Soc 126*, 13208-9.

(83) De, P., Li, M., Gondi, S. R., and Sumerlin, B. S. (2008) Temperature-regulated activity of responsive polymer-protein conjugates prepared by grafting-from via RAFT polymerization. *J Am Chem Soc 130*, 11288-9.

(84) Raja, K. S., Wang, Q., Gonzalez, M. J., Manchester, M., Johnson, J. E., and Finn, M. G. (2003) Hybrid virus-polymer materials. 1. Synthesis and properties of PEG-decorated cowpea mosaic virus. *Biomacromolecules 4*, 472-6.

(85) Cheng, X., Ming, X., and Croyle, M. A. (2003) PEGylated adenoviruses for gene delivery to the intestinal epithelium by the oral route. *Pharm Res 20*, 1444-51.

(86) Ogawara, K., Rots, M. G., Kok, R. J., Moorlag, H. E., Van Loenen, A. M., Meijer, D. K., Haisma, H. J., and Molema, G. (2004) A novel strategy to modify adenovirus tropism and enhance transgene delivery to activated vascular endothelial cells in vitro and in vivo. *Hum Gene Ther 15*, 433-43.

(87) Fisher, K. D., Stallwood, Y., Green, N. K., Ulbrich, K., Mautner, V., and Seymour, L. W. (2001) Polymer-coated adenovirus permits efficient retargeting and evades neutralising antibodies. *Gene Ther 8*, 341-8.

(88) Green, N. K., Herbert, C. W., Hale, S. J., Hale, A. B., Mautner, V., Harkins, R., Hermiston, T., Ulbrich, K., Fisher, K. D., and Seymour, L. W. (2004) Extended plasma circulation time and decreased toxicity of polymer-coated adenovirus. *Gene Ther 11*, 1256-63.

(89) Kochendoerfer, G. G. (2005) Site-specific polymer modification of therapeutic proteins. *Curr Opin Chem Biol 9*, 555-60.

(90) Gaberc-Porekar, V., Zore, I., Podobnik, B., and Menart, V. (2008) Obstacles and pitfalls in the PEGylation of therapeutic proteins. *Curr Opin Drug Discov Devel 11*, 242-50.

(91) Filpula, D., and Zhao, H. (2008) Releasable PEGylation of proteins with customized linkers. *Adv Drug Deliv Rev 60*, 29-49.

(92) Shechter, Y., Mironchik, M., Rubinraut, S., Tsubery, H., Sasson, K., Marcus, Y., and Fridkin, M. (2008) Reversible pegylation of insulin facilitates its prolonged action in vivo. *Eur J Pharm Biopharm 70*, 19-28.

(93) Duncan, R., Gilbert, H. R., Carbajo, R. J., and Vicent, M. J. (2008) Polymer masked-unmasked protein therapy. 1. Bioresponsive dextrin-trypsin and -

melanocyte stimulating hormone conjugates designed for alpha-amylase activation. *Biomacromolecules 9*, 1146-54.

(94) M. G. Savage (1992) *Avidin-Biotin Chemistry: A Handbook*, *Pierce Chemical company*, *Rockford, Illinois*.

(95) Daehne, S., Resch-Genger, U., and Wolfbeis, O. S. (1998) *Near-Infrared Dyes for High Technology Applications*, Vol. 52, Kluwer Academic, Dordrecht.

(96) Michalet, X., Pinaud, F. F., Bentolila, L. A., Tsay, J. M., Doose, S., Li, J. J., Sundaresan, G., Wu, A. M., Gambhir, S. S., and Weiss, S. (2005) Quantum dots for live cells, in vivo imaging, and diagnostics. *Science 307*, 538-44.

(97) Dubertret, B., Skourides, P., Norris, D. J., Noireaux, V., Brivanlou, A. H., and Libchaber, A. (2002) In vivo imaging of quantum dots encapsulated in phospholipid micelles. *Science 298*, 1759-62.

(98) So, M. K., Xu, C., Loening, A. M., Gambhir, S. S., and Rao, J. (2006) Self-illuminating quantum dot conjugates for in vivo imaging. *Nat Biotechnol 24*, 339-43.

(99) Ballou, B., Lagerholm, B. C., Ernst, L. A., Bruchez, M. P., and Waggoner, A. S. (2004) Noninvasive imaging of quantum dots in mice. *Bioconjug Chem 15*, 79-86.

(100) Bhaumik, S., and Gambhir, S. S. (2002) Optical imaging of Renilla luciferase reporter gene expression in living mice. *Proc Natl Acad Sci U S A 99*, 377-82.

(101) Contag, C. H., and Bachmann, M. H. (2002) Advances in in vivo bioluminescence imaging of gene expression. *Annu Rev Biomed Eng 4*, 235-60.

(102) Cheng, Z., Levi, J., Xiong, Z., Gheysens, O., Keren, S., Chen, X., and Gambhir, S. S. (2006) Near-infrared fluorescent deoxyglucose analogue for tumor optical imaging in cell culture and living mice. *Bioconjug Chem 17*, 662-9.

(103) Weissleder, R., Tung, C. H., Mahmood, U., and Bogdanov, A., Jr. (1999) In vivo imaging of tumors with protease-activated near-infrared fluorescent probes. *Nat Biotechnol 17*, 375-8.

(104) Becker, A., Hessenius, C., Licha, K., Ebert, B., Sukowski, U., Semmler, W., Wiedenmann, B., and Grotzinger, C. (2001) Receptor-targeted optical imaging of tumors with near-infrared fluorescent ligands. *Nat Biotechnol 19*, 327-31.

(105) Hilderbrand, S. A., Kelly, K. A., Weissleder, R., and Tung, C. H. (2005) Monofunctional near-infrared fluorochromes for imaging applications. *Bioconjug Chem 16*, 1275-81.

(106) Lin, Y., Weissleder, R., and Tung, C. H. (2002) Novel near-infrared cyanine fluorochromes: synthesis, properties, and bioconjugation. *Bioconjug Chem 13*, 605-10.

(107) Mader, O., Reiner, K., Egelhaaf, H. J., Fischer, R., and Brock, R. (2004) Structure property analysis of pentamethine indocyanine dyes: identification of a new dye for life science applications. *Bioconjug Chem 15*, 70-8.

(108) Zhao, W., and Carreira, E. M. (2006) Conformationally restricted aza-BODIPY: highly fluorescent, stable near-infrared absorbing dyes. *Chemistry- A European Journal 12*, 7254-63.

(109) Liu, J., Diwu, Z., Leung, W.-Y., Lu, Y., Patch, B., and Haugland, R. P. (2003) Rational design and synthesis of a novel class of highly fluorescent rhodamine

dyes that have strong absorption at long wavelengths. *Tetrahedron Letters 44*, 4355-4359.

(110) Bandichhor, R., Petrescu, A. D., Vespa, A., Kier, A. B., Schroeder, F., and Burgess, K. (2006) Synthesis of a new water-soluble rhodamine derivative and application to protein labeling and intracellular imaging. *Bioconjug Chem 17*, 1219-25.

(111) Jose, J., and Burgess, K. (2006) Benzophenoxazine-based fluorescent dyes for labeling biomolecules. *Tetrahedron Letters 62*, 11021-11037.

(112) Patonay, G., Salon, J., Sowell, J., and Strekowski, L. (2004) Noncovalent labeling of biomolecules with red and near- infrared dyes. *Molecules 9*, 40-9.

(113) Tung, C. H. (2004) Fluorescent peptide probes for in vivo diagnostic imaging. *Biopolymers 76*, 391-403.

(114) Zaheer, A., Lenkinski, R. E., Mahmood, A., Jones, A. G., Cantley, L. C., and Frangioni, J. V. (2001) In vivo near-infrared fluorescence imaging of osteoblastic activity. *Nat Biotechnol 19*, 1148-54.

(115) Anand, P., Kunnumakkara, A. B., Newman, R. A., and Aggarwal, B. B. (2007) Bioavailability of curcumin: problems and promises. *Mol Pharm 4*, 807-18.

(116) Chattopadhyay, I., Biswas, K., Bandyopadhyay, U., and Banerjee, R. K. (2004) Turmeric and curcumin: Biological actions and medicinal applications. *Current Science 87*, 44-53.

(117) Aggarwal, B. B., Kumar, A., and Bharti, A. C. (2003) Anticancer potential of curcumin: preclinical and clinical studies. *Anticancer Res 23*, 363-98.

(118) Sharma, O. P. (1976) Antioxidant activity of curcumin and related compounds. *Biochem Pharmacol 25*, 1811-2.

(119) Ruby, A. J., Kuttan, G., Babu, K. D., Rajasekharan, K. N., and Kuttan, R. (1995) Anti-tumour and antioxidant activity of natural curcuminoids. *Cancer Lett 94*, 79-83.

(120) Sugiyama, Y., Kawakishi, S., and Osawa, T. (1996) Involvement of the beta-diketone moiety in the antioxidative mechanism of tetrahydrocurcumin. *Biochem Pharmacol 52*, 519-25.

(121) Srimal, R. C., and Dhawan, B. N. (1973) Pharmacology of diferuloyl methane (curcumin), a non-steroidal anti-inflammatory agent. *J Pharm Pharmacol 25*, 447-52.

(122) Jordan, W. C., and Drew, C. R. (1996) Curcumin--a natural herb with anti-HIV activity. *J Natl Med Assoc 88*, 333.

(123) Mahady, G. B., Pendland, S. L., Yun, G., and Lu, Z. Z. (2002) Turmeric (Curcuma longa) and curcumin inhibit the growth of Helicobacter pylori, a group 1 carcinogen. *Anticancer Res 22*, 4179-81.

(124) Kim, M. K., Choi, G. J., and Lee, H. S. (2003) Fungicidal property of Curcuma longa L. rhizome-derived curcumin against phytopathogenic fungi in a greenhouse. *J Agric Food Chem 51*, 1578-81.

(125) Reddy, R. C., Vatsala, P. G., Keshamouni, V. G., Padmanaban, G., and Rangarajan, P. N. (2005) Curcumin for malaria therapy. *Biochem Biophys Res Commun 326*, 472-4.

(126) Kuttan, R., Bhanumathy, P., Nirmala, K., and George, M. C. (1985) Potential anticancer activity of turmeric (Curcuma longa). *Cancer Lett 29*, 197-202.

(127) Kiso, Y., Suzuki, Y., Watanabe, N., Oshima, Y., and Hikino, H. (1983) Antihepatotoxic principles of Curcuma longa rhizomes. *Planta Med 49*, 185-7.

(128) Venkatesan, N. (1998) Curcumin attenuation of acute adriamycin myocardial toxicity in rats. *Br J Pharmacol 124*, 425-7.

(129) Venkatesan, N., Punithavathi, D., and Arumugam, V. (2000) Curcumin prevents adriamycin nephrotoxicity in rats. *Br J Pharmacol 129*, 231-4.

(130) Srivastava, R., Dikshit, M., Srimal, R. C., and Dhawan, B. N. (1985) Anti-thrombotic effect of curcumin. *Thromb Res 40*, 413-7.

(131) Dikshit, M., Rastogi, L., Shukla, R., and Srimal, R. C. (1995) Prevention ofischaemia-induced biochemical changes by curcumin & quinidine in the cat heart. *Indian J. Med. Res. 101*, 31-35.

(132) Nirmala, C., and Puvanakrishnan, R. (1996) Protective role of curcumin against isoproterenol induced myocardial infarction in rats. *Mol Cell Biochem 159*, 85-93.

(133) Nirmala, C., and Puvanakrishnan, R. (1996) Effect of curcumin on certain lysosomal hydrolases in isoproterenol-induced myocardial infarction in rats. *Biochem Pharmacol 51*, 47-51.

(134) Srinivasan, M. (1972) Effect of curcumin on blood sugar as seen in a diabetic subject. *Indian J. Med. Sci. 26*, 269-270.

(135) Babu, P. S., and Srinivasan, K. (1995) Influence of dietary curcumin and cholesterol on the progression of experimentally induced diabetes in albino rat. *Mol Cell Biochem 152*, 13-21.

(136) Babu, P. S., and Srinivasan, K. (1997) Hypolipidemic action of curcumin, the active principle of turmeric (Curcuma longa) in streptozotocin induced diabetic rats. *Mol Cell Biochem 166*, 169-75.

(137) Arun, N., and Nalini, N. (2002) Efficacy of turmeric on blood sugar and polyol pathway in diabetic albino rats. *Plant Foods Hum Nutr 57*, 41-52.

(138) Deodhar, S. D., Sethi, R., and Srimal, R. C. (1980) Preliminary study on antirheumatic activity of curcumin (diferuloyl methane). *Indian J Med Res 71*, 632-4.

(139) Shankar, T. N., Shantha, N. V., Ramesh, H. P., Murthy, I. A., and Murthy, V. S. (1980) Toxicity studies on turmeric (Curcuma longa): acute toxicity studies in rats, guineapigs & monkeys. *Indian J Exp Biol 18*, 73-5.

(140) Qureshi, S., Shah, A. H., and Ageel, A. M. (1992) Toxicity studies on Alpinia galanga and Curcuma longa. *Planta Med 58*, 124-7.

(141) Lao, C. D., Demierre, M. F., and Sondak, V. K. (2006) Targeting events in melanoma carcinogenesis for the prevention of melanoma. *Expert Rev Anticancer Ther 6*, 1559-68.

(142) Lao, C. D., Ruffin, M. T. t., Normolle, D., Heath, D. D., Murray, S. I., Bailey, J. M., Boggs, M. E., Crowell, J., Rock, C. L., and Brenner, D. E. (2006) Dose escalation of a curcuminoid formulation. *BMC Complement Altern Med 6*, 10.

(143) Cheng, A. L., Hsu, C. H., Lin, J. K., Hsu, M. M., Ho, Y. F., Shen, T. S., Ko, J. Y., Lin, J. T., Lin, B. R., Ming-Shiang, W., Yu, H. S., Jee, S. H., Chen, G. S., Chen, T. M., Chen, C. A., Lai, M. K., Pu, Y. S., Pan, M. H., Wang, Y. J., Tsai, C. C., and Hsieh, C. Y. (2001) Phase I clinical trial of curcumin, a chemopreventive

agent, in patients with high-risk or pre-malignant lesions. *Anticancer Res 21*, 2895-900.

(144) Shoba, G., Joy, D., Joseph, T., Majeed, M., Rajendran, R., and Srinivas, P. S. (1998) Influence of piperine on the pharmacokinetics of curcumin in animals and human volunteers. *Planta Med 64*, 353-6.

(145) Wahlstrom, B., and Blennow, G. (1978) A study on the fate of curcumin in the rat. *Acta Pharmacol Toxicol (Copenh) 43*, 86-92.

(146) Ravindranath, V., and Chandrasekhara, N. (1980) Absorption and tissue distribution of curcumin in rats. *Toxicology 16*, 259-65.

(147) Ravindranath, V., and Chandrasekhara, N. (1981) Metabolism of curcumin--studies with [3H]curcumin. *Toxicology 22*, 337-44.

(148) Pan, M. H., Huang, T. M., and Lin, J. K. (1999) Biotransformation of curcumin through reduction and glucuronidation in mice. *Drug Metab Dispos 27*, 486-94.

(149) Perkins, S., Verschoyle, R. D., Hill, K., Parveen, I., Threadgill, M. D., Sharma, R. A., Williams, M. L., Steward, W. P., and Gescher, A. J. (2002) Chemopreventive efficacy and pharmacokinetics of curcumin in the min/+ mouse, a model of familial adenomatous polyposis. *Cancer Epidemiol Biomarkers Prev 11*, 535-40.

(150) Sharma, R. A., Euden, S. A., Platton, S. L., Cooke, D. N., Shafayat, A., Hewitt, H. R., Marczylo, T. H., Morgan, B., Hemingway, D., Plummer, S. M., Pirmohamed, M., Gescher, A. J., and Steward, W. P. (2004) Phase I clinical trial of oral curcumin: biomarkers of systemic activity and compliance. *Clin Cancer Res 10*, 6847-54.

(151) Yang, K. Y., Lin, L. C., Tseng, T. Y., Wang, S. C., and Tsai, T. H. (2007) Oral bioavailability of curcumin in rat and the herbal analysis from Curcuma longa by LC-MS/MS. *J Chromatogr B Analyt Technol Biomed Life Sci 853*, 183-9.

(152) Marczylo, T. H., Verschoyle, R. D., Cooke, D. N., Morazzoni, P., Steward, W. P., and Gescher, A. J. (2007) Comparison of systemic availability of curcumin with that of curcumin formulated with phosphatidylcholine. *Cancer Chemother Pharmacol 60*, 171-7.

(153) Holder, G. M., Plummer, J. L., and Ryan, A. J. (1978) The metabolism and excretion of curcumin (1,7-bis-(4-hydroxy-3-methoxyphenyl)-1,6-heptadiene-3,5-dione) in the rat. *Xenobiotica 8*, 761-8.

(154) Sharma, R. A., McLelland, H. R., Hill, K. A., Ireson, C. R., Euden, S. A., Manson, M. M., Pirmohamed, M., Marnett, L. J., Gescher, A. J., and Steward, W. P. (2001) Pharmacodynamic and pharmacokinetic study of oral Curcuma extract in patients with colorectal cancer. *Clin Cancer Res 7*, 1894-900.

(155) Garcea, G., Jones, D. J., Singh, R., Dennison, A. R., Farmer, P. B., Sharma, R. A., Steward, W. P., Gescher, A. J., and Berry, D. P. (2004) Detection of curcumin and its metabolites in hepatic tissue and portal blood of patients following oral administration. *Br J Cancer 90*, 1011-5.

(156) Hoehle, S. I., Pfeiffer, E., Solyom, A. M., and Metzler, M. (2006) Metabolism of curcuminoids in tissue slices and subcellular fractions from rat liver. *J Agric Food Chem 54*, 756-64.

(157) Ireson, C., Orr, S., Jones, D. J., Verschoyle, R., Lim, C. K., Luo, J. L., Howells, L., Plummer, S., Jukes, R., Williams, M., Steward, W. P., and Gescher, A. (2001)

Characterization of metabolites of the chemopreventive agent curcumin in human and rat hepatocytes and in the rat in vivo, and evaluation of their ability to inhibit phorbol ester-induced prostaglandin E2 production. *Cancer Res 61*, 1058-64.

(158) Sandur, S. K., Pandey, M. K., Sung, B., Ahn, K. S., Murakami, A., Sethi, G., Limtrakul, P., Badmaev, V., and Aggarwal, B. B. (2007) Curcumin, demethoxycurcumin, bisdemethoxycurcumin, tetrahydrocurcumin and turmerones differentially regulate anti-inflammatory and anti-proliferative responses through a ROS-independent mechanism. *Carcinogenesis 28*, 1765-73.

(159) Pfeiffer, E., Hoehle, S. I., Walch, S. G., Riess, A., Solyom, A. M., and Metzler, M. (2007) Curcuminoids form reactive glucuronides in vitro. *J Agric Food Chem 55*, 538-44.

(160) Kim, J. M., Araki, S., Kim, D. J., Park, C. B., Takasuka, N., Baba-Toriyama, H., Ota, T., Nir, Z., Khachik, F., Shimidzu, N., Tanaka, Y., Osawa, T., Uraji, T., Murakoshi, M., Nishino, H., and Tsuda, H. (1998) Chemopreventive effects of carotenoids and curcumins on mouse colon carcinogenesis after 1,2-dimethylhydrazine initiation. *Carcinogenesis 19*, 81-5.

(161) Okada, K., Wangpoengtrakul, C., Tanaka, T., Toyokuni, S., Uchida, K., and Osawa, T. (2001) Curcumin and especially tetrahydrocurcumin ameliorate oxidative stress-induced renal injury in mice. *J Nutr 131*, 2090-5.

(162) Naito, M., Wu, X., Nomura, H., Kodama, M., Kato, Y., and Osawa, T. (2002) The protective effects of tetrahydrocurcumin on oxidative stress in cholesterol-fed rabbits. *J Atheroscler Thromb 9*, 243-50.

(163) Pari, L., and Amali, D. R. (2005) Protective role of tetrahydrocurcumin (THC) an active principle of turmeric on chloroquine induced hepatotoxicity in rats. *J Pharm Pharm Sci 8*, 115-23.

(164) Murugan, P., and Pari, L. (2006) Effect of tetrahydrocurcumin on plasma antioxidants in streptozotocin-nicotinamide experimental diabetes. *J Basic Clin Physiol Pharmacol 17*, 231-44.

(165) Ryu, E. K., Choe, Y. S., Lee, K. H., Choi, Y., and Kim, B. T. (2006) Curcumin and dehydrozingerone derivatives: synthesis, radiolabeling, and evaluation for beta-amyloid plaque imaging. *J Med Chem 49*, 6111-9.

(166) Cruz-Correa, M., Shoskes, D. A., Sanchez, P., Zhao, R., Hylind, L. M., Wexner, S. D., and Giardiello, F. M. (2006) Combination treatment with curcumin and quercetin of adenomas in familial adenomatous polyposis. *Clin Gastroenterol Hepatol 4*, 1035-8.

(167) Verma, S. P., Salamone, E., and Goldin, B. (1997) Curcumin and genistein, plant natural products, show synergistic inhibitory effects on the growth of human breast cancer MCF-7 cells induced by estrogenic pesticides. *Biochem Biophys Res Commun 233*, 692-6.

(168) Fang, J. Y., Hung, C. F., Chiu, H. C., Wang, J. J., and Chan, T. F. (2003) Efficacy and irritancy of enhancers on the in-vitro and in-vivo percutaneous absorption of curcumin. *J Pharm Pharmacol 55*, 1175.

(169) Balasubramanian, S., and Eckert, R. L. (2004) Green tea polyphenol and curcumin inversely regulate human involucrin promoter activity via opposing

effects on CCAAT/enhancer-binding protein function. *J Biol Chem 279*, 24007-14.

(170) Bisht, S., Feldmann, G., Soni, S., Ravi, R., Karikar, C., and Maitra, A. (2007) Polymeric nanoparticle-encapsulated curcumin ("nanocurcumin"): a novel strategy for human cancer therapy. *J Nanobiotechnology 5*, 3.

(171) Tiyaboonchai, W., Tungpradit, W., and Plianbangchang, P. (2007) Formulation and characterization of curcuminoids loaded solid lipid nanoparticles. *Int J Pharm 337*, 299-306.

(172) Li, L., Ahmed, B., Mehta, K., and Kurzrock, R. (2007) Liposomal curcumin with and without oxaliplatin: effects on cell growth, apoptosis, and angiogenesis in colorectal cancer. *Mol Cancer Ther 6*, 1276-82.

(173) Kunwar, A., Barik, A., Pandey, R., and Priyadarsini, K. I. (2006) Transport of liposomal and albumin loaded curcumin to living cells: an absorption and fluorescence spectroscopic study. *Biochim Biophys Acta 1760*, 1513-20.

(174) Suresh, D., and Srinivasan, K. (2007) Studies on the in vitro absorption of spice principles--curcumin, capsaicin and piperine in rat intestines. *Food Chem Toxicol 45*, 1437-42.

(175) Ma, Z., Shayeganpour, A., Brocks, D. R., Lavasanifar, A., and Samuel, J. (2007) High-performance liquid chromatography analysis of curcumin in rat plasma: application to pharmacokinetics of polymeric micellar formulation of curcumin. *Biomed Chromatogr 21*, 546-52.

(176) Gatti, G., and Perucca, E. (1994) Plasma concentrations of free and conjugated silybin after oral intake of a silybin-phosphatidylcholine complex (silipide) in healthy volunteers. *Int J Clin Pharmacol Ther 32*, 614-7.

(177) Kimura, T., Takeda, K., Kageyu, A., Toda, M., Kurosaki, Y., and Nakayama, T. (1989) Intestinal absorption of dolichol from emulsions and liposomes in rats. *Chem Pharm Bull (Tokyo) 37*, 463-6.

(178) Liu, A., Lou, H., Zhao, L., and Fan, P. (2006) Validated LC/MS/MS assay for curcumin and tetrahydrocurcumin in rat plasma and application to pharmacokinetic study of phospholipid complex of curcumin. *J Pharm Biomed Anal 40*, 720-7.

(179) Letchford, K., Liggins, R., and Burt, H. (2008) Solubilization of hydrophobic drugs by methoxy poly(ethylene glycol)-block-polycaprolactone diblock copolymer micelles: theoretical and experimental data and correlations. *J Pharm Sci 97*, 1179-90.

(180) Mishra, S., Narain, U., Mishra, R., and Misra, K. (2005) Design, development and synthesis of mixed bioconjugates of piperic acid-glycine, curcumin-glycine/alanine and curcumin-glycine-piperic acid and their antibacterial and antifungal properties. *Bioorg Med Chem 13*, 1477-86.

(181) John, V. D., Kuttan, G., and Krishnankutty, K. (2002) Anti-tumour studies of metal chelates of synthetic curcuminoids. *J Exp Clin Cancer Res 21*, 219-24.

(182) Sui, Z., Salto, R., Li, J., Craik, C., and Ortiz de Montellano, P. R. (1993) Inhibition of the HIV-1 and HIV-2 proteases by curcumin and curcumin boron complexes. *Bioorg Med Chem 1*, 415-22.

(183) Eybl, V., Kotyzova, D., and Bludovska, M. (2004) The effect of curcumin on cadmium-induced oxidative damage and trace elements level in the liver of rats and mice. *Toxicol Lett 151*, 79-85.

(184) Vajragupta, O., Boonchoong, P., Watanabe, H., Tohda, M., Kummasud, N., and Sumanont, Y. (2003) Manganese complexes of curcumin and its derivatives: evaluation for the radical scavenging ability and neuroprotective activity. *Free Radic Biol Med 35*, 1632-44.

(185) Vajragupta, O., Boonchoong, P., and Berliner, L. J. (2004) Manganese complexes of curcumin analogues: evaluation of hydroxyl radical scavenging ability, superoxide dismutase activity and stability towards hydrolysis. *Free Radic Res 38*, 303-14.

(186) Eybl, V., Kotyzova, D., Leseticky, L., Bludovska, M., and Koutensky, J. (2006) The influence of curcumin and manganese complex of curcumin on cadmium-induced oxidative damage and trace elements status in tissues of mice. *J Appl Toxicol 26*, 207-12.

(187) Thompson, K. H., Bohmerle, K., Polishchuk, E., Martins, C., Toleikis, P., Tse, J., Yuen, V., McNeill, J. H., and Orvig, C. (2004) Complementary inhibition of synoviocyte, smooth muscle cell or mouse lymphoma cell proliferation by a vanadyl curcumin complex compared to curcumin alone. *J Inorg Biochem 98*, 2063-70.

(188) Mohammadi, K., Thompson, K. H., Patrick, B. O., Storr, T., Martins, C., Polishchuk, E., Yuen, V. G., McNeill, J. H., and Orvig, C. (2005) Synthesis and

characterization of dual function vanadyl, gallium and indium curcumin complexes for medicinal applications. *J Inorg Biochem 99*, 2217-25.

(189) Shen, L., and Ji, H. F. (2007) Theoretical study on physicochemical properties of curcumin. *Spectrochim Acta A Mol Biomol Spectrosc 67*, 619-23.

(190) Mosley, C. A., Liotta, D. C., and Snyder, J. P. (2007) Highly active anticancer curcumin analogues. *Adv Exp Med Biol 595*, 77-103.

(191) Ohori, H., Yamakoshi, H., Tomizawa, M., Shibuya, M., Kakudo, Y., Takahashi, A., Takahashi, S., Kato, S., Suzuki, T., Ishioka, C., Iwabuchi, Y., and Shibata, H. (2006) Synthesis and biological analysis of new curcumin analogues bearing an enhanced potential for the medicinal treatment of cancer. *Mol Cancer Ther 5*, 2563-71.

(192) Shi, W., Dolai, S., Rizk, S., Hussain, A., Tariq, H., Averick, S., L'Amoreaux, W., El ldrissi, A., Banerjee, P., and Raja, K. (2007) Synthesis of monofunctional curcumin derivatives, clicked curcumin dimer, and a PAMAM dendrimer curcumin conjugate for therapeutic applications. *Org Lett 9*, 5461-4.

(193) Ihara, N., Schmitz, S., Kurisawa, M., Chung, J. E., Uyama, H., and Kobayashi, S. (2004) Amplification of inhibitory activity of catechin against disease-related enzymes by conjugation on poly(epsilon-lysine). *Biomacromolecules 5*, 1633-6.

(194) Aggarwal, B. B., and Shishodia, S. (2006) Molecular targets of dietary agents for prevention and therapy of cancer. *Biochem Pharmacol 71*, 1397-421.

(195) Hermanson, G. T. (1996) *Bioconjugate Techniques*, Academic Press, San Diego, California.

Chapter II

(1) Ehrlich, P. (1960) *The Collected Papers of Paul Ehrlich*, Pergamon, London.

(2) Mullin, R. (2005) *C&En. 83*.

(3) Hata, K. (2006) Efficacy of Mylotarg for acute myeloid leukemia. *Annual Review Ketsueki*, 114-123.

(4) Wu, A. M., and Senter, P. D. (2005) Arming antibodies: prospects and challenges for immunoconjugates. *Nat Biotechnol 23*, 1137-46.

(5) Hermenson, G. T. (2008) *Bioconjugate Techniques, 2nd Ed.*, Academic Press, San Diego, California.

(6) Raja, K., McDonald, R., Tuck, S., Rodriguez, R., Milley, B., and Traquina, P. (2007) One-pot synthesis, purification, and formulation of bionanoparticle-CpG oligodeoxynucleotide hepatitis B surface antigen conjugate vaccine via tangential flow filtration. *Bioconjug Chem 18*, 285-8.

(7) Raja, K. S., Wang, Q., Gonzalez, M. J., Manchester, M., Johnson, J. E., and Finn, M. G. (2003) Hybrid virus-polymer materials. 1. Synthesis and properties of PEG-decorated cowpea mosaic virus. *Biomacromolecules 4*, 472-6.

(8) Shi, W., Dolai, S., Rizk, S., Hussain, A., Tariq, H., Averick, S., L'Amoreaux, W., El ldrissi, A., Banerjee, P., and Raja, K. (2007) Synthesis of monofunctional curcumin derivatives, clicked curcumin dimer, and a PAMAM dendrimer curcumin conjugate for therapeutic applications. *Org Lett 9*, 5461-4.

(9) Hannink, J. M., Cornelissen, J. J., Farrera, J. A., Foubert, P., De Schryver, F. C., Sommerdijk, N. A., and Nolte, R. J. (2001) Protein-Polymer Hybrid Amphiphiles. *Angew Chem Int Ed Engl 40*, 4732-4734.

(10) Velonia, K., Rowan, A. E., and Nolte, R. J. (2002) Lipase polystyrene giant amphiphiles. *J Am Chem Soc 124*, 4224-5.

(11) Kochendoerfer, G. G., Chen, S. Y., Mao, F., Cressman, S., Traviglia, S., Shao, H., Hunter, C. L., Low, D. W., Cagle, E. N., Carnevali, M., Gueriguian, V., Keogh, P. J., Porter, H., Stratton, S. M., Wiedeke, M. C., Wilken, J., Tang, J., Levy, J. J., Miranda, L. P., Crnogorac, M. M., Kalbag, S., Botti, P., Schindler-Horvat, J., Savatski, L., Adamson, J. W., Kung, A., Kent, S. B., and Bradburne, J. A. (2003) Design and chemical synthesis of a homogeneous polymer-modified erythropoiesis protein. *Science 299*, 884-7.

(12) Kovar, M., Strohalm, J., Etrych, T., Ulbrich, K., and Rihova, B. (2002) Star structure of antibody-targeted HPMA copolymer-bound doxorubicin: a novel type of polymeric conjugate for targeted drug delivery with potent antitumor effect. *Bioconjug Chem 13*, 206-15.

(13) Kulkarni, S., Schilli, C., Grin, B., Muller, A. H., Hoffman, A. S., and Stayton, P. S. (2006) Controlling the aggregation of conjugates of streptavidin with smart block copolymers prepared via the RAFT copolymerization technique. *Biomacromolecules 7*, 2736-41.

(14) Sen Gupta, S., Raja, K. S., Kaltgrad, E., Strable, E., and Finn, M. G. (2005) Virus-glycopolymer conjugates by copper(I) catalysis of atom transfer radical polymerization and azide-alkyne cycloaddition. *Chem Commun (Camb)*, 4315-7.

(15) Sen Gupta, S., Kuzelka, J., Singh, P., Lewis, W. G., Manchester, M., and Finn, M. G. (2005) Accelerated bioorthogonal conjugation: a practical method for the ligation of diverse functional molecules to a polyvalent virus scaffold. *Bioconjug Chem 16*, 1572-9.

(16) Hou, S., Sun, X. L., Dong, C. M., and Chaikof, E. L. (2004) Facile synthesis of chain-end functionalized glycopolymers for site-specific bioconjugation. *Bioconjug Chem 15*, 954-9.

(17) Vazquez-Dorbatt, V., and Maynard, H. D. (2006) Biotinylated glycopolymers synthesized by atom transfer radical polymerization. *Biomacromolecules 7*, 2297-302.

(18) Lele, B. S., Murata, H., Matyjaszewski, K., and Russell, A. J. (2005) Synthesis of uniform protein-polymer conjugates. *Biomacromolecules 6*, 3380-7.

(19) De, P., Li, M., Gondi, S. R., and Sumerlin, B. S. (2008) Temperature-regulated activity of responsive polymer-protein conjugates prepared by grafting-from via RAFT polymerization. *J Am Chem Soc 130*, 11288-9.

(20) Bontempo, D., Heredia, K. L., Fish, B. A., and Maynard, H. D. (2004) Cysteine-reactive polymers synthesized by atom transfer radical polymerization for conjugation to proteins. *J Am Chem Soc 126*, 15372-3.

(21) Bontempo, D., and Maynard, H. D. (2005) Streptavidin as a Macroinitiator for Polymerization: In Situ Protein-Polymer Conjugate Formation. *Journal of the American Chemical Society 127*, 6508-6509.

(22) Geng, J., Mantovani, G., Tao, L., Nicolas, J., Chen, G., Wallis, R., Mitchell, D. A., Johnson, B. R., Evans, S. D., and Haddleton, D. M. (2007) Site-directed

conjugation of "clicked" glycopolymers to form glycoprotein mimics: binding to mammalian lectin and induction of immunological function. *J Am Chem Soc 129*, 15156-63.

(23) Law, K.-Y. (1993) Organic photoconductive materials: recent trends and developments. *Chemical Reviews 93*, 449-486.

(24) Fabian, J., Nakazumi, H., and Matsuoka, M. (1992) Near-infrared absorbing dyes. *Chemical Review 92*, 1197-1226.

(25) Mishra, A., Behera, R. K., Behera, P. K., Mishra, B. K., and Behera, G. B. (2000) Cyanines during the 1990s: A Review. *Chem Rev 100*, 1973-2012.

(26) Zhao, W., and Carreira, E. M. (2005) Conformationally restricted aza-bodipy: a highly fluorescent, stable, near-infrared-absorbing dye. *Angew Chem Int Ed Engl 44*, 1677-9.

(27) Patonay, G., Salon, J., Sowell, J., and Strekowski, L. (2004) Noncovalent labeling of biomolecules with red and near- infrared dyes. *Molecules 9*, 40-9.

(28) Tung, C. H. (2004) Fluorescent peptide probes for in vivo diagnostic imaging. *Biopolymers 76*, 391-403.

(29) Zaheer, A., Lenkinski, R. E., Mahmood, A., Jones, A. G., Cantley, L. C., and Frangioni, J. V. (2001) In vivo near-infrared fluorescence imaging of osteoblastic activity. *Nat Biotechnol 19*, 1148-54.

(30) Wang, J.-S., and Matyjaszewski, K. (1995) Controlled/"living" radical polymerization. atom transfer radical polymerization in the presence of transition-metal complexes. *Journal of the American Chemical Society 117*, 5614-5615.

(31) Shi, W., Dolai, S., Averick, S., Fernando, S. S., Saltos, J. A., L'Amoreaux, W., Banerjee, P., and Raja, K. (2009) A General Methodology Toward Drug/Dye Incorporated Living Copolymer-Protein Hybrids: (NIRF Dye-Glucose) Copolymer-Avidin/BSA Conjugates as Prototypes. *Bioconjug Chem*, 1595–1601.

(32) Luxenhofer, R., and Jordan, R. (2006) Click Chemistry with Poly(2-oxazoline)s. . *Macromolecules 39*, 3509-3516.

Chapter III

(1) Harris, J. M. (1992) *Poly (ethylene glycol) chemistry; Biotechnical and Biomedical Applications.*, Plenum Press, New York.

(2) Nicolas, J., Mantovani, G., and Haddleton, D. M. (2007) Living Radical Polymerization as a Tool for the Synthesis of Polymer-Protein/Peptide Bioconjugates. *Macromol. Rapid Commun. 28*, 1083-1111.

(3) Raja, K. S., Dolai, S., Shi, W., and Wang, Q. (2009) in *Dekker Encyclopedia of Nanoscience and Nanotechnology, Second Edition* (Schwarz, J. A., Contescu, C. I., and Putyera, K., Eds.) pp 386-396, Taylor and Francis Group.

(4) Vriezema, D. M., Comellas Aragones, M., Elemans, J. A., Cornelissen, J. J., Rowan, A. E., and Nolte, R. J. (2005) Self-assembled nanoreactors. *Chem Rev 105*, 1445-89.

(5) Douglas, T., and Young, M. (2006) Viruses: making friends with old foes. *Science 312*, 873-5.

(6) Klok, H.-A. (2009) Peptide/Protein-Synthetic Polymer Conjugates: Quo Vadis. *Macromolecules 42*, 7990-8000.

(7) Miyamoto, M., Naka, K., Shiozaki, M., Chujo, Y., and Saegusa, T. (1990) Preparation and enzymic activity of poly[(N-acylimino)ethylene]-modified catalase. *Macromolecules 23*, 3201-3205.

(8) Bailon, P., and Won, C.-Y. (2009) PEG-modified biopharmaceuticals. *Expert Opinion on Drug Delivery 6*, 1-16.

(9) Kozlowski, A., and Harris, J. M. (2001) Improvements in protein PEGylation: pegylated interferons for treatment of hepatitis C. *J Control Release 72*, 217-24.

(10) Chapman, A. P., Antoniw, P., Spitali, M., West, S., Stephens, S., and King, D. J. (1999) Therapeutic antibody fragments with prolonged in vivo half-lives. *Nat Biotechnol 17*, 780-3.

(11) Rajender, R., K., Modi, M. W., and Pedder, S. (2002) Use of peginterferon alfa-2a (40 KD) (Pegasys) for the treatment of hepatitis C. *Advanced Drug Delivery Reviews 54*, 571-586.

(12) Kitamura, K., Takahashi, T., Yamaguchi, T., Noguchi, A., Takashina, K., Tsurumi, H., Inagake, M., Toyokuni, T., and Hakomori, S. (1991) Chemical engineering of the monoclonal antibody A7 by polyethylene glycol for targeting cancer chemotherapy. *Cancer Res 51*, 4310-5.

(13) Pedley, R. B., Boden, J. A., Boden, R., Begent, R. H., Turner, A., Haines, A. M., and King, D. J. (1994) The potential for enhanced tumour localisation by poly(ethylene glycol) modification of anti-CEA antibody. *Br J Cancer 70*, 1126-30.

(14) Veronese, F. M., and Pasut, G. (2005) PEGylation, successful approach to drug delivery. *Drug Discov Today 10*, 1451-8.

(15) Krishna, O. D., and Kiick, K. L. (2010) Protein- and peptide-modified synthetic polymeric biomaterials. *Biopolymers 94*, 32-48.

(16) Kochendoerfer, G. G., Chen, S. Y., Mao, F., Cressman, S., Traviglia, S., Shao, H., Hunter, C. L., Low, D. W., Cagle, E. N., Carnevali, M., Gueriguian, V., Keogh, P. J., Porter, H., Stratton, S. M., Wiedeke, M. C., Wilken, J., Tang, J., Levy, J. J., Miranda, L. P., Crnogorac, M. M., Kalbag, S., Botti, P., Schindler-Horvat, J., Savatski, L., Adamson, J. W., Kung, A., Kent, S. B., and Bradburne, J. A. (2003) Design and chemical synthesis of a homogeneous polymer-modified erythropoiesis protein. *Science 299*, 884-7.

(17) Tao, L., Kaddis, C. S., Loo, R. R. O., Grover, G. N., Loo, J. A., and Maynard, H. D. (2009) Synthetic approach to homodimeric protein-polymer conjugates. *Chemical Communications 16*, 2148-2150.

(18) Maynard, H. D., Heredia, K. L., Li, R. C., Parra, D. P., and Vazquez-Dorbatt, V. (2007) Thermoresponsive biohybrid materials synthesized by ATRP. *Journal of Materials Chemistry 17*, 4015-4017.

(19) Heredia, K. L., and Maynard, H. D. (2007) Synthesis of protein-polymer conjugates. *Org Biomol Chem 5*, 45-53.

(20) Bontempo, D., Heredia, K. L., Fish, B. A., and Maynard, H. D. (2004) Cysteine-reactive polymers synthesized by atom transfer radical polymerization for conjugation to proteins. *J Am Chem Soc 126*, 15372-3.

(21) Romanini, D. W., and Francis, M. B. (2008) Attachment of peptide building blocks to proteins through tyrosine bioconjugation. *Bioconjugate chemistry 19*, 153-157.

(22) Gilmore, J. M., Scheck, R. A., Esser-Kahn, A. P., Joshi, N. S., and Francis, M. B. (2006) N-terminal protein modification through a biomimetic transamination reaction. *Angewandte Chemie, International Edition 45*, 5307-5311.

(23) Esser-Kahn, A. P., and Francis, M. B. (2008) Protein-cross-linked polymeric materials through site-selective bio-conjugation. *Angewandte Chemie, International Edition 47*, 3751-3754.

(24) Carrico, Z. M., Romanini, D. W., Mehl, R. A., and Francis, M. B. (2008) Oxidative coupling of peptides to a virus capsid containing unnatural amino acids. *Chem Commun (Camb)*, 1205-7.

(25) Kulkarni, S., Schilli, C., Grin, B., Muller, A. H., Hoffman, A. S., and Stayton, P. S. (2006) Controlling the aggregation of conjugates of streptavidin with smart block copolymers prepared via the RAFT copolymerization technique. *Biomacromolecules 7*, 2736-41.

(26) Boyer, C., Bulmus, V., Liu, J., Davis, T. P., Stenzel, M. H., and Barner-Kowollik, C. (2007) Well-defined protein-polymer conjugates via in situ RAFT polymerization. *J Am Chem Soc 129*, 7145-54.

(27) Tao, L., Mantovani, G., Lecolley, F., and Haddleton, D. M. (2004) Alpha-aldehyde terminally functional methacrylic polymers from living radical polymerization: application in protein conjugation "pegylation". *J Am Chem Soc 126*, 13220-1.

(28) Qi, K., Ma, Q., Remsen, E. E., Clark, C. G., Jr., and Wooley, K. L. (2004) Determination of the bioavailability of biotin conjugated onto shell cross-linked (SCK) nanoparticles. *J Am Chem Soc 126*, 6599-607.

(29) Sen Gupta, S., Raja, K. S., Kaltgrad, E., Strable, E., and Finn, M. G. (2005) Virus-glycopolymer conjugates by copper(I) catalysis of atom transfer radical polymerization and azide-alkyne cycloaddition. *Chem Commun (Camb)*, 4315-7.

(30) Hou, S., Sun, X. L., Dong, C. M., and Chaikof, E. L. (2004) Facile synthesis of chain-end functionalized glycopolymers for site-specific bioconjugation. *Bioconjug Chem 15*, 954-9.

(31) Bontempo, D., and Maynard, H. D. (2005) Streptavidin as a macroinitiator for polymerization: in situ protein-polymer conjugate formation. *Journal of the American Chemical Society 127*, 6508-6509.

(32) Lele, B. S., Murata, H., Matyjaszewski, K., and Russell, A. J. (2005) Synthesis of uniform protein-polymer conjugates. *Biomacromolecules 6*, 3380-7.

(33) Ayres, L., Vos, M. R. J., Adams, P. J. H. M., Shklyarevskiy, I. O., and Van Hest, J. C. M. (2003) Elastin-Based Side-Chain Polymers Synthesized by ATRP. *Macromolecules 36*, 5967-5973.

(34) Klok, H.-A. (2005) Biological-synthetic hybrid block copolymers: Combining the best from two worlds. *Journal of Polymer Science, Part A: Polymer Chemistry 43*, 1-17.

(35) Kohn, M., and Breinbauer, R. (2004) The Staudinger ligation-a gift to chemical biology. *Angew Chem Int Ed Engl 43*, 3106-16.

(36) Saxon, E., and Bertozzi, C. R. (2000) Cell surface engineering by a modified Staudinger reaction. *Science 287*, 2007-10.

(37) Kiick, K. L., Saxon, E., Tirrell, D. A., and Bertozzi, C. R. (2002) Incorporation of azides into recombinant proteins for chemoselective modification by the

Staudinger ligation. *Proceedings of the National Academy of Sciences of the United States of America 99*, 19-24.

(38) Rostovtsev, V. V., Green, L. G., Fokin, V. V., and Sharpless, K. B. (2002) A stepwise huisgen cycloaddition process: copper(I)-catalyzed regioselective "ligation" of azides and terminal alkynes. *Angew Chem Int Ed Engl 41*, 2596-9.

(39) Link, A. J., and Tirrell, D. A. (2003) Cell surface labeling of Escherichia coli via copper(I)-catalyzed [3+2] cycloaddition. *J Am Chem Soc 125*, 11164-5.

(40) Deiters, A., Cropp, T. A., Summerer, D., Mukherji, M., and Schultz, P. G. (2004) Site-specific PEGylation of proteins containing unnatural amino acids. *Bioorg Med Chem Lett 14*, 5743-5.

(41) Nicolas, J., Khoshdel, E., and Haddleton, D. M. (2007) Bioconjugation onto biological surfaces with fluorescently labeled polymers. *Chem Commun (Camb)*, 1722-4.

(42) Shi, W., Dolai, S., Rizk, S., Hussain, A., Tariq, H., Averick, S., L'Amoreaux, W., El ldrissi, A., Banerjee, P., and Raja, K. (2007) Synthesis of monofunctional curcumin derivatives, clicked curcumin dimer, and a PAMAM dendrimer curcumin conjugate for therapeutic applications. *Org Lett 9*, 5461-4.

(43) Sen Gupta, S., Kuzelka, J., Singh, P., Lewis, W. G., Manchester, M., and Finn, M. G. (2005) Accelerated bioorthogonal conjugation: a practical method for the ligation of diverse functional molecules to a polyvalent virus scaffold. *Bioconjug Chem 16*, 1572-9.

(44) Kiessling, L. L., Gestwicki, J. E., and Strong, L. E. (2006) Synthetic multivalent ligands as probes of signal transduction. *Angew. Chem. Int. Ed. 45*, 2348-2368.

(45) Andrews, D. L. (2008) Mechanistic principles and applications of resonance energy transfer. *Can. J. Chem. 86*, 855-870.

Chapter IV

(1) Chattopadhyay, I., Biswas, K., Bandyopadhyay, U., and Banerjee, R. K. (2004) Turmeric and curcumin: Biological actions and medicinal applications. *Current Science 87*, 44-53.

(2) Strimpakos, A. S., and Sharma, R. A. (2008) Curcumin: preventive and therapeutic properties in laboratory studies and clinical trials. *Antioxid Redox Signal 10*, 511-45.

(3) Aggarwal, B. B., and Shishodia, S. (2006) Molecular targets of dietary agents for prevention and therapy of cancer. *Biochem Pharmacol 71*, 1397-421.

(4) Leyon, P. V., and Kuttan, G. (2003) Studies on the role of some synthetic curcuminoid derivatives in the inhibition of tumour specific angiogenesis. *J Exp Clin Cancer Res 22*, 77-83.

(5) Shi, W., Dolai, S., Rizk, S., Hussain, A., Tariq, H., Averick, S., L'Amoreaux, W., El ldrissi, A., Banerjee, P., and Raja, K. (2007) Synthesis of monofunctional curcumin derivatives, clicked curcumin dimer, and a PAMAM dendrimer curcumin conjugate for therapeutic applications. *Org Lett 9*, 5461-4.

(6) Nurfinal, A. N., Reksohadiprodjo, M. S., Timmerman, H., Jenie, U. A., Sugiyant, D., and van der Goot, H. (1997) Synthesis of some symmetrical curcumin derivatives and their antiinflammatory activity. *European Journal of Medicinal Chemistry 32*, 321-328.

(7) Yang, F., Lim, G. P., Begum, A. N., Ubeda, O. J., Simmons, M. R., Ambegaokar, S. S., Chen, P. P., Kayed, R., Glabe, C. G., Frautschy, S. A., and Cole, G. M. (2005) Curcumin inhibits formation of amyloid beta oligomers and fibrils, binds plaques, and reduces amyloid in vivo. *J Biol Chem 280*, 5892-901.

(8) Kumar, S., Narain, U., Tripathi, S., and Misra, K. (2001) Syntheses of Curcumin Bioconjugates and Study of Their Antibacterial Activities against beta-Lactamase-Producing Microorganisms. *Bioconjug Chem 12*, 464-9.

(9) Shishodia, S., Amin, H. M., Lai, R., and Aggarwal, B. B. (2005) Curcumin (diferuloylmethane) inhibits constitutive NF-kappaB activation, induces G1/S arrest, suppresses proliferation, and induces apoptosis in mantle cell lymphoma. *Biochem Pharmacol 70*, 700-13.

(10) Cole, G. M., Teter, B., and Frautschy, S. A. (2007) Neuroprotective effects of curcumin. *Adv Exp Med Biol 595*, 197-212.

(11) Cheng, A. L., Hsu, C. H., Lin, J. K., Hsu, M. M., Ho, Y. F., Shen, T. S., Ko, J. Y., Lin, J. T., Lin, B. R., Ming-Shiang, W., Yu, H. S., Jee, S. H., Chen, G. S., Chen, T. M., Chen, C. A., Lai, M. K., Pu, Y. S., Pan, M. H., Wang, Y. J., Tsai, C. C., and Hsieh, C. Y. (2001) Phase I clinical trial of curcumin, a chemopreventive agent, in patients with high-risk or pre-malignant lesions. *Anticancer Res 21*, 2895-900.

(12) Anand, P., Kunnumakkara, A. B., Newman, R. A., and Aggarwal, B. B. (2007) Bioavailability of curcumin: problems and promises. *Mol Pharm 4*, 807-18.

(13) Pfeiffer, E., Hoehle, S. I., Walch, S. G., Riess, A., Solyom, A. M., and Metzler, M. (2007) Curcuminoids form reactive glucuronides in vitro. *J Agric Food Chem 55*, 538-44.

(14) Shoba, G., Joy, D., Joseph, T., Majeed, M., Rajendran, R., and Srinivas, P. S. (1998) Influence of piperine on the pharmacokinetics of curcumin in animals and human volunteers. *Planta Med 64*, 353-6.

(15) Ryu, E. K., Choe, Y. S., Lee, K. H., Choi, Y., and Kim, B. T. (2006) Curcumin and dehydrozingerone derivatives: synthesis, radiolabeling, and evaluation for beta-amyloid plaque imaging. *J Med Chem 49*, 6111-9.

(16) Bisht, S., Feldmann, G., Soni, S., Ravi, R., Karikar, C., and Maitra, A. (2007) Polymeric nanoparticle-encapsulated curcumin ("nanocurcumin"): a novel strategy for human cancer therapy. *J Nanobiotechnology 5*, 3.

(17) Tiyaboonchai, W., Tungpradit, W., and Plianbangchang, P. (2007) Formulation and characterization of curcuminoids loaded solid lipid nanoparticles. *Int J Pharm 337*, 299-306.

(18) Li, L., Braiteh, F. S., and Kurzrock, R. (2005) Liposome-encapsulated curcumin: in vitro and in vivo effects on proliferation, apoptosis, signaling, and angiogenesis. *Cancer 104*, 1322-31.

(19) Li, L., Ahmed, B., Mehta, K., and Kurzrock, R. (2007) Liposomal curcumin with and without oxaliplatin: effects on cell growth, apoptosis, and angiogenesis in colorectal cancer. *Mol Cancer Ther 6*, 1276-82.

(20) Maiti, K., Mukherjee, K., Gantait, A., Saha, B. P., and Mukherjee, P. K. (2007) Curcumin-phospholipid complex: Preparation, therapeutic evaluation and pharmacokinetic study in rats. *Int J Pharm 330*, 155-63.

(21) Kumar, V., Lewis, S. A., Mutalik, S., Shenoy, D. B., Venkatesh, and Udupa, N. (2002) Biodegradable microspheres of curcumin for treatment of inflammation. *Indian J Physiol Pharmacol 46*, 209-17.

(22) Raja, K. S., Balambika, R., Dolai, S., and Shi, W. (2009) The concept of a green drug, curcumin and it's derivatives as a model system. *Mini-Reviews in Organic Chemistry 6*, 152-158.

(23) Mosley, C. A., Liotta, D. C., and Snyder, J. P. (2007) Highly active anticancer curcumin analogues. *Adv Exp Med Biol 595*, 77-103.

(24) Thompson, K. H., Bohmerle, K., Polishchuk, E., Martins, C., Toleikis, P., Tse, J., Yuen, V., McNeill, J. H., and Orvig, C. (2004) Complementary inhibition of synoviocyte, smooth muscle cell or mouse lymphoma cell proliferation by a vanadyl curcumin complex compared to curcumin alone. *J Inorg Biochem 98*, 2063-70.

(25) Sharma, K. K., Chandra, S., and Basu, D. K. (1987) Synthesis and antiarthritic study of a new orally active diferuloylmethane (curcumin) gold complex. *Inorganica Chimica Acta 135*, 47-48.

(26) Krishnankutty, K., and Venugopalan, P. (1998) Metal chelates of curcuminoids. *Synthesis and Reactivity in Inorganic and Metal-Organic Chemistry 28*, 1313-1325.

(27) Barik, A., Mishra, B., Kunwar, A., Kadam, R. M., Shen, L., Dutta, S., Padhye, S., Satpati, A. K., Zhang, H. Y., and Priyadarsini, K. I. (2007) Comparative study of copper(II)-curcumin complexes as superoxide dismutase mimics and free radical scavengers. *European Journal of Medicinal Chemistry 42*, 431-439.

(28) Vajragupta, O., Boonchoong, P., Watanabe, H., Tohda, M., Kummasud, N., and Sumanont, Y. (2003) Manganese complexes of curcumin and its derivatives: evaluation for the radical scavenging ability and neuroprotective activity. *Free Radic Biol Med 35*, 1632-44.

(29) Hermanson, G. T. (1996) *Bioconjugate Techniques*, Academic Press, San Diego, California.

(30) Shi, W., Dolai, S., Averick, S., Fernando, S. S., Saltos, J. A., L'Amoreaux, W., Banerjee, P., and Raja, K. (2009) A General Methodology Toward Drug/Dye Incorporated Living Copolymer-Protein Hybrids: (NIRF Dye-Glucose) Copolymer-Avidin/BSA Conjugates as Prototypes. *Bioconjug Chem*, 1595–1601.

Chapter V

(1) Chattopadhyay, I., Biswas, K., Bandyopadhyay, U., and Banerjee, R. K. (2004) Turmeric and curcumin: Biological actions and medicinal applications. *Current Science 87*, 44-53.

(2) Aggarwal, B. B., and Shishodia, S. (2006) Molecular targets of dietary agents for prevention and therapy of cancer. *Biochem Pharmacol 71*, 1397-421.

(3) Leyon, P. V., and Kuttan, G. (2003) Studies on the role of some synthetic curcuminoid derivatives in the inhibition of tumour specific angiogenesis. *J Exp Clin Cancer Res 22*, 77-83.

(4) Nurfinal, A. N., Reksohadiprodjo, M. S., Timmerman, H., Jenie, U. A., Sugiyant, D., and van der Goot, H. (1997) Synthesis of some symmetrical curcumin derivatives and their antiinflammatory activity. *European Journal of Medicinal Chemistry 32*, 321-328.

(5) Yang, F., Lim, G. P., Begum, A. N., Ubeda, O. J., Simmons, M. R., Ambegaokar, S. S., Chen, P. P., Kayed, R., Glabe, C. G., Frautschy, S. A., and Cole, G. M. (2005) Curcumin inhibits formation of amyloid beta oligomers and fibrils, binds plaques, and reduces amyloid in vivo. *J Biol Chem 280*, 5892-901.

(6) Mazumder, A., Neamati, N., Sunder, S., Schulz, J., Pertz, H., Eich, E., and Pommier, Y. (1997) Curcumin Analogs with Altered Potencies against HIV-1 Integrase as Probes for Biochemical Mechanisms of Drug Action. *Journal of Medicinal Chemistry 40*, 3057-3063.

(7) Cheng, A. L., Hsu, C. H., Lin, J. K., Hsu, M. M., Ho, Y. F., Shen, T. S., Ko, J. Y., Lin, J. T., Lin, B. R., Ming-Shiang, W., Yu, H. S., Jee, S. H., Chen, G. S., Chen, T. M., Chen, C. A., Lai, M. K., Pu, Y. S., Pan, M. H., Wang, Y. J., Tsai, C. C., and Hsieh, C. Y. (2001) Phase I clinical trial of curcumin, a chemopreventive agent, in patients with high-risk or pre-malignant lesions. *Anticancer Res 21*, 2895-900.

(8) Folkman, J., Hahnfeldt, P., and Hlatky, L. (2000) Cancer: looking outside the genome. *Nat Rev Mol Cell Biol 1*, 76-9.

(9) Soto, A. M., and Sonnenschein, C. (2004) The somatic mutation theory of cancer: growing problems with the paradigm? *Bioessays 26*, 1097-107.

(10) Gibbs, W. W. (2003) Untangling the roots of cancer. *Sci Am 289*, 56-65.

(11) Prehn, R. T. (1994) Cancers beget mutations versus mutations beget cancers. *Cancer Res 54*, 5296-300.

(12) Vogelstein, B., and Kinzler, K. W. (2004) Cancer genes and the pathways they control. *Nature Medicine 10*, 789-799.

(13) Garcea, G., Berry, D. P., Jones, D. J. L., Singh, R., Dennison, A. R., Farmer, P. B., Sharma, R. A., Steward, W. P., and Gescher, A. J. (2005) Consumption of the Putative Chemopreventive Agent Curcumin by Cancer Patients: Assessment of Curcumin Levels in the Colorectum and their Pharmacodynamic Consequences. *Cancer Epidemiology, Biomarkers & Prevention 14*, 120-125.

(14) Lopez-Lazaro, M. (2008) Anticancer and carcinogenic properties of curcumin: considerations for its clinical development as a cancer chemopreventive and chemotherapeutic agent. *Molecular nutrition & food research 52*, S103-S127.

(15) Hanahan, D., and Weinberg, R. A. (2000) The hallmarks of cancer. *Cell 100*, 57-70.

(16) Samaha, H. S., Kelloff, G. J., Steele, V., Rao, V., and Reddy, B. S. (1997) Modulation of apoptosis by sulindac, curcumin, phenylethyl-3-methylcaffeate and 6-phenylhexyl isothiocyanate: apoptotic index as a biomarker in colon cancer chemoprevention and promotion. *Cancer Research 57*, 1301-1305.

(17) Volate, S. R., Davenport, D. M., Muga, S. J., and Wargovich, M. J. (2005) Modulation of aberrant crypt foci and apoptosis by dietary herbal supplements (quercetin, curcumin, silymarin, ginseng and rutin). *Carcinogenesis 26*, 1450-6.

(18) Li, L., Braiteh, F. S., and Kurzrock, R. (2005) Liposome-encapsulated curcumin: in vitro and in vivo effects on proliferation, apoptosis, signaling, and angiogenesis. *Cancer 104*, 1322-31.

(19) Li, L., Ahmed, B., Mehta, K., and Kurzrock, R. (2007) Liposomal curcumin with and without oxaliplatin: effects on cell growth, apoptosis, and angiogenesis in colorectal cancer. *Molecular Cancer Therapeutics 6*, 1276-1282.

(20) Karin, M. (2006) Nuclear factor-kappaB in cancer development and progression. *Nature 441*, 431-6.

(21) Chuang, S. E., Cheng, A. L., Lin, J. K., and Kuo, M. L. (2000) Inhibition by curcumin of diethylnitrosamine-induced hepatic hyperplasia, inflammation, cellular gene products and cell-cycle-related proteins in rats. *Food Chem Toxicol 38*, 991-5.

(22) Leclercq, I. A., Farrell, G. C., Sempoux, C., dela Pena, A., and Horsmans, Y. (2004) Curcumin inhibits NF-kappaB activation and reduces the severity of experimental steatohepatitis in mice. *J Hepatol 41*, 926-34.

(23) Klaunig, J. E., and Kamendulis, L. M. (2004) The role of oxidative stress in carcinogenesis. *Annu Rev Pharmacol Toxicol 44*, 239-67.

(24) Lopez-Lazaro, M. (2007) Excessive superoxide anion generation plays a key role in carcinogenesis. *Int J Cancer 120*, 1378-80.

(25) Lopez-Lazaro, M. (2007) Dual role of hydrogen peroxide in cancer: possible relevance to cancer chemoprevention and therapy. *Cancer Lett 252*, 1-8.

(26) Kratz, F., Muller, I. A., Ryppa, C., and Warnecke, A. (2008) Prodrug strategies in anticancer chemotherapy. *ChemMedChem 3*, 20-53.

(27) Panchal, R. G. (1998) Novel therapeutic strategies to selectively kill cancer cells. *Biochem Pharmacol 55*, 247-52.

(28) Zangemeister-Wittke, U. (2005) Antibodies for targeted cancer therapy -- technical aspects and clinical perspectives. *Pathobiology 72*, 279-86.

(29) Wu, A. M., and Senter, P. D. (2005) Arming antibodies: prospects and challenges for immunoconjugates. *Nat Biotechnol 23*, 1137-46.

(30) Ricart, A. D., and Tolcher, A. W. (2007) Technology insight: cytotoxic drug immunoconjugates for cancer therapy. *Nat Clin Pract Oncol 4*, 245-55.

(31) Senter, P. D. (2009) Potent antibody drug conjugates for cancer therapy. *Curr Opin Chem Biol 13*, 235-44.

(32) Carter, P. J., and Senter, P. D. (2008) Antibody-drug conjugates for cancer therapy. *Cancer J 14*, 154-69.

(33) Tomalia, D. A. (2003) *Handbook of Nanoscience, Engineering and Technology*, CRC Press, Boca Raton, FL.

(34) Tomalia, D. A., Huang, B., Swanson, D. R., Brothers, H. M., and Klimash, J. W. (2003) Structure control within poly(amidoamine) dendrimers: size, shape and regio-chemical mimicry of globular proteins. *Tetrahedron Letters 59*, 3799-3813.

(35) Zhang, C., and Tomalia, D. A. (2001) *Dendrimers and Other Dendritic Polymers*, Wiley, Chichester.

(36) Brothers, H. M., Piehler, L. T., and Tomalia, D. A. (1998) Slab-gel and capillary electrophoretic characterization of polyamidoamine dendrimers. *Journal of Chromatography, A 814*, 233-248.

(37) Esfand, R., and Tomalia, D. A. (2001) Poly(amidoamine) (PAMAM) dendrimers: from biomimicry to drug delivery and biomedical applications. *Drug Discovery Today 6*, 427-436.

(38) Tomalia, D. A., Brothers, H. M., 2nd, Piehler, L. T., Durst, H. D., and Swanson, D. R. (2002) Partial shell-filled core-shell tecto(dendrimers): a strategy to surface differentiated nano-clefts and cusps. *Proc Natl Acad Sci U S A 99*, 5081-7.

(39) Tomalia, D. A., Naylor, A. M., and Goddard, W. A., III. (1990) Starburst dendrimers: control of size, shape, surface chemistry, topology and flexibility in the conversion of atoms to macroscopic materials. *Angewandte Chemie, International Edition 102*, 119-157.

(40) Hecht, S., and Frechet, J. M. J. (2001) Dendritic encapsulation of function: applying nature's site isolation principle from biomimetics to materials science. *Angewandte Chemie, International Edition 40*, 74-91.

(41) Piotti, M. E., Rivera, F., Jr., Bond, R., Hawker, C. J., and Frechet, J. M. J. (1999) Synthesis and Catalytic Activity of Unimolecular Dendritic Reverse Micelles with "Internal" Functional Groups. *Journal of the American Chemical Society 121*, 9471-9472.

(42) Tomalia, D. A., and Frechet, J. M. (2005) Introduction to "Dendrimers and dendritic polymers". *Progress in Polymer Science 30*, 217-219.

(43) Adronov, A., and Frechet, J. M. J. (2000) Light-harvesting dendrimers. *Chemical Communications 18*, 1701-1710.

(44) Jensen, A. W., Maru, B. S., Zhang, X., Mohanty, D. K., Fahlman, B. D., Swanson, D. R., and Tomalia, D. A. (2005) Preparation of fullerene-shell dendrimer-core nanoconjugates. *Nano Lett 5*, 1171-3.

(45) DeMattei, C. R., Huang, B., and Tomalia, D. A. (2004) Designed Dendrimer Syntheses by Self-Assembly of Single-Site, ssDNA Functionalized Dendrons. *Nano Letters 4*, 771-777.

(46) Kubasiak, L. A., and Tomalia, D. A. *Polymeric Gene Delivery Principles and Applications*, CRC Press, Boca Raton.

(47) Kim, T.-I., Seo, H. J., Choi, J. S., Jang, H.-S., Baek, J., Kim, K., and Park, J.-S. (2004) PAMAM-PEG-PAMAM: novel triblock copolymer as a biocompatible and efficient gene delivery carrier. *Biomacromolecules 5*, 2487-2492.

(48) Singh, P. (2001) *Dendrimers and Dendritic Polymers.*, Wiley, Chichester.

(49) Singh, P., Moll, F., III, Lin, S. H., and Ferzli, C. (1996) Starburst dendrimers: A novel matrix for multifunctional reagents in immunoassays. *Clinical Chemistry 42*, 1567-1569.

(50) Jiang, Y.-H., Emau, P., Cairns, J. S., Flanary, L., Morton, W. R., McCarthy, T. D., and Tsai, C.-C. (2005) SPL7013 gel as a topical microbicide for prevention of vaginal transmission of SHIV89.6P in macaques. *AIDS Research and Human Retroviruses 21*, 207-213.

(51) Ariga, T., and Hamano, M. (1990) Antioxidative properties of proanthocyanidins. Part II. radical scavenging action and its mode in procyanidins B-1 and B-3 from

Azuki beans to peroxyl radicals. *Agricultural and Biological Chemistry 54*, 2499-2504.

(52) Saito, M., Hosoyama, H., Ariga, T., Kataoka, S., and Yamaji, N. (1998) Antiulcer Activity of Grape Seed Extract and Procyanidins. *Journal of Agricultural and Food Chemistry 46*, 1460-1464.

(53) Hagerman, A. E., Riedl, K. M., Jones, G. A., Sovik, K. N., Ritchard, N. T., Hartzfeld, P. W., and Riechel, T. L. (1998) High molecular weight plant polyphenolics (tannins) as biological antioxidants. *Journal of Agricultural and Food Chemistry 46*, 1887-1892.

(54) Ihara, N., Schmitz, S., Kurisawa, M., Chung, J. E., Uyama, H., and Kobayashi, S. (2004) Amplification of inhibitory activity of catechin against disease-related enzymes by conjugation on poly(epsilon-lysine). *Biomacromolecules 5*, 1633-6.

(55) Puchtler, H., Sweat, F., and Levine, M. (1962) The binding of Congo red by amyloid. *Journal of Histochemistry and Cytochemistry 10*, 355-364.